Cretaceous tectonism and volcanism in the eastern Scotian Basin, offshore Nova Scotia

by

Sarah Bowman

A Thesis Submitted to Saint Mary's University, Halifax, Nova Scotia,
in Partial Fulfillment of the Requirements for the
Degree of Master of Science in Applied Science

September 2010, Halifax, Nova Scotia

Approved: Dr. Georgia Pe-Piper
               Supervisor
               Department of Geology

Approved: Dr. Brendan Murphy
               External Examiner
               Department of Earth Sciences
               St. Francis Xavier University

Approved: Dr. David Piper
               Supervisory Committee Member
               Department of Geology and Bedford
               Institute of Oceanography

Approved: Dr. Cristian Suteanu
               Supervisory Committee Member
               Department of Geography and
               Environmental Studies Program

Approved: Dr. Andrew MacRae
               Program Representative

Approved: Dr. Kevin Vessey
               Dean of Graduate Studies

Date: September 22, 2010

Canada

Cretaceous tectonism and volcanism in the eastern Scotian Basin, offshore, Nova Scotia

by Sarah J. Bowman

Abstract

Early Cretaceous tectonism and volcanism is widespread in the eastern Mesozoic-Cenozoic Scotian Basin. The precise stratigraphic position of volcanic rocks within wells has been re-evaluated and the volcanological character of the rocks refined by study of cuttings and well logs. Hauterivian-Barremian volcanic rocks on the SW Grand Banks and Aptian-Albian volcanic rocks in the Orpheus Graben and SE Scotian Shelf are likely the result of Strombolian type eruptions. The timing of regional unconformities appears to mark the onset of different components of the volcanic system. The distribution of volcanism is related to the complex opening history of Europe from North America. Widespread volcanic activity indicates a regional and long-lived magma source, which resulted in elevated regional heat flow. Effects of this heat flow are seen in sediments within the Sable sub-basin, but was insufficient to significantly influence the petroleum system.

September 22, 2010

Acknowledgements

TABLE OF CONTENTS

<u>**LIST OF FIGURES**</u>

LIST OF TABLES

CHAPTER 1
INTRODUCTION AND OBJECTIVES

1.1 Introduction

This study is concerned with the impact of Cretaceous tectonism and volcanism on the petroleum system located in the eastern Scotian Basin, offshore eastern Canada. The Scotian Basin is a passive-margin, Mesozoic-Cenozoic basin flanked to the southwest by the Yarmouth Arch and to the northeast by the Avalon Uplift (Wade and MacLean, 1990). The Scotian Basin comprises interconnected sedimentary sub-basins: the Shelburne, Sable, Abenaki, Laurentian and South Whale sub-basins, and the Orpheus Graben, which contain relatively thicker sediments. The study area for this thesis comprises the eastern Scotian Basin and includes the Orpheus Graben, the eastern portion of the Abenaki sub-basin, the Laurentian sub-basin and the South Whale sub-basin (Figure 1.1). The Orpheus Graben is located on the northeastern corner of the Scotian Shelf, extending from the Chedabucto Bay in the east to the Laurentian Channel to the west (Jansa and Wade, 1975). It is bounded to the north by the Scatarie Ridge and to the south by the Canso Ridge. Structurally, the graben is surrounded by a series of discontinuous subparallel faults (Weir-Murphy, 2004). The Abenaki sub-basin is located on the southeastern portion of the Scotian Shelf. Within this study the Abenaki sub-basin will be referred to as the SE Scotian Shelf. In this study, although the Orpheus Graben is located on the Scotian Shelf, it will be referred to separately from the SE Scotian Shelf as the two areas are distinctly different structurally. The Laurentian sub-basin is located at the mouth of the Laurentian Channel and extends onto the southwest Grand Banks. The South Whale sub-basin is located farther west on the southwest Grand Banks. The

1
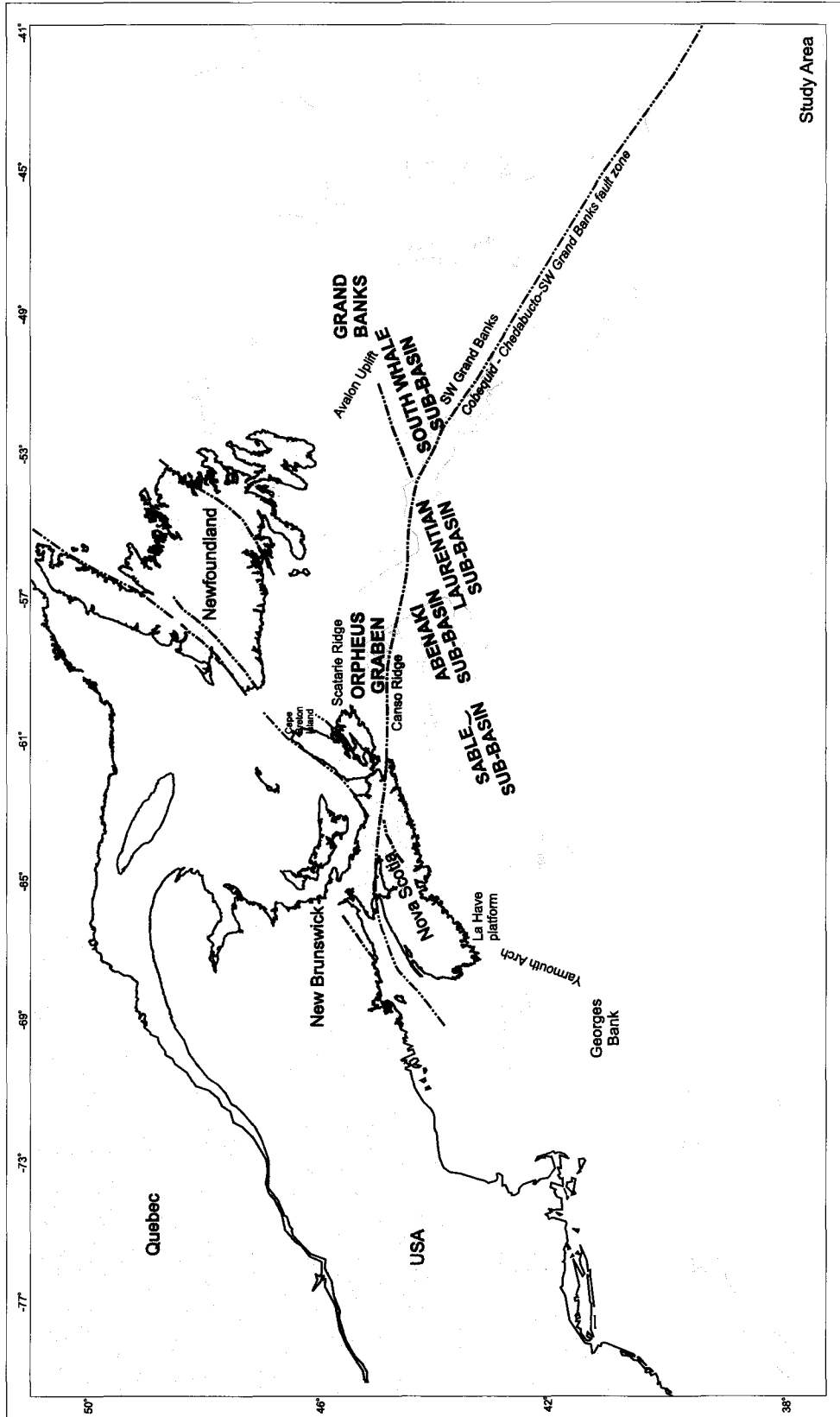
Figure 1.1: Map showing location of study area in blue

Laurentian and South Whale sub-basins together will be referred to as the SW Grand Banks in this study.

1.1.1 Tectonic history

The development of the Scotian Basin can be divided into two main phases: one that caused the formation of sub-basins on the Scotian Shelf (including the Orpheus Graben), and one that caused the formation of sub-basins on the SW Grand Banks. The first phase began in the early part of the Mesozoic (approximately 210-230 Ma, in the late Triassic) with the initiation of south to north rifting between North America and Africa and the development of northeast trending grabens and half-grabens bounded by normal faults on the Scotian Shelf (Keen et al., 1990; Wade and MacLean, 1990). It has been suggested that bounding Mesozoic extensional faults are likely to be reactivated Paleozoic faults such as the Cobequid-Chedabucto fault system (Jansa and Pe-Piper, 1985; Tankard and Welsink, 1989; MacLean and Wade, 1992). Rifting is thought to have ceased in the Orpheus Graben and on the Scotian Shelf by the middle Jurassic (~180 Ma).

The SW Grand Banks was affected by both the rifting which had occurred on the Scotian Shelf to the south, and the second phase of rifting between Newfoundland and Iberia. This second phase has been interpreted by Tucholke et al. (2007) to have occurred in three stages: Berriasian, Valanginian to Hauterivian and Barremian to end Aptian (~112 Ma). On the Grand Banks, the tectonic history is dominated by uplift and erosion as well as by subsidence within its sedimentary basins. The Grand Banks comprises a series of intracratonic basins and ridges similar to those on the Scotian Shelf

(Enachescu, 1988). An important tectonic element is the Avalon Uplift, which has been considered to be late Jurassic to early Cretaceous (Wade and MacLean, 1990). According to MacLean and Wade (1992), the uplift was generated by rifting between the Grand Banks and Iberia and resulted in significant erosion and reworking of sediments during the early Cretaceous. These sediments were then deposited into the basins of the Grand Banks and the Scotian Basin.

It is important to understand the more localized tectonic history of the study area and how it relates to the regional tectonic history of the Scotian margin and Grand Banks. Understanding the timing of tectonic movement may aid in determining a more exact time of emplacement of volcanic rocks, the extent of the volcanic rocks, and potential pathways for magma migration.

1.1.2 Depositional history

Stratigraphic nomenclature in the Scotian Basin is based on McIver (1971) and Wade and MacLean (1990) (Figure 1.2). The plot on Figure 1.2 has been corrected to the Gradstein et al. (2008) timescale. The interconnected sub-basins of the Scotian Shelf underwent prolonged subsidence resulting in sediment accumulations of up to 12 km in thickness (Wade and MacLean, 1990). Syn-rift Triassic continental redbeds and evaporites of the Eurydice and Argo formations were deposited first, followed by early Jurassic continental clastic sedimentary rocks and evaporitic dolostones. At this time a small amount of volcanic and sub-volcanic rocks were emplaced, which are discussed in the next section. During the middle to late Jurassic, post-rift clastic rocks and carbonate rocks of the Mohawk, Mic Mac, Abenaki and Verrill Canyon formations were deposited

4

Ma	Period	Epoch	Age	Scotian Basin stratigraphy

Laurentian Fm

PLE
PLI

10

20

OLIGOC. — Chattian / Rupelian

30

Priabonian / Bartonian

40

EOCENE — Lutetian

50

Ypresian

Banquereau Fm

PALEOC. — Thanetian / Selandian / Danian

60

Maastrichtian

70

Campanian

UPPER

80

Wyandot Fm

Santonian / Coniacian

Dawson Canyon Fm

90

Turonian

Cenomanian

Marmora Mb

100

Sable Mb

Albian

Logan Canyon Fm   Cree Mb

110

Aptian

120

Naskapi Mb

Barremian / Hauterivian / Valanginian / Berriasian

130

Upper Mb

(O Marker

Misslsauga Fm

Middle Mb   Lower Mb

140

Verrill Canyon Fm

Tithonian

150

UPPER

Kimmeridgian

Mic Mac Fm

Abenaki Fm

Mic Mac Fm

Oxfordian

160

Callovian

MIDDLE — Bathonian / Bajocian / Aalenian

170

Mohican Fm

180

Iroquois Fm

190

200

Rhaetian

Argo Fm

Norian

210

UPPER

220

Carnian

Eurydice Fm

230

240

Figure 1.2: Generalized stratigraphy of the Scotian Basin, including the SW Grand Banks (modified from Pe-Piper and Piper, *in press*). The timescale is that of Gradstein et al. (2008).

5

along the basin margin. Following this was the deposition of the units of importance to this study: the thick fluvial-deltaic sediments of the early Cretaceous Mississauga Formation and the mid-Cretaceous Logan Canyon Formation, both of which pass seaward into the Verrill Canyon Formation.

During the Cretaceous, there were fluctuations in sea level which influenced the deposition of sandstones of the Mississauga Formation and the mix of transgressive shales and regressive sandstones of the Logan Canyon Formation (Jansa and Wade, 1975). The Mississauga Formation can be divided into three members: lower, middle and upper, although the lower member is not present in the eastern part of the Scotian Basin (Wade and MacLean, 1990) where the equivalent strata are referred to as the upper part of the Mic Mac Formation (Figure 1.2). The middle and upper members are separated by a transgressive limestone unit called the "O" marker, which is not found within the Orpheus Graben and is found only locally on the SW Grand Banks (Wade and MacLean, 1990). The Mississauga Formation is generally considered to be Berriasian to Barremian (Williams, 1975; Wade and MacLean, 1990). The Logan Canyon Formation can be divided into four members: the basal transgressive shale of the Naskapi Member, the sandstone dominated Cree Member, the shale dominated Sable Member and the sandstone dominated Marmora Member (Wade and MacLean, 1990). The Logan Canyon Formation is considered to be Aptian to Cenomanian (Williams, 1975).

In the late Cretaceous, transgressive marine shales of the Dawson Canyon Formation and the chalk and marl of the Wyandot Formation were deposited. Sedimentary rocks deposited after these formations are considered part of the Tertiary Banquereau Formation. The general stratigraphy of the SW Grand Banks is very similar

to that of the Orpheus Graben and Scotian Shelf and thus the stratigraphic nomenclature of the Scotian Shelf and Orpheus Graben will also be used for the SW Grand Banks.

Understanding the depositional history of the study area is important as changes in depositional patterns often are indications of tectonic movement. It is also important to understand the stratigraphic position of the volcanic rocks in order to properly interpret timing and environment of emplacement.

1.1.3 Igneous rocks

The continental margin off Nova Scotia is considered a non-volcanic rifted margin as early Jurassic rift-related volcanic and sub-volcanic rocks are sparse (Louden and Lau, 2001). However, Cretaceous volcanic rocks and intrusions are widespread on the Scotian Shelf (Jansa and Pe-Piper, 1985). The volcanism is also found on the SW Grand Banks (Jansa and Pe-Piper, 1988; Pe-Piper et al., 1994; Pe-Piper et al., 2007). Data from wells drilled for hydrocarbon exploration have shown that there were episodes of post-rifting volcanic activity synchronous with major regional tectonic events on the SE Scotian Shelf and in the Orpheus Graben and syn-rift volcanic activity on the SW Grand Banks (Jansa and Pe-Piper, 1988).

There is evidence of volcanism within five wells on the Scotian Shelf. These wells are the Argo F-38, Hercules G-15 and Jason C-20 wells within the Orpheus Graben, and the Hesper I-52 and Hesper P-52 wells on the SE Scotian Shelf. On the SW Grand Banks, volcanic and intrusive rocks have been found within the Emerillon C-56, Mallard M-45, Brant P-87, Narwhal F-99 and Twillick G-49 wells (Figure 1.3). According to Pe-Piper et al. (1990), occurrences of igneous rocks on the SW Grand Banks and within the

7

Figure 1.3: Map showing location of Cretaceous volcanic rocks in eastern Canada (Strong and Harris, 1974; Schlee et al., 1976; Keen et al., 1977; Hall et al., 1977; McHone,1978; Houghton et al., 1979; Jansa and Pe-Piper, 1985)

Orpheus Graben and SE Scotian Shelf are very important elements in discerning the tectonic history of the area, since igneous activity reflects tectonic processes and different types of igneous rocks are formed in different tectonic environments. Beyond the Scotian Shelf and SW Grand Banks, Cretaceous igneous occurrences are found in many other areas on the North American margin such as the New England seamounts, Baltimore Canyon, J-Anomaly ridge, Fogo seamounts, Newfoundland seamounts and inland in the White Mountains and Monteregian Hills (New England-Quebec Igneous Province) (Strong and Harris, 1974; Schlee et al., 1976; Keen et al., 1977; Hall et al., 1977; Houghton et al., 1979; McHone, 1980; Jansa and Pe-Piper, 1985) (Figure 1.3).

1.1.4 Thermal history

The thermal history of an area is a key component to hydrocarbon exploration as hydrocarbons are formed by the effect of heat on organic matter. Understanding the thermal maturation of sediments can assist in advancing oil and gas exploration. The thermal effects of volcanism in the Scotian Basin have been previously considered only in terms of the local effects of a single thick basalt flow (e.g. Lyngberg, 1984), but as our understanding of the regional extent of the volcanism improves it is clear that the effects of regional high heat flow must also be considered. The intrusion of volcanic material into the sedimentary system would introduce a heat flow beyond what would be expected from normal burial and compaction, but the magnitude of this effect needs to be determined to assess its role in the maturation of potential petroleum resources.

1.2 Previous work in the Scotian Basin

The Scotian Basin has been investigated by industry and many researchers following the first petroleum exploration near Sable Island by Mobil Oil Canada Ltd. in 1958 (Keen and Piper, 1990). Since then, more than 140 wells have been drilled and thousands of kilometers of seismic reflection have been shot within the Scotian Basin. Information from wells and seismic exploration has led to a greater understanding of the tectonic, depositional and hydrocarbon history of the Scotian Basin. The general stratigraphy of the area has been investigated in detail by McIver (1971), Jansa and Wade (1975), Given (1977), Grant and McAlpine (1990), Wade and MacLean (1990) and MacLean and Wade (1992, 1993). Weir-Murphy (2004) further refined the stratigraphy of Cretaceous rocks within wells in the Orpheus Graben and one well on the SE Scotian Shelf. The tectonic history of the Scotian Basin has been studied by many authors including Jansa and Wade (1975), Enachescu (1988), Welsink et al. (1989a, 1989b), Tankard and Welsink (1989), Louden (2002), Pe-Piper and Piper (2004) and Tucholke et al. (2007).

The thermal evolution of the Scotian Basin has been investigated in terms of regional lithospheric and crustal stretching models. Royden and Keen (1980), Keen and Beaumont (1990), Dehler and Keen (1993), Keen and Dehler (1993) and Williamson et al. (1995) have all investigated the effects of rifting and subsidence on the thermal evolution of the Scotian margin. Keen et al. (1993) studied decompression melting at rift margins to determine whether or not models can predict the occurrences of igneous rocks in the Scotian Basin. The authors found that rift-related volcanism can occur tens of millions of years after the end of rifting, but their model did not predict the observed

igneous occurrences in the study area. Williamson et al. (1995) generated a model of lithospheric stretching and associated melting to predict the volume and rare earth element composition of basaltic magmas generated during rifting. They concluded that that under certain conditions, the first magmas generated by decompression melting are alkaline magmas not exceeding 1 km in thickness. All of these studies have focused on volcanism related to Triassic-early Jurassic rifting and not heat flow related to Cretaceous igneous activity in the Scotian Basin.

The thermal history in the Scotian Basin has also been investigated from studies of the sedimentary rocks. Apatite fission track dating has been used by Grist et al. (1991) and Li et al. (1995), who discovered thermal overprints in samples from the central Scotian Basin, west of the study area of this thesis. Wierzbecki et al. (2006) investigated fluid inclusions from the Deep Panuke field in the Sable sub-basin and proposed that the dissolution and dolomitization of carbonates in that area was due to hydrothermal fluids derived from either igneous activity or overpressures rising through reactivated strike-slip faults. Karim et al. (2010) have investigated fluid inclusions in diagenetic carbonate cements and quartz overgrowths within the Mississauga and Logan Canyon formations in sandstones from the Venture field in the Sable sub-basin. The fluid inclusions have shown unexpectedly elevated temperatures at some point during the Cretaceous.

There have also been many investigations into Cretaceous igneous occurrences both onshore, in the New England-Quebec Igneous Province, and offshore of eastern Canada (Strong and Harris, 1974; Schlee et al., 1976; Keen et al., 1977; Hall et al., 1977, McHone et al., 1980; Houghton et al., 1979; Jansa and Pe-Piper, 1985; Eby, 1985, 1992). The main focus of these investigations has been radiometric dating and the geochemistry

of the igneous rocks, in an effort to determine their age, origin and potential relationships to each other. The igneous rocks in the Orpheus Graben have been studied by Jansa and Pe-Piper (1985) who determined that the basalts found within wells in the Orpheus Graben were within-plate oceanic alkali basalts ranging in age from 102-125± 5 Ma. They also suggested the volcanism could be an expression of the reactivation of the Cobequid-Chedabucto transform fault zone. Jansa and Pe-Piper (1986, 1988), Pe-Piper and Jansa (1987) and Pe-Piper et al. (1990, 1992, 1994) studied similar rock occurrences in the Baltimore Canyon, Newfoundland seamounts, Grand Banks and the New England seamounts. They determined all the studied rocks were emplaced between 95-135 Ma and all were alkali basalts with differing rare earth element enrichments and incompatible trace elements. They thus separated these volcanic rocks into the Grand Banks-Scotian Shelf igneous province and the Georges Bank-Baltimore Canyon igneous province. Jansa (1991) published a map in the East Coast Basin Atlas series depicting the extent of the igneous occurrences in the Orpheus Graben. Pe-Piper et al. (2007) investigated the petrology and tectonic setting of the Fogo Seamounts located south of the SW Grand Banks.

1.3 Objectives

Previous work has largely focused on regional lithospheric stretching models and the geochemistry of igneous rocks in the Scotian Basin. No systematic attempt has been made to trace the extent of the volcanic rocks using seismic profiles, evaluate their overall relation to the tectonic history of the area, or model their thermal effects on the sediment system. The main purpose of this research is to determine the impact of

Cretaceous tectonism and volcanism on the petroleum system in the Orpheus Graben, SE Scotian Shelf and SW Grand Banks. This will be achieved through four sub-objectives:

1) Revise the seismo-stratigraphic correlation of Cretaceous rocks within the Orpheus Graben to the SE Scotian Shelf and the SW Grand Banks

2) Improve the understanding of the character and timing of the reactivation of the SW Grand Banks-Chedabucto-Cobequid fault system using improved seismic stratigraphy

3) Evaluate the extent and volcanological character of volcanic rocks in the Orpheus Graben, SE Scotian Shelf and the SW Grand Banks using well data and seismic interpretation

4) Model the thermal effects of known volcanism in the Orpheus Graben, SE Scotian Shelf and the SW Grand Banks and validate these models by comparison with organic maturation data from wells

CHAPTER 2
METHODS

2.1 Lithostratigraphic interpretations

Initial lithostratigraphic interpretations of the volcanic rocks in the study area were aided by previously interpreted lithostratigraphic boundaries by MacLean and Wade (1993) and the CNLOPB (2007). Biostratigraphic picks were based on many authors, as summarized in the BASIN database (http://basin.gdr.nrcan.gc.ca/index_e.php). Descriptions of ditch cuttings and sidewall cores, where available, were found in the Well History Reports for each well archived at the Bedford Institute of Oceanography. These descriptions were used as a rough guide in interpreting the lithology and stratigraphy of the volcanic rocks. All conversions of stages to numerical ages are based on the timescale of Gradstein et al. (2008).

2.1.1 Coarse fraction well cuttings

Coarse fraction drill cuttings (>2 mm) were available from the Jason C-20 and Argo F-38 wells. The cuttings were viewed with a binocular microscope to identify the presence of volcanic rocks within these wells in an attempt to determine depth ranges of the volcanic rocks and to confirm the work of Weir-Murphy (2004)

2.1.2 Thin sections of cuttings

Thin sections were available at the Geological Survey of Canada (Atlantic) for all wells containing volcanic rocks used in this study. The thin sections were prepared from washed but unsorted drill cuttings for the Argo F-38, Hercules G-15, Jason C-20 wells as

described in Jansa and Pe-Piper (1985). The limitation of the thin sections stems from the fact they were made from drill cuttings. Drill cuttings are taken from a range of depths, generally every 3-10 m and thus samples represent lithologies over a 3-10 m interval. Secondly, drill cutting size is generally only a few mm and thus nothing larger than lapilli can be recognized in a volcanic rock sequence. Thirdly, cavings from overlying intervals may contaminate a sample. Thin sections were viewed using a petrographic microscope to identify volcanic material.

2.1.3 Well logs

Where available, electrical well logs (gamma ray, sonic, resistivity, density, spontaneous potential and dip meter) were used to identify volcanic and pyroclastic rocks and to correlate intervals between wells. The well logs were digitized by HIS Accumap and are available in the BASIN database.

2.2 Seismic interpretation

Publicly released 2D seismic reflection data acquired by industry and the Geological Survey of Canada from the 1970's to the 2000's were interpreted using The KINGDOM Suite 8.5 32-bit seismic interpretation software (SMT, 2009). The Kingdom Suite project was built and extended from the Scotian Shelf and Orpheus Graben seismic project of Weir-Murphy (2004). The project used Zone 20N for a UTM projection coordinate system with WGS 1984 as a geodetic datum in conjunction with a WGS 1984 Ellipsoid. The quality of data used in the project varies widely as it is a compilation of seismic data from multiple sources and multiple processors over the past 35 years. Much

of the data in the Orpheus Graben and Scotian Shelf are publicly released microfiche

copies of seismic reflection data obtained from the CNSOPB which were scanned and

converted into digital data by Weir-Murphy (2004). The rest of the data used was digital

data made available by GSC (Atlantic). As seismic reflection data is displayed in two-

way time (TWT), data from velocity survey profiles completed after the drilling of a well

were entered into The KINGDOM Suite software to determine the depth in metres at the

well site. With depths determined at the well site, previously interpreted

lithostratigraphic and biostratigraphic picks could be correlated at each well. Seismic

data used in this study can be found in Table 4.1 with their locations shown in Figure 4.1

2.3 Basin modeling

Basin modeling is a tool used to mathematically simulate the geological history of

an area based on geological, geochemical, geophysical, paleontological and seismic data.

PetroMod 10 modeling software (Schlumberger, 2007) was used in this study to generate

a 1D model. Inputs required for the generation of a 1D model are: formation names,

formation depths, ages of deposition, and lithologies of formations. The major source of

error is the inferred depositional ages from biostratigraphy, which are not absolute ages,

and in many cases have errors or are incomplete for the well.

Model results can be compared with certain measured well data. Such data

includes, where available, vitrinite reflectance and downhole temperature data. The

quality of the vitrinite data is at times questionable due to the many different analysts and

dates of analysis for wells, as well as the possibility of reworked vitrinite. Log header

bottom hole temperatures were used after being corrected using a Horner correction

16

(Zetaware, 2003). Model results also depend on boundary conditions such as paleo-water depth, sediment water interface temperature, and heat flow. Paleo-water depths can be estimated from the depositional environment of each formation based on facies descriptions taken from core descriptions of each well and from some biostratigraphic data. Sensitivity of the outputs to water depth is very low for water depth changes of ~200 m. For the majority of wells used in this study water depth has not changed radically over time (>200 m) and thus no attempts were made to determine paleo-water depth over time. Since the water depth at time of drilling was known, it was used in the model.

There is some evidence, such as sedimentological and geochemical evidence, that sea floor temperatures were as much as 30°C higher during the Cretaceous than the present day seafloor temperature of ~4°C (Littler et al., 2009). For simplicity, changes in sediment water interface temperature over time were not calculated and an assumed present day ocean bottom temperature of 4°C was used. It is assumed that the effect of a higher seafloor temperature on vitrinite reflectance values is significantly smaller than the effect of heat flow. For this study, the most important parameter in the boundary conditions was the heat flow, which is discussed in depth in Chapter 5.

In a 1D model, the outputs are burial history plots with overlays of expected temperatures based on lithologies present and depth and length of time of burial. Model outputs correct for compaction over time. Another overlay is the heat flow based on manually inputted heat flows. Graphs can also be generated showing measured values of Horner corrected BHT's versus model computed expected temperatures, and measured vitrinite reflectance profiles vs model computed vitrinite reflectance. Model outputs use

a Sweeney and Burnham (1990) calculation of vitrinite reflectance and appropriate

thermal conductivity values based on the entered lithologies.

CHAPTER 3
STRATIGRAPHY AND FACIES OF VOLCANIC ROCKS

It is commonly difficult to distinguish lava flows from sills in seismic reflection profiles and from well cuttings. As a result, the term "volcanic" has been used loosely in some previous literature and has been applied to sub-volcanic rocks. Likewise the term pyroclastic has been used loosely and may include volcaniclastic intervals. In this study, the term "volcanic" is restricted to rocks interpreted as extrusive and "sub-volcanic" is used for fine-grained igneous rocks of hypabyssal origin. The term "pyroclastic" is restricted to intervals interpreted as exclusively or predominantly of pyroclastic rocks: ejecta derived directly from a volcanic vent. The term "volcaniclastic" implies sedimentary rocks in which detritus reworked from pyroclastic and volcanic rocks is the principal component.

Occurrences of volcanic and sub-volcanic rock have been found in wells in the Orpheus Graben (Argo F-38, Jason C-20 and Hercules G-15), SE Scotian Shelf (Hesper P-52 and Hesper I-52) and on the SW Grand Banks (Emerillon C-56, Mallard M-45, Brant P-87, Twillick G-49 and Narwhal F-99). The stratigraphic position of these volcanic and sub-volcanic rocks could give clues as to the style and timing of volcanic activity on the eastern margin of Canada. It may also be possible to correlate events between wells and determine whether volcanic activity occurred as one or multiple pulses.

All radiometric dating reported in the literature and discussed in this chapter was carried out by whole rock K/Ar analysis on mafic material, with the exception of the Mallard M-45 well in which analyses were also carried out on felsic rocks and the

Emerillon C-56 well in which K/Ar analysis was carried out on a biotite separate from a monzodiorite sample. Limitations of whole rock K/Ar dating are mainly a result of either ^{40}Ar loss due to alteration and high temperatures or excess ^{40}Ar retention. If there is a loss of ^{40}Ar, the calculated K/Ar age will be younger than the true age, while with ^{40}Ar retention, the calculated age will be older (New Mexico Tech, 2008). All K/Ar dates reported have been corrected based on Steiger and Jager (1977), and modified to recent calibrations by Renne et al. (1998) and Schoene and Bowring (2006).

Lithostratigraphic picks for the wells in the Orpheus Graben and SE Scotian Shelf (MacLean and Wade, 1993) and the SW Grand Banks (CNLOPB, 2007) were used as a basis for stratigraphic interpretation. Published biostratigraphic picks were also used to aid in interpreting the age of emplacement of the volcanic rocks in these areas. However, there are some inherent inconsistencies within the biostratigraphic data, as biostratigraphic studies on material from these areas was carried out over many years, by different authors using different methods, such as palynology or micropaleontology. Also, cavings from higher in the well are often integrated into studied samples and may influence the age interpretation. The biostratigraphic data used for this thesis are listed in Table 3.1.

The volcanic rock sequence within the Brant P-87 and Mallard M-45 wells is much thicker than any other occurrence in wells investigated by this study. The thicker volcanic sequences allowed for a more detailed interpretation of the volcanic stratigraphy within these wells. Thus, the stratigraphy of the wells on the SW Grand Banks will be discussed first, as interpretations of the volcanic stratigraphy of wells in the Orpheus

Well Name	Year	Author	Method
Argo F-38	1979	BUJAK, J.P.	PALYNOLOGY
Hercules G-15	1979	WILLIAMS, G.L.	PALYNOLOGY
Jason C-20	1975	UNION OIL COMPANY OF CANADA LTD	PALYNOLOGY
	1988	ASCOLI, P.	OSTRACODS
	1988	ASCOLI, P.	CALC BENTH FORAMS
Hesper I-52	2003	THOMAS, F.C.	MICROPALEO
Sachem D-76	2005	ASCOLI, P.	MICROPALEO
Dauntless D-35	1988	ASCOLI, P.	MICROPALEO
			CALC BENTH FORAMS
			PLANKTONIC FORAMS
Emerillon C-56	1993	FORD, J.H.	PALYNOLOGY
Hermine E-94	2006	WILLIAMS, G.L.	PALYNOLOGY
Puffin B-90	1988	ASCOLI, P.	PLANKTONIC FORAMS
			MICROPALEO
			CALC BENTH FORAMS
Brant P-87	1977	GRADSTEIN, F.M.	MICROPALEO
Mallard M-45	2008	ASCOLI, P.	MICROPALEO

Table 3.1: List of biostratigraphic data used in this study

Graben and SE Scotian Shelf were at times made by analogy to the wells on the SW Grand Banks.

3.1 Grand Banks

3.1.1 Brant P-87

Brant P-87 was drilled by Amoco Imperial Skelly in November 1973 targeting a high on the mid-Cretaceous unconformity. Brant P-87 is located on the SW Grand Banks (44°16'59.9"N, 52°42'19.5"W). The well is 3587 m deep, penetrating sediments from the Banquereau Formation (including the Eocene Chalk), Dawson Canyon Formation (Petrel Member), Logan Canyon Formation and the Mississauga Formation (CNLOPB, 2007).

The well encountered three volcanic units within the Mississauga Formation consisting of: an upper volcanic unit from 2790-2908 m (9150-9540 ft), a middle volcanic unit from 3100-3445 m (10,170-11,305 ft), and a lower volcanic unit from 3485-3587 m (11,435-11,760 ft). Biostratigraphy indicates the upper unit occurs within the Barremian, while the middle unit occurs within the undivided Neocomian and the lower unit was deemed barren. Whole rock K/Ar dating of basalt from the lower volcanic unit at 3535 m indicates an age of 136.3±6 Ma, placing it within the Hauterivian.

Pe-Piper and Jansa (1987) previously interpreted the volcanic rocks as two units, a lower unit of diabase sills or flows and an upper unit of basalt and pyroclastic rocks. Jansa and Pe-Piper (1988) stated that the systematic changes in crystal sizes through the individual bodies and the presence of vesicles in the lower basaltic unit followed by the presence of overlying pyroclastics and the occurrence of certain nannofossils suggest that

the lower basaltic rocks are mainly flows extruded in a submarine environment. They also state that the upper volcanic unit is compositionally similar to the lower igneous units found within Hercules G-15, Jason C-20 and Argo F-38 wells in the Orpheus Graben.

The lower volcanic unit (unit A) is readily identified on well logs based on its distinct blocky appearance of the gamma and sonic velocity logs, as well as a sharp decrease in gamma, increase in density and sharp increase in sonic velocity and resistivity in comparison with overlying material. The lower volcanic unit shows near uniform gamma, sonic velocity and resistivity log responses of ~40 API, 200 μs/m and ~20 mmho/m. The middle volcanic unit (unit B) is readily identified on well logs based on fairly uniform gamma, sonic velocity and resistivity log responses of ~90 API, 300 μs/m and 2800 kg/m^3 throughout the unit, compared to intervals above and below. The upper volcanic unit (unit C) is identified on well logs based on a sharp increase in the gamma ray log at the top of the unit which then decreases through the unit. From the well logs, the lower volcanic unit is approximately 102 m (335 ft) thick; however, the well did not fully penetrate this interval. The middle volcanic unit is approximately 345.5 m (1, 133 ft) thick. The thickness of the upper volcanic unit is more difficult to determine as there appears to be gradation into this unit from a conglomerate below; however, based on the well logs an approximate thickness is 120 m (390 ft) (Figure 3.1).

Thin sections made from washed but unsorted well cuttings (Jansa and Pe-Piper, 1988), in conjunction with cutting and sidewall core descriptions from the Well History Report, were reviewed for the three volcanic units. The cuttings and sidewall core descriptions indicate the lower volcanic unit was interpreted by the logging geologists as
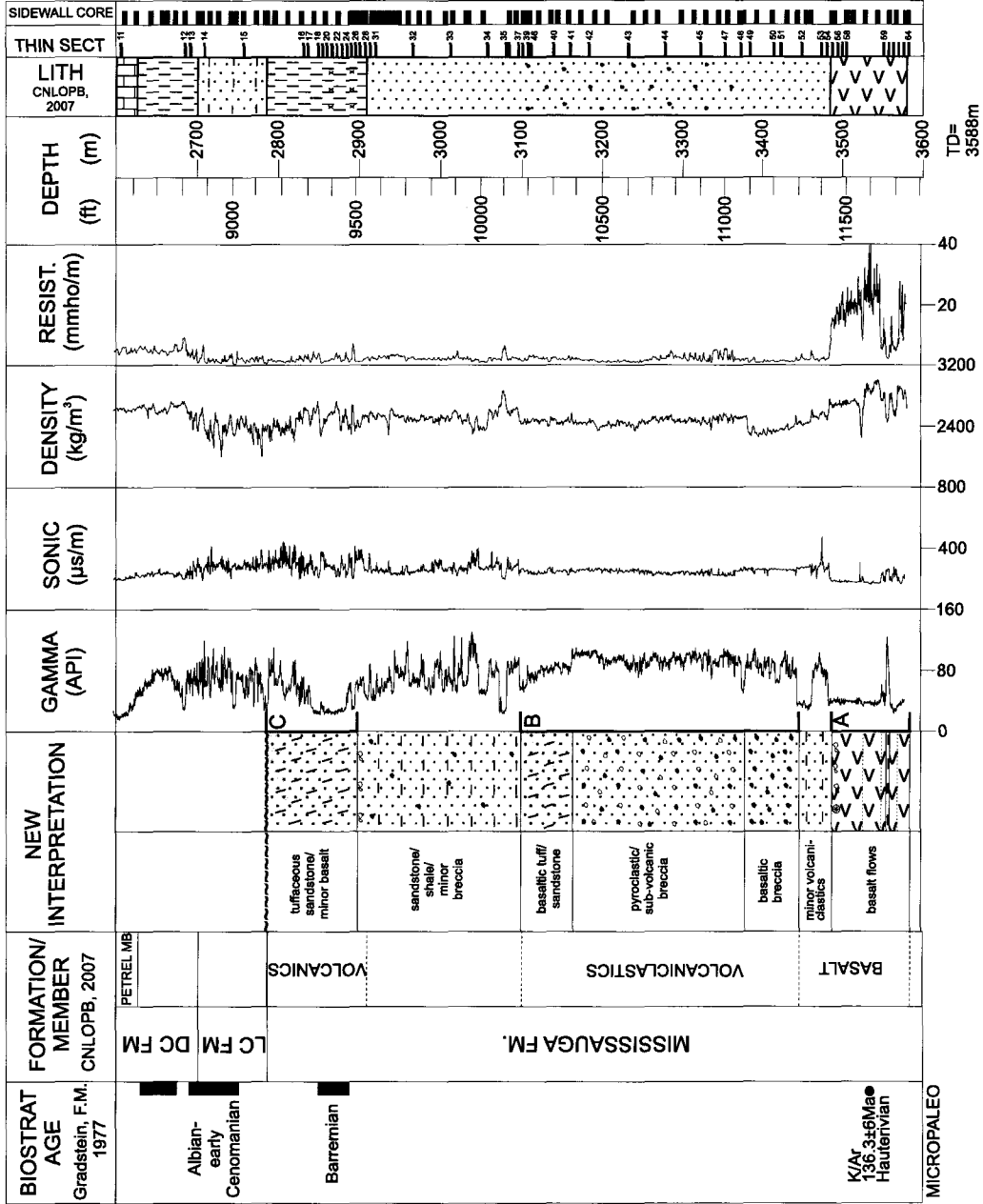
Figure 3.1: Summary of well data from Brant P-87. A indicates the basalt unit, B indicates the middle unit, and C indicates the upper unit. LC= Logan Canyon Formation, DC= Dawson Canyon Formation

24

very finely crystalline diabase. Diabase is a hypabyssal intrusive igneous rock, and thus it is possible that the lower volcanic unit is a shallow sill or dyke. As the well did not penetrate fully through the unit, it is unclear if sediments below show the effects of an intruding sill or dyke. However, many thick basalt flows have interiors that are texturally similar to fine grained diabase. Based on the character of the well logs (peaks in sonic velocity and density logs), the lower volcanic unit can be divided into five or more subunits of diabase or basalt of which the thickest is approximately 41 m thick. Thin sections of cuttings within the sub-units consist of mainly diabase or basalt while between sub-units, where thin sections were available; there is a greater abundance of quartz, feldspar and minor limestone. This indicates the possibility of some sedimentation between the sub-units. Within the sub-units, where thin sections were available, the diabase or basalt is finer grained at the top and bottom of the sub-units. The uppermost sub-unit of the lower unit contains vesicular basalt, glass and minor hyaloclastites at its top. The presence of possible sedimentation between sub-units, finer grained edges of sub-units, the presence of vesicles and glass at the top of the sequence, and the lack of alteration in sediments directly overlying the lower volcanic unit indicates the probability that the lower volcanic unit consists of multiple basalt flows. Hyaloclastites are observed at the surface of lavas which have been in contact with water, whether from submarine eruption or from a subaerial flow interacting with water at a paleoshore (Silvestri, 1961). Jansa and Pe-Piper (1988) have already suggested that the occurrence of marine nannofossils in interbedded sands and shales pointed to an eruption of volcanic material into a subaqueous environment. The presence of hyaloclastites and minor limestone within this lower volcanic unit agrees with their interpretation.

Overlying the lower volcanic unit is a 40 m unit in which the cuttings consist of sandy shale with minor vesicular basalt. It is unclear whether the basalt fragments are cavings or are in-situ.

The middle volcanic unit appears to comprise three sub-units based on interpretations of sidewall cores, cuttings descriptions and a review of thin sections of cuttings. According to the sidewall core and cuttings descriptions in the Well History Report, the entire middle volcanic unit consists of varying degrees of predominantly felsic breccia with mafic rock fragments. The term breccia has been broadly used to describe volcanic, pyroclastic and volcaniclastic rocks >2 mm composed of predominantly angular fragments within a finer grained or glassy matrix (Fisher and Schmincke, 1984; Cornen et al., 1996). Thin sections of cuttings from the basal sub-unit of the middle volcanic unit show a predominance of highly angular fragments of basalt with minor amounts of highly angular fragments of quartz, feldspar and plagioclase. However, cuttings used to make the thin sections are typically <2 mm and thus the basal sub-unit is interpreted as a basaltic breccia from sidewall cores in the Well History Report. Overlying the basaltic breccia, within the middle sub-unit, thin sections contain a greater abundance of angular felsic fragments, including quartz with a granophyric texture. The minor basaltic material in this sub-unit is slightly reddish in color. Near the top of this middle sub-unit, the minor basaltic material is glassy. Based on the angularity of the fragments, the predominance of felsic material and granophyric quartz, the reddening of basalt (which may indicate alteration or weathering), and the sidewall core and cuttings descriptions in the Well History Report, the middle sub-unit is interpreted as a pyroclastic or volcanic breccia. The lack of hyaloclastites in this sub-unit, along with

the presence of reddened basaltic material may indicate subaerial eruption. Thin sections from the upper sub-unit of the middle volcanic unit show slightly less angular fragments of finer grained reddened basalt and fragments of sandstone. This sub-unit is interpreted as a basaltic tuff within sandstone. Based on the presence of reddened basaltic material and absence of hyaloclastites, this sub-unit is interpreted as subaerial.

Overlying the middle volcanic unit and underlying the upper volcanic unit, thin sections contain cuttings of sandstone and shale, with minor cuttings of similar breccias and mafic rock fragments as in the middle unit. Thin sections from the upper volcanic unit contain spherulitic glass, minor basalt and minor hyaloclastites, as well as sandstone and limestone cuttings. Halfway through the upper volcanic unit, based on thin sections, cuttings become predominantly felsic, including what appear to be cuttings of trachyte. The mafic and felsic cuttings in the upper volcanic unit are much less angular and are finer grained than similar cuttings of the underlying middle volcanic unit. Based on the grain size, the upper volcanic unit is interpreted as a tuffaceous felsic pyroclastic unit with minor basaltic material. The presence of hyaloclastites and minor limestone indicate extrusion into water. This unit is truncated at the top by the mid-Cretaceous unconformity, at the base of the Logan Canyon Formation (MacLean and Wade, 1993).

3.1.2 Mallard M-45

Mallard M-45 was drilled by Amoco Imperial Skelly in February, 1973 targeting a stratigraphic pinchout of Lower Cretaceous-Upper Jurassic strata. Mallard M-45 is located on the SW Grand Banks (44°16'46.2"N, 52°07'22.4"W). The well was drilled to a depth of 3522 m penetrating sediments from the Banquereau Formation (including the

Eocene Chalk), Dawson Canyon Formation (Petrel Member), Logan Canyon Formation, Mississauga Formation and the Rankin Formation, which is equivalent to the Mic Mac Formation found in the main Scotian Basin (CNLOPB, 2007).

The well encountered three volcanic units within the Mississauga Formation consisting of: a lower volcanic unit from 2651-3150 m (8700-10, 334 ft), a middle volcanic unit from 2475-2630 m (8130-8630 ft), and an upper volcanic unit from 2268-2475 m (7440-8130 ft). According to the CNLOPB (2007), the volcanic rocks overlie the base Cretaceous unconformity. Biostratigraphy indicates the volcanic rocks lie within the interval between the Albian to the Jurassic. Whole rock K/Ar dating was carried out on both basalt and felsic rocks in this well. A basalt sample taken from the lower volcanic unit at 2950 m (9678 ft) yielded an age of 128.3±4 Ma, within the Barremian. Two felsic samples taken from the lower volcanic unit at 2840 m (9318 ft) and 2660 m (8727 ft) yielded ages of 135.3±3 Ma and 134.3±3 Ma, within the Hauterivian. A second basalt sample was taken at the base of the middle unit at 2600 m (8530 ft) yielding an age of 129.3±3 Ma, placing it within the Barremian.

Jansa and Pe-Piper (1988) indicated that volcanic rocks within the Mallard M-45 well represent a bimodal suite of mixed felsic and mafic igneous rocks (rhyolite, trachyte, basalt) and volcaniclastics. In 1994, Pe-Piper et al. proposed separating the volcanic interval into four units (A, B, C and D). Unit A of thin basalt flows and unit B of basalt lapilli tuff and thin basalt flows correspond to the lower volcanic unit of this study. Unit C was described as an 18 m thick basalt flow and lapilli tuffs as well as felsic hypabyssal rocks. The lower portion of unit C (basalt flows and hypabyssal rocks) is equivalent to the middle volcanic unit. Unit D is described as basaltic lapilli tuff and volcaniclastic

strata. This unit corresponds to the upper volcanic unit. Pe-Piper et al. (1994) also suggested that the felsic rocks in Mallard M-45 were alkali feldspar granites.

The volcanic units within the Mallard M-45 well do not exhibit well log responses as distinctive as the well log responses of the volcanic units in the Brant P-87 well. The lower volcanic unit (unit A) is identified on well logs based on a fairly uniform gamma ray log response, averaging ~45 API throughout the unit, compared to overlying and underlying strata. The resistivity, density and sonic velocity logs are quite variable in the lower volcanic unit. The middle volcanic unit is identified on well logs based on a more variable gamma ray response compared to intervals above and below. Again, the resistivity, density and sonic velocity logs are variable. The upper volcanic unit is identified on well logs based on a fairly uniform and generally low gamma ray response (~30 API) compared to intervals above and below. From the well logs, the lower volcanic unit is approximately 500 m (1650 ft) thick, the middle volcanic unit is approximately 155 m (500 ft) thick and the upper volcanic unit is approximately 207 m (680 ft) thick (Figure 3.2).

Thin sections made from washed but unsorted well cuttings (Pe-Piper et al., 1994), in conjunction with sidewall core descriptions from the Well History Report were reviewed for the three volcanic units. Individual sidewall cores in the lower volcanic unit described by H.W. Nelson (presumably a staff geologist with Amoco-Imperial-Skelly) show the following stratigraphic section from base to top: lapilli tuff, overlain by tuffaceous sandstone and tuffaceous shale, then volcanic breccia, a second interval of lapilli tuff, basaltic lapilli tuff and a second interval of tuffaceous sandstone. In the underlying Rankin Formation, sidewall cores are of shales and limestones. Thin sections
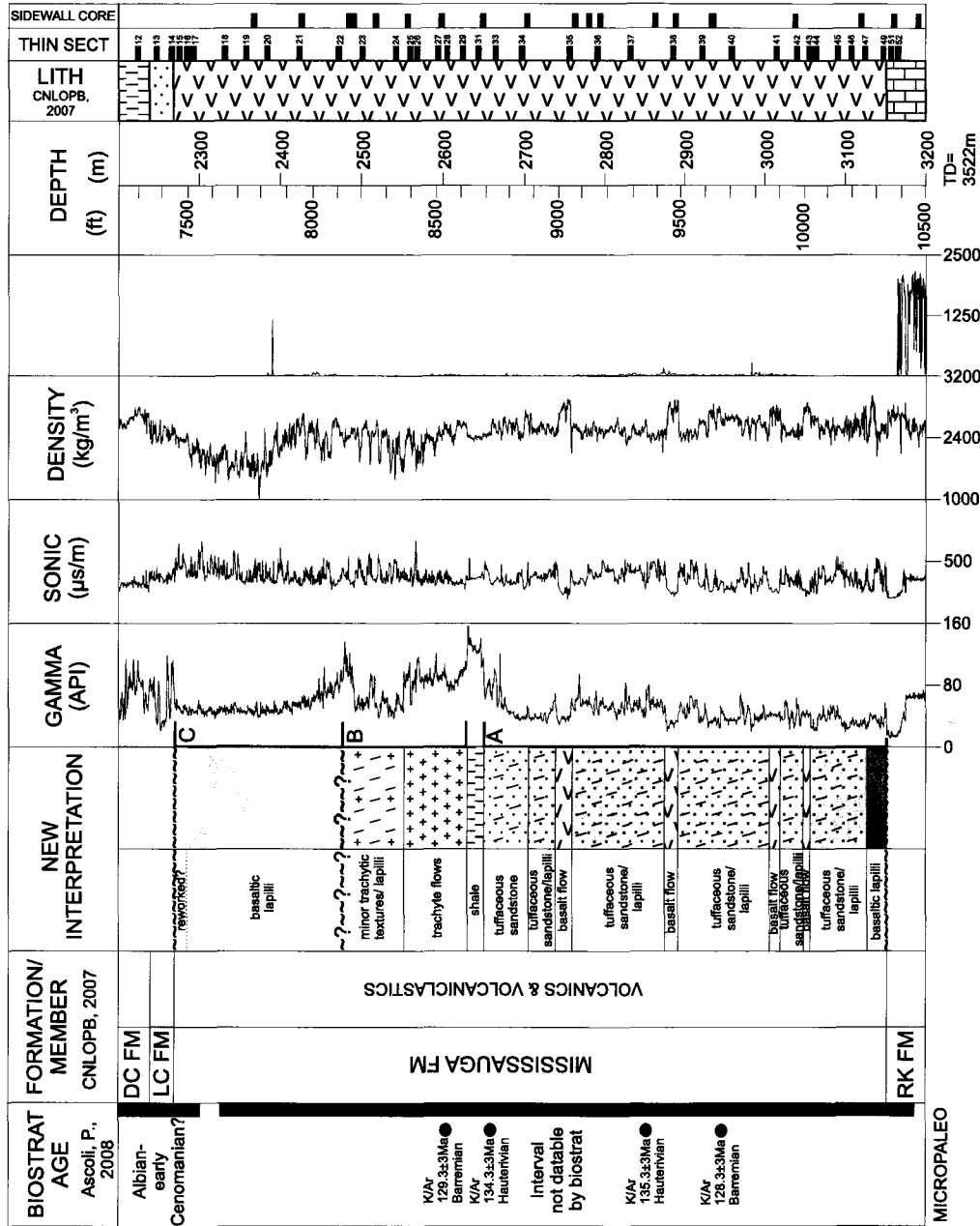
Figure 3.2: Summary of well data from Mallard M-45. A indicates the basalt unit, B indicates the middle unit, and C indicates the upper unit. RK= Rankin Formation, LC= Logan Canyon Formation, DC= Dawson Canyon Formation

of cuttings directly underlying the lower volcanic unit confirm the presence of predominantly limestone. Two thin sections from the basal 21 m of the lower volcanic unit contain fine grained basalt, spherulitic glass and homogeneous glass as well as grains of limestone. Based on the presence of spherulitic glass and basalt grains, this basal 21 m of the lower volcanic unit is interpreted as pyroclastic basaltic lapilli tuff. Overlying the basaltic lapilli tuff, thin sections of cuttings from 3110-3060 m contain fragments of fine grained basalt, minor glass and limestone. A thin section of cuttings at 3054 m consists almost exclusively of basalt fragments which are finer grained than the basalt fragments below. Thin sections of cuttings from 3038-2923 m contain fine grained basalt similar to that found in thin sections from 3110-3060 m, however, there is a greater proportion of felsic grains. A thin section of cuttings at 2886 m consists almost exclusively of finer grained basalt fragments similar to those found at 3054 m. Thin sections of cuttings from 2832-2795 m contain minor fine grained basalt but consist predominantly of felsic grains (trachyte or rhyolite). A thin section of cuttings at 2758 m consists almost exclusively of finer grained basalt fragments, similar to those at 3054 m and 2886 m. Thin sections of cuttings from 2700-2650 m contain predominantly felsic grains, some with granophyric textures. Based on the grain size and predominance of felsic material, the lower volcanic unit is interpreted as a pyroclastic unit of tuffaceous sandstone and lapilli tuff.

Paleoenvironmental data based on fossils and palynomorphs is available for the Mallard M-45 well (Ascoli, 2008) and indicate a marginal marine environment at the time of extrusion of the lower pyroclastic unit. In addition, the presence of limestone near the base of the unit, as well as glassy basaltic material, indicates possible extrusion into a submarine environment. A review of the well logs for the lower pyroclastic unit of

tuffaceous sandstone and lapilli tuff indicate three 15 m thick and one 18.5 m thick sections showing higher resistivity and sonic velocity compared to the rest of the unit. Thin sections of cuttings previously described in three of the four sections (at 3054 m, 2886 m and 2758 m) contain fine grained basalt. The increases in resistivity and sonic velocity are very similar in character to the well log response of the basaltic lower volcanic unit within the Brant P-87 well (Figure 3.1). Thus, by analogy with the Brant P-87 well, these four sections of increased resistivity and sonic velocity response are interpreted as basaltic. These basaltic intervals within the lower pyroclastic unit are presumed to be basalt flows similar to those found in the lower basaltic unit at the Brant P-87 well.

Overlying the lower volcanic unit is 18 m of shale. The middle volcanic unit was interpreted by H.M. Nelson from sidewall cores in the Well History Report as trachyte with overlying lapilli tuff. Thin sections of cuttings confirm the presence of abundant trachyte in the basal portion of the middle volcanic unit. Thin sections of cuttings from the upper portion of the middle volcanic unit, contains an upward-decreasing amount of trachyte and an increasing amount of fine-grained basalt. Thus, the middle volcanic unit is interpreted as a volcanic unit of trachyte flows at the base grading up into a pyroclastic trachytic lapilli tuff. The very top of the middle volcanic/pyroclastic unit was interpreted in sidewall core as reworked lapilli tuff containing plant material, which may indicate a subaerial erosion surface. Paleoenvironmental data (Ascoli, 2008) indicate a change from a marginal marine environment throughout the volcanic and pyroclastic units to a neritic environment above these units.

The upper volcanic unit directly overlies the middle volcanic/pyroclastic unit. Sidewall cores interpreted by H.M. Nelson and described in the Well History Report indicate the upper volcanic unit consists of basaltic lapilli tuff. The gamma ray log is very uniform throughout the unit, unlike units A and B. Thin sections of cuttings from the upper volcanic unit show an abundance of fine-grained basalt fragments and minor glassy material which appears to have a felty texture common to devitrified glass. Based on the sidewall core descriptions and the presence of fine grained basalt and glass in the thin sections, the upper volcanic unit has been interpreted as pyroclastic basaltic lapilli tuff. Thus, the thin sections of cuttings can be calibrated against the interpretation of the sidewall cores of basaltic lapilli tuff and may be used to interpret lapilli tuff elsewhere. According to the CNLOPB (2007), the upper pyroclastic unit is topped by the mid-Cretaceous unconformity at the base of the Logan Canyon Formation (Figure 3.2).

3.1.3 Twillick G-49

Twillick G-49 was drilled by Amoco-Imperial-Skelly in March, 1974 and is located on the SW Grand Banks (44°18'25.7"N, 51°21'28.1"W). The well was drilled to a depth of 1301 m (4270 ft) and penetrated sediments from the Banquereau Formation, Dawson Canyon Formation (including the Petrel Member), Logan Canyon Formation and the Mississauga Formation (CNLOPB, 2007). The well bottomed in a volcanic rock unit from 1287-1301.5 m (4220-4270 ft) within the Mississauga Formation. Biostratigraphy indicates the volcanic rock interval is found within sediments of indeterminate age. Sediments 48 m (157 ft) above the volcanic interval are Coniacian. Whole rock K/Ar dating of material from the bottom of the well within the volcanic unit yielded a date of

118.2±5 Ma which, if correct, places the unit within the Aptian. This date is unexpected as the Mississauga Formation is thought to be Tithonian-Barremian in age while the Logan Canyon Formation is considered to be Aptian and younger. However, as in the Mallard M-45 and Brant P-87 wells, MacLean and Wade (1993) interpreted a mid-Cretaceous unconformity separating the Mississauga Formation from the overlying Logan Canyon Formation. The volcanic units in the Brant P-87 and Mallard M-45 wells are capped by this unconformity and thus by analogy it is presumed this is the case with the Twillick G-49 well and a similar age for the volcanic unit in this well would be expected. The date yielded by K-Ar analysis may be due to alteration which could lead to ^{40}Ar loss and thus an age younger than the true age.

Jansa and Pe-Piper (1988) noted that the igneous unit is a 15 m thick porphyritic diabase which is overlain by an oxidized red clay containing highly altered diabase fragments interpreted as a weathering surface. They also determined the crystal size decreases towards the top of the unit and therefore is most likely a shallow sill or a thick subaerial flow.

The volcanic unit is identifiable on well logs based on its distinct blocky appearance and sharp increase in sonic velocity, density and resistivity in comparison with overlying rock. It is not possible to determine the true thickness of the volcanic unit as the well bottomed in the unit and most likely did not fully penetrate the interval. What is visible in the logs is 15 m of the volcanic unit. One cuttings description was available in the Well History Report from within the volcanic unit, which was interpreted by logging geologists as diorite. Also in the Well History Report is a thin section description of material of the junk sub recovery from the well bottom. An interpretation was made

by the geologist studying the thin section that the material was from an alkaline volcanic flow of andesitic composition. A review of the few thin sections made from samples taken from the conventional core (Jansa and Pe-Piper, 1988) available from this unit showed it to consist of fine grained diabase or basalt. It is unclear whether this unit is volcanic or sub-volcanic (Figure 3.3).

3.1.4 Emerillon C-56

Emerillon C-56 was drilled by Elf et al. in December 1973 targeting a salt pillow. Emerillon is located on the western edge of the Grand Banks (45°15'04.8"N, 54°23'16.9"W). The well was drilled to a depth of 3276 m penetrating sediments from the Banquereau Formation, Wyandot Formation, Dawson Canyon Formation (including Petrel Member), Eider Unit, Voyager Formation, Downing Formation and the Carboniferous Windsor Group Evaporites (CNLOPB, 2007).

The well encountered an igneous rock unit from 2964-3002 m (9724-9849 ft) within the Downing Formation. Biostratigraphy places the unit within lower Jurassic Pliensbachian sediments. K/Ar dating was carried out on a biotite from a monzodiorite sample taken near the base of the unit at 2990 m (9810 ft) which yielded a date of 97.4±3.8 Ma placing it within the mid-Cretaceous Cenomanian. Ditch cuttings and core descriptions in the Well History Report from within the igneous rock interval were interpreted by logging geologists as containing "salt and pepper" sandstone underlain by arkose (Figure 3.4).

Jansa and Pe-Piper (1988) determined the cuttings of "salt and pepper" sandstone and arkose were igneous in nature and were interpreted then as one or possibly more

Figure 3.3: Summary of well data from Twillick G-49. MISS= Mississauga Formation, LC= Logan Canyon Formation, PET= Petrel Member
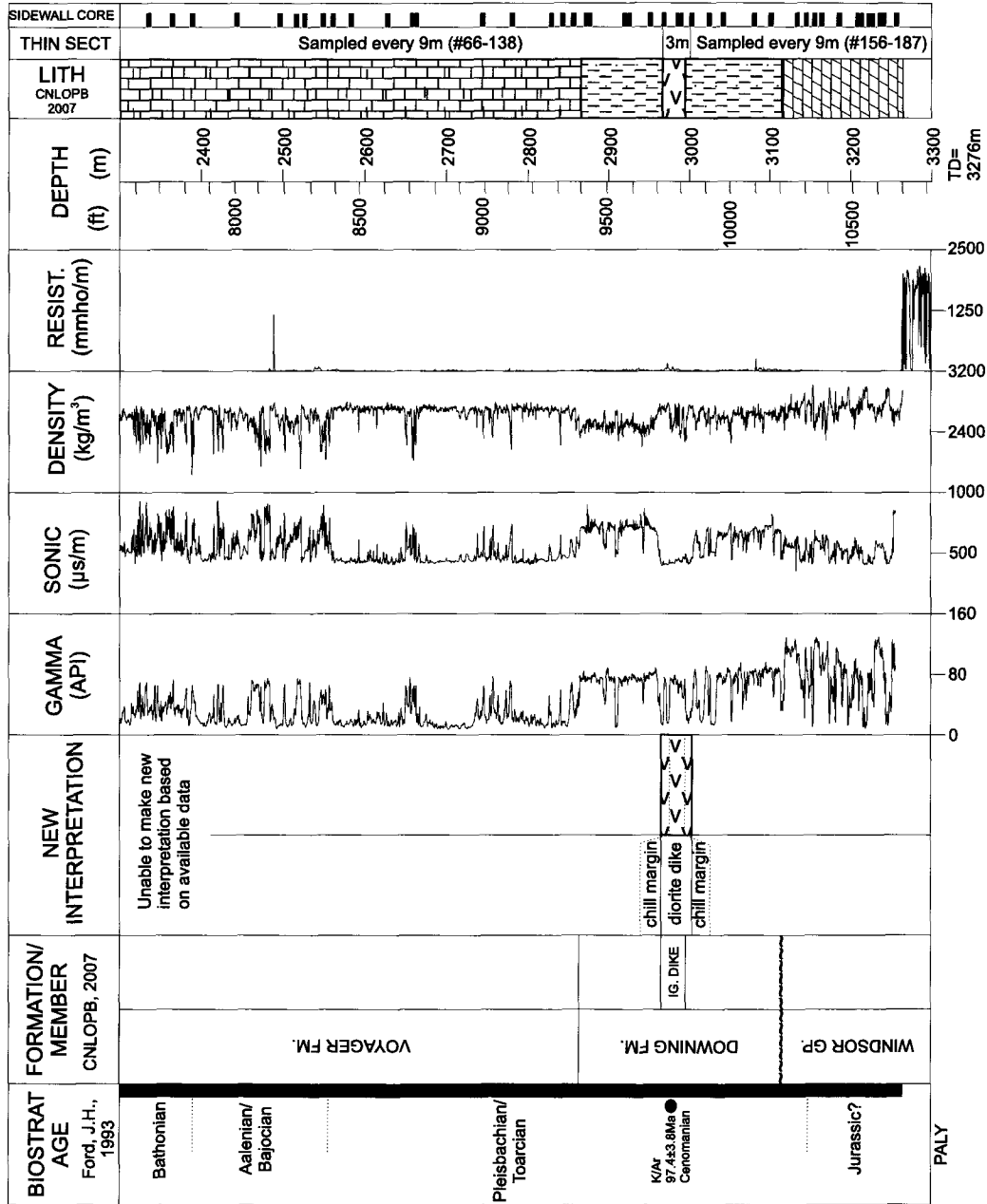
Figure 3.4: Summary of well data from Emerillon C-56

diorite dykes. The dyke was identified geochemically as trachyandesite. They also determined that the diorite is very fine grained and altered at the top. It coarsens and becomes less altered with depth, although at the base there is again more intense alteration. Volcaniclastic and pyroclastic material were absent from drilling chips. Based on the physical attributes of the unit, alterations of the top and bottom of the unit, and the absence of volcaniclastic or pyroclastics material, the unit was interpreted to be a sill or dyke.

The volcanic unit is readily identifiable on well logs based on its distinct blocky appearance and sharp increase in resistivity and sonic velocity in comparison with overlying and underlying material. From the well logs, the volcanic unit is approximately 38 m thick. Based on peaks in the resistivity and sonic velocity logs within the volcanic unit there may be 5 or more distinct volcanic subunits ranging in thickness from 3 to 9 m each.

There were no sidewall core descriptions available in the Well History Report, as it appears that no sidewall cores were taken, and the cuttings descriptions of "salt and pepper" sandstone and arkose were not useful in interpreting the volcanic unit. Thin sections made from washed but unsorted drill cuttings show variably altered medium grained diorite. The grain size and the K-Ar date of 97.4±3.8 Ma , which is much younger than the biostratigraphic age of the surrounding Pliensbachian sediments (189.6-189.3 Ma) both indicate that the diorite is sub-volcanic. However, it is unclear whether the sub-volcanic rock unit is a sill or a dyke.

Dipmeter data indicate a change from the regional ~10°S dip to 66°SE within the sub-volcanic unit. This change in dip would seem to indicate a sub-vertical dyke which

may be cross-cutting strata. However, it is unclear whether just the sub-volcanic unit is dipping, or if it is the entire sedimentary unit which is dipping at this level within this well. Also in question is the origin of multiple sub-units as interpreted from the well logs, which might represent multiple dykes or a layered sill. A review of seismic profiles in the next chapter may aid in resolving this matter.

3.1.5 Narwhal F-99

Narwhal F-99 was drilled by Northcor et al. in July, 1987 targeting a deep-seated structure. Narwhal is located in deep water just off the western edge of the SW Grand Banks (44°18'22.0"N, 53°44'35.1"W). The well was drilled to a depth of 4585 m penetrating the Banquereau Formation (including the Eocene Chalk), Dawson Canyon Formation (Petrel Member), Shortland Shale and the Verrill Canyon Formation (deepwater equivalent of Mississauga Formation) (CNLOPB, 2007). The well bottomed in a flat-topped volcanic basement high which has been interpreted by Pe-Piper et al. (2007) to be part of the Fogo Seamounts. Biostratigraphy indicates the sediments directly above the volcanic rocks are Tithonian-Berriasian (Figure 3.5).

3.1.6 SW Grand Banks well correlation

The volcanic units found on the SW Grand Banks are similar in age range but vary in character (Figure 3.6). The volcanic units in the Brant P-87, Mallard M-45 and Twillick G-49 wells all occur within the Mississauga Formation and have been dated radiometrically from Hauterivian to Barremian. The Aptian age at Twillick G-49 is inconsistent with the regional stratigraphy. The volcanic unit in the Narwhal F-99 well is

Figure 3.5: Summary of well data from Narwhal F-99
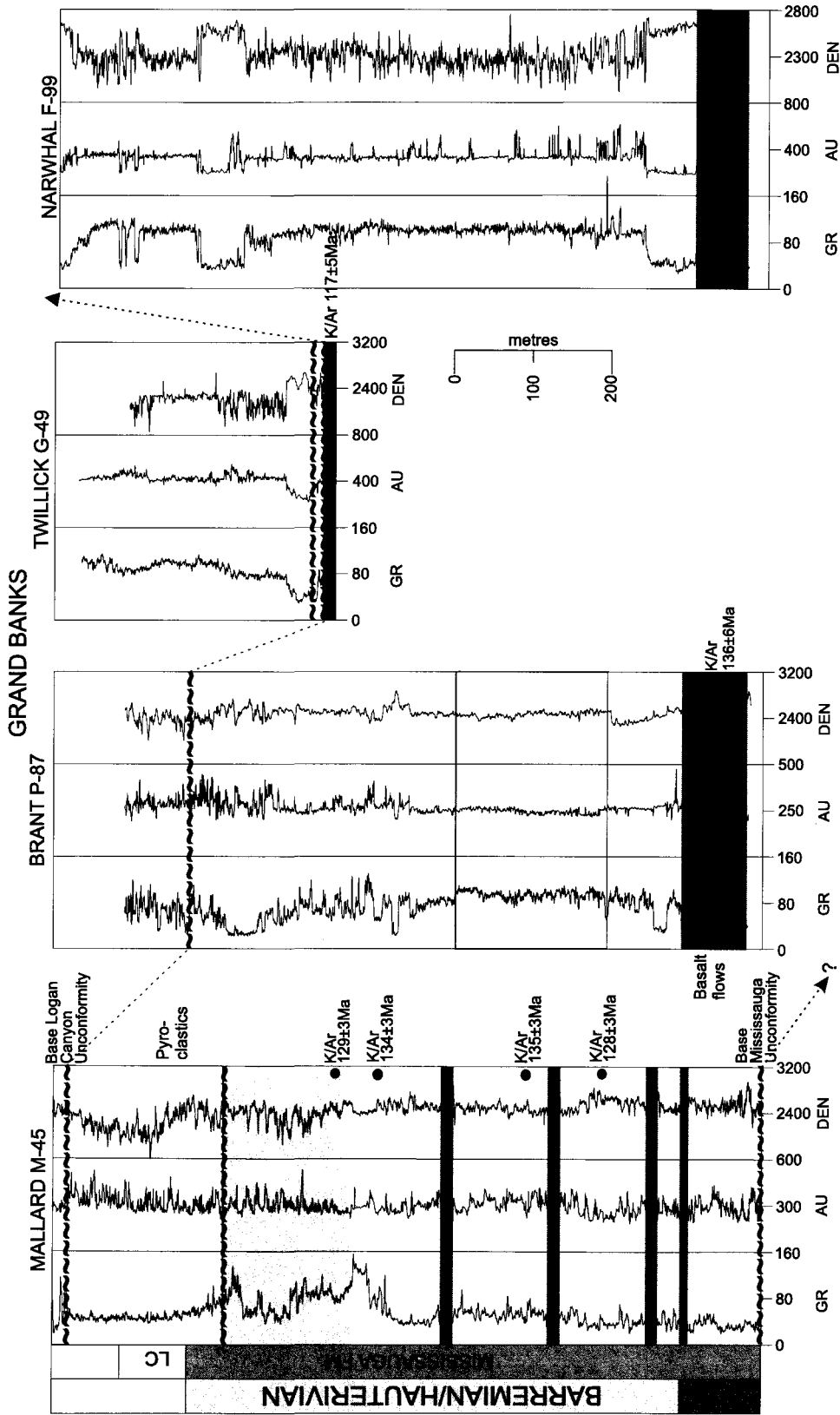
Figure 3.6: SW Grand Banks well correlation. Basalt flows are shown in red, while pyroclastic deposits are shown in yellow and trachyte flows in green. On the Grand Banks, there are multiple events of pyroclastic output with some events of basalt and trachyte output. The true thickness of the volcanics in Brant P-87, Twillick G-49 and Narwhal F-99 is unclear as the well bottomed in basalt.

41

biostratigraphically dated as Berriasian or older. The Narwhal F-99 and Twillick G-49

wells bottomed in basalt with no associated pyroclastics. The Brant P-87 and Mallard M-

45 wells consist of approximately 900 m of basalt flows and thick pyroclastic units

varying from predominantly breccia in Brant P-87 to basaltic lapilli tuff in Mallard M-45.

Trachyte occurs near the top of the volcanic and pyroclastic sequence in both these wells,

in unit B in the Mallard M-45 well (Figure 3.2) and unit C in the Brant P-87 well (Figure

3.1) Trachyte is generally considered to be a highly evolved end member of alkalic

magma and may indicate the waning of magma supply and final stages of volcanic

activity (Clague, 1987; Vazquez et al., 2007). The thicker basal basalt flows and more

brecciated pyroclastic material indicates Brant P-87 was most likely closer to a volcanic

centre than Mallard M-45, where pyroclastic material apparently is finer. The source of

the volcanic rocks will be discussed in a later chapter. As all but Mallard M-45 bottomed

in the volcanic unit it is unclear whether or not the volcanic rocks on the SW Grand

Banks were erupted on top of the Base Mississauga unconformity. All radiometric ages

for the volcanic units are Hauterivian or Barremian, suggesting that no Berriasian-

Valanginian volcanic rocks are present.

3.2 Orpheus Graben and SE Scotian Shelf

3.2.1 Argo F-38

Argo F-38 was drilled by Shell Canada in December 1970, targeting a rollover

anticline play. Argo F-38 is located within the Orpheus Graben (45°27'23.2"N,

58°50'24.4"W). The well is 3386 m deep and penetrates sediment from the Dawson

Canyon Formation (including Petrel Member), Logan Canyon Formation (Marmora Member, Sable Member, Cree Member and possibly Naskapi Member), Mississauga Formation (Upper and Middle Member), Mic Mac Formation, Mohican Formation, Iroquois Formation, Argo Formation, Eurydice Formation and the Meguma Group basement rocks (MacLean and Wade, 1993).

The well encountered two volcanic units within the Logan Canyon Formation from 979-998 m (3210-3280 ft) and 1024-1042 m (3360-3419 ft) (Figure 3.2). Further refinement of the stratigraphy by Weir-Murphy (2004) placed the volcanic units within the Cree Member. Biostratigraphy indicates the volcanic units are found under- and overlain by Aptian-Albian sediments.

Previous investigation by Jansa and Pe-Piper (1985) determined that the lower volcanic unit consists of a subaerial basalt flow overlying proximal debris reworked from another immediately underlying flow while the upper volcanic unit was interpreted to be a pyroclastic unit, due to the presence of altered glass and fragments of quartz trachytes in cuttings. Dipmeter data of the lower unit indicates a change in dip of up to 20° from the regional dip of 2° (Jansa and Pe-Piper, 1985).

The two volcanic units are readily identified in sonic, resistivity and density well logs based on their distinct blocky appearance and sharp increase in gamma, sonic velocity, density and resistivity in contrast to overlying and underlying rocks. From the well logs, the lower volcanic unit is approximately 18 m thick and can be separated into five sub-units based on coincident variation in the sonic velocity and density logs. The upper volcanic unit displays a similar increase in sonic velocity, resistivity and density

log response as the lower volcanic unit and is approximately 19 m thick. This unit can also be separated into five sub-units, on the same basis (Figure 3.7, 3.7a).

Ditch cutting descriptions from the Well History Report were interpreted by the logging geologists as "dark green, amphibolitic rock with minor magnetite" in the lower volcanic unit and "arkosic sandstone" in the upper volcanic unit. A single thin section from cuttings was available from the lower volcanic unit at 1033-1036 m (3390-3400 ft) which contained cuttings of basalt, sandstone and shale. Based on the presence of basalt in thin section and the well log response similar to basalts found in wells on the SW Grand Banks, the lower volcanic unit is interpreted as multiple basalt flows. The lack of limestone, glassy material and hyaloclastites seems to indicate a subaerial extrusion of the lower volcanic unit.

There was only one ditch cutting sample taken within the interval of 945-1033 m (3100-3390 ft) from which a thin section was made. The thin section contained predominantly basalt, with lesser sandstone and minor shale. This interval spans both the upper and lower volcanic unit and thus it is unclear whether the basalt found in this interval is sourced from the upper or lower volcanic unit. However, both units exhibit similar log responses indicating a similar lithology (Figure 3.7, 3.7a). Thus the thin sections did not aid in differentiating the two units

Although Jansa and Pe-Piper (1985) suggested that the upper volcanic unit was a pyroclastic unit, the well log character suggests the presence of five subunits similar to those of the lower unit and thus the upper volcanic unit has been interpreted as multiple basalt flows. The interpretation of the upper volcanic unit as pyroclastic by Jansa and Pe-Piper was based on the presence of trachyte and glass identified in thin section, although
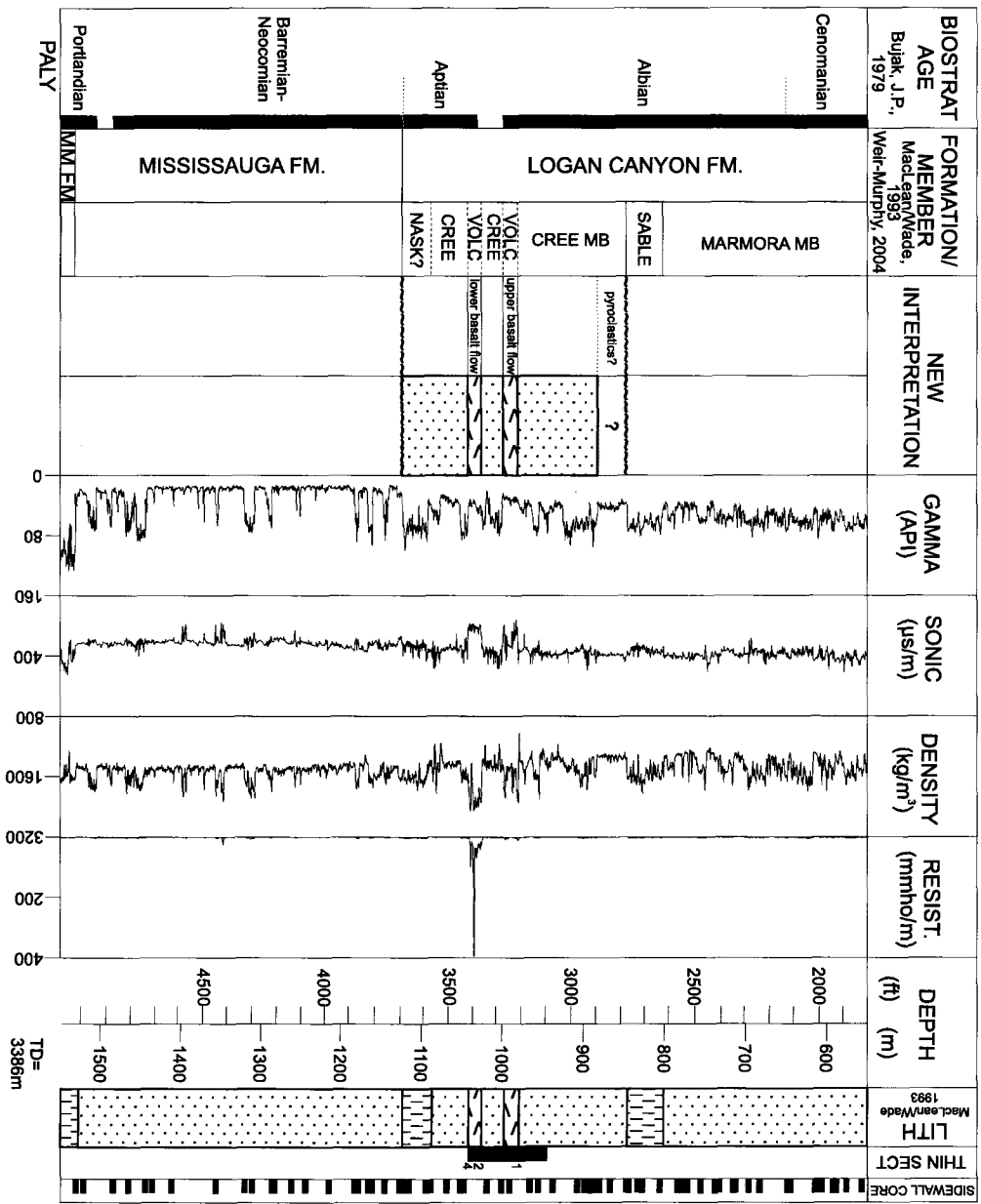
Figure 3.7: Summary of well data from Argo F-38. MM= Mic Mac Formation, NASK= Naskapi Member, VOLC= Volcanic
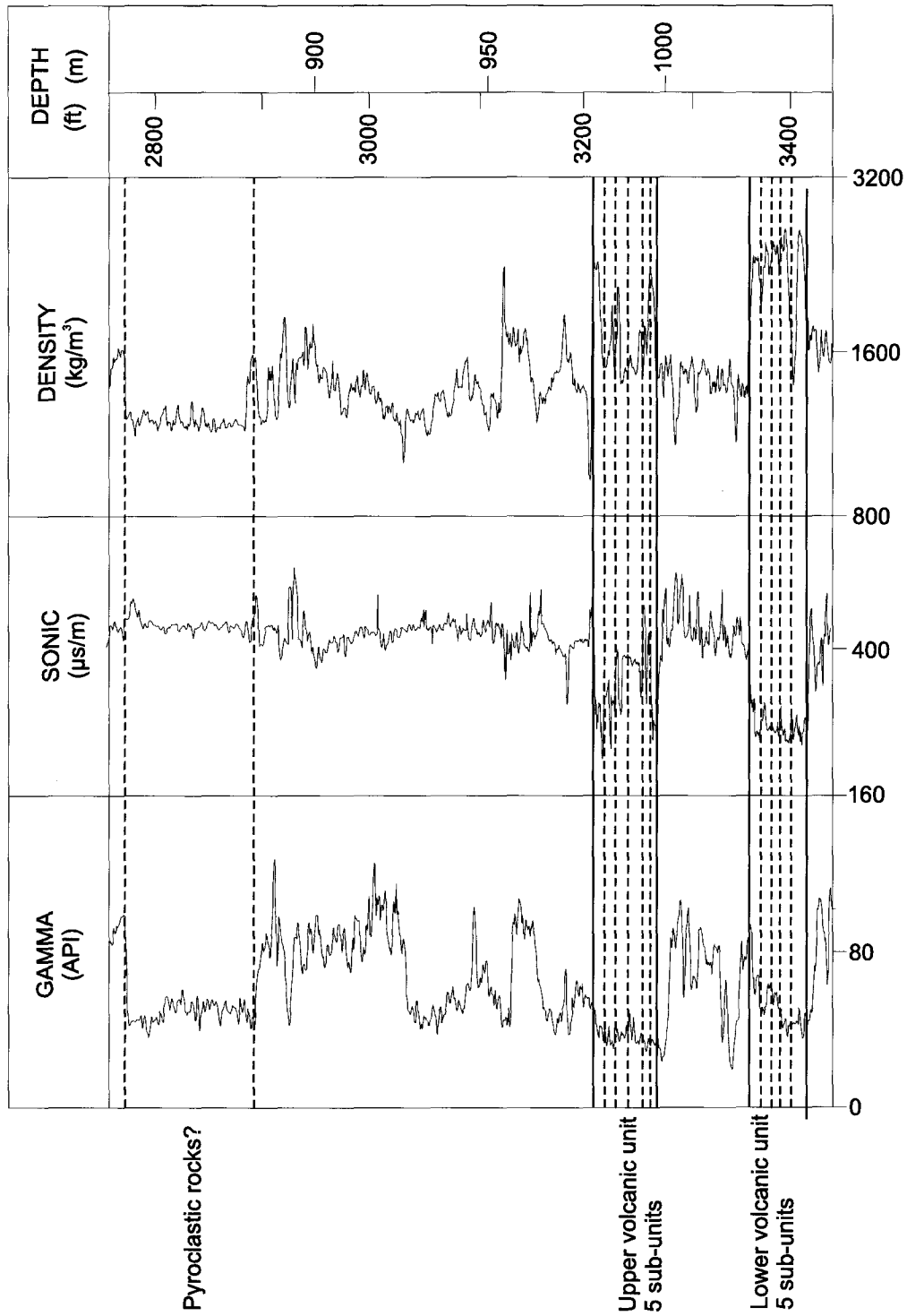
Figure 3.7a: Detailed well log interpretation for the Argo F-38 well

a review of the thin section from cuttings available from this interval did not contain trachyte. However, as discussed in section 3.1.6, trachyte may indicate the final stages of predominantly basaltic volcanic activity (Clague, 1987; Vazquez et al., 2007). Thus, the presence of trachyte would not be unexpected at the very top of the upper volcanic unit as volcanic activity ended.

There is a very uniform well log response in Argo F-38 over 40 m, above the two basaltic units, from 842.7-884 m (2765-2900 ft) within the Cree Member (and topped by the Top Cree unconformity), which is very similar to the well log responses of the pyroclastic units found within Jason C-20 and Hercules G-15 and at the same stratigraphic level. The ditch cuttings and sidewall core descriptions from the well report of Argo F-38 indicate the presence of poor samples in this interval which contain principally very fine grained quartzose sandstone.

Weir-Murphy (2004) claimed to have found two volcanic units within the Middle Mississauga member from 1344-1350 m and 1392-1398 m. This interpretation was based on density peaks and sonic velocity spikes in the wireline logs and basalt/diabase cuttings found below this interval. Weir-Murphy (2004) claimed the two units were flows based on the work of Lyngberg (1984), who stated spores found beneath an igneous interval were noticeably darkened while spores were not darkened above the interval. However, the two volcanic units of Weir-Murphy are found above and below the interval stated by Lyngberg (1984). The igneous interval of Lyngberg (1984) is suspect, as there is no basis for this interval stated in the study and the depth of the interval is curiously the exact same depth as that stated for an igneous unit in the Jason C-20 well, which has been confirmed by others (Jansa and Pe-Piper, 1985; MacLean and

47

Wade, 1993). It would appear that the depth stated for an igneous interval in the Mississauga Formation in the Argo F-38 by Lyngberg (1984) was a typographic error. Although there are spikes in the density and sonic velocity logs corresponding to the depths of the volcanic units of Weir-Murphy (2004) within the Mississauga Formation, my review of coarse fraction (>2 mm) well cuttings could not confirm the presence of volcanic rocks. Weir-Murphy (2004) claimed to have found 60 chips of basalt within the interval, thus, if there were volcanic rocks within cuttings, they were removed by for analysis. It is unclear whether the volcanic rocks were in-situ or downhole cavings but based on the scarcity of cuttings of volcanic rocks it is presumed they are downhole cavings from the overlying basalt flows of the lower unit of this thesis.

3.2.2 Jason C-20

Jason C-20 was drilled by Union et al. in July 1974, targeting a tilted fault block play. Jason C-20 is located within the Orpheus Graben (45°29'05.5"N, 58°32'28.3"W). The well is 2483 m deep and penetrates sediment from the Dawson Canyon Formation (including Petrel Member), Logan Canyon Formation (Marmora Member, Sable Member, and Cree Member), Mississauga Formation, Mic Mac Formation, Mohican Formation, an interval noted as caprock and the Argo Formation (MacLean and Wade, 1993).

The well encountered two volcanic units from 1245-1320 m (4085-4330 ft) and 1359-1375 m (4459-4511 ft) at the base of what was interpreted as the Naskapi Member of the Logan Canyon Formation by MacLean and Wade (1993). Lithostratigraphic correlation by Weir-Murphy (2004) indicates the absence of the Naskapi Member and the

presence of volcanic rocks within the Cree Member. Biostratigraphy indicates the upper volcanic unit is interbedded with sediments of Aptian age, while the lower volcanic unit is placed imprecisely within sediments of Aptian-probable Jurassic age. The Jurassic taxa are presumably reworked.

Jansa and Pe-Piper (1985) identified the lower volcanic unit as three basalts, with the thickest being a 9 m thick holocrystalline basalt with a highly altered top of chloritized glass which they interpreted to indicate shallow subsurface intrusion or extrusion of magma into wet unconsolidated sediments. The upper volcanic unit was interpreted as a volcaniclastic unit containing volcanic clasts and chloritized glass mixed with sediment and basaltic detritus. Dipmeter data shows no change in dip of the lower unit in comparison to underlying strata, while the upper unit indicates an increase from 6° at the base to 22° at the top. This may indicate a buildup of volcaniclastic material near the source, which is yet unknown.

The 16 m (52 ft) thick lower volcanic unit is readily identified in sonic and resistivity well logs based on its distinct blocky appearance and sharp increase in sonic velocity and resistivity in contrast to overlying and underlying rocks (Figure 3.8, 3.8a). From the well logs, the lower volcanic unit can be divided into two subunits. The lower subunit is approximately 8 m thick while the upper subunit is approximately 5 m thick. The two subunits are separated by approximately 3 m of rock with lower density and sonic velocity. The upper volcanic unit is also readily identified on well logs based on fairly uniform gamma ray, sonic velocity and resistivity log responses throughout the unit compared to intervals above and below. The upper volcanic unit is approximately 75 m (245 ft) thick. Within this unit are two positive spikes in the sonic velocity and resistivity
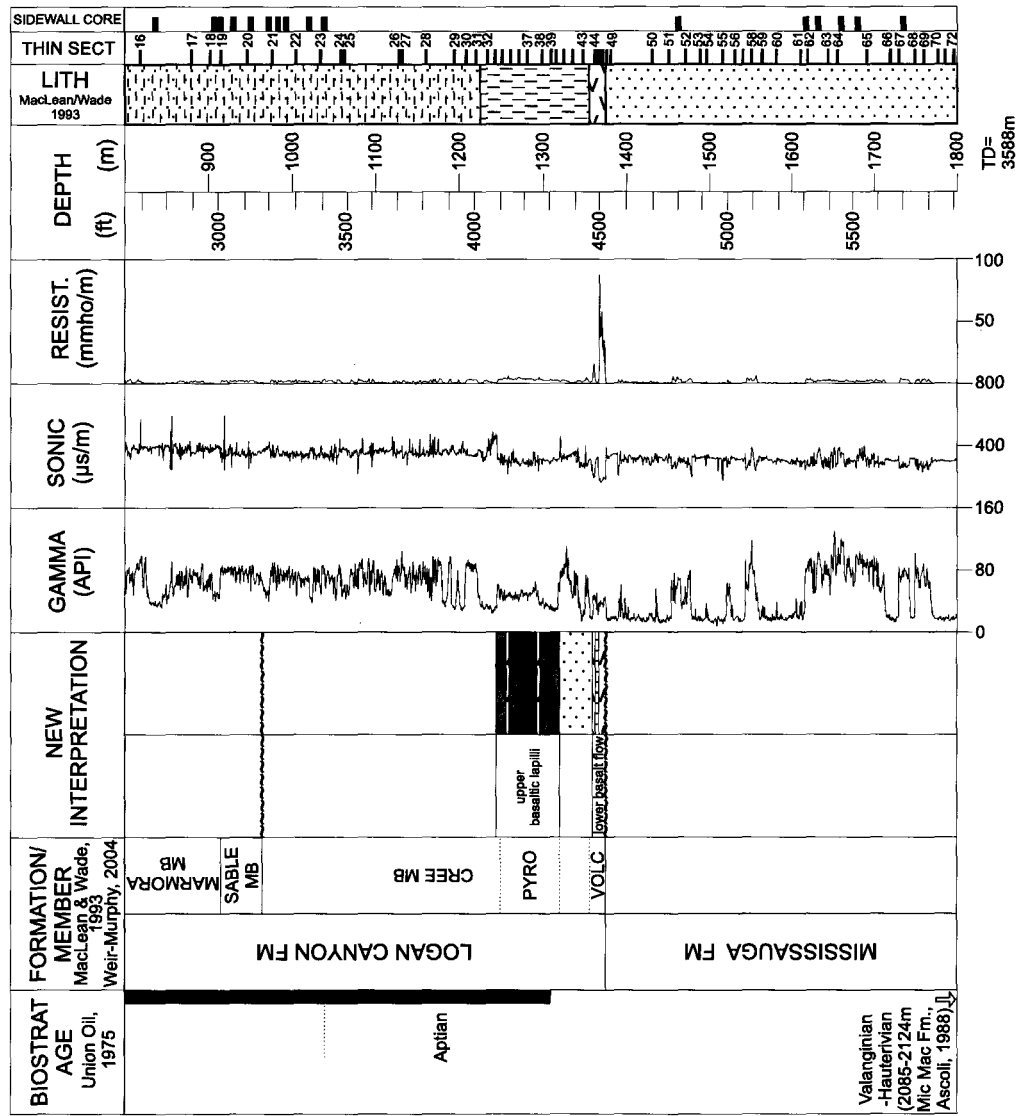
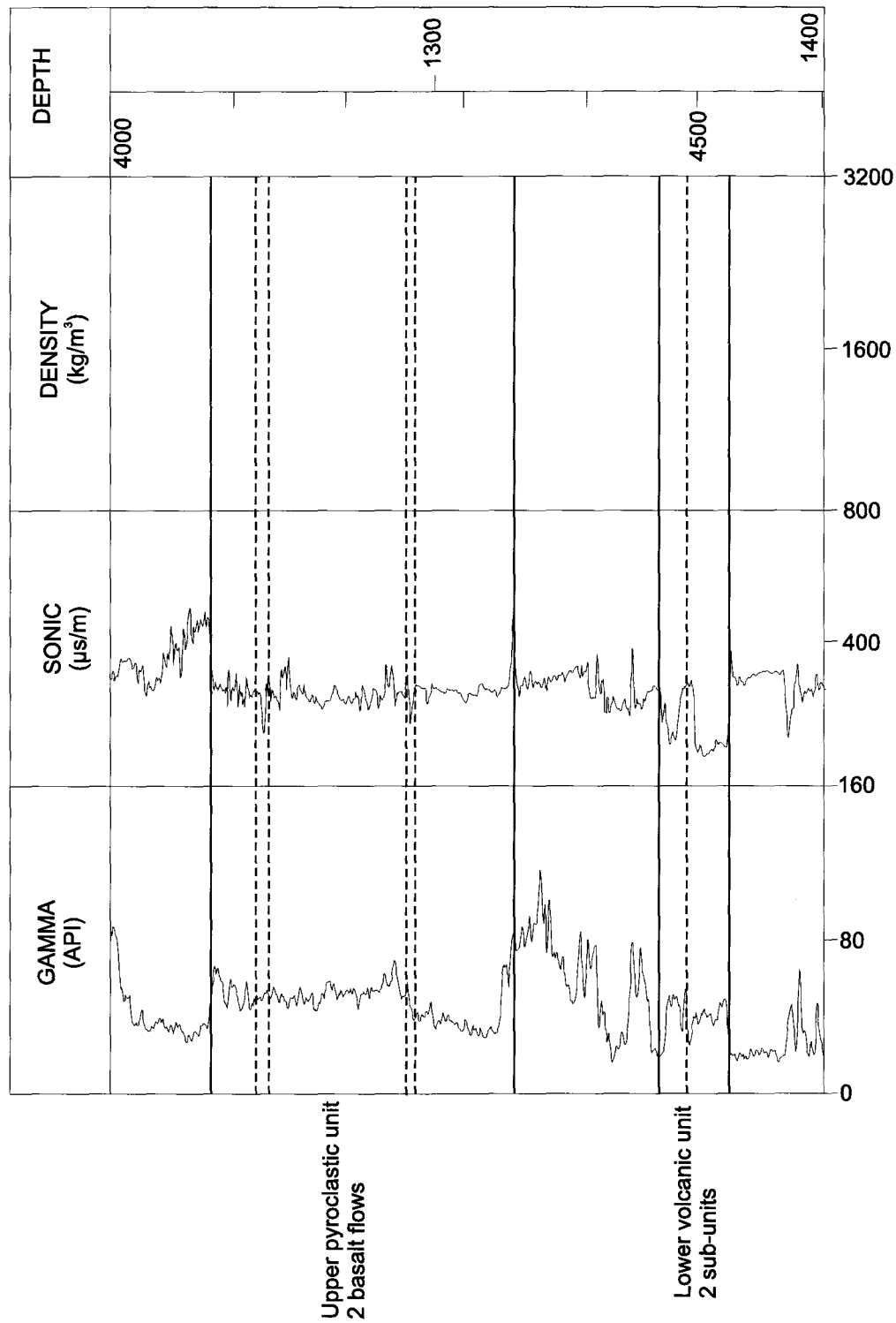Figure 3.8: Summary of well data from Jason C-20. VOLC= Volcanic, PYRO= Pyroclastic

50

Figure 3.8a: Detailed well log interpretation for the Jason C-20 well

51

logs at 1259 m (4130 ft) and 1295 m (4250 ft). The increase in the sonic velocity and resistivity are similar to the well log response of the lower volcanic unit and thus these two spikes within the upper volcanic unit may represent a similar lithology to the lower volcanic unit.

Ditch cutting descriptions in the Well History Report from the lower volcanic unit indicate the cuttings were interpreted by logging geologists as mottled light grey to black volcanic rock with some magnetite in a kaolinitic clay matrix representing 90% of the sample with the other 10% of the sample composed of sandstones. Study of thin sections made from coarse drill cuttings shows the lower sub-unit of the lower volcanic unit to be glassy basalt becoming coarser towards the middle and fining at the top with more glassy material. The overlying sub-unit in the lower volcanic unit had only one thin section which shows cuttings of very fine grained basalt in a glassy matrix. Based on the presence of basalt with glassy material at the top, the two subunits have been interpreted as basalt flows. The lack of limestone and hyaloclastites seems to indicate a subaerial extrusion of the lower volcanic unit.

The ditch cuttings from the upper volcanic unit, as interpreted by logging geologists in the Well History Report, consist of white bentonite throughout the unit. Based on thin sections, the upper volcanic unit shows a relatively homogeneous unit of fine grained vesicular basalt with some spherulites intermixed with fragments of quartz and other felsic material. The vesicular material has an almost frothy appearance. The thin sections confirm the interpretation of Jansa and Pe-Piper (1985) that the upper volcanic unit is a pyroclastic unit. The grain size, presence of basaltic material and analogous well log response to unit C (2268-2475 m) in the Mallard M-45 well lead to an

interpretation of the pyroclastic unit as basaltic lapilli tuff. At the level of the two spikes found in the well logs within the upper pyroclastic unit, no sidewall cores were taken, however, cuttings of crystalline basalt were found within the thin sections. These data suggest that there are two thin (less than 1 m thick) basalt flows within the upper pyroclastic unit (Figure 3.8).

3.2.3 Hercules G-15

Hercules G-15 was drilled by Union et al. in July 1974, targeting a stratigraphic pinchout play in the Lower Cretaceous and Upper Jurassic. Hercules G-15 is located within the Orpheus Graben (45°34'20.6"N, 58°47'13.1"W). The well was drilled to a depth of 1081 m, penetrating sediments from the Logan Canyon Formation (Marmora Member, Sable Member, and Cree Member), Mic Mac Formation, a limestone facies, Mohican Formation, Iroquois Formation and the Argo Formation. Noticeably absent is the Mississauga Formation (MacLean and Wade, 1993).

The well encountered two volcanic units from 751-774 m (2465-2540 ft) and 634-712 m (2080-2335 ft) within the Logan Canyon Formation at the base of the Cree Member. Published biostratigraphy indicates the upper volcanic unit occurs within Berriasian-Hauterivian sediments while the lower volcanic unit occurs within sediments dated as Berriasian. Whole rock K/Ar dating was carried out on two holocrystalline basalt samples from the base of the upper volcanic unit at 713 m (2340 ft). The analysis was carried out by two different laboratories which yielded dates of 120.2±5 Ma (Aptian) and 103.9±2.6 Ma (Albian). According to Jansa and Pe-Piper (1985), "discrepancies in the dates between these two laboratories are not systematic and result from differences in

^{40}Ar content, which may be due to different retention of argon in slightly altered volcanic material". As pointed out by Weir-Murphy (2004), there is a large discrepancy between the biostratigraphic age of Berriasian-Hauterivian and the stratigraphic age based on lithology, well logs, seismic study, and K/Ar dating which places the Logan Canyon Formation within the Aptian-Albian. However, based on seismic correlation (MacLean and Wade, 1993), the Mississauga Formation is absent in the Hercules G-15 well. The Berriasian-Hauterivian taxa may be reworked (Weir-Murphy, 2004).

Jansa and Pe-Piper (1985) interpreted that the lower volcanic unit consists of two homogeneous holocrystalline basalts 14 m and 9 m thick, separated by 2 m of shale. They interpreted the upper volcanic unit to be a pyroclastic unit consisting of sedimentary rocks which may have originated from a mudflow intermixed with highly altered vesicular and porphyritic basalt and quartz trachyte both in a glassy matrix.

The 23 m (75 ft) thick lower volcanic unit is readily identified in sonic and resistivity well logs based on its distinct blocky appearance and sharp increase in sonic velocity and resistivity in contrast to overlying and underlying material. From the well logs, the lower volcanic unit can be divided into two sub-units. The lower sub-unit is approximately 15 m thick while the overlying sub-unit is approximately 3.5 m thick. The two sub-units are separated by approximately 4.5 m of shale. The upper volcanic unit is also readily identified on well logs based on fairly uniform gamma ray, sonic velocity and resistivity log responses throughout the unit compared to intervals above and below. The upper volcanic unit is approximately 78 m (255 ft) thick and is overlain by the Top Cree Member unconformity (Weir-Murphy, 2004) (Figure 3.9, 3.9a).
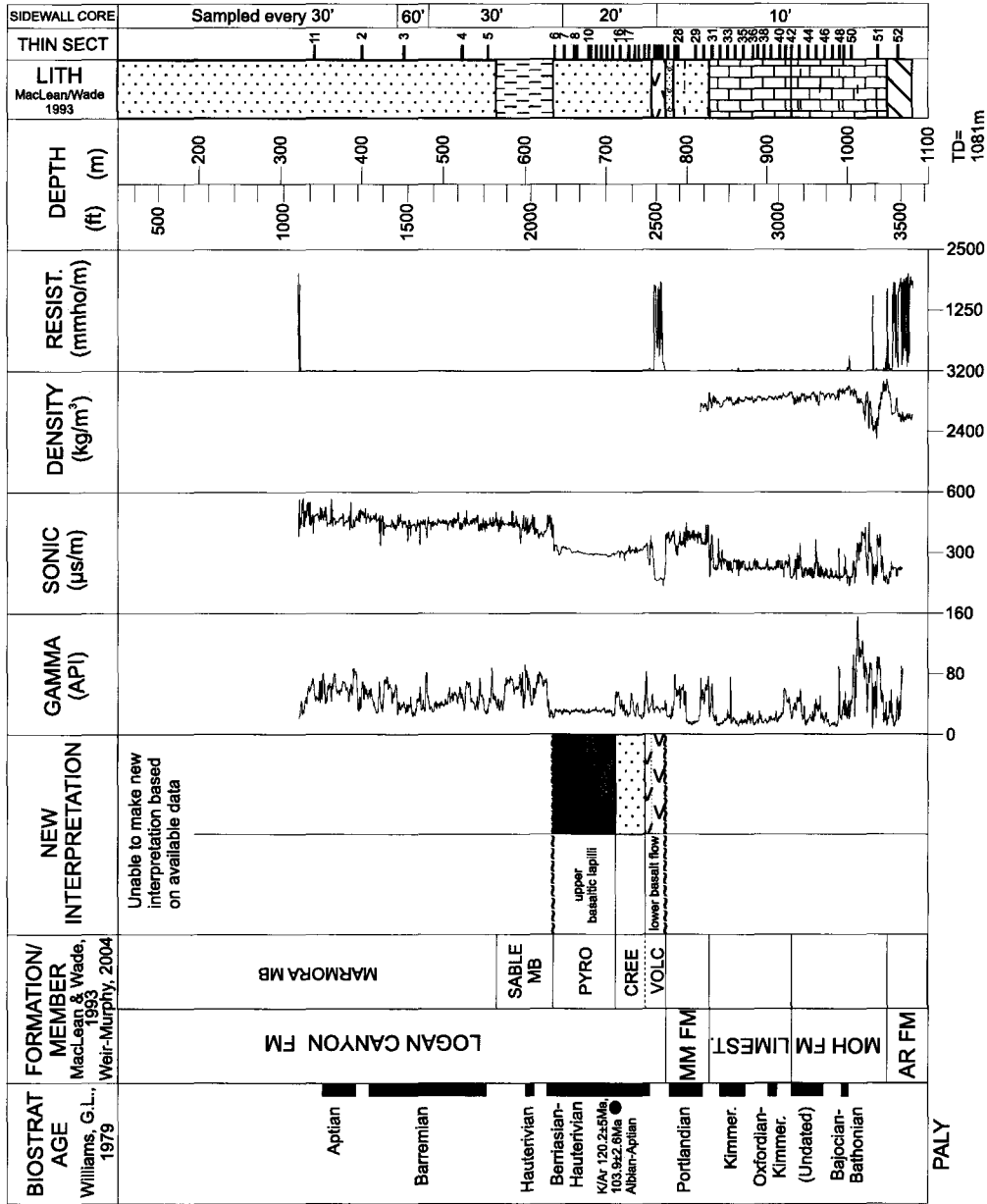
Figure 3.9: Summary of well data from Hercules G-15. AR= Argo Formation, MOH= Mohican Formation, LIMEST= Limestone, MM= Mic Mac Formation, VOLC= Volcanic, PYRO= Pyroclastic
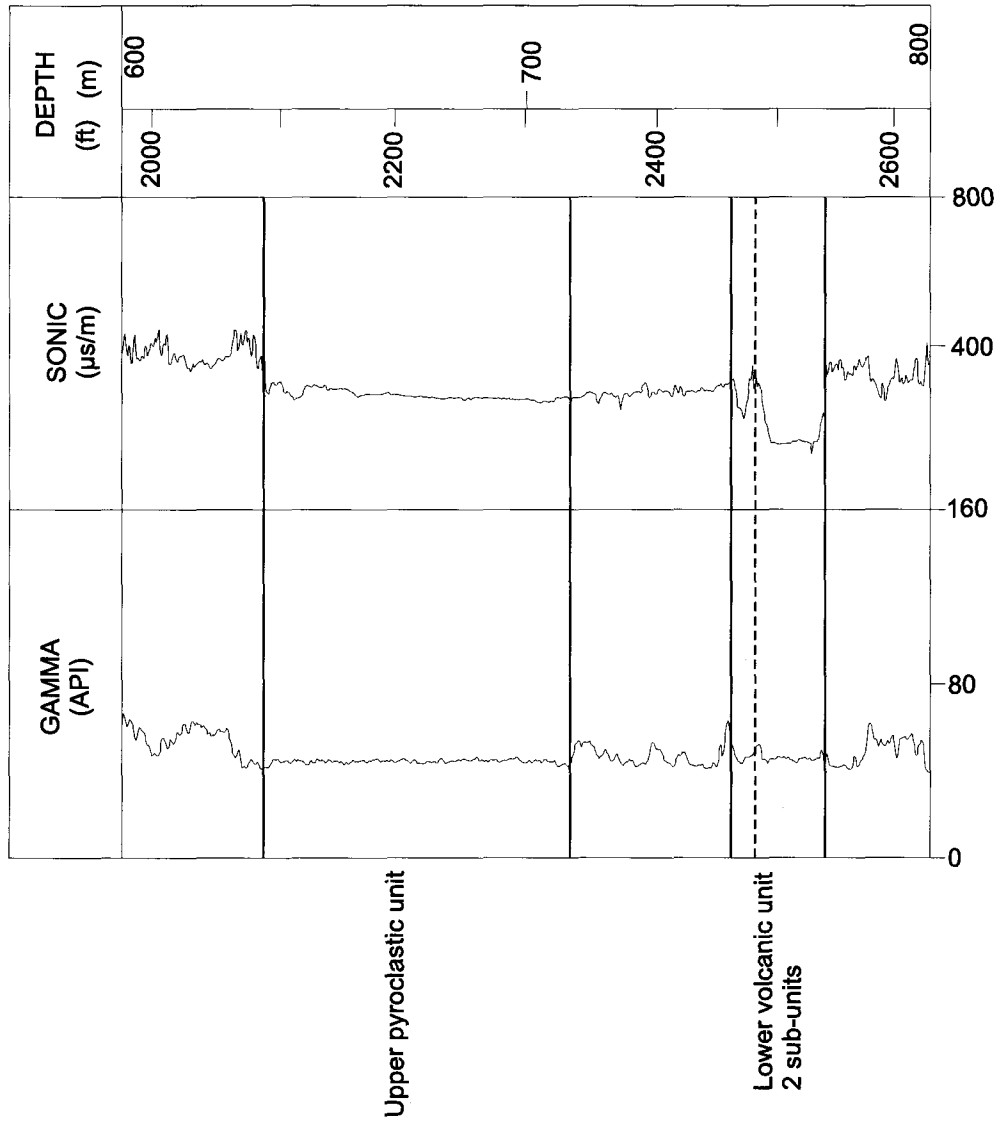
55

Figure 3.9a: Detailed well log interpretation for the Hercules G-15 well

Descriptions in the Well History Report of ditch cuttings interpreted by logging geologists from the lower volcanic unit indicate black, aphanitic volcanic material with magnetite and related dark minerals overlying conglomeratic sandstone. Study of the thin sections made from coarse drill cuttings shows both sub-units of the lower volcanic unit consist of vesicular basalt and spherulitic glassy basalt. The thin sections of cuttings for the tops of each sub-unit have a higher proportion of fine-grained basalt. The lower volcanic unit is interpreted to be two holocrystalline basalts which is in agreement with previous observations by Jansa and Pe-Piper (1985). Based on the presence of vesicular basalt and similarity to the well log response and thin sections of the lower volcanic unit in the Jason C-20 well, the sub-units are interpreted to be two distinct basalt flows (Figure 3.9). The lower volcanic unit and upper volcanic unit are separated by approximately 38 m (125 ft) of sandstone and minor shale based on cuttings and log response. Thin sections of cuttings for these intervals contain a few volcanic chips interpreted as cavings.

Ditch cutting descriptions in the Well History Report in the upper volcanic unit do not specifically indicate the presence of pyroclastic material as interpreted by Jansa and Pe-Piper (1985), stating only the presence of a bentonitic siltstone. Thin sections within the upper volcanic unit show a fairly consistent interval of fragmented quartz and fine grained basalt in a glassy matrix with an abundance of vesicles and some spherulites. Basalt cuttings become coarser grained and more vesicular near the top of the unit. The thin sections in this upper volcanic unit appear very similar to the thin sections from the upper pyroclastic unit of the Jason C-20 well. Based on observation within the thin sections of fine grained fragmented felsic and mafic material, abundant vesicular and

glassy material and similarity to the upper pyroclastic unit in the Jason C-20 well, the upper volcanic unit is interpreted as pyroclastic basaltic lapilli tuff. The principal new finding from this well is a redefining of the thicknesses of the basalt flows within the lower volcanic unit from 14 m and 9 m determined by Jansa and Pe-Piper (1985) to 15 m and 3.5 m.

3.2.4 Hesper I-52 and Hesper P-52

The Hesper I-52 and Hesper P-52 wells were drilled 450 m apart and thus intersect a very similar stratigraphic sequence. To avoid repetition, only the Hesper I-52 well will be discussed in this thesis. Hesper I-52 was drilled by Petro-Canada Mobil in May 1976 targeting an amplitude anomaly. Hesper I-52 lies on the eastern the Scotian Shelf (45°41'40.3"N, 57°52'32.2"W). The well was drilled to a depth of 2804 m encountering sediments from the Banquereau Formation, Wyandot Formation, Dawson Canyon Formation (including Petrel Member), Logan Canyon Formation (Marmora Member, Sable Member, Cree and Naskapi Member) and the Mississauga Formation (MacLean and Wade, 1993).

The well penetrated a volcanic unit near the base of the Naskapi Member of the Logan Canyon Formation from 2726-2745 m (8944-9005 ft). Biostratigraphy indicates the volcanic unit is found within sediments of indeterminate age, but sediments 168 m (550 ft) above the volcanic unit are Albian in age. Whole rock K/Ar dating was carried out on two holocrystalline basalt samples at 2743 m (9000 ft) at the base of the volcanic unit, yielding ages of 113±5 Ma and 127±3.2 Ma, which fall within the Aptian. As with

the Hercules G-15 well, the analyses were carried out by two different laboratories and the discrepancies between the ages were discussed above in section 3.2.3.

Jansa and Pe-Piper (1985) determined the volcanic unit consists of holocrystalline basalt that is coarser crystalline in the middle while the top and base are more finely crystalline and highly altered. They interpreted this unit to be a sill or dyke.

The 19 m (62 ft) thick volcanic unit is readily identified in sonic and resistivity well logs based on its distinct blocky appearance and sharp increase in sonic velocity and resistivity in contrast to overlying and underlying intervals. From the well logs, the volcanic unit appears not to be composite, unlike the wells in the Orpheus Graben within which multiple basalt flows were interpreted within the lower volcanic units. Based on the well logs, there is no other readily identifiable volcanic unit as seen in wells in the Orpheus Graben (Figure 3.10, 3.10a).

Ditch cutting and core descriptions in the Well History Report from within the volcanic unit were interpreted by logging geologists as an intrusive body consisting of "quartz crystalline rock and intermixed magnetic material with a minor weathered appearance". Thin sections made from coarse drill cuttings from the base of the volcanic unit consist of fine grained basalt and minor glass, coarser basalt in the middle and the finest grained basalt with chlorite alteration at the top. The presence of fine grained basalt and chlorite at the top of the unit may indicate interaction with water, although whether a submarine extrusion or extrusion onto wet sediments is unclear. Based on a review of well logs, ditch cuttings and sidewall core descriptions and a review of thin sections, no associated pyroclastic material was found within this well which may
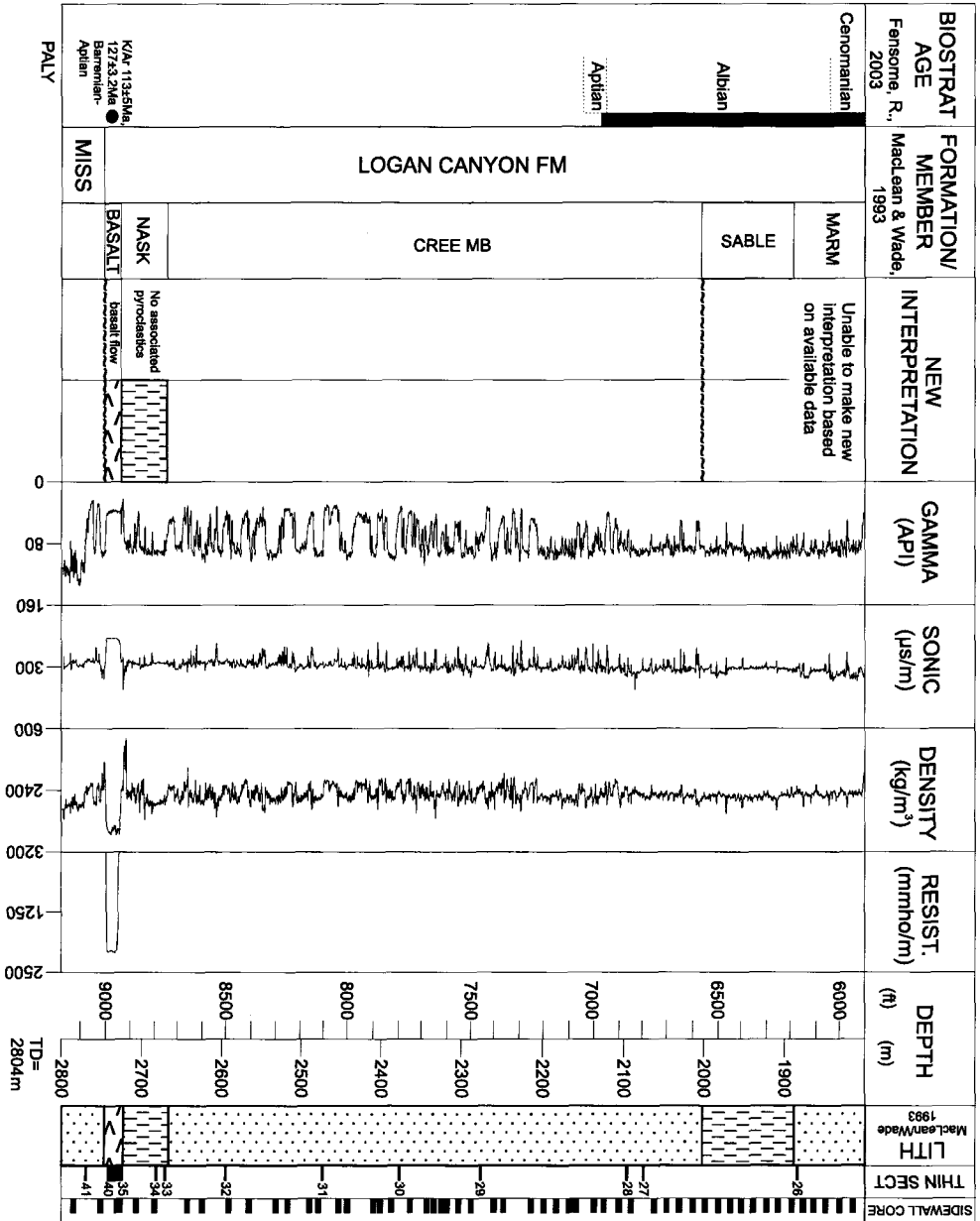
Figure 3.10: Summary of well data from Hesper I-52. MISS= Mississauga Formation, NASK= Naskapi Member, MARM= Marmora Member
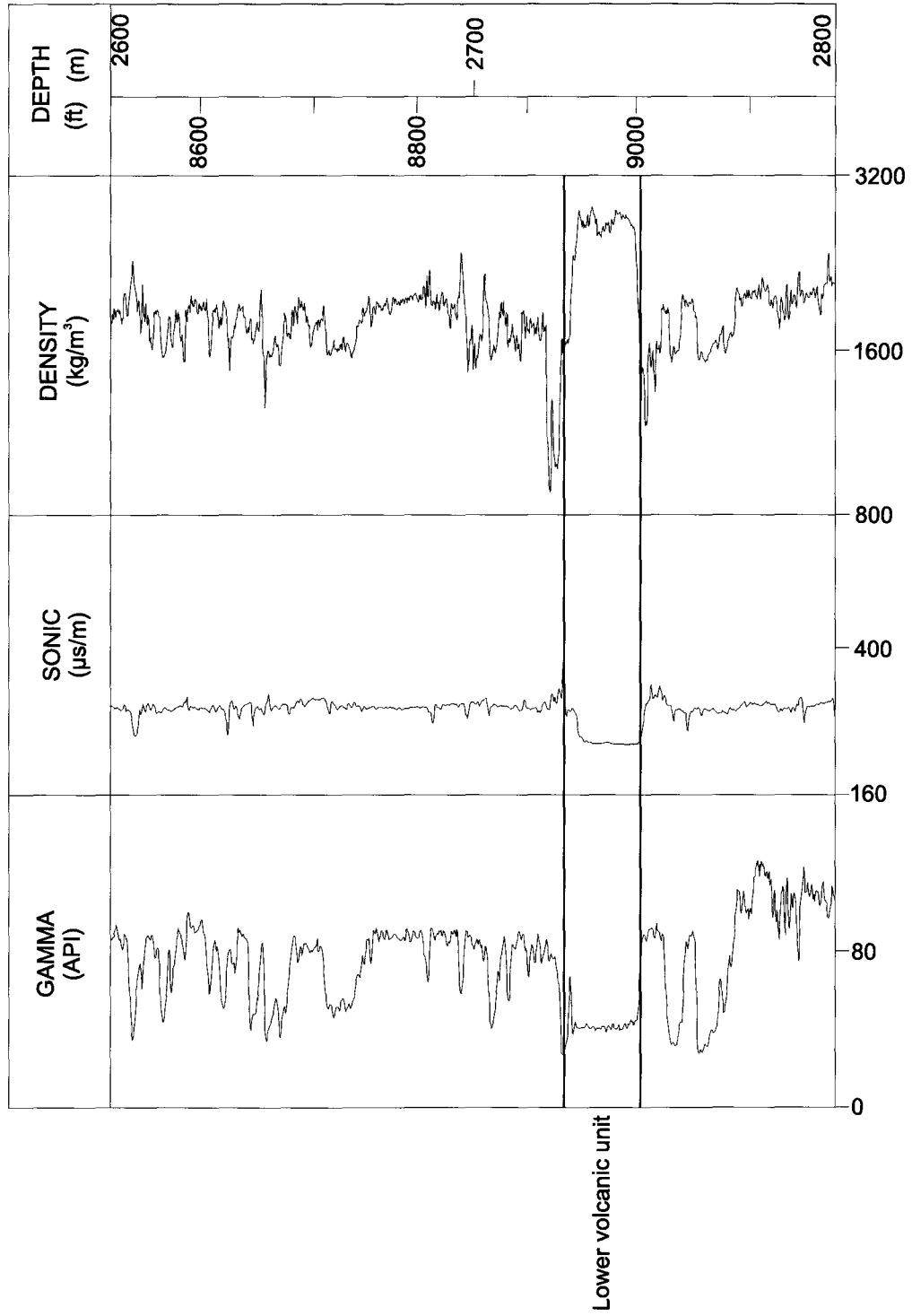
Figure 3.10a: Detailed well log interpretation for the Hesper I-52 well

indicate that the basaltic unit is a flow located at a distance from the source beyond which pyroclastic material would be expected.

3.2.5 Orpheus Graben and SE Scotian Shelf well correlation

The volcanic rock intervals encountered within the Orpheus Graben are similar in age and character (Figure 3.11). Basalt flows found in the lower basaltic units in Argo F-38, Hercules G-15 and Jason C-20 all consist of 18-23 m (60-75 ft) thick basalt flows near the base of the Logan Canyon Formation. Biostratigraphic and K/Ar dating indicate that all volcanic units are Aptian to Albian in age.

In the Jason C-20 and Hercules G-15 wells, the extrusion of the lower basaltic unit occurred almost directly above the base Logan Canyon unconformity. In Argo F-38, the lower basaltic unit was extruded nearly 80 m above the unconformity. In question is the stratigraphic position of the lower basaltic unit in the Argo F-38 well. Jansa and Pe-Piper (1985) have shown that the Argo F-38 volcanics rest upon unconsolidated pebbly sand. This relationship may record the true stratigraphic location of the base Logan Canyon unconformity. However, Bujak (1979) identified this underlying interval as Aptian. The presence of the Naskapi Member and the placement of the base of the Logan Canyon Formation is unclear. MacLean and Wade (1993) indicate uncertainty as to the presence of this member by recording it as "Naskapi Mb?". The Naskapi Member is considered to be a transgressive shale unit with variable amounts of interbedded sand (McIver, 1971). McIver (1971) also states the Naskapi Member becomes sandier towards the northeast (near the Orpheus Graben) compared to its type location near Sable Island and thus it may be either indistinguishable from the overlying sandy Cree Member or
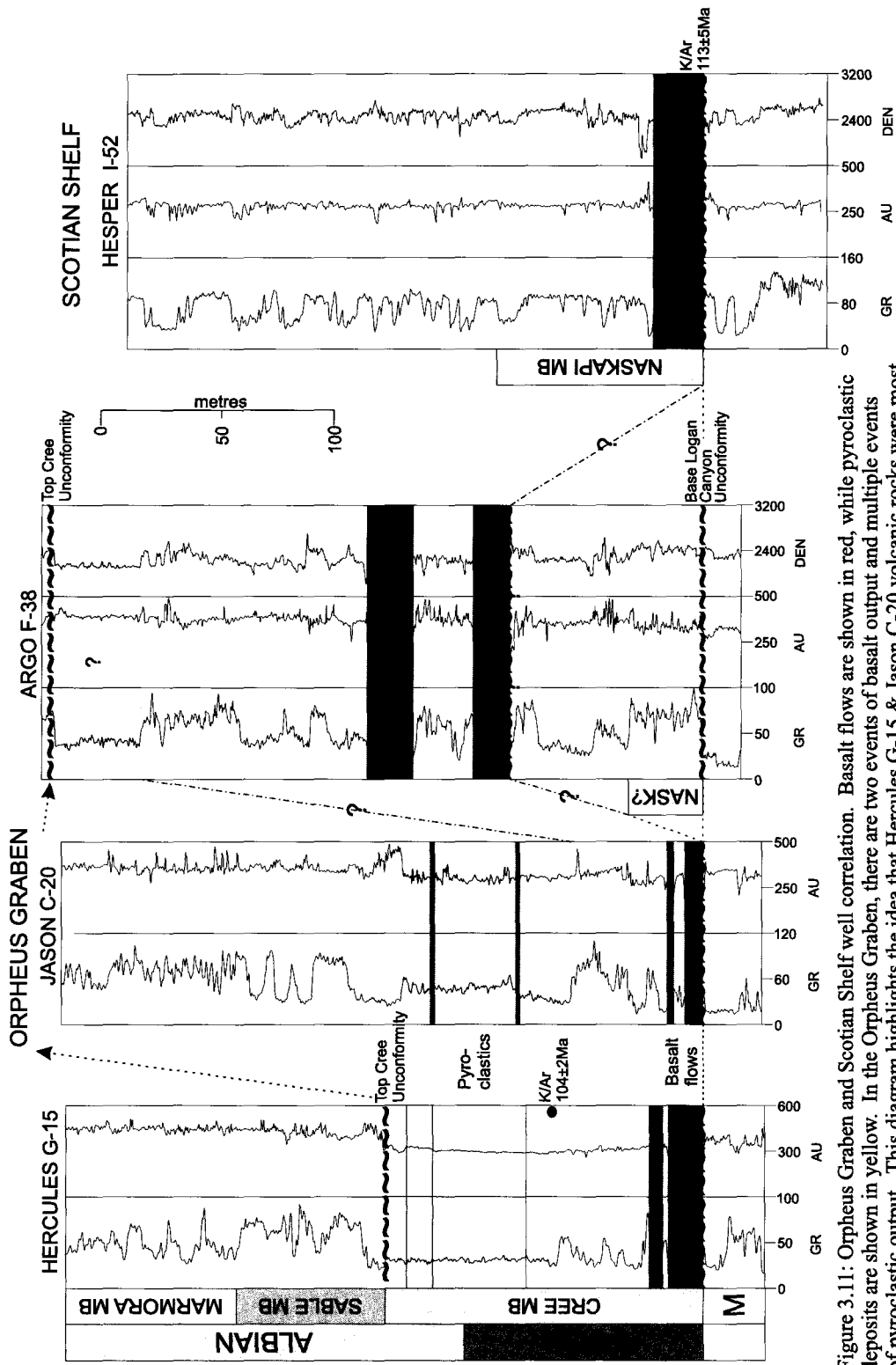
Figure 3.11: Orpheus Graben and Scotian Shelf well correlation. Basalt flows are shown in red, while pyroclastic deposits are shown in yellow. In the Orpheus Graben, there are two events of basalt output and multiple events of pyroclastic output. This diagram highlights the idea that Hercules G-15 & Jason C-20 volcanic rocks were most likely from the same source based on their stratigraphic similarity. It is unclear whether or not Argo F-38 was dervied from the same source due to questions of stratigraphic placement of the Base Logan Canyon unconformity.

may be absent altogether. According to Weir-Murphy (2004), the Cree Member is divided into an upper and lower section with the lower section characterized by medium to coarse grained sandstone beds interbedded with shale, mudstone and silty mudstone. Sidewall cores and ditch cuttings from the potential Naskapi interval indicate mudstone with coarsening upwards sand. The two nearest wells, Jason C-20 and Hercules G-15 do not have a Naskapi Mb and thus, unless Argo F-38 was located in a depositional low, it might be expected that the Naskapi Member is absent in this well.

The upper volcanic unit in Argo F-38 is 26 m (85 ft) above the lower basaltic unit and is 20 m (66 ft) thick. The lack of samples makes it unclear whether this upper unit is a basalt flow or pyroclastic unit based on the lack of samples; however, the well log response is similar to the lower basaltic unit and it is therefore interpreted as a basalt flow. There is a question as to whether a pyroclastic unit does exist in Argo F-38 in the upper Cree Member, as might be expected based on the presence of pyroclastic units in the nearby Jason C-20 and Hercules G-15. The Hercules G-15 and Jason C-20 wells intersected a pyroclastic unit 75-78 m (246-256 ft) thick approximately 40 m (131 ft) above the lower basaltic unit, while the Hesper I-52 well does not contain any higher volcanic units.

Whether the volcanic unit at Hesper I-52 is a basalt flow or a sill cannot be determined exclusively from thin sections and well logs. The basalt sits on top of the base Logan Canyon unconformity (Weir-Murphy, 2004) at the same stratigraphic level as basalt flows in the Orpheus Graben of a similar age and is of similar thickness. Thus, if the basalt at Hesper I-52 is to be considered a sill or dyke as stated by Jansa and Pe-Piper

(1985), it would have to be a very shallow intrusion if correlated with the Orpheus graben volcanic flows.

The lower basaltic units in the Hercules G-15 and Jason C-20 wells were extruded soon after the base Logan Canyon unconformity. The basalt flows and pyroclastic rocks in the Jason C-20, Hercules G-15 and Argo F-38 wells, and one of the basalt flows in the Hesper I-52 well correlate among themselves. Previous interpretations place the volcanic and pyroclastic rocks in the Jason C-20, Hercules G-15 and Argo F-38 wells within the base Cree Member, while the basalt flow at the Hesper I-52 well was interpreted as within the Naskapi Member. This implies the base of the Cree Member is diachronous with the Naskapi Member, or the identification of the Naskapi Member is wrong. The Jason C-20, Argo F-38 and Hercules G-15 wells were located inboard of the marine transgression which deposited the diachronous Naskapi Member shale at Hesper I-52, and thus the Cree Member in the Orpheus Graben and the Naskapi Member on the Scotian Shelf may be time equivalent.

CHAPTER 4
SEISMIC INTERPRETATION

Seismic data used in this study are all 2D seismic reflection data acquired by industry in the 1970's through to the early 2000's. The seismic data is important to this study, as they can be used to determine the extent of the volcanism in the Orpheus Graben, Scotian Shelf and SW Grand Banks. The data also can provide insight into the tectonic history during the Cretaceous in these areas. Seismic data used in this study can be found in Table 4.1 with their locations shown in Figure 4.1.

The vertical resolution of the data varies throughout the project from 6.25-18.75 m based on the quality of the seismic data. Vertical resolution of the data refers to the minimum required thickness a bed must be so that it is distinguishable from an overlying or underlying bed. Vertical resolution can be determined by:

$$R = v / 4f,$$

where R is resolution, v is velocity and f is the dominant frequency (Yilmaz, 1987). Kingdom Suite 8.5 has a Survey Spectrum function which displays the frequencies used in the seismic profile. To determine the minimum thickness of a bed which is resolvable in the data, the equation stated above is used. In this equation, $v = 1500$ ms^{-1} which is the velocity of water and $f =$ the highest frequency used in the seismic profile. For example, for profile 83-4449BA, the Survey Spectrum shows dominant frequencies ranging from 5-40 Hz (Figure 4.2). Thus, using the above equation,

$$R = 1500 \text{ ms}^{-1} / 4 \cdot 40 \text{ Hz}, \ R = 9.4 \text{ m}$$

And so, 9.4 m is the thinnest bed within which the top and bottom of the bed can be distinguished in that seismic profile. Applying this equation to the multitude of seismic
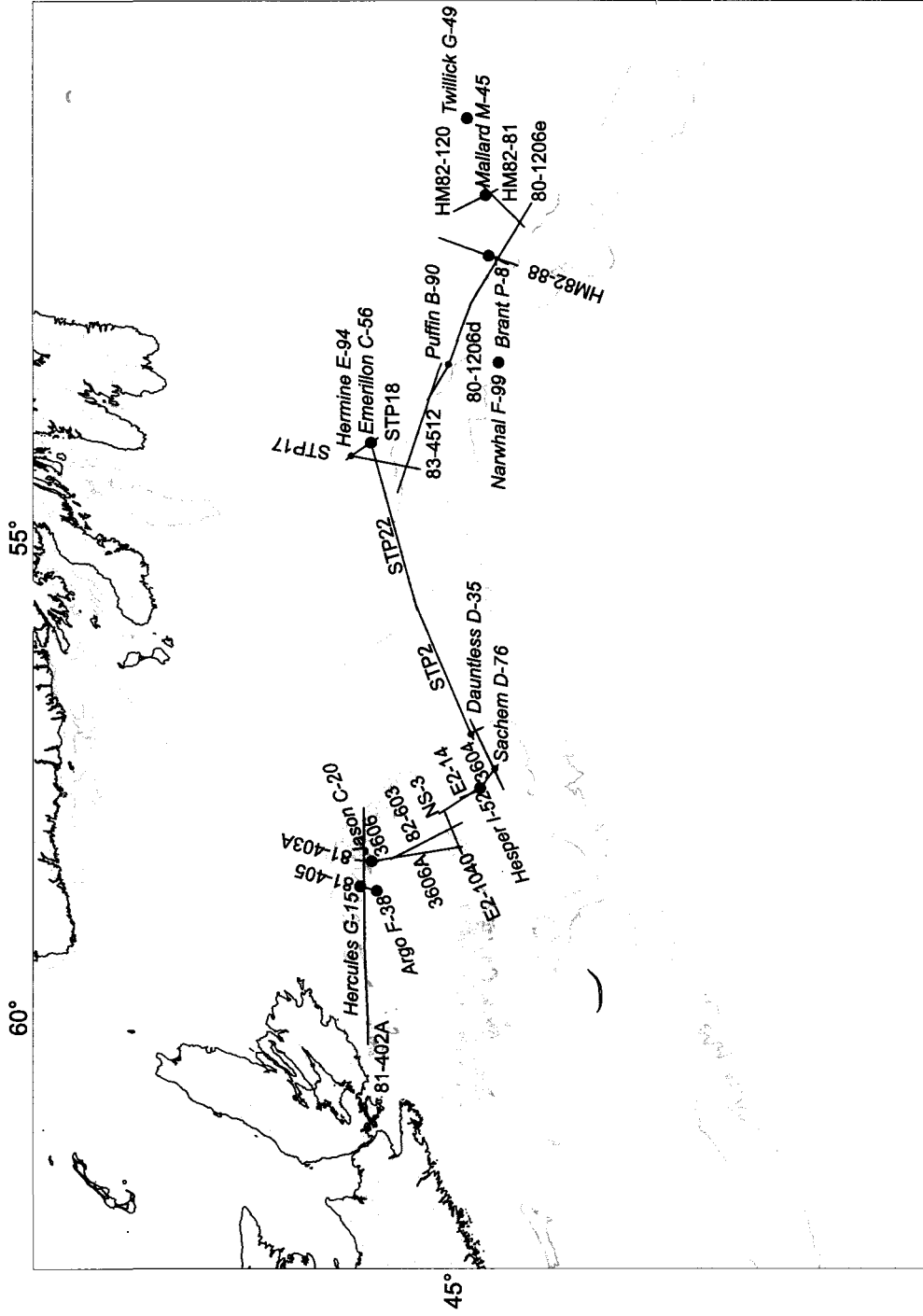
Figure 4.1: Map showing all profiles in the seismic project (blue), profiles shown in this study (red) and relevant well locations (black; wells with volcanic rocks shown in orange)
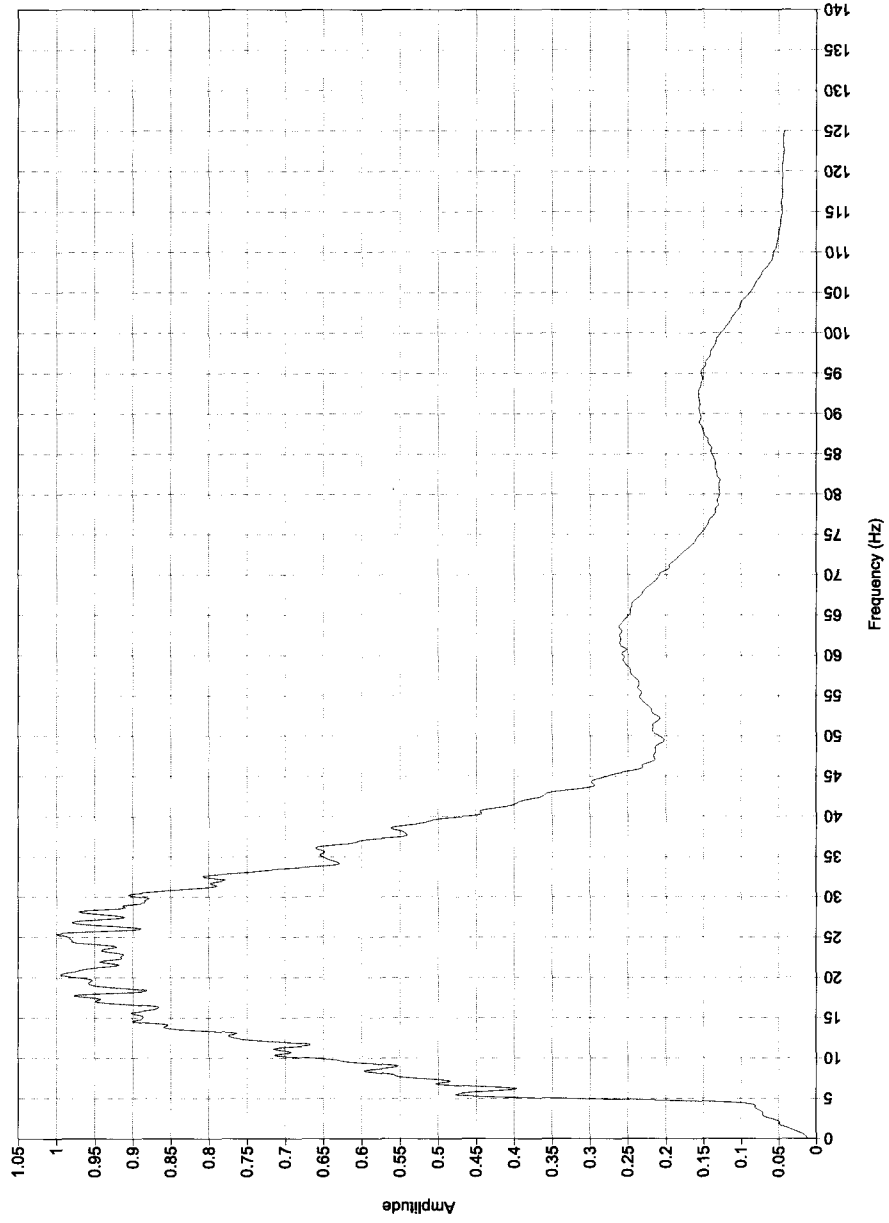
67

Figure 4.2: Example of the Survey Spectrum generated by Kingdom Suite for the profile 83-4449BA. The usable frequency of this spectrum is from ~5 Hz to 40 Hz, and thus 40 Hz is used in the equation to determine the vertical resolution of a seismic profile

profiles in this study, the vertical resolution ranged from as small as 6.25 m to as large as 18.75 m.

Previously interpreted lithostratigraphic and biostratigraphic picks from wells found within the GSC BASIN database were used to determine age of reflectors and seismic stratigraphy. For wells in the Orpheus Graben and SE Scotian Shelf, lithostratigraphic picks were made by MacLean and Wade (1993), while on the SW Grand Banks, lithostratigraphic picks were made by the CNLOPB (2007). Biostratigraphic picks for wells were made by multiple authors over multiple years and are listed for each well in Chapter 3 (Table 3.1).

Seismic reflection profiles record two-way travel time and not depth. Thus, to make well-to-seismic ties, velocity survey data for each well was used to convert two-way time (TWT) to metres depth at the wellbore. With the well in metres, biostratigraphic and lithostratigraphic picks could be placed on the seismic at the well site. Based on the biostratigraphic and lithostratigraphic picks, nine seismic horizons were picked throughout the seismic project where possible. These horizons are listed in Table 4.2.

Of the nine seismic horizons listed above, four are considered unconformities: the Base Tertiary unconformity, the mid-Albian Top Cree Member unconformity, the base Aptian Top Mississauga Formation unconformity and the base Cretaceous Base Mississauga Formation unconformity. The unconformities range from very obvious angular unconformities to completely conformable horizons that are at times difficult or impossible to trace throughout the entire study area. The Base Tertiary, Top Mississauga and Base Mississauga horizons are all positive reflections with a generally

YEAR	COMPANY	PROJECT	PROFILE
1972	Canadian Superior	8624-C020-001E	E2-14
			E2-1040
1973	Amoco Canada	8620-A004-006E	3123a
1981	Petro-Canada	8624-P028-007E	80-1206d
			80-1206e
		8624-P028-030E	81-402A
			81-403A
			81-405
1982	Canterra Energy	8624-C055-003E	NS-3
	Husky Oil	8620-H006-004E	HM82-81
			HM82-88
			HM82-120
			HM82-138
	Bow Valley	8624-B011-003E	82-603
1983	Soquip	8620-S014-006E	83-1430B
			83-4449BA
			83-4449BB
		8620-S014-010E	83-4512
	Western Geophysical/ GSC(A)	ST.PIERRE SURVEY	STP2
			STP17
			STP18
			STP22
1985	Petro-Canada	8624-P028-072E	3604
			3606
			3606A
	Petro-Canada	8624-P028-081E	6309

Table 4.1: List of seismic lines used in this study

HORIZON	COLOR	APPROX. AGE
Base Tertiary unconformity	Yellow	Base Tertiary
Top Wyandot	Purple	
Top Petrel	Pink	
Top Logan Canyon Formation	Green	
Top Cree Member unconformity	Turquoise	Mid-Albian
Top Mississauga Formation unconformity	Lime Green	Base Aptian
"O" marker	Blue	
Base Mississauga Formation unconformity	Red	Base Cretaceous
Top Volcanic	Orange	

Table 4.2: List of horizons picked throughout the seismic project

strong acoustic impedance contrast throughout much of the study area. The Top Cree horizon is also a positive reflector but does not have as strong of an acoustic impedance contrast as the others, making it more difficult to trace across the study area. The change from an unconformity to a conformable horizon is due to the fact that the study area covers a large geographic region encompassing multiple sub-basins and intervening highs, as well as slightly different tectonic histories. Where the unconformities do not display unconformable relationships to underlying or overlying strata, their position was determined from lithostratigraphic and biostratigraphic picks within wells and then were correlated along seismic profiles between wells. The nature of the unconformities will be discussed, with examples shown in seismic profiles, within this chapter in the section regarding tectonic movement.

In this chapter, the well-to-seismic ties and regional correlations will be dealt with first. Where volcanic rocks are detectable seismically they will be briefly mentioned, however, they will be discussed in the following section on the seismic evidence of volcanic rocks and the evidence of the tectonic history. Only the seismic profiles showing well-to-seismic ties, volcanic features or tectonic features will be shown in the main body of this thesis. Seismic profiles used for correlation can be found in Appendix 1.

4.1 Well ties and regional correlation

The Sachem D-76 well on the SE Scotian Shelf was chosen as the starting point for the seismic project as it is a) centrally located between the Orpheus Graben and the SW Grand Banks, b) contains a well defined lithostratigraphic section and c) has fairly

recent biostratigraphic picks from Ascoli (2005). The lithostratigraphic and biostratigrahic picks show good correlation with the NW-SE seismic profile 3604 with the exception of the Base Mississauga Formation horizon. At the well, biostratigraphy places the horizon as older than Kimmeridgian, though elsewhere it is considered Tithonian-Barremian (Figure 4.3a). Also present on this profile is the well-to-seismic tie for the Hesper I-52 well. As with the Sachem D-76 well, lithostratigraphic and biostratigraphic picks from the Hesper I-52 well both correlate with the seismic profile shown in Figure 4.3a. All horizons along this profile are conformable. Correlation between the two wells along this profile is generally consistent but with some uncertainty due to the quality of the seismic data. The biggest uncertainty is with the Top Logan Canyon Formation horizon, which is difficult to trace across the profile. The thickness of the Logan Canyon sedimentary rocks between the Top Logan Canyon horizon and the Top Cree Member horizon appears to vary between the two wells, being thicker at the Hesper I-52 well than at the Sachem D-76 well. The basalt flow at the Hesper I-52 well, described in Chapter 3 (Figure 3.5), was traced in the profile and will be discussed later in the chapter. The basalt flow is shown in Figure 4.3b without the interpretation to highlight the double reflection of the flow at the Hesper I-52 well. Correlations from this initial profile at the Sachem D-76 and Hesper I-52 wells were then made first northwestwards into the Orpheus Graben and then eastwards across the Laurentian Channel and onto the SW Grand Banks.
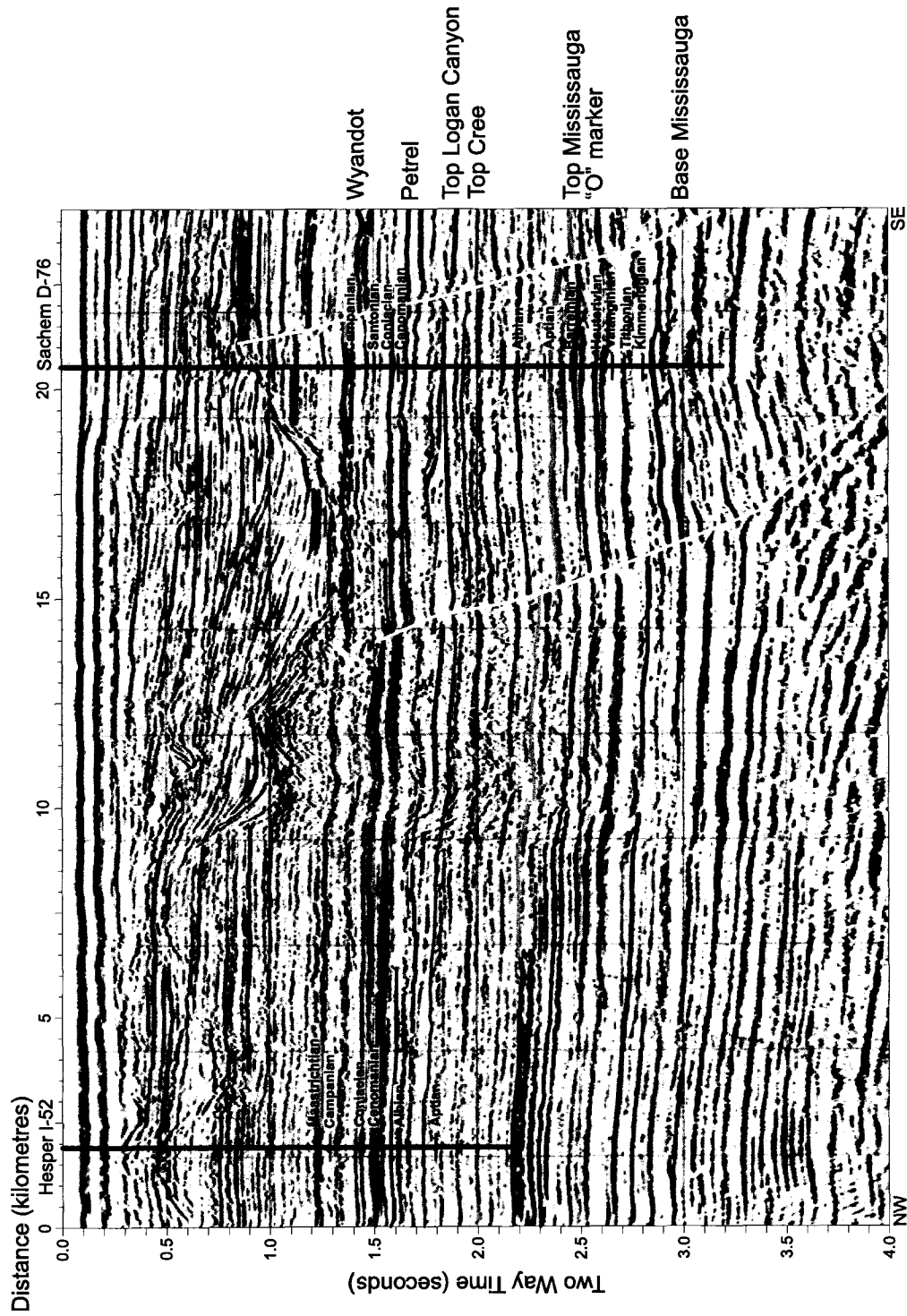
Figure 4.3a: NW-SE profile 3604 showing the well-to-seismic tie for the Hesper I-52 and the Sachem D-76 well. This profile also shows the correlation between the two wells1

73

Figure 4.3b: NW-SE profile 3604 highlighting the double reflection of the volcanic horizon and abrupt ending of the volcanic horizon at the Hesper I-52 well

74

4.1.1 Correlation to Orpheus Graben

From the Hesper I-52 well, correlation was made in a northwestward direction along profile NS-3 (Figure 4.4a). In this profile all horizons are conformable and are traceable with reasonable certainty with the exception of the Top Logan Canyon and Top Cree horizons. These horizons can only be traced in the NNW section of the profile. The Top Cree horizon is obscured by artifacts of an overlying channel at 15 km and can only be traced from 15-30 km, while the reflector traced as the Top Logan Canyon horizon has a very low acoustic impedance contrast and can only be traced from 20-30 km. The transition from Logan Canyon sediments to the overlying Dawson Canyon sediments may be gradual and thus there may not be a well developed acoustic impedance contrast between them to generate a strong and consistent reflector at the top of the Logan Canyon Formation. The basalt flow near the Hesper I-52 well was intersected in this profile and is shown in greater detail in Figure 4.4b.

Correlation was continued in a northwestwards direction along profile E2-14 (Figure 4.5a, b). The seismic profile is a paper copy which has been scanned and then turned into digital data by Weir-Murphy (2004) and is thus of a low quality. However, correlations were possible with some inherent uncertainty due to the quality of the data. In this profile, the "O" marker appears to onlap the Base Mississauga. The Top Mississauga and the Base Mississauga merge into one reflector northwards. As the two unconformities have merged together, the reflector is picked as the Base Mississauga horizon north of this profile though there is uncertainty as to which unconformity is actually being picked. There is also uncertainty as to where these unconformities transition again into separate and distinct unconformities as seen in the Orpheus Graben.
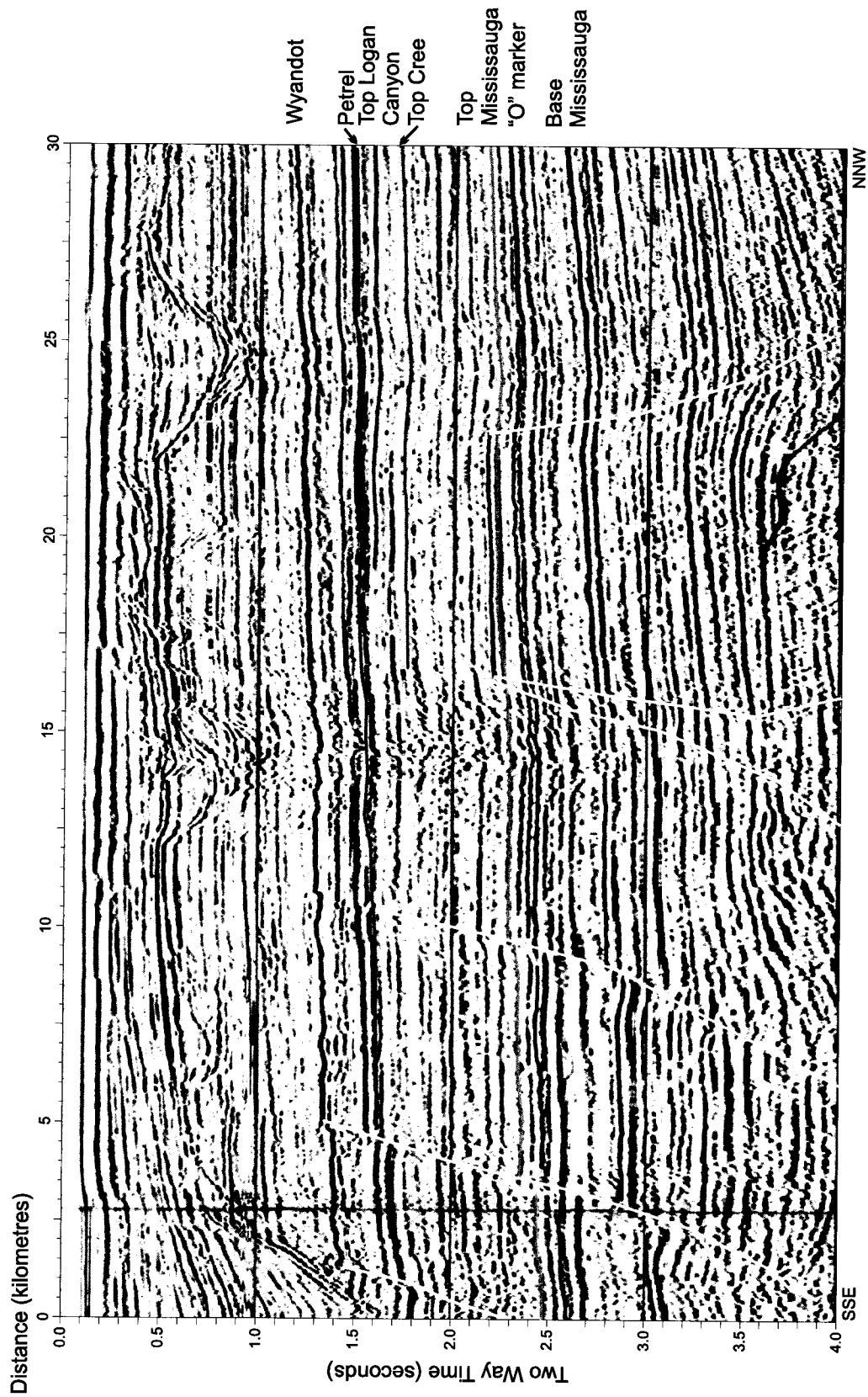
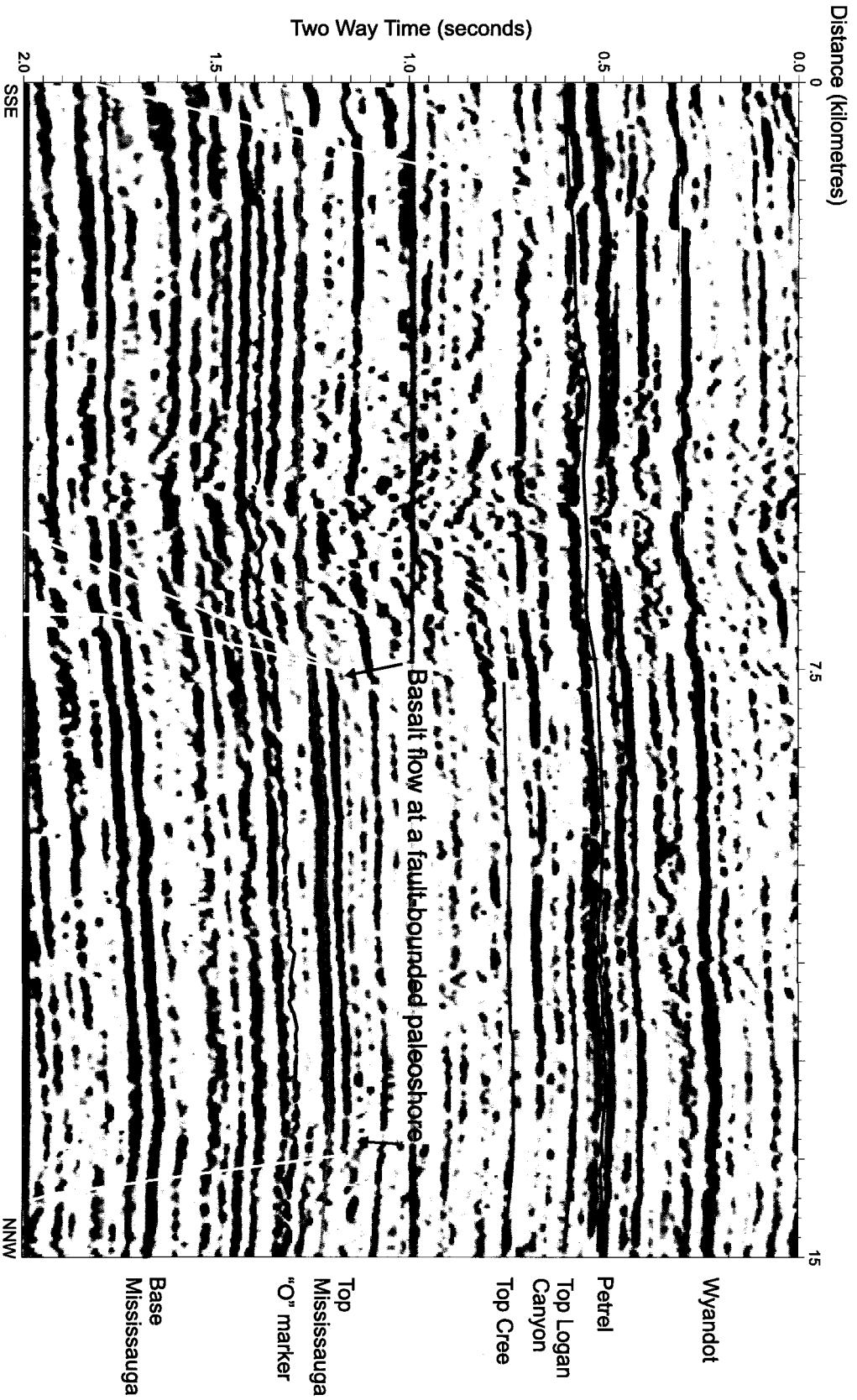Figure 4.4a: NNW-SSE profile NS-3 correlation northwestwards toward the Orpheus Graben

Figure 4.4b: NNW-SSE profile NS-3 highlights the Aptian basalt flow intersected by the Hesper I-52 well
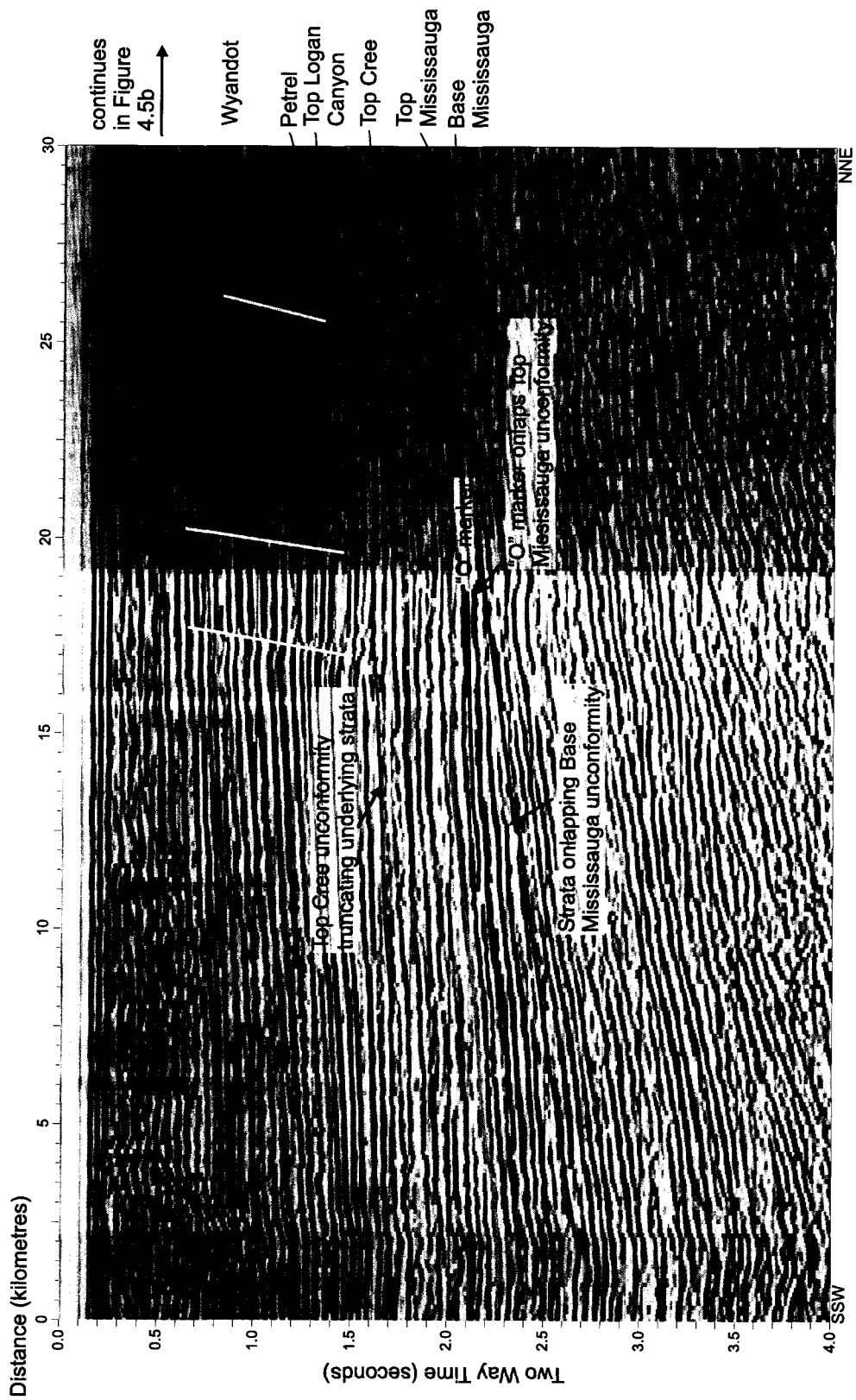
Figure 4.5a: NNE-SSW profile E2-14 (part 1) correlating from the Hesper I-52 well towards the Orpheus Graben. This profile also highlights the tilting of Cretaceous strata inboard of the shelf edge
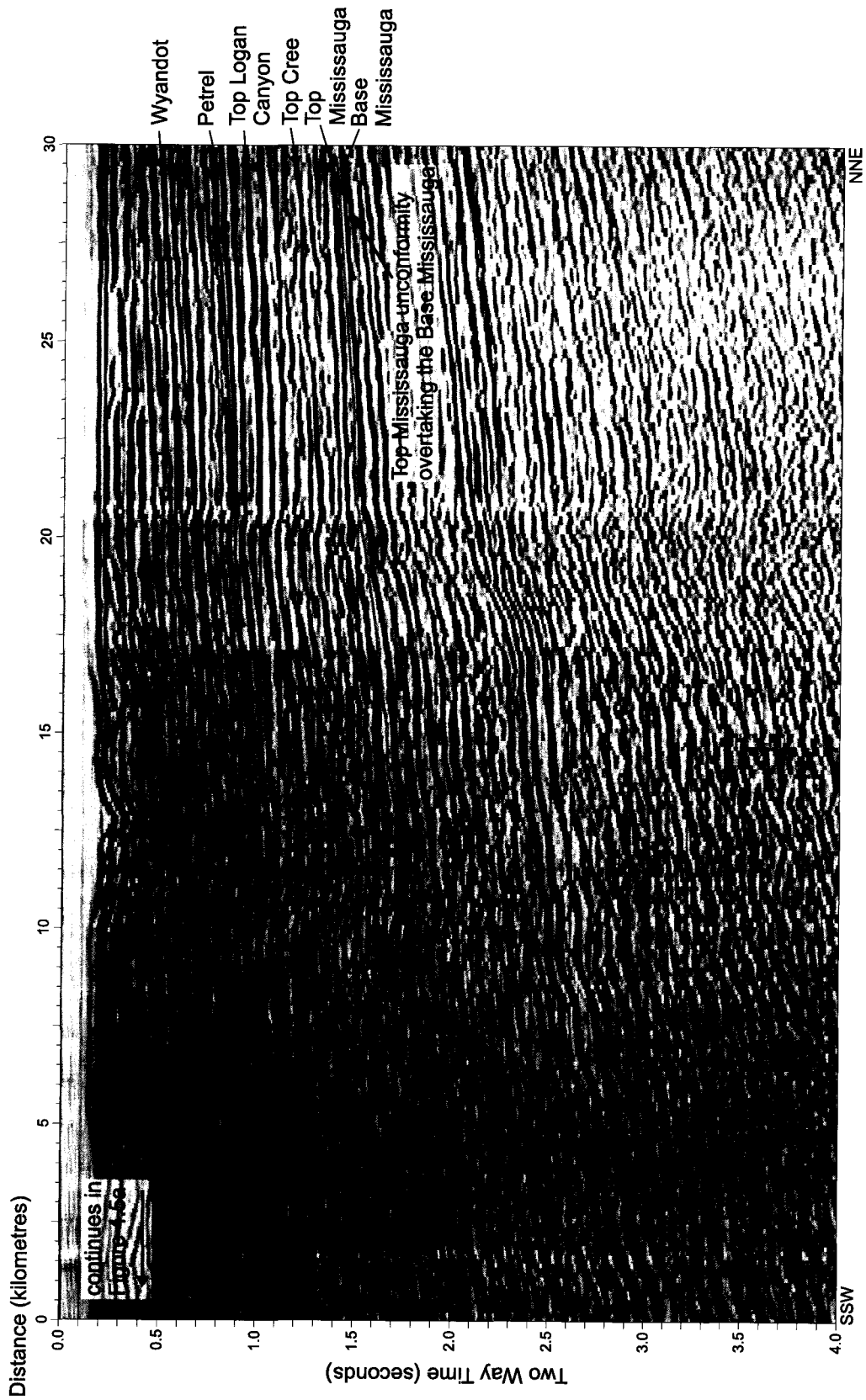
Figure 4.5b: NNE-SSW profile E2-14 (part 2) correlating from the Hesper I-52 well towards the Orpheus Graben. This profile also highlights the tilting of Cretaceous strata inboard of the shelf edge.

79

Continuing northwestwards towards the Orpheus Graben, correlations are made along more scanned paper copies of poor quality seismic data in profiles E2-1040 and 3606A (Appendix Figures 1.1 and 1.2a, b). There is uncertainty in the Top Logan Canyon and Top Cree horizons, which cannot be followed from E2-1040 to 3606A, due to the poor quality of the profiles. It is within these profiles that full correlation of horizons on the Scotian Shelf and the Orpheus Graben breaks down due to the uncertainty caused by the poor quality data and the presence of the Canso Ridge which could have altered depositional and erosional patterns in the area.

Within the Orpheus Graben, profile 3606 intersects the Jason C-20 well and a well-to-seismic tie can be made (Figure 4.6). Unfortunately, there are only four biostratigraphic picks from two different authors available for this well; however, the work of Weir-Murphy (2004) clearly defines the lithostratigraphy of the Jason C-20 well. The volcanic rocks discussed in Chapter 3 (Figure 3.8) for the Jason C-20 well are detected seismically. Correlation westwards from the Jason C-20 well towards the Argo F-38 and Hercules G-15 wells is possible along profiles 81-403A and 81-402A (Appendix Figures 1.3 and 1.4). These profiles are poor quality scanned profiles and thus there is some inherent uncertainty in the horizons, mainly with the Top Cree, Top Logan Canyon and Petrel horizons.

Correlation between the Argo F-38 and Hercules G-15 wells can be made along profile 81-405 (Figure 4.7). This profile also shows the well-to-seismic ties for both the Argo F-38 and Hercules G-15 wells. The biostratigraphic and lithostratigraphic picks correlate with the seismic data for the Argo F-38 well; however, the biostratigraphic picks for the Hercules G-15 well does not correlate with the seismic data at all. The
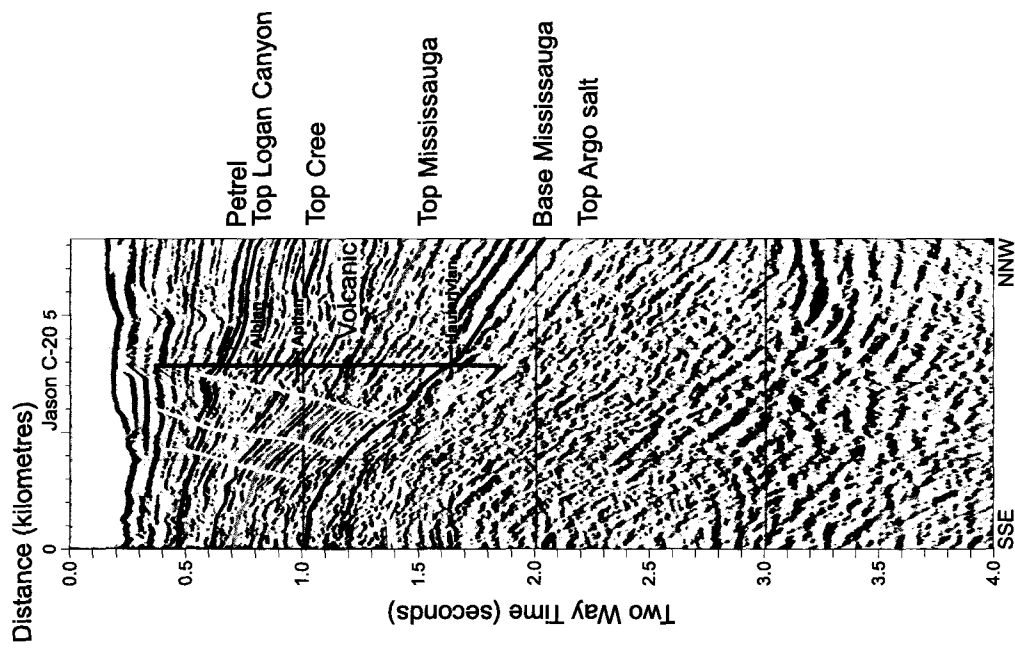
Figure 4.6: SSE-NNW profile 3606 showing the well-to-seismic tie for the Jason C-20 well
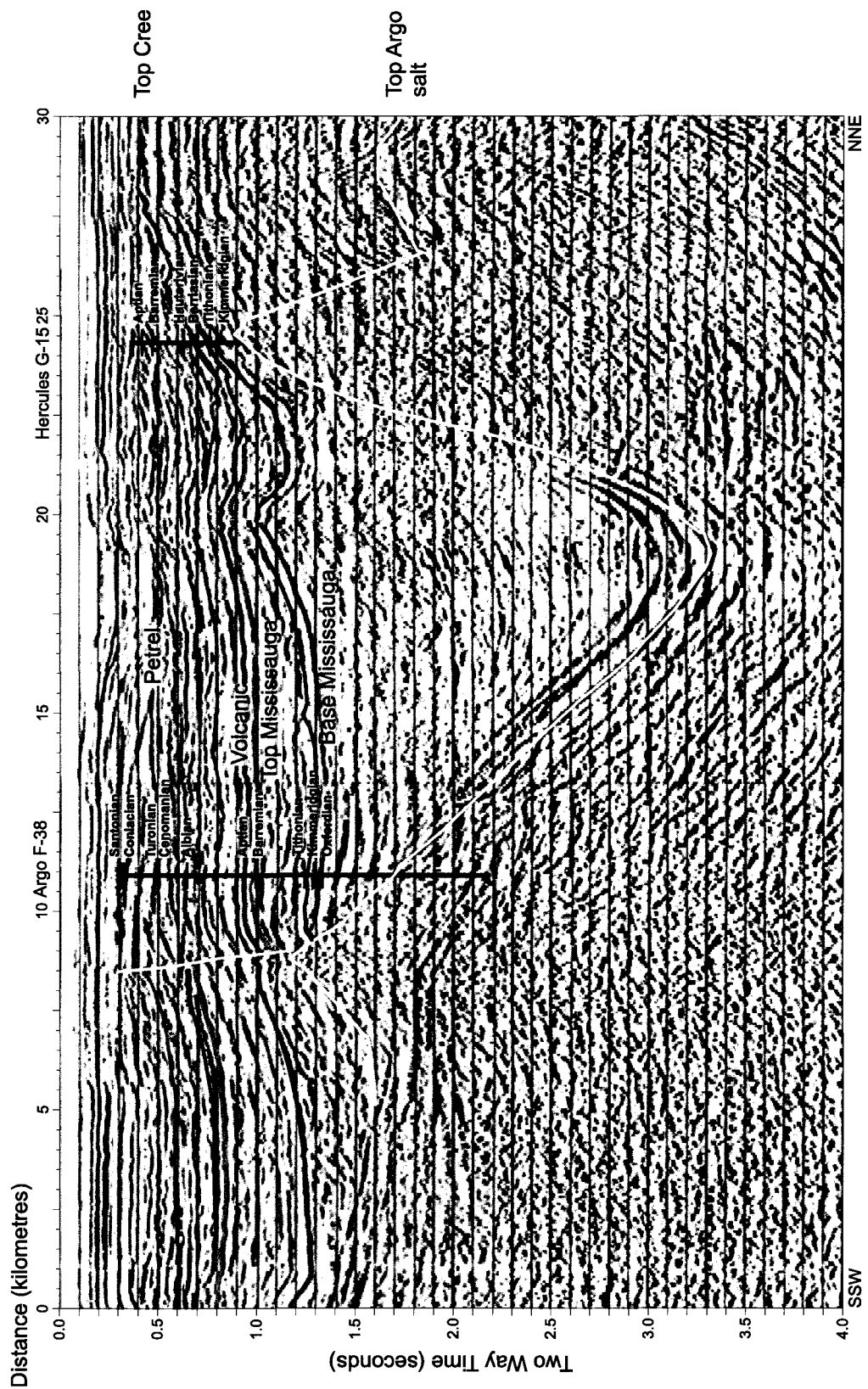
81

Figure 4.7: SSW-NNE profile 81-405 showing the well-to-seismic ties for the Argo F-38 and Hercules G-15 wells. This profile also shows the correlation between the wells

issues with the biostratigraphy were discussed in Chapter 3 and by Weir-Murphy (2004). Although there is some interruption of seismic reflectors between the Argo F-38 and Hercules G-15 wells due to salt movement, the lithostratigraphic picks are correlatable between the wells. The volcanic rocks discussed in Chapter 3 for the Argo F-38 (Figure 3.7) and Hercules G-15 (Figure 3.9) wells are detectable seismically and are correlatable between the two wells.

4.1.2 Correlation to SW Grand Banks

Correlation from the Sachem D-76 well was also carried out across the Laurentian Channel and onto the SW Grand Banks. From the Sachem D-76 well, correlation was made along profile 83-4449BB, 83-4449BA and 83-1430B (Appendix Figures 1.5, 1.6 and 1.7). Along these profiles all horizons were conformable and were correlated with good certainty to the Dauntless D-35 well at the southeastern edge of the Scotian Shelf.

A well-to-seismic tie was made for the Dauntless D-35 well on profile STP2 (Figure 4.8, Appendix Figures 1.8a, b, c, d, e). This profile is part of a high quality digital data set covering the St. Pierre region over the Laurentian Channel and onto the SW Grand Banks. The lithostratigraphic and biostratigraphic picks show an excellent match to the seismic correlation. Along this profile, the Wyandot Formation is topped by the Base Tertiary horizon; however, at the well site the Base Tertiary is not listed in the lithostratigraphic picks. Biostratigraphy by Williams (1995) indicates the base of Tertiary sediments is found at 1418 m while lithostratigraphy of MacLean and Wade place the top of the Wyandot Formation at 1432 m. The Banquereau Formation overlies the Wyandot Formation and in some parts of the Scotian Basin, the Banquereau
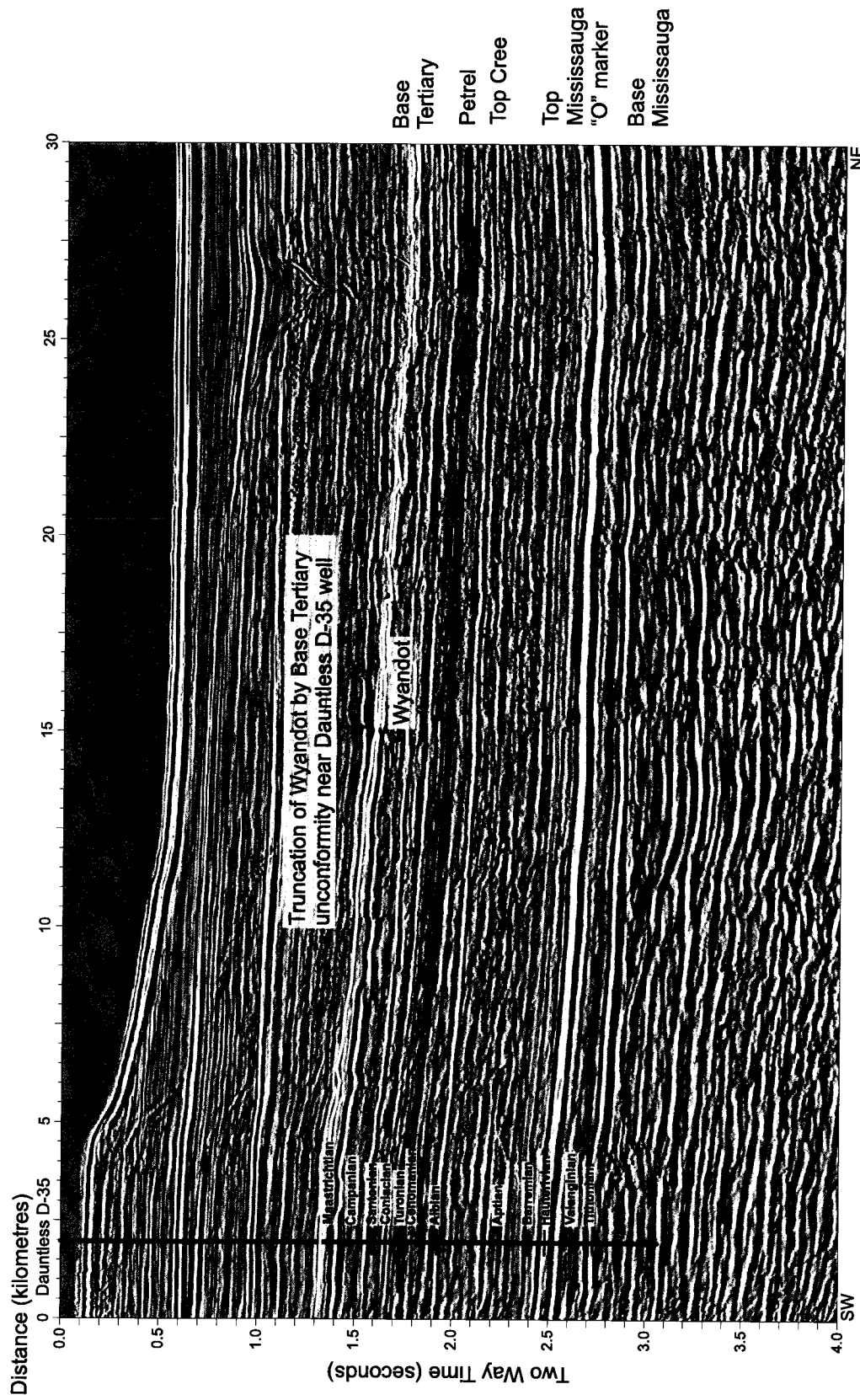
Figure 4.8: NE-SW profilee STP2 (part 1) showing the well-to-seismic tie of the Dauntless D-35 well. This profile also shows the correlation between the SE Scotian Shelf and the SW Grand Banks

84

Formation has been dated biostratigraphically as Maastrichtian (latest Cretaceous) (Ascoli 1988, 2005). Thus the top Wyandot/ base Banquereau does not always mark the base of the Tertiary. The Base Tertiary unconformity may not be recognizable in lithostratigraphic studies at the Dauntless D-35 well, as it could be conformable at the well site. Within the seismic profile, the Base Tertiary reflector is unresolvable from the Wyandot reflector. This reflector is conformable at the well site; however, within 15 km east of the Dauntless D-35 well the unconformable relationship of the Base Tertiary horizon to the underlying Wyandot Formation becomes apparent as the Base Tertiary truncates the Wyandot horizon. On this profile, the reflector on which the Top Logan Canyon horizon is picked loses its medium amplitude within 10 km of the Dauntless D-35 well. This horizon is not detected on seismic profiles east of this point with the exception of the easternmost part of the study area. The Petrel and Top Cree horizons are truncated by the Base Tertiary horizon as the unconformity erodes through the strata, eventually forming a ~10 km wide channel which eroded below the Top Cree horizon but not to the level of the Top Mississauga horizon. The Base Tertiary horizon is the only recognizably unconformable horizon in this profile.

Correlation was continued across the Laurentian Channel in profile STP22 which ultimately ends at the Emerillon C-56 well (Appendix Figure 1.9a, b, c, d). This profile is similar to the previous STP2 profile in that the Base Tertiary horizon is unconformable; however, it is in this profile that the Base Mississauga horizon also can be seen as unconformable. In this profile, the "O" marker onlaps the Base Mississauga, marking the inboard edge of the "O" marker limestone. The east end of the profile shows the well-to-

seismic tie of the Emerillon C-56 well (Figure 4.9). The lithostratigraphic and biostratigraphic picks match the seismic data.

Well-to-seismic ties can also be made on profile STP18 for both the Emerillon C-56 and Hermine E-94 wells (Figure 4.10). For the Hermine E-94 well, as with the Emerillon C-56 well, the lithostratigraphic and biostratigraphic picks confirm the seismic correlation. This profile shows the unconformable relationship of the Base Tertiary and the Base Mississauga horizons to underlying strata, highlighting the very obvious angular unconformity of the Base Mississauga horizon in this part of the study area. The diabase sill or dyke in the Emerillon C-56 well is detectable in the seismic.

Correlation across the SW Grand Banks was continued with the N-S profile STP17 and the NW-SE profile 83-4512 (Appendix Figures 1.10a, b and 1.11a, b). The Base Tertiary, Top Mississauga and Base Mississauga can be correlated across these profiles. The Petrel horizon cannot be correlated from profile STP17 to the NW section of the 83-4512 profile as the acoustic impedance contrast becomes very low. The Top Cree horizon was truncated by the Base Tertiary horizon along the previously described profile STP2 and the position of the horizon could not be re-established eastward. The Logan Canyon Formation on the SW Grand Banks at the Emerillon C-56 and Hermine E-94 wells is approximately 100 m thick or less, and thus resolving a Top Cree horizon was impossible. However, southeastward of the STP17 profile, sediments thicken and the Top Cree horizon could be established along profile 83-4512 from correlation to a well-to-seismic tie in the Puffin B-90 well to the east. The "O" marker horizon, which had onlapped the Base Mississauga in STP2 is also re-established along profile 83-4512 from correlation with the Puffin B-90 well.

Distance (kilometres)

Two Way Time (seconds)

Emerillon C-56

SW   NE

Base Tertiary

Petrel

Top Mississauga
Base Mississauga

Volcanic
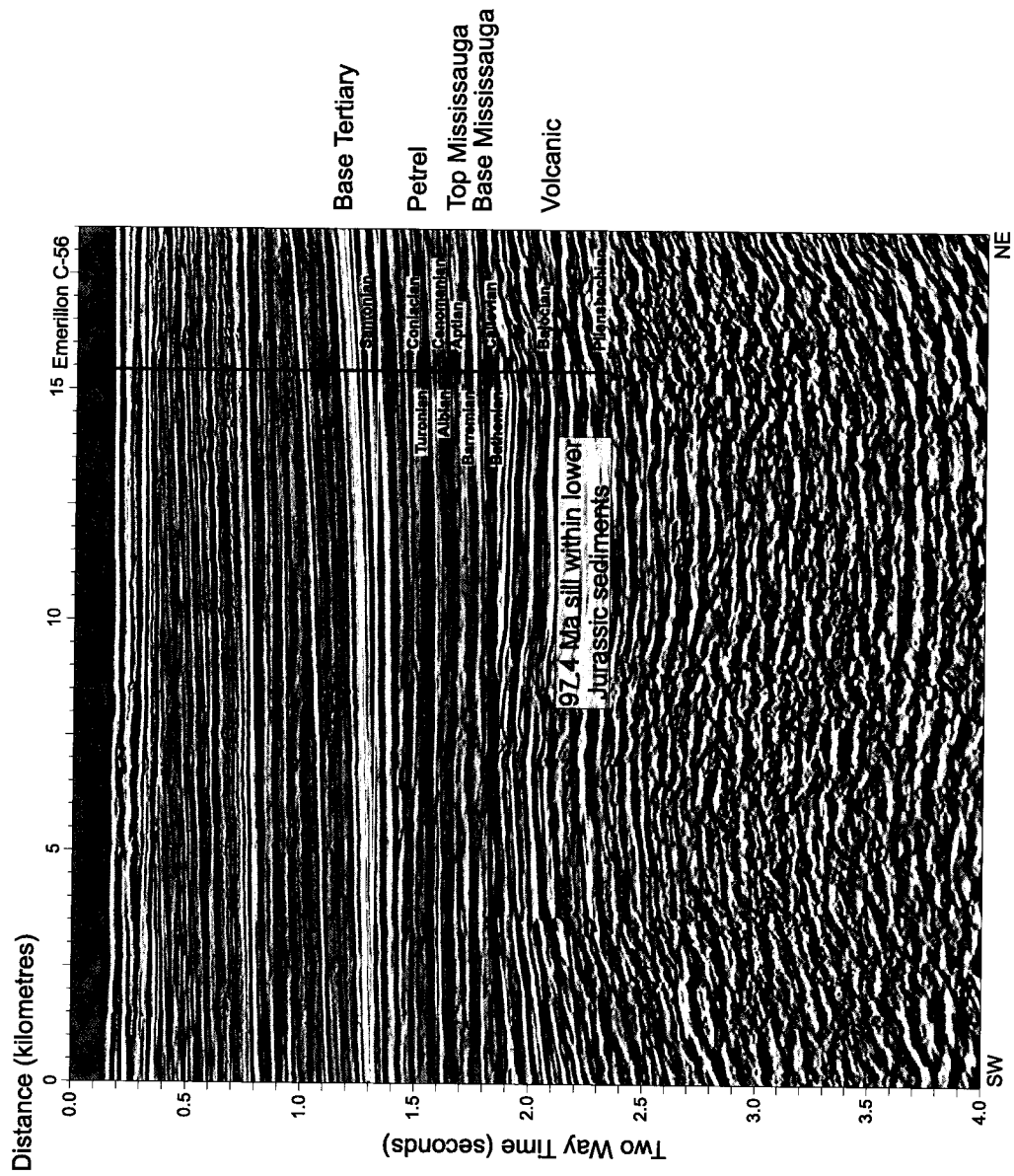
97.4 Ma sill within lower
Jurassic sediments

Figure 4.9: NE-SW profile STP22 (part 5) showing the well-to-seismic tie for the Emerillon C-56 well. This profile also shows the correlation of the SE Scotian Shelf with the SW Grand Banks
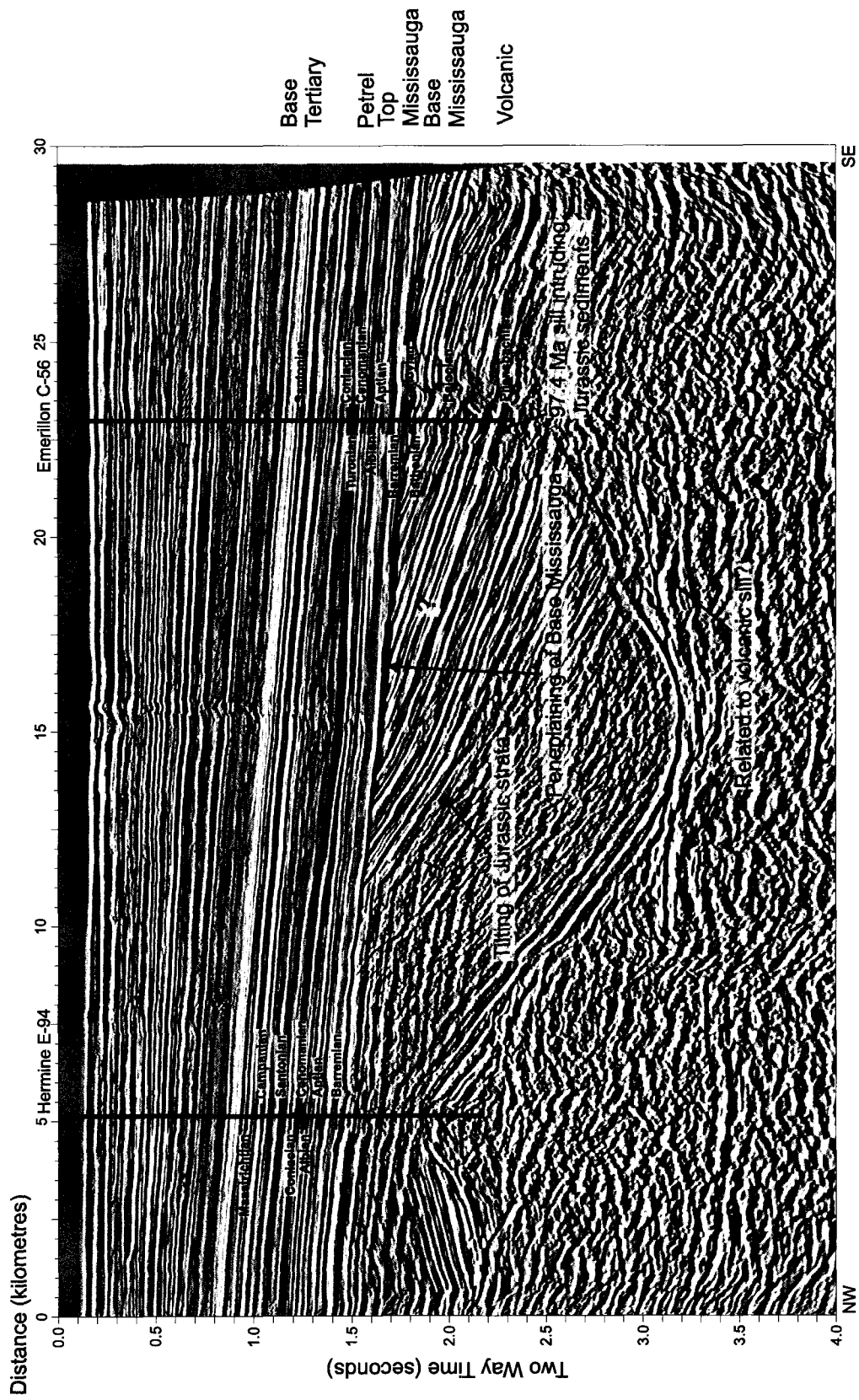
87

Figure 4.10: SE-NW profile STP18 showing the well-to-seismic ties of the Hermine E-94 and Emerillon C-56 wells. This profile also shows the correlation between the wells, the sill at the Emerillon C-56 well, tilting of Jurassic strata and the unconformable relationship of the Base Mississauga

88

Correlations were also made across profile 80-1206d and 801206e with a well-to-seismic tie with the Puffin B-90 well along profile 80-1206d (Figure 4.11, Appendix 1.12a, b and 1.13a, b, c). These profiles can be correlated with reasonable certainty at the Base Tertiary, Petrel, Top Logan Canyon, Top Mississauga and Base Mississauga horizons, while the Top Cree and "O" marker horizons are only correlated through 80-1206d. The lithostratigraphic and biostratigraphic picks for the Puffin B-90 well confirm the seismic correlation, except for the Base Mississauga horizon, as there is no biostratigraphic data to date the horizon. Along these profiles, the Mississauga and Logan Canyon formations become much thicker in places than in the Orpheus Graben, SE Scotian Shelf and the edge of the SW Grand Banks; however, by the eastern end of these profiles, the majority of the Mississauga Formation becomes confined to mini-basins, and the Logan Canyon formation is thinned to the point of being almost unresolvable in the seismic profiles. Correlations in this portion of the SW Grand Banks, east of profile STP17, were made more difficult due to the presence of salt domes. An example of a salt dome of the type often seen in the seismic profiles in this region is shown in Figure 4.12b.

At the eastern edge of the study area, correlations are made along profiles HM82-88 (intersecting the Brant P-87 well), HM82-81, and HM82-120 (intersecting the Mallard M-45 well). The lithostratigraphic and biostratigraphic picks for the Brant P-87 well along profile HM82-88 correlate only at some horizons (Figure 4.12a, b). The Base Tertiary is placed lithostratigraphically and in the seismic profiles above a biostratigraphic pick of Eocene (Gradstein, 1977: micropaleontology). Also there is no biostratigraphic data below the Barremian pick just under the Top Mississauga horizon,
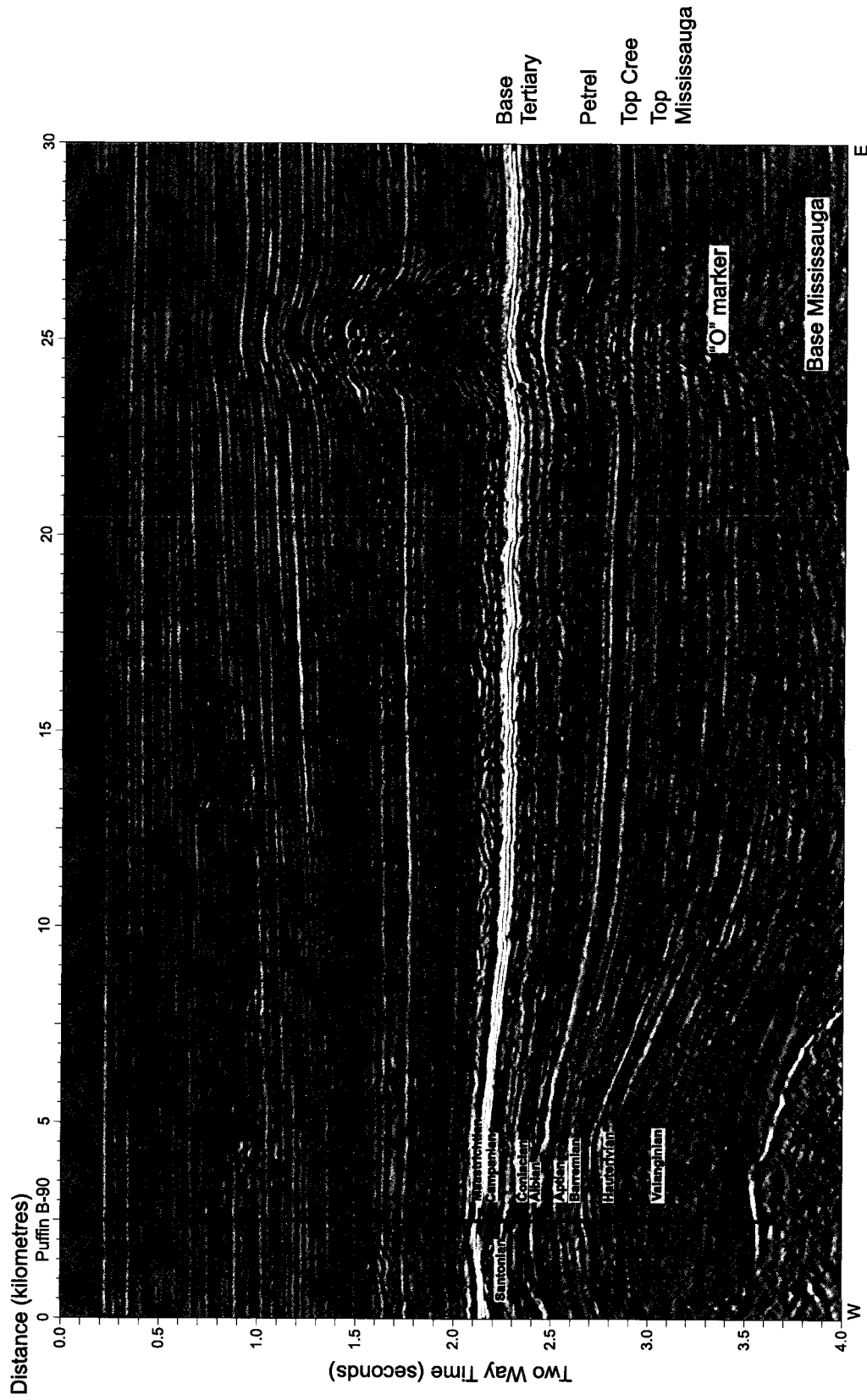
Figure 4.11: E-W profile 80-1206d (part 2) showing the well-to-seismic tie of the Puffin B-90 well. This profile also shows the correlation with the SW Grand Banks
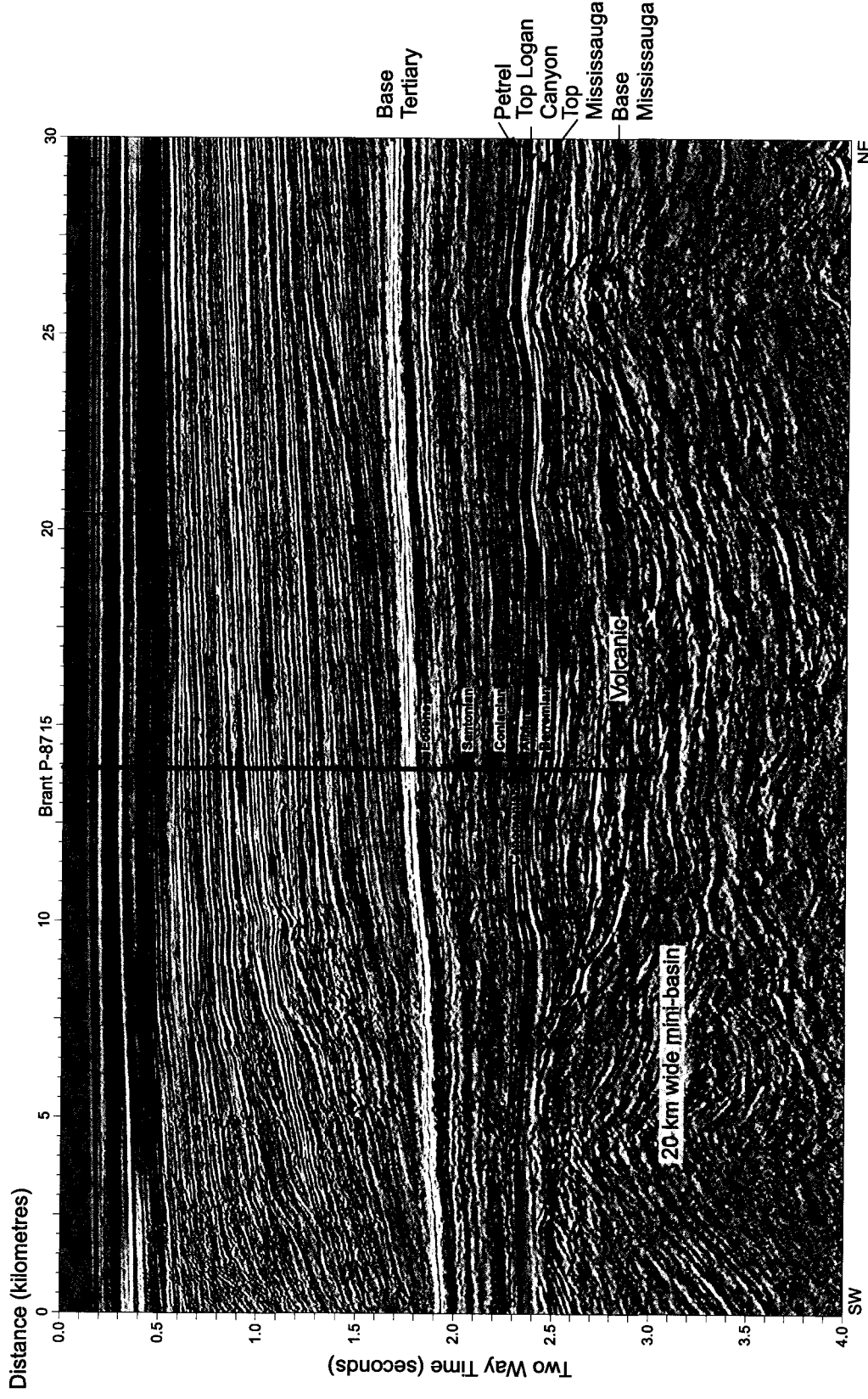
90

Figure 4.12a: NE-SW profile HM82-88 (part 1) showing the well-to-seismic tie of the Brant P-87 well. This profile also shows the correlation to the SW Grand Banks, and the formation of mini-basins in this part of the study area.
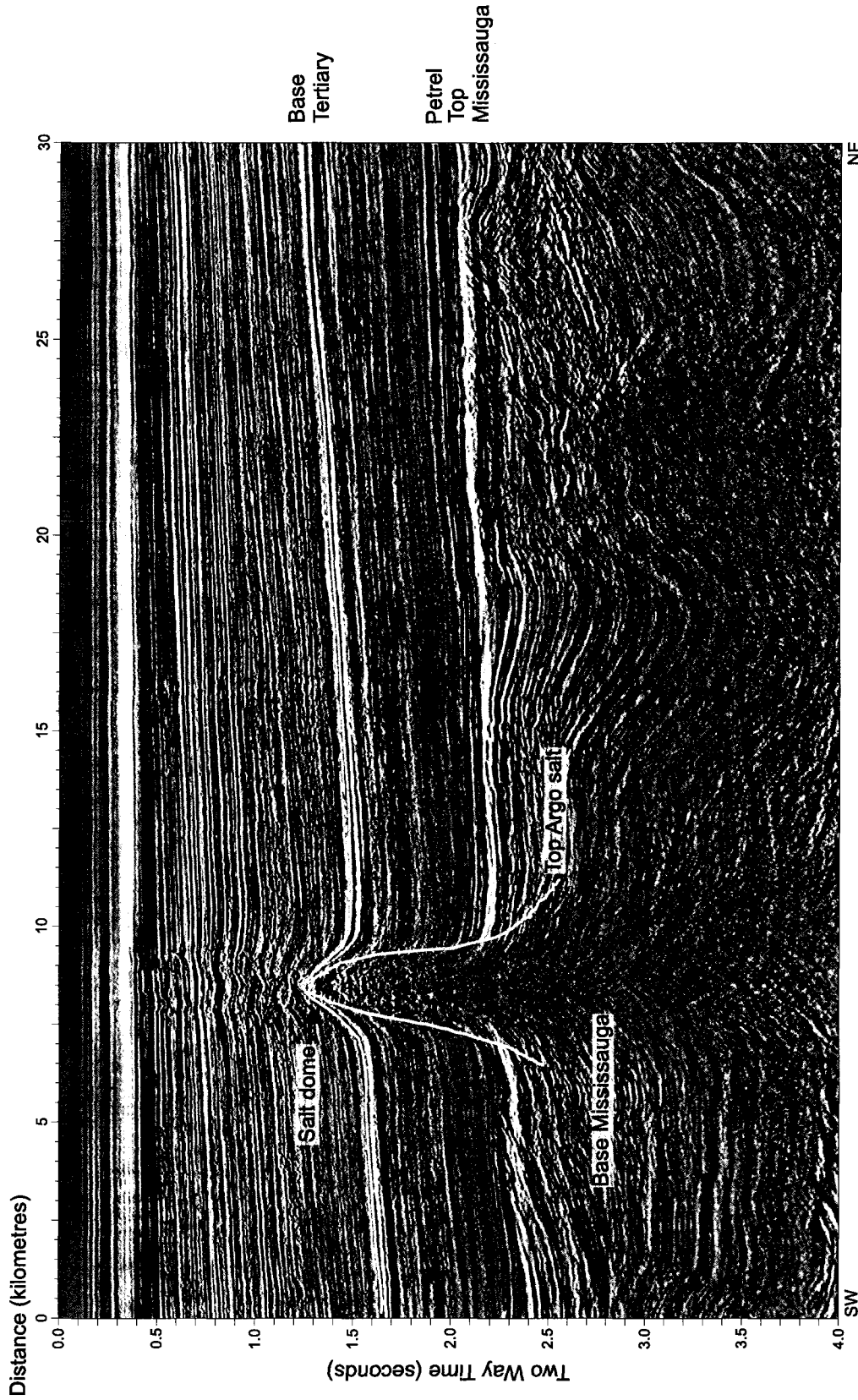
91

Figure 4.12b: NE-SW profile HM82-88 (part 2) correlating the SW Grand Banks and highlighting an example of the salt domes encountered in the seismic throughout the SW Grand Banks

within the volcanic interval of this well discussed in Chapter 3 (Figure 3.1). The volcanic rocks were detected seismically. Also, the well does not penetrate the Base Mississauga reflector and thus this horizon was placed based on direct seismic correlation with surrounding profiles and is inherently uncertain.

Correlation from the Brant P-87 well towards the Mallard M-45 well was made along profiles HM82-81 (Appendix Figure 1.14) and HM82-120 which intersected the Mallard M-45 well (Figure 4.13). The lithostratigraphic and biostratigraphic picks confirm the seismic correlation to this well. The volcanic rock interval discussed in Chapter 3 (Figure 3.2) is detected seismically. Correlation to the Twillick G-49 well was impossible as the seismic profile intersecting this well did not intersect other seismic profiles. The volcanic rock in the Twillick G-49 well discussed in Chapter 3 (Figure 3.3) could not be resolved seismically.

4.2 Seismic evidence of volcanic rocks

4.2.1 Orpheus Graben

Volcanic rocks have been intersected in Argo F-38, Hercules G-15, Jason C-20, Hesper I-52, Emerillon C-56, Brant P-87 and Mallard M-45 and can be identified in seismic data. In the Orpheus Graben wells (Argo F-38, Hercules G-15 and Jason C-20), the basalt flows are thin and the quality of the seismic data is poor, making correlation of the flows difficult. The basalt flows are marked by a very strong reflection at the top of the highest flow. The volcanic horizons in the Argo F-38 and Hercules G-15 wells are imaged in Figure 4.7 along profile 81-405. In the Argo F-38 well, there are two 18-19 m
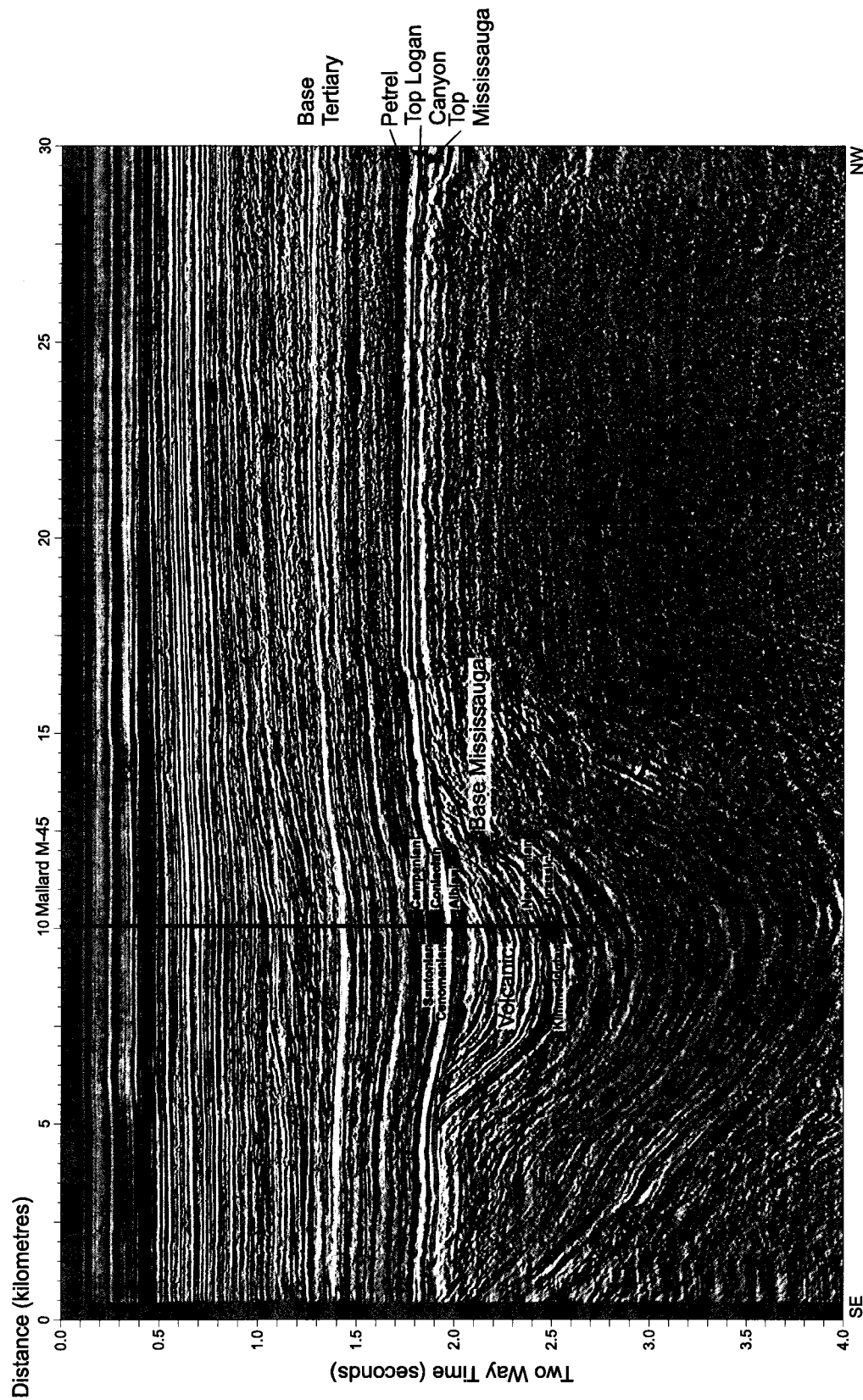
Figure 4.13: NW-SE profile HM82-120 showing the well-to-seismic tie of the Mallard M-45 well. This profile also shows the correlation with the SW Grand Banks and the foramtion of mini-basins encountered in this part of the study area

thick basalt flows separated by 25 m of sediments (Figure 3.7). The resolution of profile 81-405 is approximately 15 m and the flows may not be fully resolvable in the profile. However, due to the strong acoustic impedance contrast of basalt compared to overlying sandstones, the top of each flow generates a strong reflection. The upper basalt flow can only be followed in the seismic profile ~2.5 km away from the well to the NNE and ~10 km away from the well in the SSW direction. The basal basalt flow, however, can be correlated to the Hercules G-15 well. The Hercules G-15 well has two basalt flows, 15 m and 4 m thick, separated by only 4 m of sediments (Figure 3.9). Thus the two flows are not resolvable within this seismic profile and only one strong reflector is seen at the top of the upper flow. In both the Argo F-38 and Hercules G-15 wells, the pyroclastic intervals are capped by the Top Cree unconformity and thus for these wells the Top Cree horizon marks the eroded top of the pyroclastic interval, which can be correlated between wells. In the Jason C-20 well, the basalt flows can only be followed in the seismic profile 3606 for less than 1 km away from the well in any direction (Figure 4.6). Flows may thin beyond the level of vertical resolution; however, even though a layer may not be thick enough to differentiate between the top and bottom of the layer, it should still generate a strong reflector due to the large contrast in acoustic impedance between overlying or underlying sands and shales in this area. The abrupt ending of strong positive reflectors corresponding to the basalt flows points to an equally abrupt ending of the basalt flows at that point. The extent to which the basalt flows can be correlated away from the wells through other seismic profiles is shown in Figure 4.14.
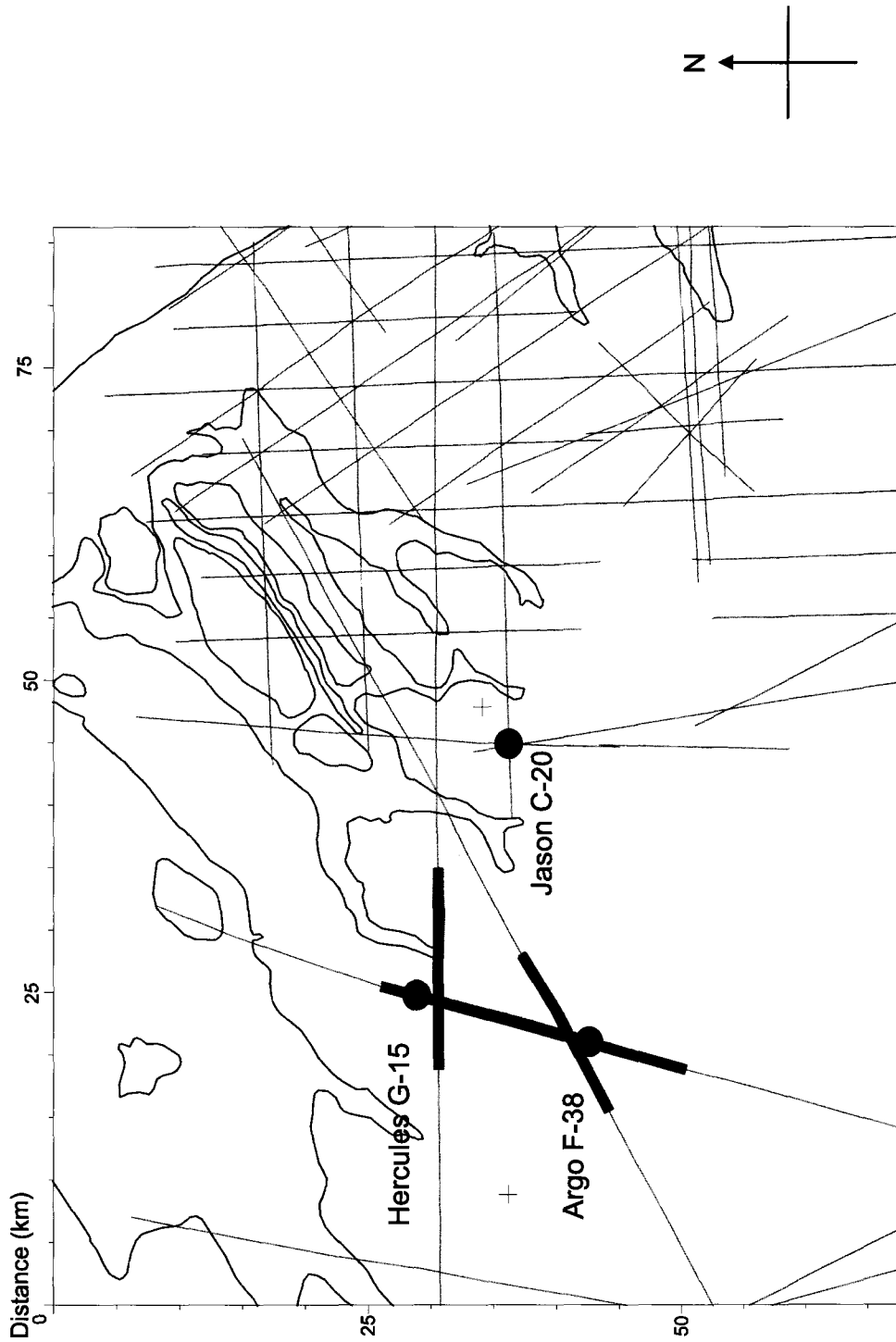
Figure 4.14: Extent of volcanic horizon picked within the Orpheus Graben (shown in red)

96

4.2.2 SE Scotian Shelf

A basalt flow is present in the Hesper I-52 well (Figure 3.10) and its seismic expression is shown in Figure 4.3a and b, appearing as two strong positive reflections at the base of the well. The basalt flow in the Hesper I-52 well is 19 m thick and the resolution of the seismic data is ~15 m. The sonic log for the Hesper I-52 well at this level (Figure 3.10) shows an abrupt increase in sonic velocity at the top of the basalt flow and an abrupt decrease in sonic velocity at the base of the basalt flow. In this profile, the flow can only be traced for ~ 4 km away from the well in the SE direction before the strong double reflection abruptly stops. Correlating horizons to an intersecting NW-SE profile NS-3, the flow also comes to an abrupt end on either side (Figure 4.4a and b). The flow appears to be located on a paleo-high bounded by faults on either side. The extent of the flow from other seismic profiles is shown in Figure 4.15

The basalt flow is not imaged at any other location on the SE Scotian Shelf in available seismic profiles. A possible explanation for the presence of the flow on the paleo-high is that the basalt, most likely sourced from the Orpheus Graben, flowed on the high until it reached a coastline defined by growth faults. The seawater cooled the flow, stopping it at the shoreline. Observations of chlorite and glass in thin sections from cuttings within the basalt flow indicate interaction with water and thus supports the interpretation of a paleoshoreline.

4.2.3 SW Grand Banks

The Emerillon C-56 well intersected a diabase sill much younger than the sediments it had intruded. Part of this sill is imaged in seismic profile STP18 shown in
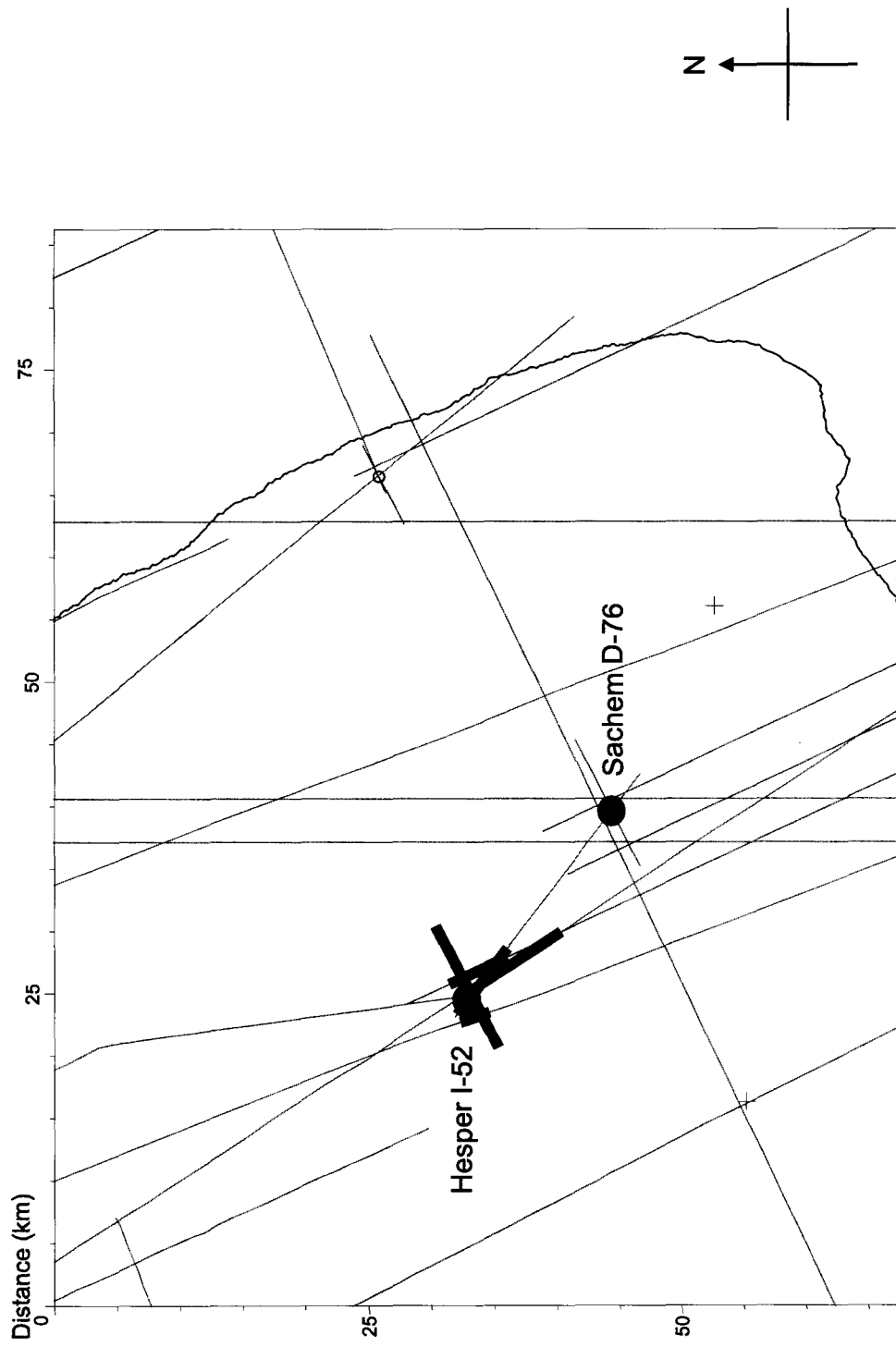
Figure 4.15: Extent of volcanic horizon picked near the Hesper I-52 well on the Scotian Shelf (shown in red)

Figure 4.10. The sill can be traced along the profile ~1 km to the NW of the well and ~2 km to the SE of the well. At each end of the sill that has been traced, the reflectors are offset which may be caused by faulting. Thus it is unclear whether the sill continues in the NW direction through the SE dipping strata until it is truncated by the Base Mississauga unconformity or whether its high amplitude reflector is a sedimentary layer. There are also many strong positive reflectors 0.75-0.95 s (TWT) below the level of the sill, suggesting that there may be a system of sills in this area.

At the Brant P-87 and Mallard M-45 wells there are large thicknesses of volcanic material allowing for a more detailed well-to-seismic tie of these intervals. As shown in Figures 4.12 and 4.13, volcanic horizons in both wells appear to be confined to mini-basins bounded by the Base Mississauga and Top Mississauga unconformities. Interpretations made in Chapter 3, as well as a sonic well log, were placed onto the seismic profiles at the wells to determine how closely the well interpretations match the seismic data.

At the Brant P-87 well, there are multiple strong positive reflectors within the volcanic interval (Figure 4.16). These reflections are strong and continuous in the profiles in the SSW direction but abruptly end halfway through the basin in the NNE direction. Near the base of the well, one of these reflectors was traced and matched the top of the basalt at the base of the well (dark blue horizon in Figure 4.12 and 4.16). A second reflector (purple horizon) was traced near the middle of the volcanic interval. This horizon corresponded to a volcanic breccia interval with no strong sonic or density log response. There are also three strong positive reflections at the top of the volcanic interval, directly under the Top Mississauga horizon. These reflections correspond to the
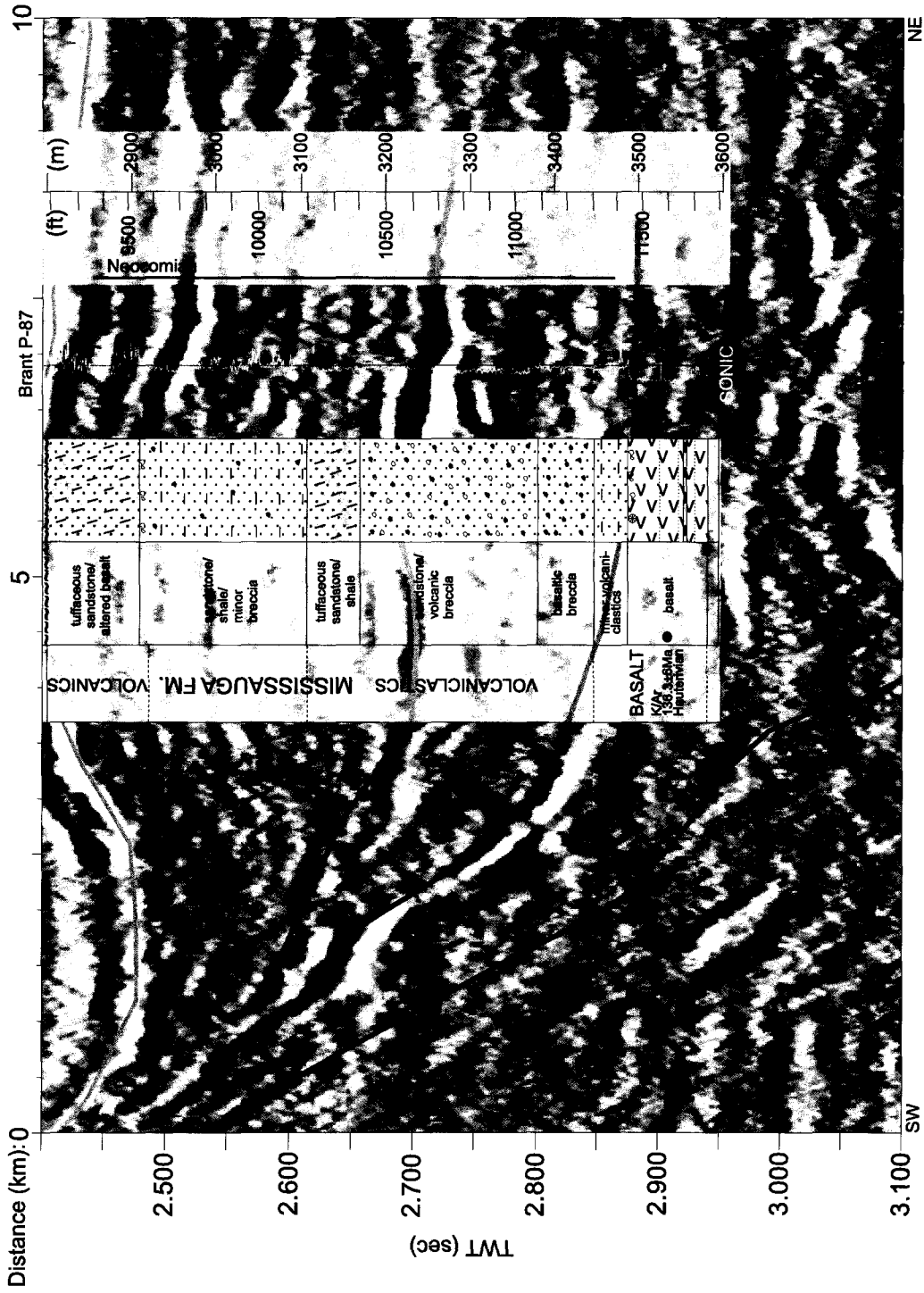
Figure 4.16: NE-SW profile HM82-88 showing a more detailed well-to-seismic tie within the volcanic section of the Brant P-87 well and its correlation to interpretations made in Chapter 3

100

tuffaceous sandstone/altered basalt interval, with moderate sonic and density log responses. Although the purple horizon and the upper reflectors did not correlate with a basalt flow in the well interpretation, it is possible that the well is offset from this seismic profile sufficiently that it did not penetrate nearby basalt flows. There is also the possibility that these flows are weathered enough to not generate a strong sonic or density log response. The blue horizon, which did correlate with the top of the basalt at the base of the well, was correlated through other profiles to attempt to determine a source direction and an extent of the flow. Unfortunately in all directions it was bounded by salt domes beyond which it could not be correlated and thus its known extent is limited to the south and west of the well (Figure 4.17). However, within what could be correlated, reflection amplitude became highest in a SSW direction, which may indicate a source in a general SW direction.

At the Mallard M-45 well, there were also multiple strong positive reflectors within the volcanic interval (Figure 4.18). As with the Brant P-87 well, the reflectors are strong at the SW edge of the basin and become slightly weaker at the NE edge. Unlike the Brant P-87 well, the reflectors within the Mallard M-45 mini-basin match with the interpreted basalt flows and their sonic responses throughout the well. These reflectors were traced as horizons; however, the only other profile onto which the horizons could be correlated (Appendix Figure 1.15) with was an almost exact replica of what was seen at the Brant P-87 well; volcanic horizons were confined to a mini-basin with strong reflectors on the eastern edge of the basin, abruptly stopping midway into the basin in the westward direction. The volcanic horizons mimic the concave shape of the mini-basin. The horizons are conformable and do not cross-cut other reflections which strengthens
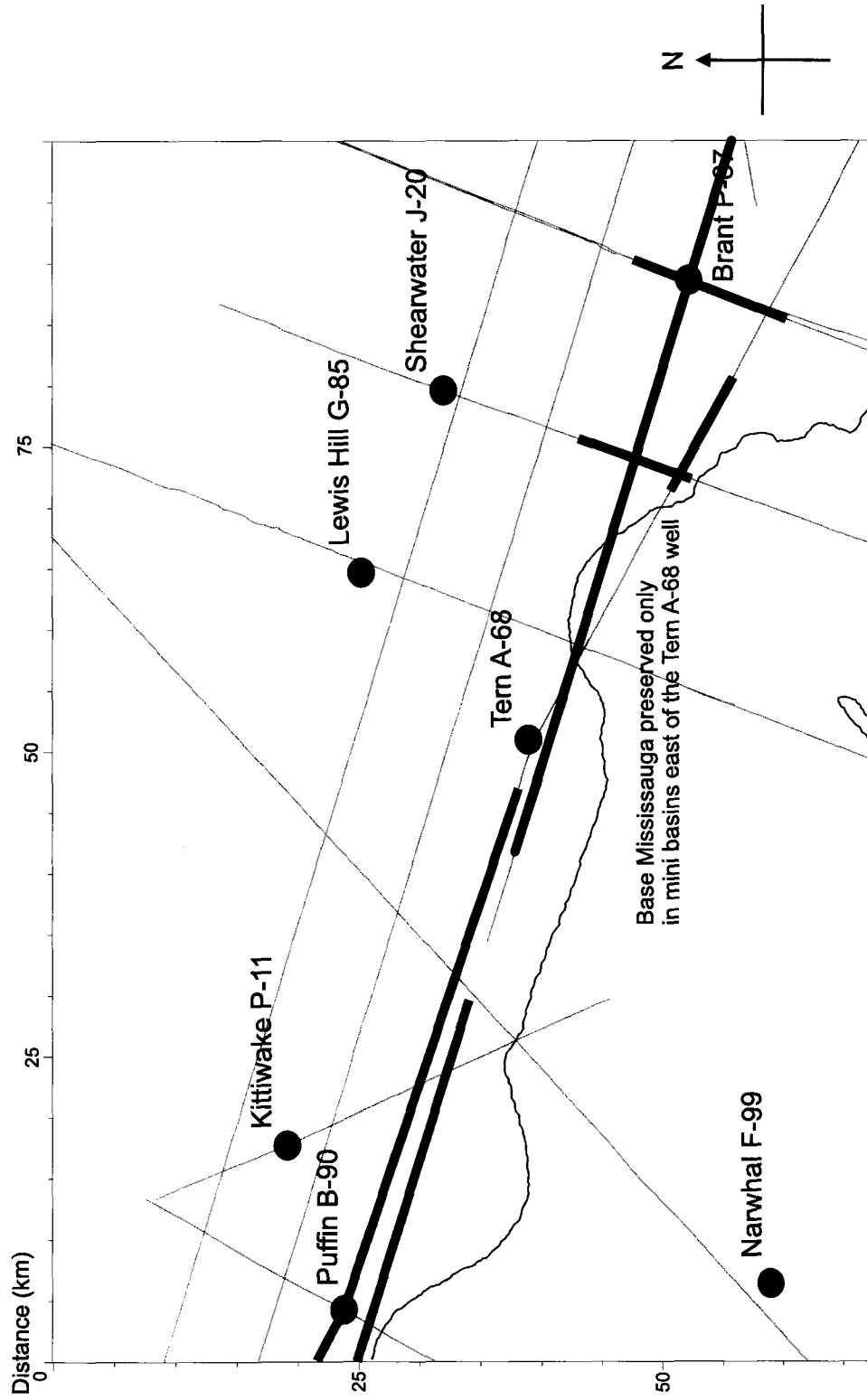
Figure 4.17: Extent of volcanic horizon picked on the SW Grand Banks from the Brant P-87 well (shown in red). Also shown is the extent of the confident picks of the Base Mississauga horizon (shown in blue)
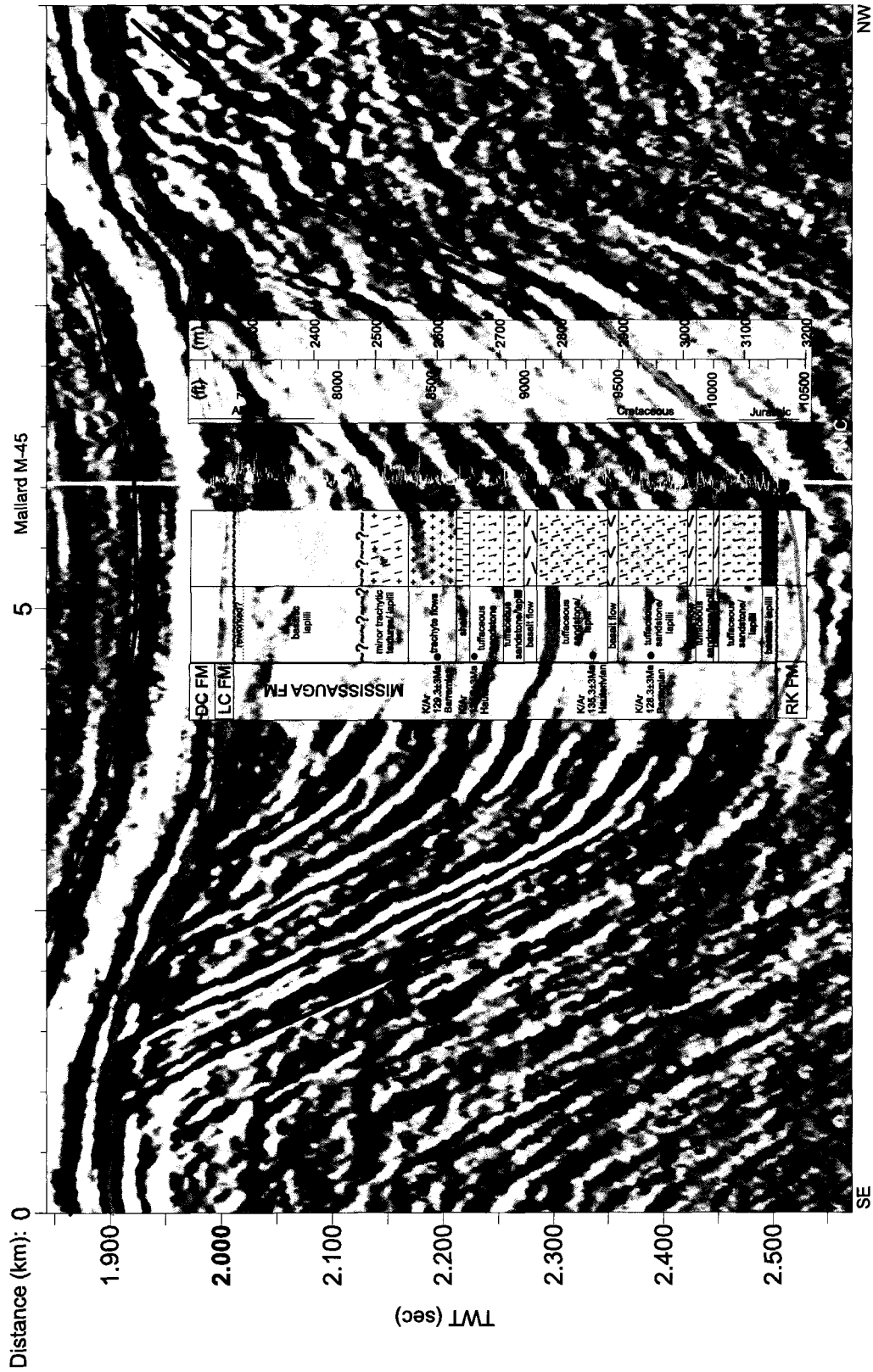
102

Figure 4.18: NW-SE profile HM82-120 showing a more detailed well-to-seismic tie within the volcanic section of the Mallard M-45 well and its correlation to interpretations made in Chapter 3.

the interpretation that the basalts in the Mallard M-45 wells are flows and not sills. Thus it seems as if the source for the Mallard M-45 flows may have been SE direction of the well.

4.3 Seismic evidence of unconformities and tectonic movement

The unconformities correlated throughout the Orpheus Graben, Scotian Shelf and SW Grand Banks are the Base Tertiary unconformity, the mid-Albian Top Cree unconformity, the Aptian Top Mississauga unconformity and the Tithonian Base Mississauga unconformity. The two most prominent unconformities are bounding horizons for this study: the Base Mississauga which is traceable throughout the entire study area, and the Base Tertiary which predominates in the SW Grand Banks area. The other unconformities are not as easily traceable throughout the study area.

The Base Mississauga unconformity represents the base of the Cretaceous sedimentary rocks. This unconformity is traceable in the Orpheus Graben and SE Scotian Shelf. The unconformable relationship to underlying Jurassic strata is much more pronounced on the SW Grand Banks, as seen by peneplanation of underlying strata, than in the Orpheus Graben or SE Scotian Shelf. The most obvious seismic expression of this unconformity is shown in Figure 4.10 along seismic profile STP18 linking the Hermine E-94 well to the Emerillon C-56 well.

The Base Tertiary unconformity marks the base of Tertiary sedimentary rocks. This unconformity is not developed in the Orpheus Graben or on the SE Scotian Shelf where sedimentation appears continuous (Pe-Piper and Piper, 2004), but is well developed within the Laurentian Channel and on the SW Grand Banks. The best

example of the unconformable relationship of this horizon to underlying strata is shown in along profile STP2 where the Base Tertiary cuts down into the Wyandot, Petrel and the Top Cree (Figure 4.8, Appendix Figure 1.8a, b, c, d).

The unconformable relationships of the Top Mississauga and Top Cree horizons can be seen in Figure 4.5a and b along profile E2-14, where both horizons truncate underlying strata. The reflector traced as the Top Cree unconformity is often subtle in seismic profiles as the reflector varies in strength, often becoming too weak to trace with confidence, thus it is not traceable throughout the entire study area. The Top Missisauga is traceable within the Orpheus Graben and SE Scotian Shelf, but it is often conformable in these areas. It becomes more prominent in the eastern portion of the SW Grand Banks as shown in Figure 4.12b along profile HM82-88, where it truncates underlying lower Cretaceous strata.

Unconformities often became more obvious on the flanks of salt domes (e.g. Top Mississauga in Figure 4.12b) and thus the presence of salt domes on the SW Grand Banks aided in identifying unconformities along profiles without closely-spaced well control.

4.3.1 Tectonic movement in the Orpheus Graben and SE Scotian Shelf

The main indicators of tectonic movement in the Orpheus Graben and SE Scotian Shelf are numerous faults and the seaward tilting of Cretaceous strata. These faults are highlighted in Figure 4.19 along NW-SE profile 82-603. The faults appear to be normal faults dipping basinwards and trending orthogonal to the profile, approximately NE-SW. They seem to have been active from the late Jurassic through to sometime within the Tertiary.
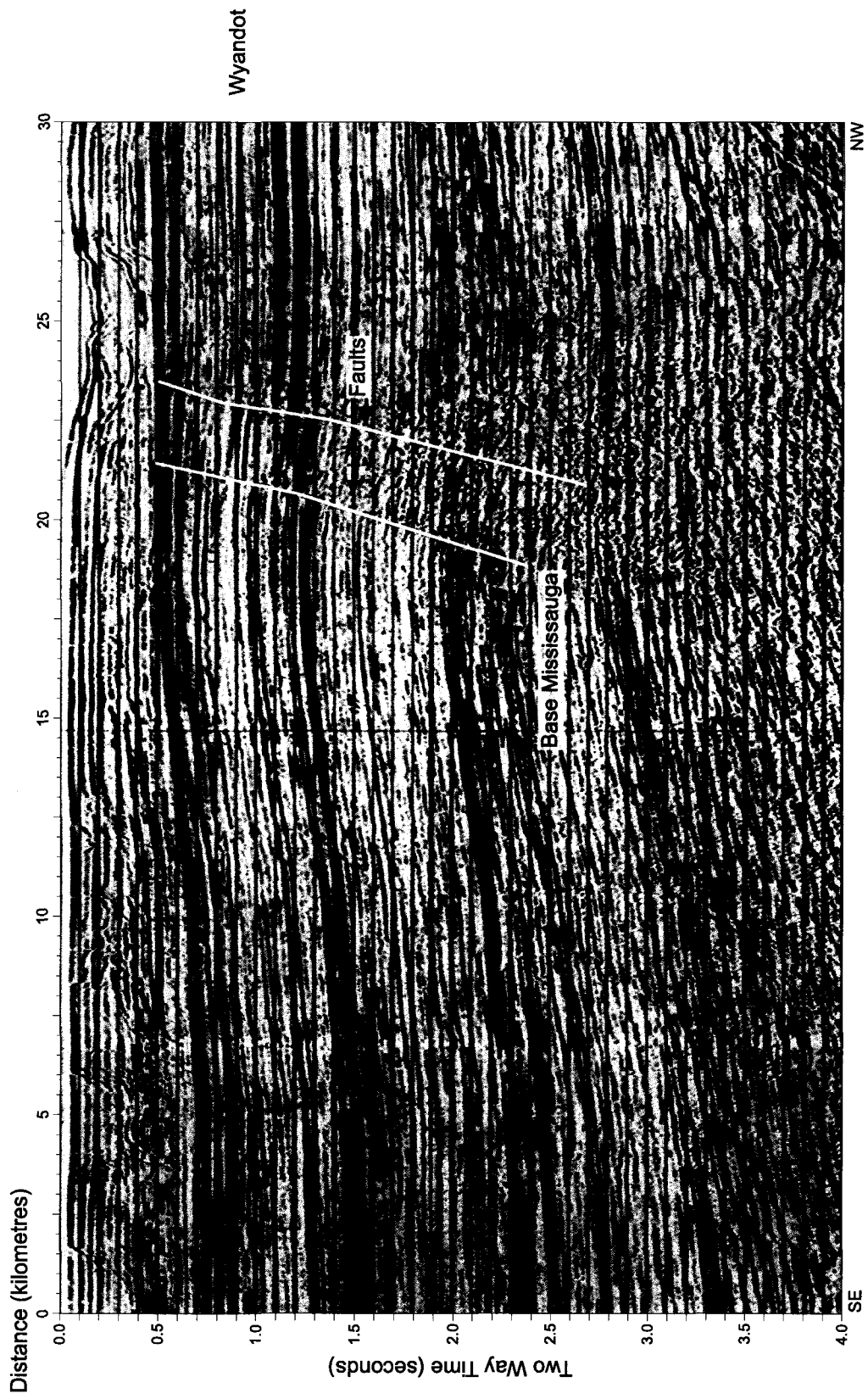
Figure 4.19: NW-SE profile 82-603 showing the typical NE-SW trending, basinward dipping faults encountered on the SE Scotian Shelf

Tilting of the Cretaceous strata can be seen in Figure 4.5a and b along NNE-SSW profile E2-14. The strata are tilted from the north basinwards to the south, which may be expected due to post-rift subsidence. However, it appears as if the tilting occurred in multiple phases during the Cretaceous. Following the Base Mississauga unconformity, the underlying strata were tilted basinwards. This is highlighted by overlying strata, such as the "O" marker, onlapping the Base Mississauga horizon. The Top Mississauga also onlaps the Base Mississauga horizon and thereby pinches out underlying early Cretaceous sediments. At the NNE end of the seismic profile, the Top Mississauga horizon merges with the Base Mississauga horizon. Strata deposited after the Top Mississauga are conformable until they are truncated by the Top Cree unconformity.

4.3.2 Tectonic movement on the SW Grand Banks

The SW Grand Banks can be subdivided into two zones based on the dominance of two different tectonic styles. The dominant indicator of tectonic movement on the SW Grand Banks is the Base Mississauga unconformity that so prominently truncates underlying Jurassic strata. However, the eastern portion of the SW Grand Banks (near the limit of the study area) is dominated by the formation of mini-basins within the lower Cretaceous.

The clearest example of the Base Mississauga unconformity truncating underlying strata was discussed in section 4.3 of this chapter and is shown in Figure 4.10 along profile STP18. This profile clearly shows tilting of Jurassic strata followed by peneplanation at the Base Mississauga unconformity. The tilting of the Jurassic sediments and peneplanation at the Base Mississauga is seen in profiles across most of

the SW Grand Banks with the exception of the eastern-most edge of the study area near the Brant P-87 and Mallard M-45 wells.

In the area of the Brant P-87 and Mallard M-45 wells there is a change in tectonic deformation as mini-basins were formed sometime between the Tithonian Base Mississauga unconformity (~145 Ma) and the Aptian Top Mississauga unconformity (~112 Ma) (Figure 4.12a and b). The mini-basins appear to be separated by eroded horsts.

4.4 Synthesis

MacLean and Wade (1992) also investigated the seismic setting of the Orpheus Graben, SE Scotian Shelf and the western portion of the SW Grand Banks (Abenaki sub-basin), while Weir-Murphy (2004) investigated the seismic setting of the Orpheus Graben and SE Scotian Shelf, using many of the same seismic profile as this study. These authors did not investigate the South Whale sub-basin. As an independent check, the results of their investigations were compared to the findings of this thesis. MacLean and Wade (1992) recognized a latest Jurassic regional unconformity which truncated underlying Jurassic strata. They termed it the Avalon Unconformity which "represents the boundary between more steeply dipping beds below and overlying conformable strata" (MacLean and Wade, 1992). The Avalon Unconformity is equivalent to the Base Mississauga unconformity previously discussed. MacLean and Wade were able to recognize the Avalon unconformity in the Orpheus Graben, across the Canso Ridge and the eastern portion of the Abenaki sub-basin. This correlates well with the Base Mississauga unconformity. However, MacLean and Wade (1992) were unable to

correlate this unconformity within the SE Scotian Shelf or the SW Grand Banks. They claimed that the unconformity cannot be correlated on the SE Scotian Shelf as it is conformable; however, with careful well-to-seismic ties, correlation of the Base Mississauga horizon is possible on the SE Scotian Shelf and is unconformable in places as shown by Figure 4.5a.

MacLean and Wade (1992) then discussed the Mississauga Formation, describing it as thick on the SE Scotian Shelf and SW Grand Banks, but thin to absent near the Emerillon C-56 and Hermine E-94 wells. They also described the "O" marker which is present on the SE Scotian Shelf but onlaps the Avalon Unconformity near the eastern edge of the Laurentian channel. This agrees with the findings of this study, though the onlapping of the "O" marker within this study is found much closer to the western edge of the Laurentian Channel. They did not recognize the Top Mississauga unconformity. This may be due to the fact that its unconformable relationship to underlying strata is the most obvious in the eastern portion of the South Whale sub-basin, which is located outside of the study area of MacLean and Wade (1992).

MacLean and Wade (1992) were unable to recognize any seismic markers within the Logan Canyon Formation. Though the Top Cree and Top Logan Canyon horizons in this study were not correlatable regionally, they were correlatable locally based on well-to-seismic ties. MacLean and Wade (1992) did recognize the regionally continuous Petrel reflector and the Base Tertiary unconformity, which agrees with this study.

The results of the study of Weir-Murphy (2004) in the Orpheus Graben and SE Scotian Shelf are quite similar to the results in this thesis. However, her study was limited to the Orpheus Graben and a very small section of the SE Scotian Shelf between

the Orpheus Graben and the Hesper I-52 well. The most significant disagreement between the work of Weir-Murphy and this thesis is the extent of the volcanic rocks. Weir-Murphy (2004) claims the seismic expression of the volcanic rocks can be traced from the Orpheus Graben east into the Laurentian Channel and south to the Hesper I-52 well on the SE Scotian Shelf. Based on the quality of seismic profiles in this area and the lack of closely spaced well control between the Orpheus Graben and the SE Scotian Shelf, it is highly unlikely a volcanic horizon could be mapped confidently across such a broad region. Also, as evidenced in seismic profile 3604 (Figure 4.3b) and NS-3 (Figure 4.4b), the basalt flow at the Hesper I-52 well appears to end abruptly to the NW and SE away from the well site.

CHAPTER 5
BASIN MODELING

5.1 Introduction

In the previous chapters it has been shown that Cretaceous volcanism in the Orpheus Graben, SE Scotian Shelf and SW Grand Banks was sustained for periods of up to 15-20 Ma in the Orpheus Graben and SE Scotian Shelf (Aptian to mid-Albian) and up to 10-20 Ma on the SW Grand Banks (Berriasian-Barremian). Such sustained volcanic activity is generally a manifestation of a high regional heat flow (Francis and Oppenheimer, 2004). A PetroMod 10 (by Schlumberger) 1D model was generated for several wells within the Scotian Basin to test hypotheses of regional heat flow as manifested by Cretaceous volcanism within the Scotian Basin. The results of the models can be compared to measured data such as present day downhole temperatures and vitrinite reflectance, and where it exists, apatite fission track and fluid inclusion data determined from samples within wells in the Scotian Basin. Vitrinite reflectance data is a good proxy for hydrocarbon maturation as it deals with a measure of maturation. Although a short-lived pulse of high heat flow would most likely not have a significant effect on vitrinite reflectance and thus on hydrocarbon maturation within the Scotian Basin, high heat flow may play an important role on the diagenesis of sediments within the basin, such as the rates at which cements precipitate. Previous basin models have focused on the effects of rifting and subsidence on the thermal evolution of Scotian Basin sediments (Royden and Keen, 1980; Keen and Beaumont, 1990; Keen et al., 1993; Dehler and Keen, 1993; Williamson et al., 1995); however, none of these models have included the effect of Cretaceous volcanism on the thermal history of the sedimentary basins.

111

5.2 Modeling procedure

All models generate calculated burial history plots, which include compaction, with a temperature overlay that shows the calculated increase and decrease of temperatures within the entire system over time as determined by the assigned heat flow input. The models also generate burial history plots with a heat flow overlay which show the increase and decrease of heat flow within the entire system over time. The models also generate downhole temperature profiles and vitrinite reflectance profiles which are compared with measured downhole temperatures and vitrinite reflectance data, the results of which will be discussed in this chapter.

Models of extensional basins generally follow two styles: a pure shear model, or a two layer model of pure and simple shear called a two layer stretching model. A pure shear model is that described by McKenzie (1978) in which the lithosphere deforms as a single layer with thinning and stretching as the ratio (β) of post-rift thickness of the lithosphere to pre-rift thickness of the lithosphere. The resultant β value therefore will be larger in areas of greater extension and lithospheric thinning and smaller in areas of lesser extension and lithospheric extension. In this model the increase of heat flow related to rifting is instantaneous followed by an exponential decay of heat flow towards equilibrium. The two layer stretching model is an evolution of the pure shear model in which the crust and lower lithosphere are separated and stretch independently of each other by a value of β in the crust and δ in the lithosphere (Royden and Keen, 1980; Hellinger and Sclater, 1983). As this study is more concerned with the thermal effect of volcanism on the sedimentary system and not a detailed extensional crustal model, a simple pure shear McKenzie-style model was used to approximate the heat flow related

to rifting. At time of writing, software licensing was not available to calculate a direct

McKenzie rift model, and thus an approximation is made which will be identified in this

study as a "McKenzie-style model".

An initial model (A) was generated based on the present day depths and

thicknesses of formations and members, their depositional ages, lithologies and present

day water depth. This was done to approximate normal burial with normal background

heat flow; no subsequent heat flow was added to the system. A second model (B) used

the McKenzie-style model to approximate the result of heat flow related to rifting. In this

model, an instantaneous heat flow increase is placed at the end of rifting, with the first

occurrence of extruded oceanic crust. Although an instantaneous rift is intuitively

unrealistic, Jarvis and McKenzie (1980) have indicated that the results of an

instantaneous stretching model do not differ significantly from true behavior as long as

the duration of rifting is less than or equal to $60/\beta^2$ Ma. Dehler and Keen (1993)

calculated the β value for the Orpheus Graben to be approximately 1.25. Plugging these

numbers into the Jarvis and McKenzie (1980) equation,

$$60/\beta^2 = 60/1.25^2 = 38.4 \text{ Ma},$$

Rifting on the Scotian margin has previously been determined to span 220-180 Ma, with

the first oceanic crust interpreted to have been extruded at 180 Ma (Sheridan, 1983; Hinz

et al., 1984; Klitgord and Schouten, 1986). Thus, this 40 Ma span is approximately equal

to the result of 38.4 Ma and fits the criteria of Jarvis and McKenzie (1980) for acceptance

of the instantaneous rifting model. On the SW Grand Banks, the β value was calculated

by Keen and Dehler (1993) to range from approximately 1.0 to 2.0. This range in β

values reflects the complex rifting history of the SW Grand Banks which has been

affected by the late Triassic-early Jurassic rifting of the Scotian margin and the early

Cretaceous rifting that separated the Grand Banks from Iberia. Using the β values

calculated for the SW Grand Banks, the Jarvis and McKenzie (1980) equation gives:

$$60/1.0^2 = 60 \text{ Ma,} \qquad \text{and} \qquad 60/2.0^2 = 15 \text{ Ma,}$$

For the purposes of this study, only the early Cretaceous rifting of the SW Grand Banks

from Iberia will be taken into account as this is the rifting stage in which ocean crust was

extruded, similar to the late Triassic-early Jurassic rifting of the Scotian margin. Rifting

of the SW Grand Banks in this second early Cretaceous stage had extension that began in

the latest Jurassic-earliest Cretaceous and culminated near the end Aptian time (Grant and

McAlpine, 1990; Tucholke et al., 2007). Therefore the rifting period of the SW Grand

Banks is inferred to have occurred from 145.5-112 Ma. This span of 33.5 Ma fits within

the upper limit of 60 Ma calculated from the Jarvis and McKenzie (1980) equation, but

does not fit with the lower limit of 15 Ma. The larger β values of >1.3 are located on

the steep continental slope and represent only a very small proportion of total β values on

the SW Grand Banks. Also, the wells being used for this study are all located in the

region of less than 1.3 β values, with the exception of the Narwhal F-99 well. For this

reason, β values greater than 1.3 will be omitted. In this case, the Jarvis and McKenzie

equation gives:

$$60/1.3^2 = 35.5 \text{ Ma,}$$

Using the more representative β values of 1.0-1.3 constrains use of the instantaneous

rifting model to rifting lasting less than or equal to 60-35.5 Ma which would include the

rifting duration of the SW Grand Banks of approximately 33.5 Ma.

A McKenzie style model requires an initial heat flow increase, followed by exponential heat flow decay over time. The initial instantaneous increase in heat flow commonly used for rift basins is 90 mW/m^2 (Jones et al., 2007). The Orpheus Graben is not located directly along the edge of the rifted margin and thus its heat flow at rifting was most likely not as high as the rest of the margin (pers. comm. Sonya Dehler, 2010). Nevertheless, the end member value of 90 mW/m^2 will be used to estimate the upper limit of heat flow related to rifting in the entire area. Similarly, as the SW Grand Banks is located along a transform margin and not directly on the rift margin, its heat flow might be expected to be slightly lower than that of the rift margin; however, the end member value of 90mW/m^2 will also be used in this area to determine an upper limit of heat flow related to rifting in the area. Present day heat flow across the Scotian Shelf and Grand Banks has been estimated to be an average of 40-50 mW/m^2 (MacKenzie et al., 1985; Issler and Beaumont, 1986, 1988) and thus an average value of 45 mW/m^2 will be used as present day heat flow. The values used to generate a McKenzie-style model for the Scotian Shelf and SW Grand Banks are listed in Table 5.1 and 5.2 and a schematic of the heat flow decay used for model B is shown in Figure 5.1 for the Scotian Shelf and Figure 5.2 for the SW Grand Banks.
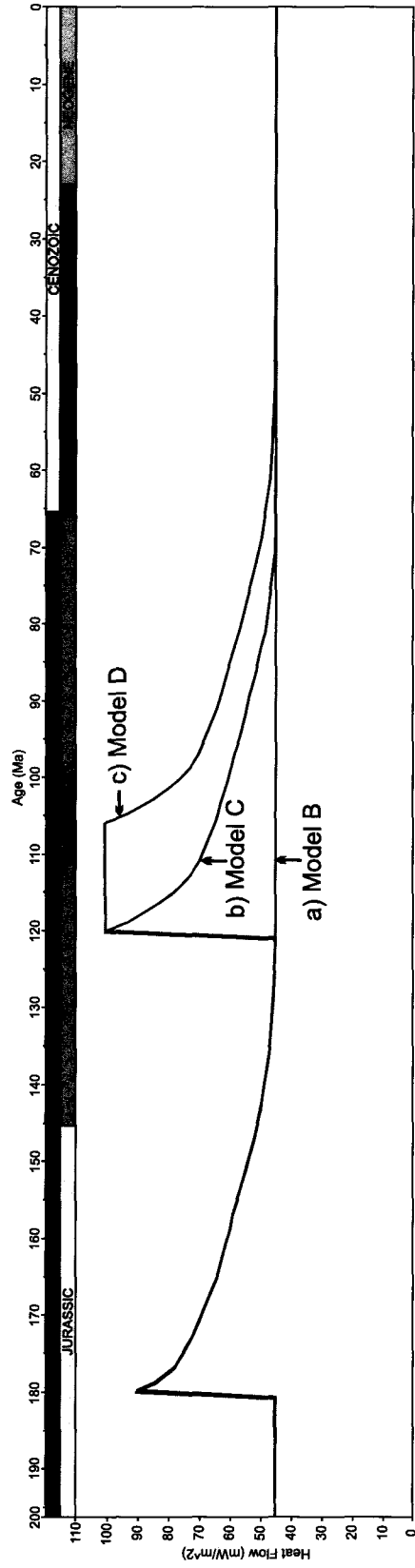
Figure 5.1: Graph showing heat flow inputs used for a) model B in green, b) model C in red and c) model D in blue, for the Orpheus Graben and Scotian Shelf

116
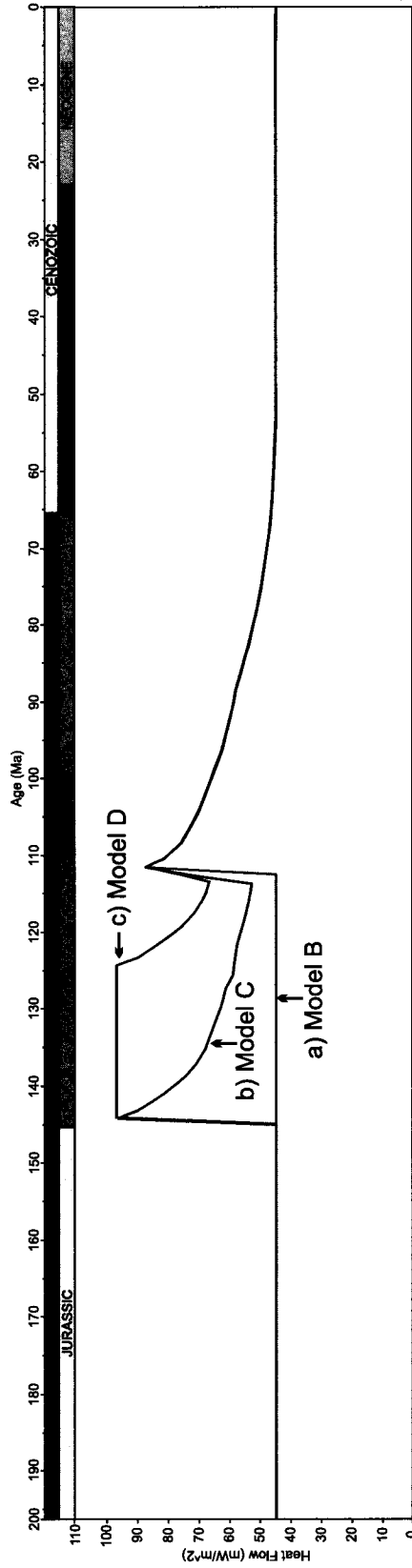
Figure 5.2: Graph showing heat flow inputs used for a) model B in green, b) model C in red and c) model D in blue, for the SW Grand Banks

117

Age (Ma)	Heat Flow (mWm^2)	Age (Ma)	Heat Flow (mWm^2)
200	45	157	59
181	45	155	57.5
180	90	153	56
179	84	151	54.5
177	78	149	53.5
175	75	147	52
173	72	145	51
171	70	143	50
169	68	135	47
167	66	130	46
165	64	125	45.5
163	62.5	120	45
159	60	0	45

Table 5.1: List of heat flow values used in Model B to simulate a McKenzie-style rifting model for the Orpheus Graben.

Age (Ma)	Heat Flow (mWm^2)	Age (Ma)	Heat Flow (mWm^2)
200	45	89	59
113	45	87	57.5
112	90	85	56
111	84	83	54.5
109	78	81	53.5
107	75	79	52
105	72	77	51
103	70	75	50
101	68	67	47
99	66	62	46
97	64	57	45.5
95	62.5	52	45
91	60	0	45

Table 5.2: List of heat flow values used in Model B to simulate a McKenzie-style rifting model for the SW Grand Banks.

A third model (C) was then generated using the McKenzie-style model discussed above to approximate heat flow related to rifting, however, in this model a second heat flow pulse at the time of volcanism in the Orpheus Graben and SW Grand Banks was added to the system. More specifically, the second heat flow pulse represents a regional heat pulse, of which the volcanism in these areas is a manifestation.

Estimating the amount of heat flow that would have been generated by upwelling magma is difficult as after more than 100 Ma, the heat flow associated with the volcanism has dissipated. Modern analogues of young volcanism such as mid-ocean ridges and the Basin and Range province of the western United States have been found to generate a heat flow from 80-120 mW/m^2 (Eldholm et al., 1999; Sarna-Wojcicki et al., 1984; Blackwell, 1983), and thus a mid-value of 100 mW/m^2 was used to estimate the heat flow associated with the volcanism in the Orpheus Graben and SW Grand Banks. Similar to heat flow related to rifting, a McKenzie style heat flow model was used with instantaneous heat flow increase and an exponential heat flow decay over time. The values used to generate a McKenzie-style model for model C of the Scotian Shelf and SW Grand Banks are listed in Table 5.3 and 5.4 and a schematic of the heat flow decay used for model C is shown in Figure 5.1 for the Scotian Shelf and Figure 5.2 for the SW Grand Banks.

Age (Ma)	Heat Flow (mW/m^2)	Age (Ma)	Heat Flow (mW/m^2)	Age (Ma)	Heat Flow (mW/m^2)
200	45	151	54.5	107	66
181	45	149	53.5	105	64
180	90	147	52	103	62.5
179	84	145	51	101	61
177	78	143	50	97	58.5
175	75	135	47	95	57
173	72	130	46	93	55.5
171	70	125	45.5	91	54.5
169	68	121	45	89	53.5
167	66	120	100	87	52
165	64	119	93	85	51
163	62.5	117	85	83	50
159	60	115	78	81	48.5
157	59	113	73	76	47
155	57.5	111	70	71	45.5
153	56	109	68	66	45
				0	45

Table 5.3: Values used in Model C to estimate heat flow due to rifting with an additional heat flow related to volcanism in the Orpheus Graben and Scotian Shelf.

Age (Ma)	Heat Flow (mW/m^2)	Age (Ma)	Heat Flow (mW/m^2)	Age (Ma)	Heat Flow (mW/m^2)
200	45	120	57	91	60
146	45	118	55.5	89	59
145	100	116	54.5	87	57.5
144	93	114	53.5	85	56
142	85	112	90	83	54.5
140	78	111	84	81	53.5
138	73	109	78	79	52
136	70	107	75	77	51
134	68	105	72	75	50
132	66	103	70	67	47
130	64	101	68	62	46
128	62.5	99	66	57	45.5
126	61	97	64	52	45
122	58.5	95	62.5	0	45

Table 5.4: Values used in Model C to estimate heat flow due to rifting with an additional heat flow related to volcanism on the SW Grand Banks.

Finally, a fourth model, Model D, was generated similar to Model C with the exception of the duration of high heat flow associated with volcanism. In Model D, the onset of a high heat flow of 100 mW/m² is instantaneous; however, the heat flow was maintained at 100 mW/m² for the maximum duration of volcanism (120-105 Ma in the Orpheus Graben and 145-125 Ma on the SW Grand Banks) before a McKenzie style decay was initiated. The values used to generate a McKenzie-style model for model D of the Scotian Shelf and SW Grand Banks are listed in Table 5.5 and 5.6 and a schematic of the heat flow decay used for model D is shown in Figure 5.1 for the Scotian Shelf and Figure 5.2 for the SW Grand Banks

Age (Ma)	Heat Flow (mW/m2)	Age (Ma)	Heat Flow (mW/m2)	Age (Ma)	Heat Flow (mW/m2)
200	45	149	53.5	94	68
181	45	147	52	92	66
180	90	145	51	88	64
179	84	143	50	84	62.5
177	78	135	47	82	61
175	75	130	46	80	58.5
173	72	125	45.5	78	57
171	70	121	45	76	55.5
169	68	120	100	74	54.5
167	66	115	100	72	53.5
165	64	110	100	70	52
163	62.5	105	100	68	51
159	60	104	93	60	50
157	59	102	85	55	48.5
155	57.5	100	78	50	47
153	56	98	73	45	45.5
151	54.5	96	70	0	45

Table 5.5: Values used in Model D to estimate heat flow due to rifting with an additional prolonged heat flow related to volcanism in the Orpheus Graben and Scotian Shelf.

Age (Ma)	Heat Flow (mW/m2)	Age (Ma)	Heat Flow (mW/m2)	Age (Ma)	Heat Flow (mW/m2)
200	45	114	68	89	59
146	45	112	90	87	57.5
145	100	111	84	85	56
140	100	109	78	83	54.5
135	100	107	75	81	53.5
130	100	105	72	79	52
125	100	103	70	77	51
124	93	101	68	75	50
122	85	99	66	67	47
120	78	97	64	62	46
118	73	95	62.5	57	45.5
116	70	91	60	52	45
				0	45

Table 5.6: Values used in Model D to estimate heat flow due to rifting with an additional prolonged heat flow related to volcanism on the SW Grand Banks

Results of the calculated burial history plot with temperature overlay are compared with measured data such as apatite fission track and fluid inclusion data which will be discussed in the next chapter. As the Cretaceous Mississauga and Logan Canyon Formations are the focus of this thesis, emphasis will be placed on results within these formations for all models.

To avoid repetition, models A through D will be described for the first well only (Jason C-20), however, any significant differences in modeled results will be highlighted. For the remaining wells on the Scotian Shelf and SW Grand Banks, only model D will be described along with associated figures. Maximum temperatures reached for each formation for each model will be listed in subsequent tables within Appendix 2, along with corresponding figures for models A-C.

5.3 Application to Orpheus Graben and Scotian Shelf

As models are generated to test hypotheses against measured data, that success depends on the availability of measured data. In the Orpheus Graben, availability and quality of measured data such as reliable biostratigraphy and vitrinite reflectance was limited and thus only the Jason C-20 well could be modeled with any degree of confidence. All four models (A-D) were run for this well. In the Orpheus Graben, the timing of volcanism is within the lower Cretaceous Aptian age, and thus models C and D were generated with heat flow introduced at 120 Ma. In an effort to test a regional heat flow hypothesis, a second well was chosen within the Sable sub-basin closer to the location of samples used by other authors to obtain thermal data, such as apatite fission track and fluid inclusion data (Li et al., 1995; Karim et al., 2010). The chosen well is Chebucto K-90.

5.3.1 Jason C-20

The results of model A produced identical results to model B, and thus only model B will be discussed here. Model B generated a burial history plot with a temperature overlay indicating maximum temperatures in all formations were reached at the maximum burial depth (Figure 5.3). The maximum temperature reached within the Mississauga Formation was 63°C while the Logan Canyon Formation reached 48°C. Unfortunately in the Jason C-20 well, there is only one Horner corrected measured downhole temperature value to compare with the modeled downhole temperature profile. The modeled temperature profile does not match the measured temperature (Figure 5.4).
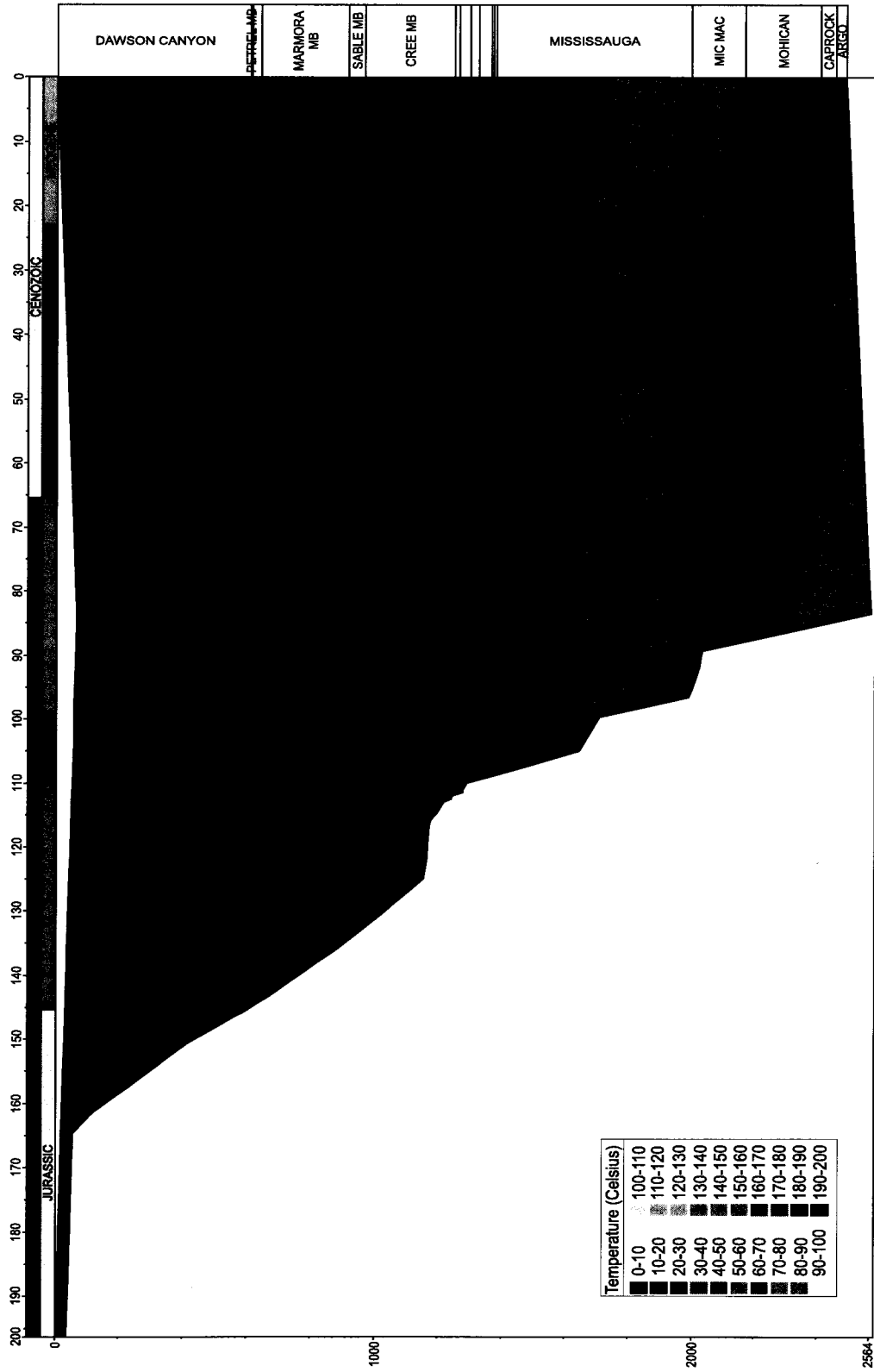
Figure 5.3: Burial history plot with temperature overlay for model B in the Jason C-20 well
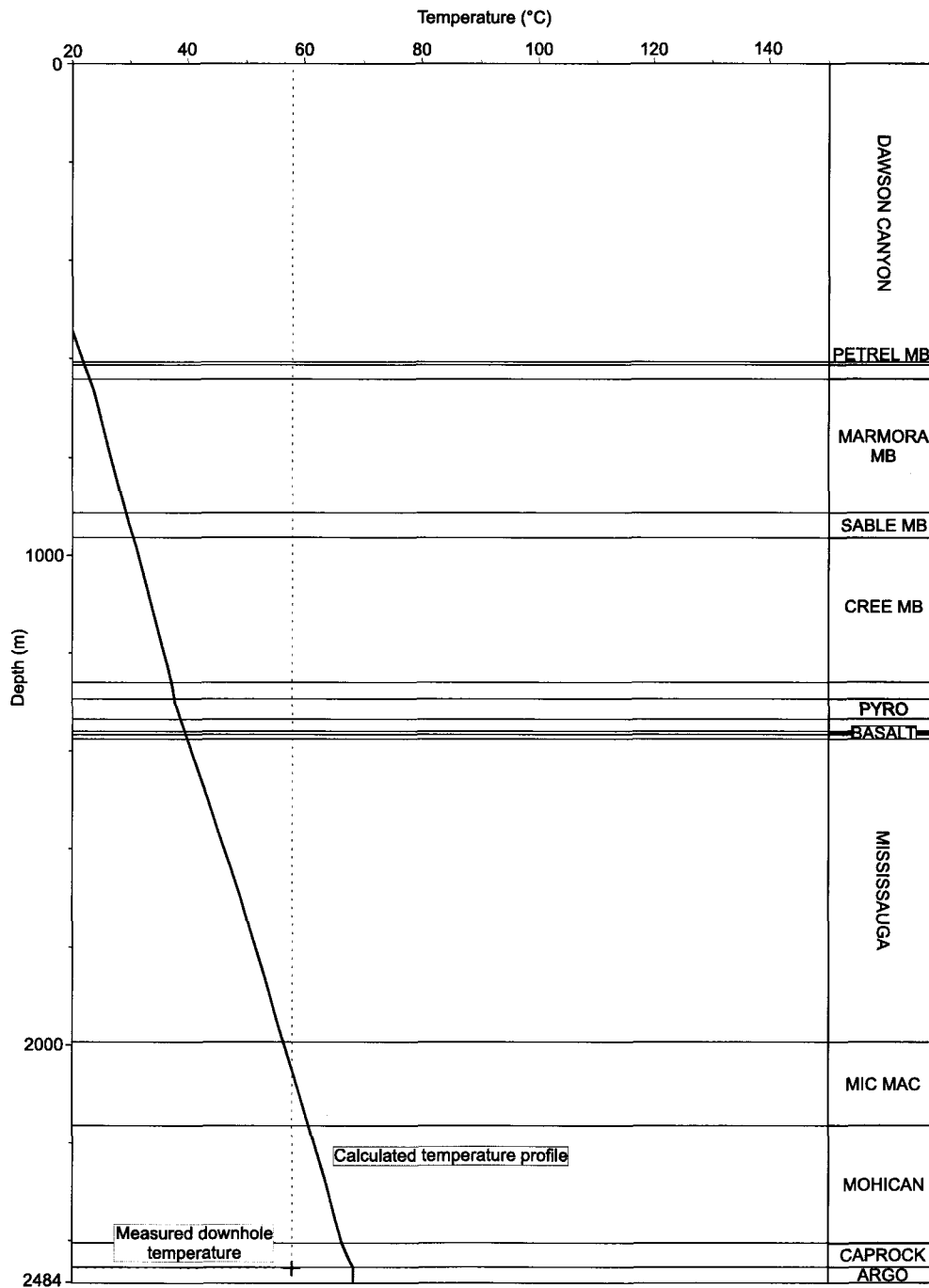
Figure 5.4: Modeled temperature profile versus measured downhole temperatures for model B in the Jason C-20 well

125
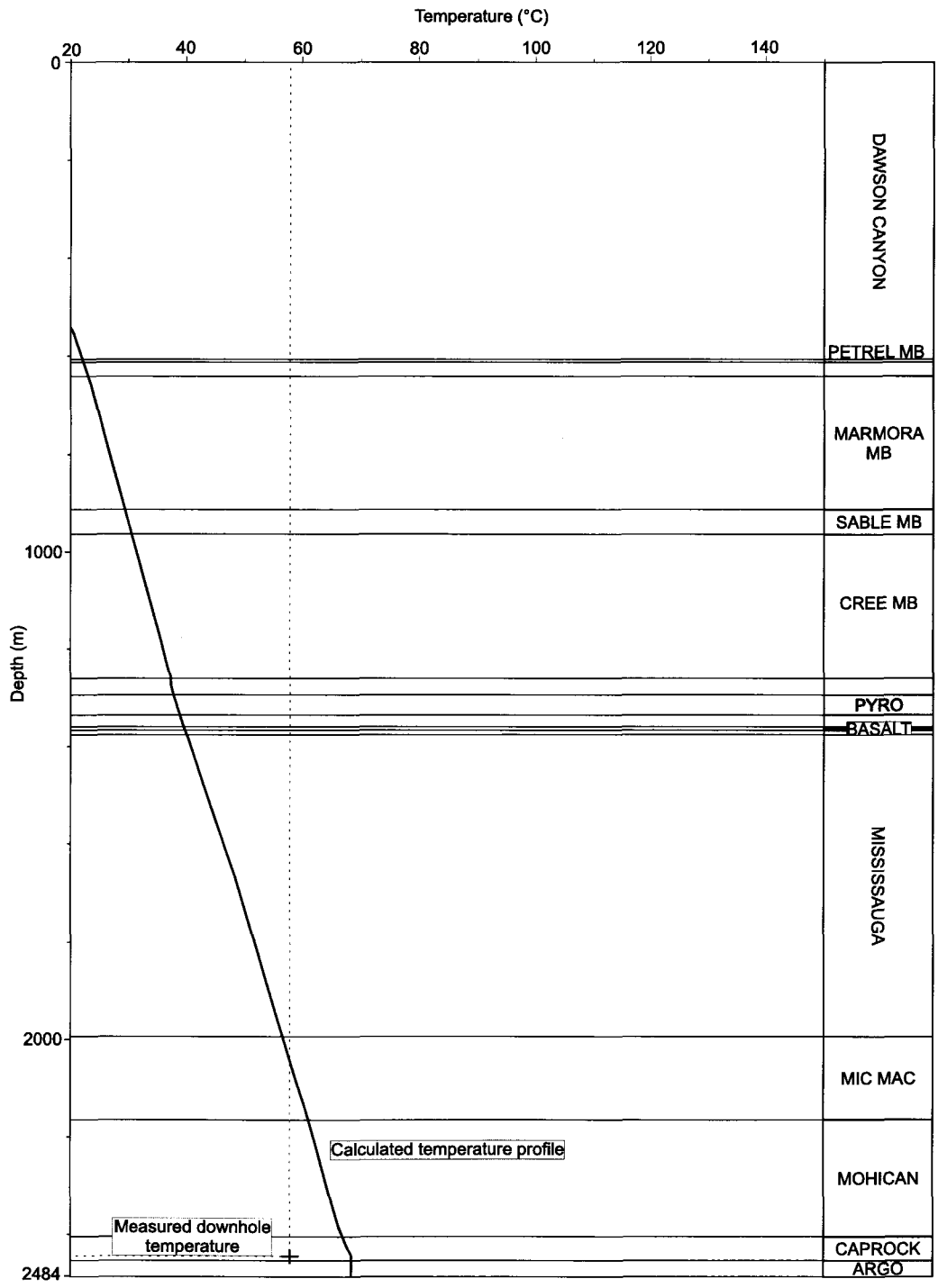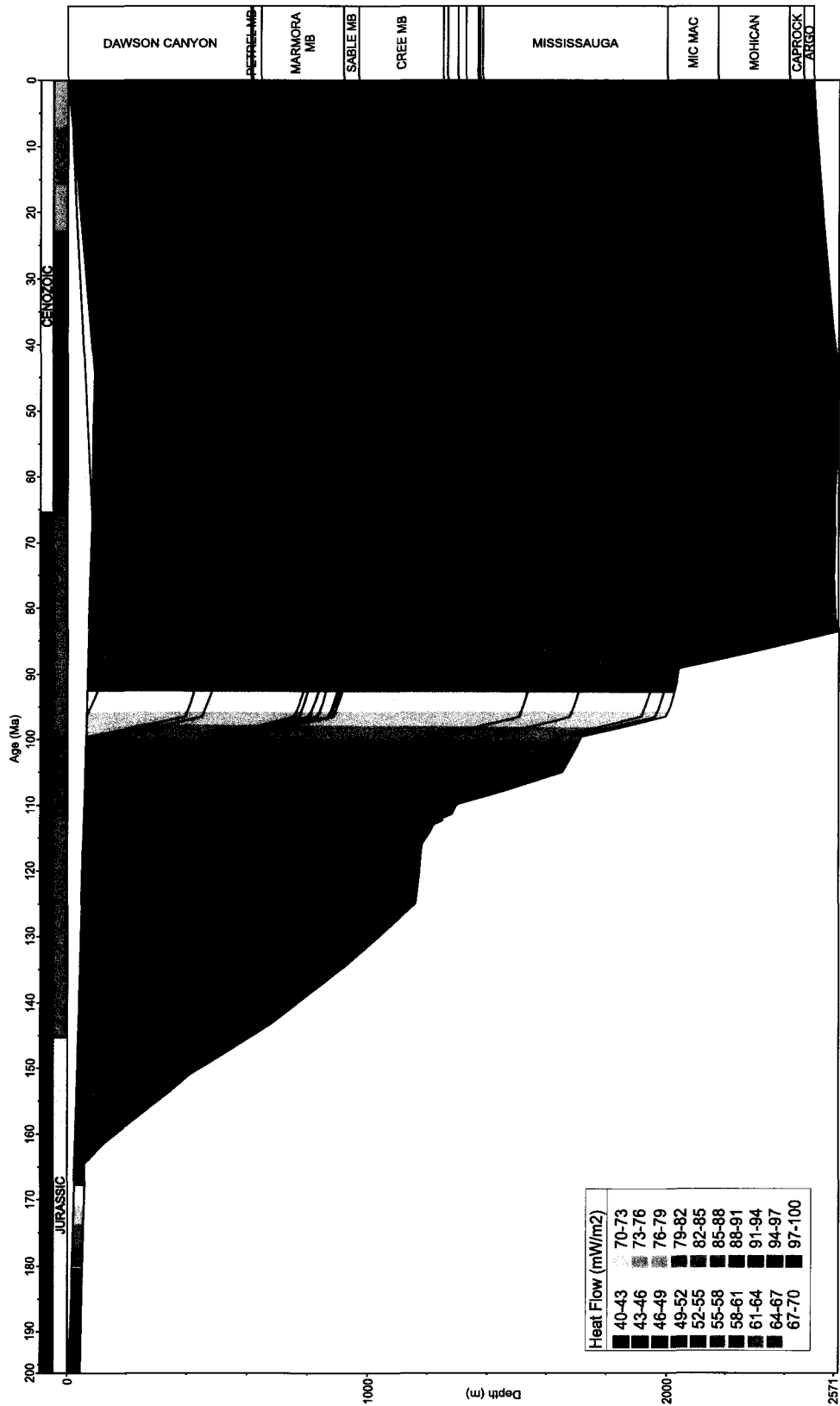
The burial history plot with a heat flow overlay is shown in Figure 5.5. The modeled profile is a close fit with the measured values of vitrinite reflectance (Figure 5.6).

Model C generated a slightly different temperature overlay than Model B, however, the results are generally the same. Although there is a temperature spike in the burial history plot with a temperature overlay at the time of volcanism, maximum temperatures in all formations were reached at maximum burial during the late Cretaceous (~85 Ma). The maximum temperatures in the Mississauga and Logan Canyon formations reached 70°C and 52°C respectively (Figure 5.7). The modeled temperature profile is the same as in model B and does not match the measured temperature (Figure 5.8). The burial history plot with a heat flow overlay is shown in Figure 5.9. The modeled vitrinite reflectance profile is almost identical to model B but with a slight shift to the right (higher Ro% values) within the Mic Mac Formation (Figure 5.10).

Model D generated a modeled result different from the result in Model C. The burial history plot with a temperature overlay shows maximum temperatures in all formations were reached at maximum burial, however; temperatures nearing maximum temperatures in all formations below the Logan Canyon Formation were reached at the time of volcanism. A maximum temperature of 81°C is reached in the Mississauga Formation during both time of volcanism at 105 Ma and at maximum burial at 85 Ma. In the Logan Canyon Formation, a maximum temperature of 58°C is reached at time of maximum burial (Figure 5.11). The modeled temperature profile is the same as in model B and C and does not match the measured temperature (Figure 5.12). The burial history plot with a heat flow overlay is shown in Figure 5.13. The modeled vitrinite reflectance
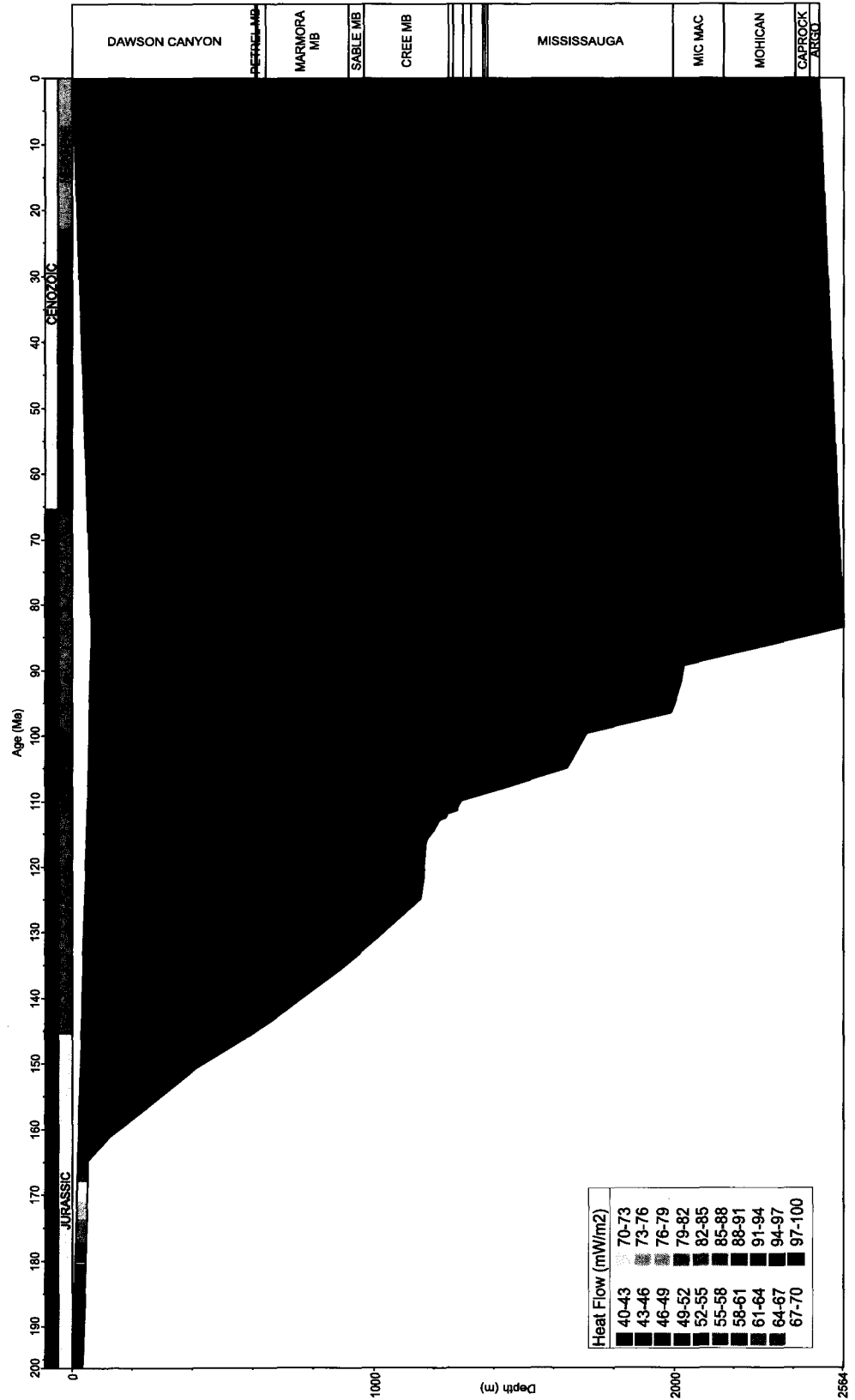
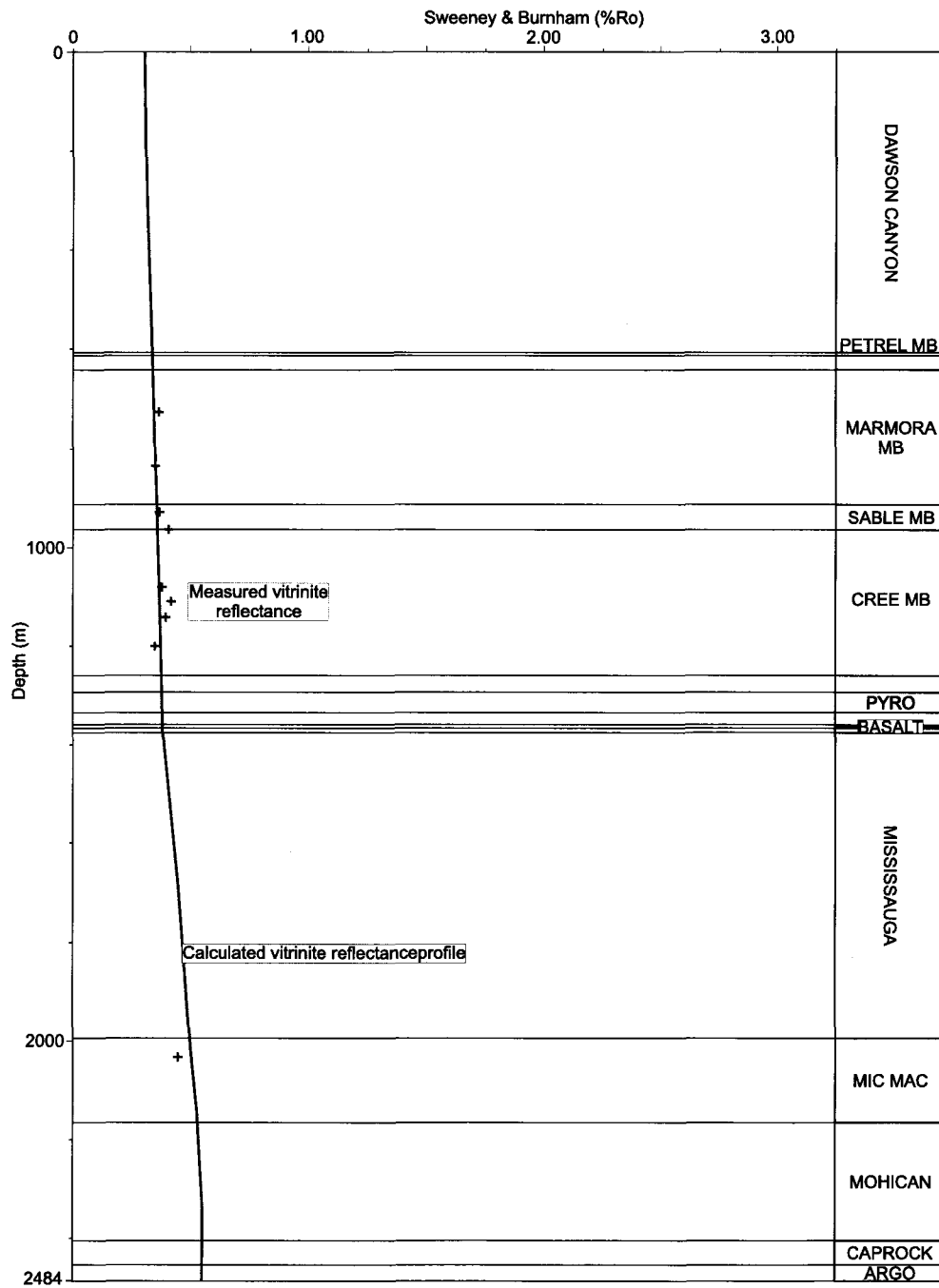Figure 5.5: Burial history plot with heat flow overlay for model B in the Jason C-20 well

127
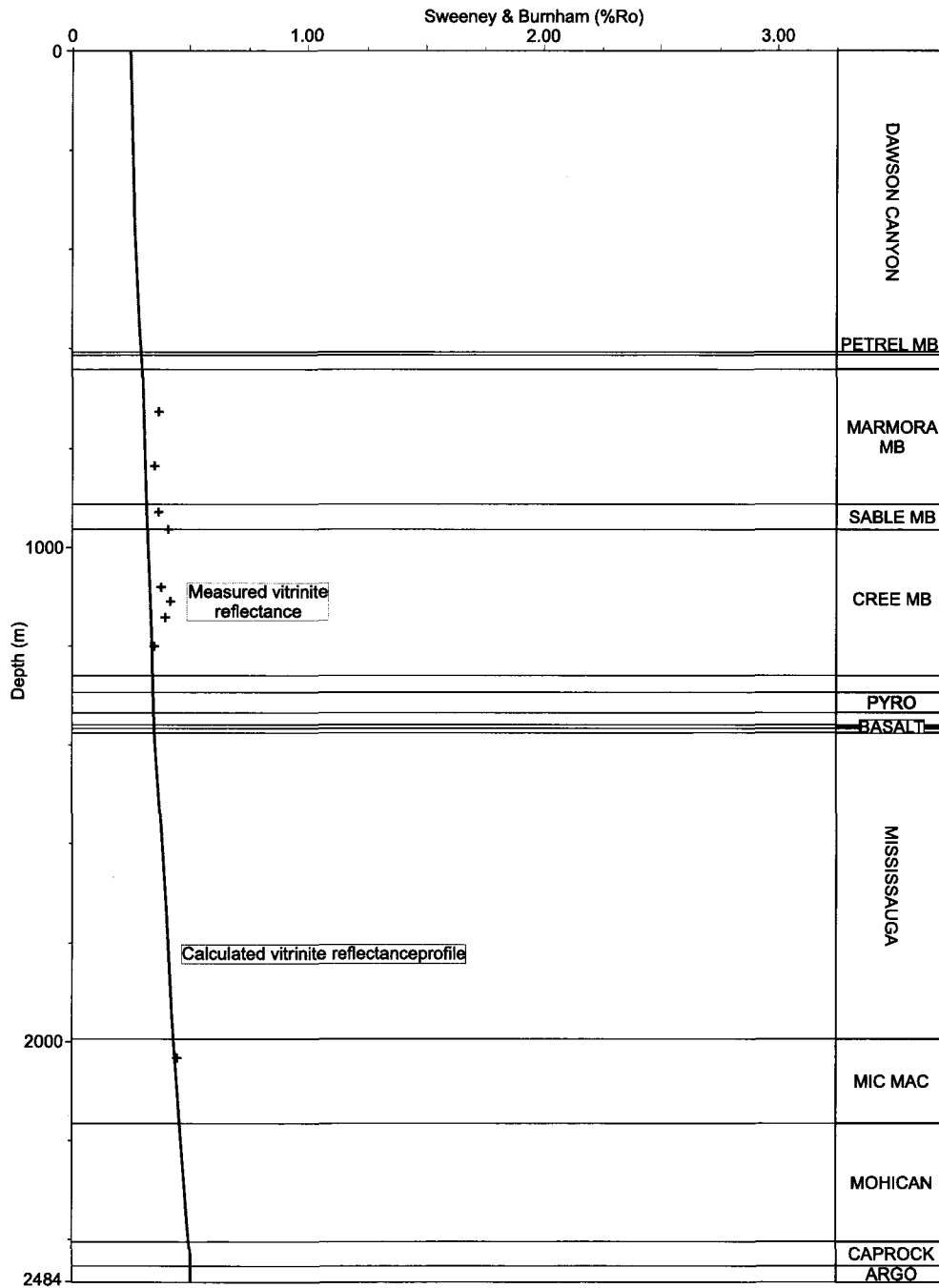
Figure 5.6: Modeled vitrinite reflectance profile versus measured vitrinite reflectance for model B in the Jason C-20 well

128
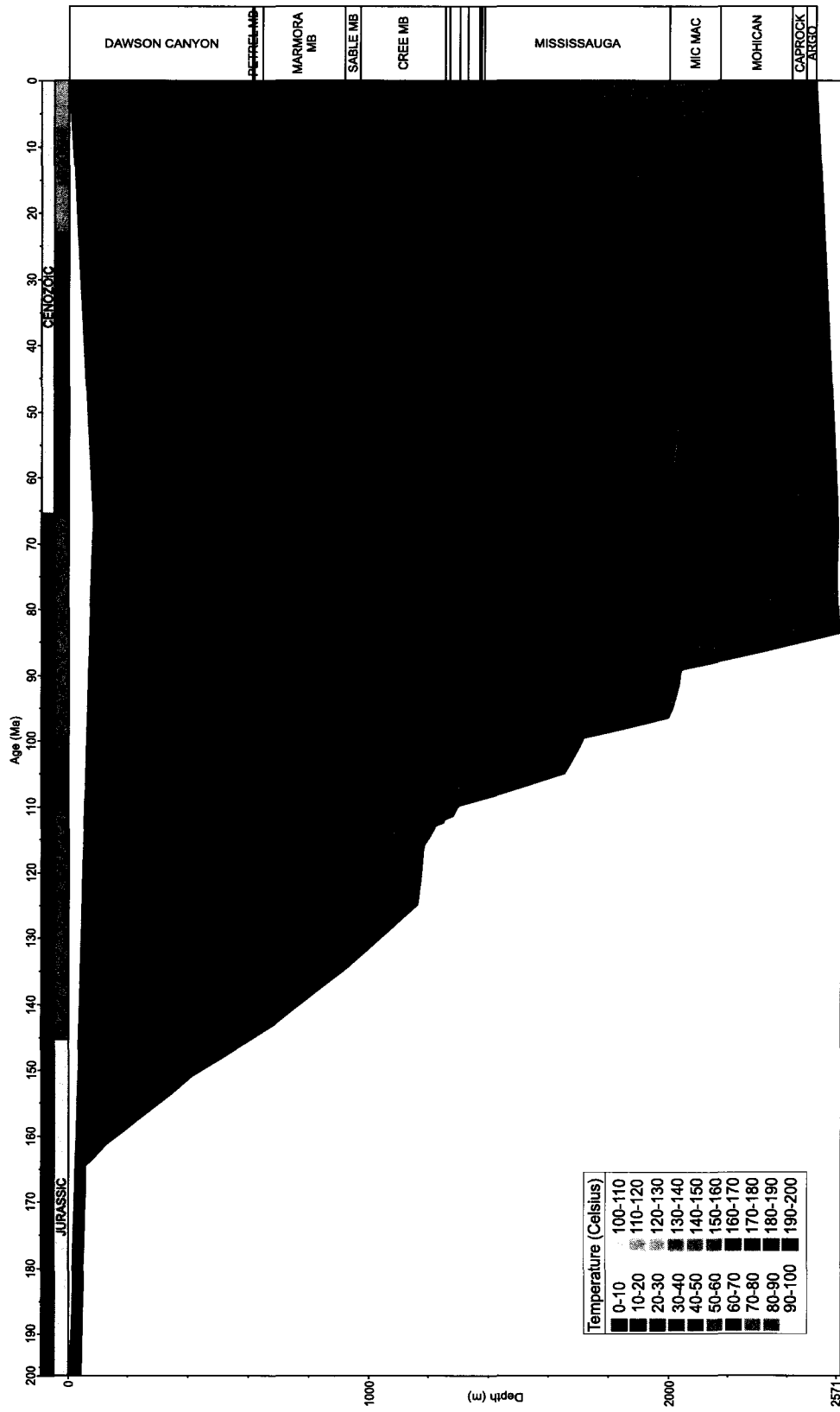
Figure 5.7: Burial history plot with temperature overlay for model C in the Jason C-20 well
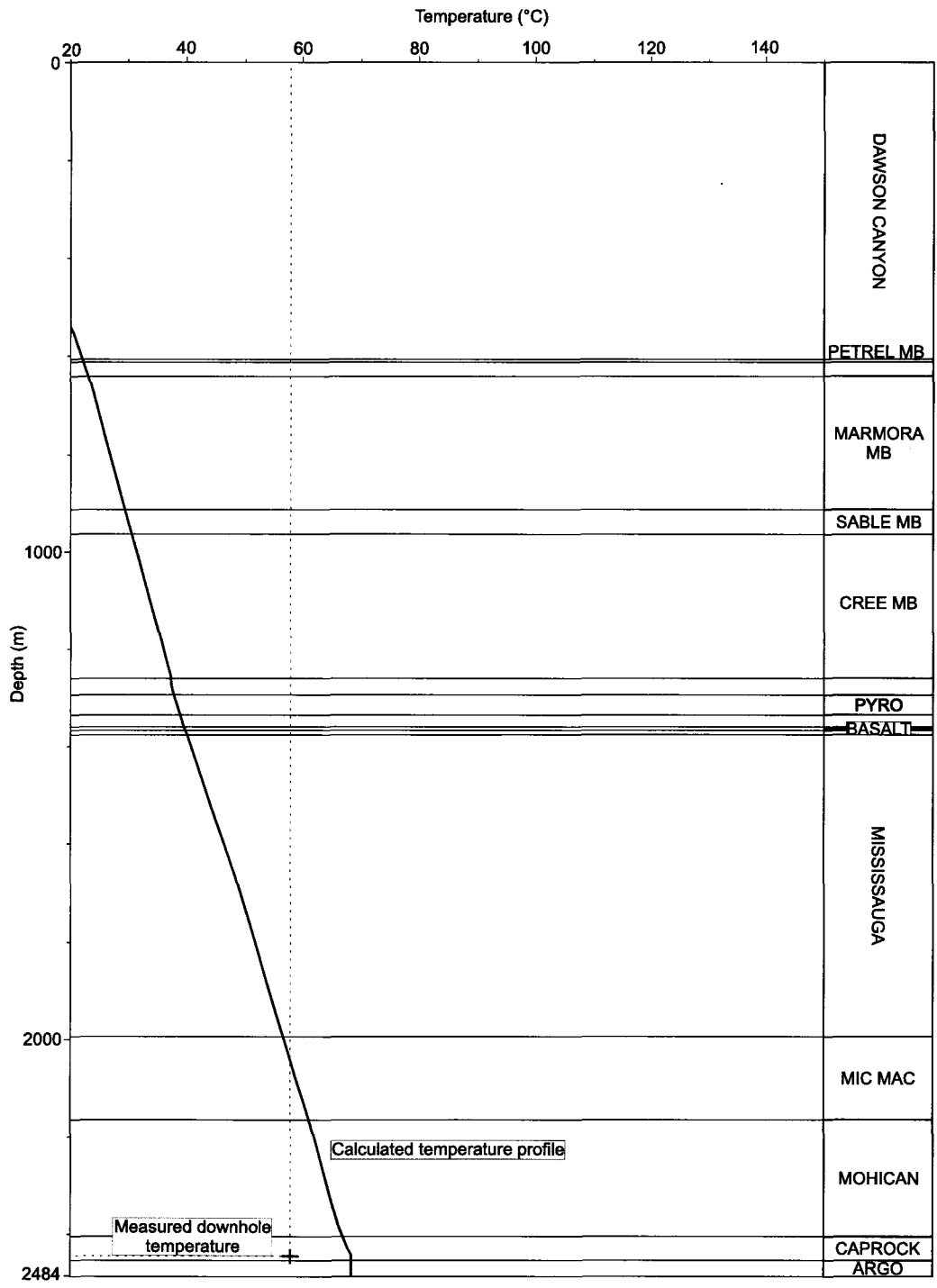
Figure 5.8: Modeled downhole temperature versus measured downhole temperature for model C
in the Jason C-20 well
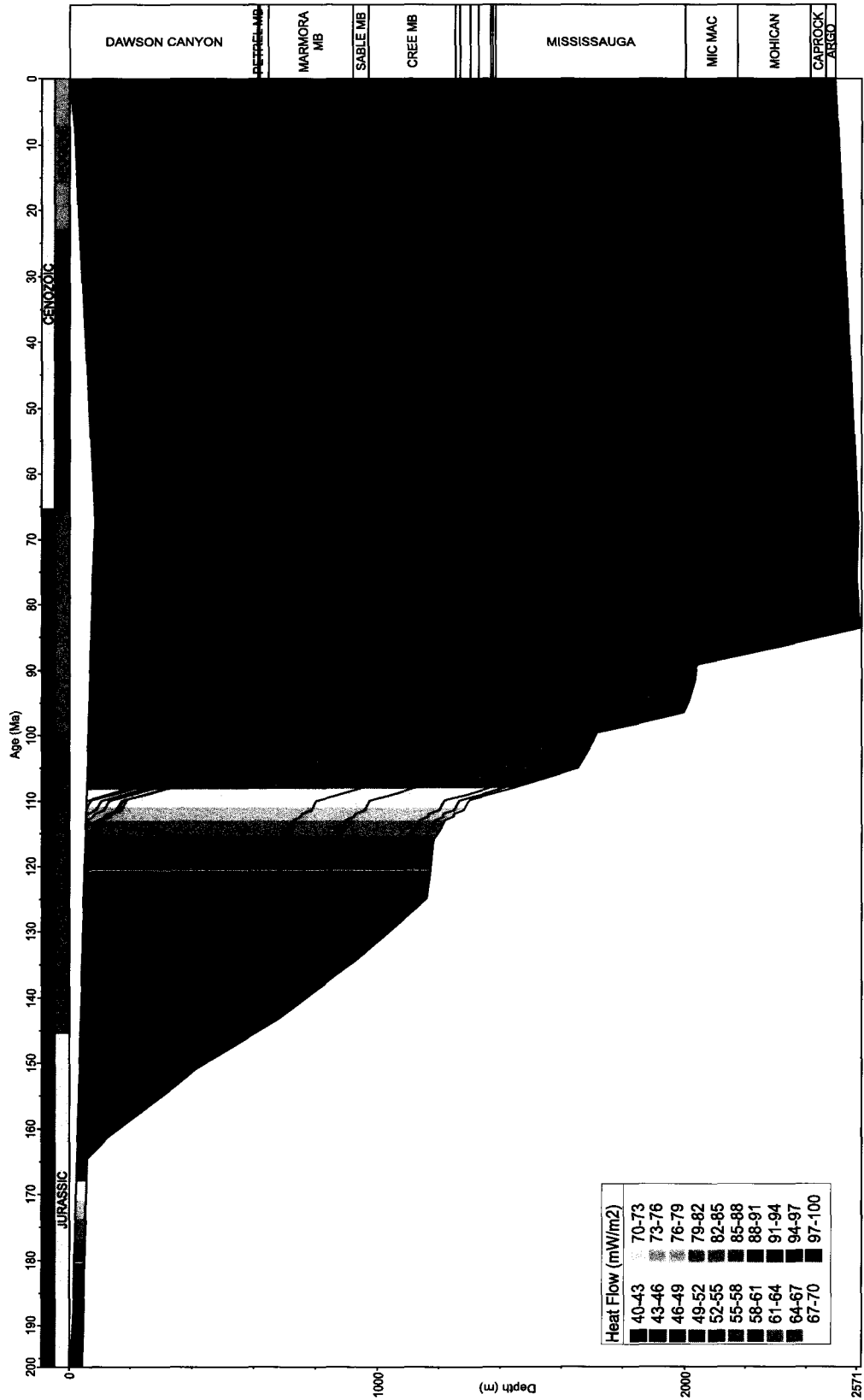
Figure 5.9: Burial history plot with heat flow overlay for model C in the Jason C-20 well

131
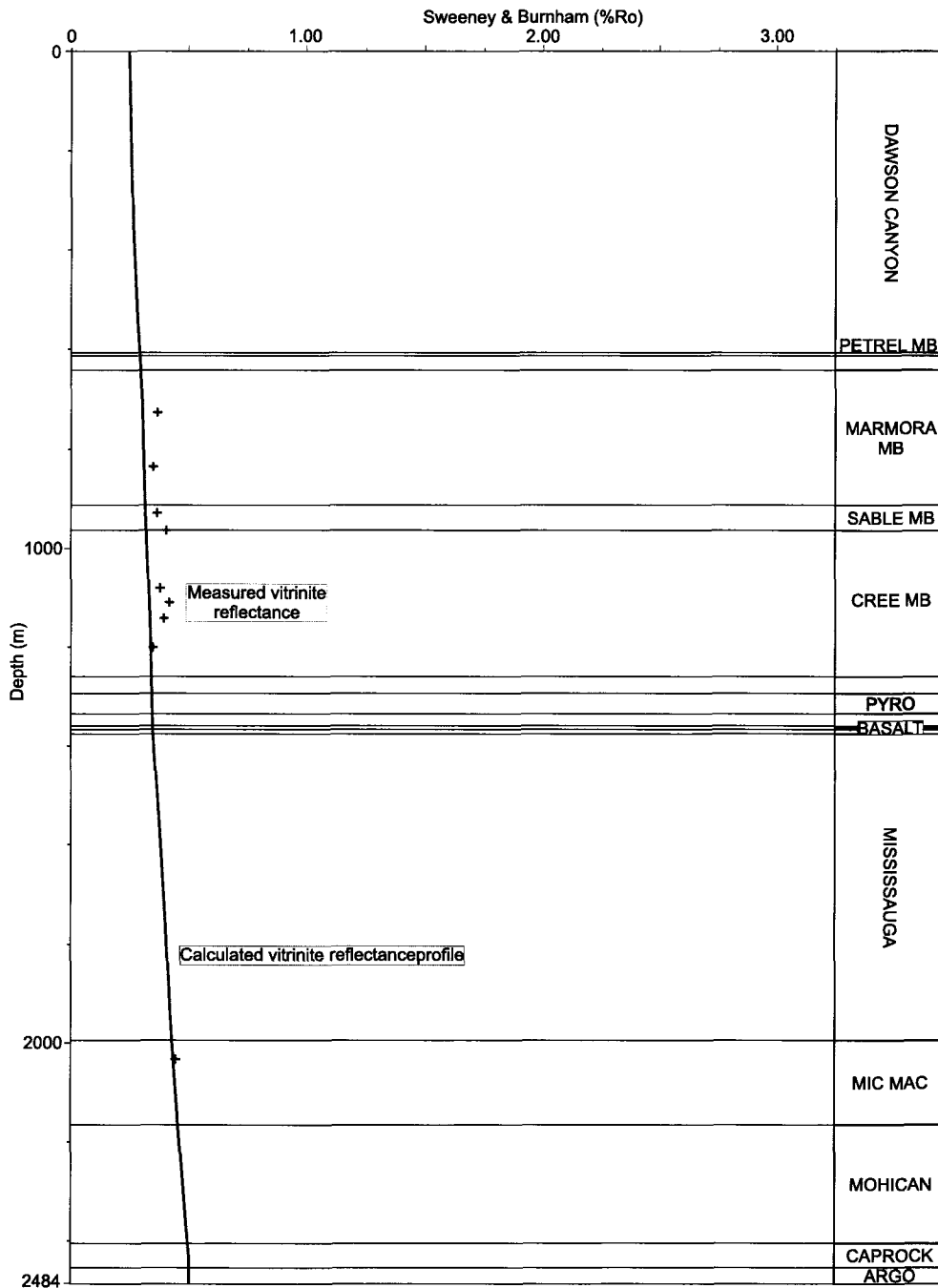
Figure 5.10: Modeled vitrinite reflectance profile versus measured vitrinite reflectance for model C in the Jason C-20 well
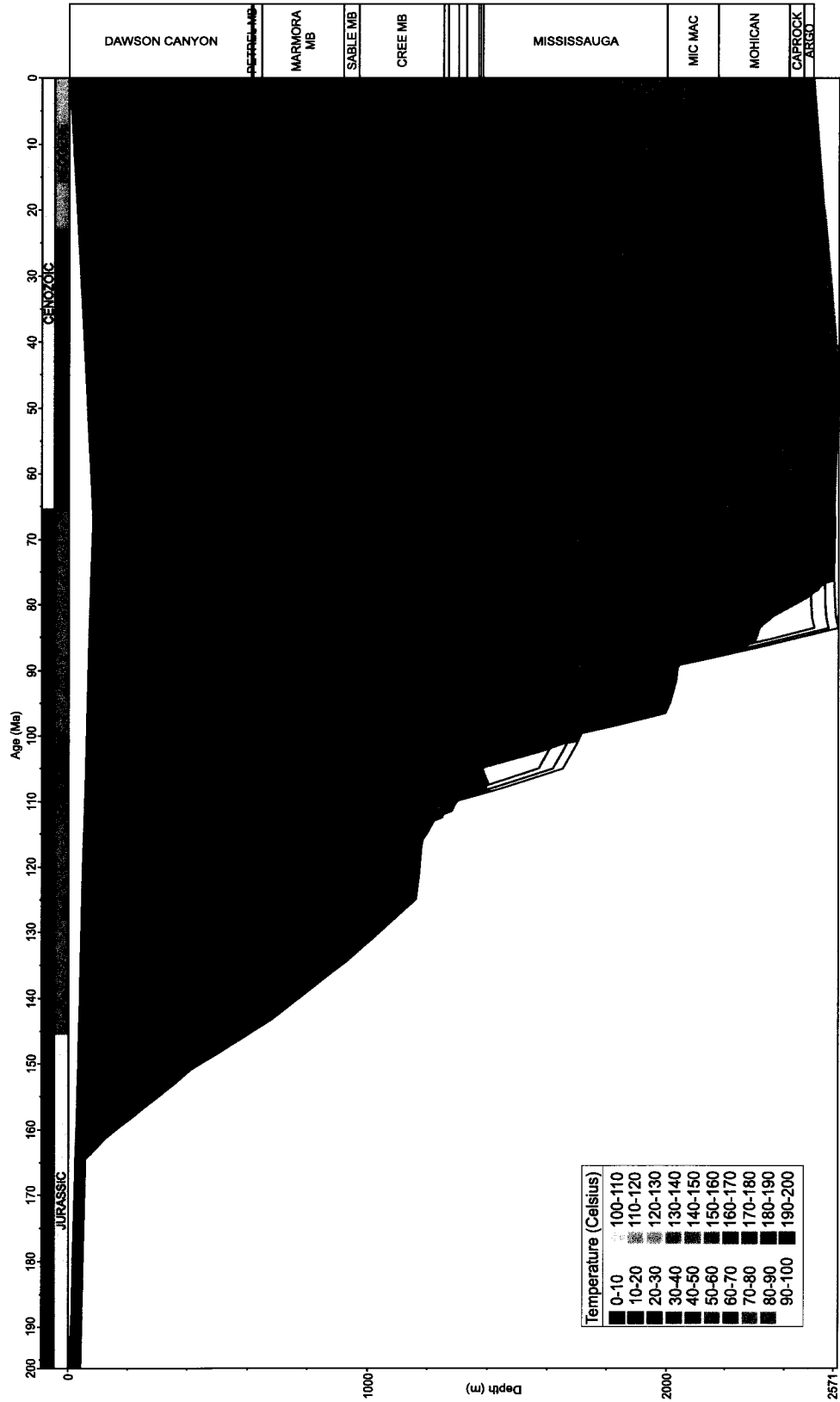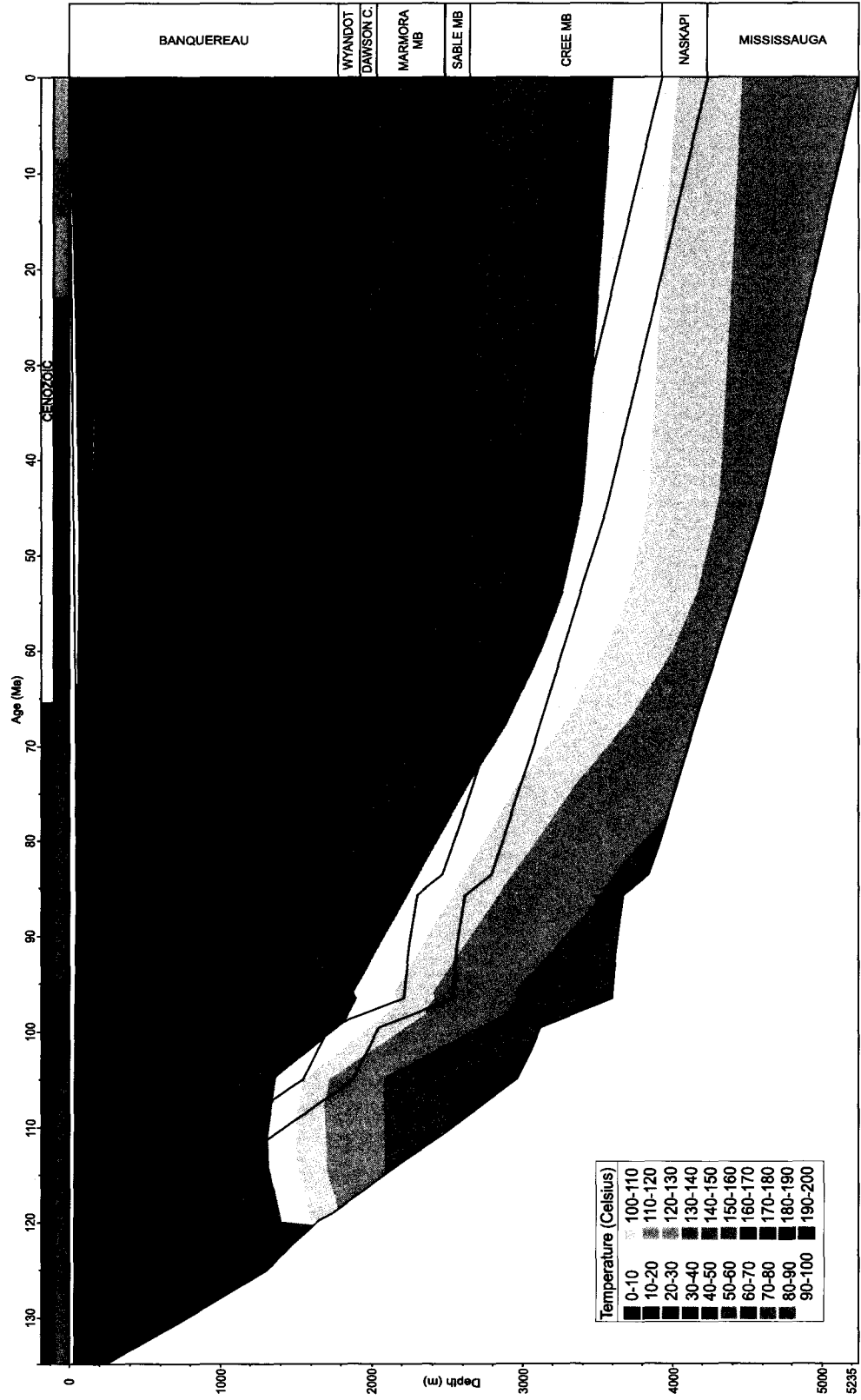
Figure 5.11: Burial history plot with temperature overlay for model D in the Jason C-20 well

133

Figure 5.12: Modeled downhole temperature versus measured downhole temperature for model D in the Jason C-20 well

Figure 5.13: Burial history plot with heat flow overlay for model D in the Jason C-20 well

profile is similar to model C but with a shift to the right (higher Ro% values) within the Mic Mac Formation from a measured value of 0.25% to the modeled value of 0.28% (Figure 5.14).

5.4.1 Chebucto K-90

In model A, maximum temperatures in all formations were reached at the maximum burial depth. In the Chebucto K-90 well, there are three Horner corrected measured downhole temperature values to compare with the modeled downhole temperature profile. The modeled temperature profile in model A does not match the measured temperature. The modeled profile is a close fit with the measured values of vitrinite reflectance until the depth of the Cree Member, where the modeled vitrinite reflectance profile follows a fairly linear trend while the measured vitrinite reflectance points increase with depth. Model B generated results similar to model A.

Model C generated maximum temperature at time of maximum burial with the exception of the Mississauga Formation which also reaches a maximum burial temperature at the time of volcanism. The modeled temperature profile is identical with model A and B and does not match the measured temperatures. The vitrinite reflectance profile is also identical to model A and B. All figures related to models A-C can be found in Appendix 2.

Model D generated a burial history plot with a temperature overlay indicating that the maximum temperature reached was 171°C in the Mississauga Formation at the time of volcanism (~105 Ma) followed by cooling to 124°C at maximum burial. The Logan Canyon Formation reached 129°C within the Naskapi Member and 100°C within the

Figure 5.14: Modeled vitrinite reflectance profile versus measured vitrinite reflectance for model D in the Jason C-20 well

Cree Member at time of volcanism (~105 Ma), cooling to 105°C and 98°C at maximum burial (Figure 5.15). The modeled temperature profile is identical with model A, B and C, and does not match the measured temperatures (Figure 5.16). The model also generated a burial history plot with a heat flow overlay which shows the increase and decay of heat flow over time within the system (Figure 5.17). The vitrinite reflectance profile is similar to model A, B and C until the depth of the Cree Member. At the depth of the Cree Member, the modeled vitrinite reflectance profile bends to the right (increase in Ro%) and, though values are lower than the measured values, the profile mimics the measured values by increasing with depth (Figure 5.18).

5.5 Synthesis of Orpheus Graben and Scotian Shelf results

Previous work on the thermal history of sedimentary rocks using apatite fission track and fluid inclusion data on the Scotian Shelf has shown evidence of unexpectedly high temperatures within the Logan Canyon and Mississauga formations during the Cretaceous that are hotter than present day temperatures (Grist et al., 1991; Li et al., 1995; Wierzbicki et al., 2006; Karim et al., 2009; Karim et al., 2010). Apatite fission track data by Grist et al. (1991) and Li et al. (1995) has shown temperatures within the Logan Canyon and Mississauga formation in studied wells of the Sable sub-basin were 1-55°C hotter during the Cretaceous than at present. Wierzbicki et al. (2006) and Karim et al. (2009, 2010) have studied fluid inclusions from dolomites and carbonate cements in the Sable sub-basin and found temperatures up to 130-147°C within the Cretaceous.

Models generated for wells in the Orpheus Graben and Scotian Shelf tested hypotheses of the presence and duration of a post-rift regional heat flow. Overall, the

Figure 5.15: Burial history plot with temperature overlay for model D in the Chebucto K-90 well

139
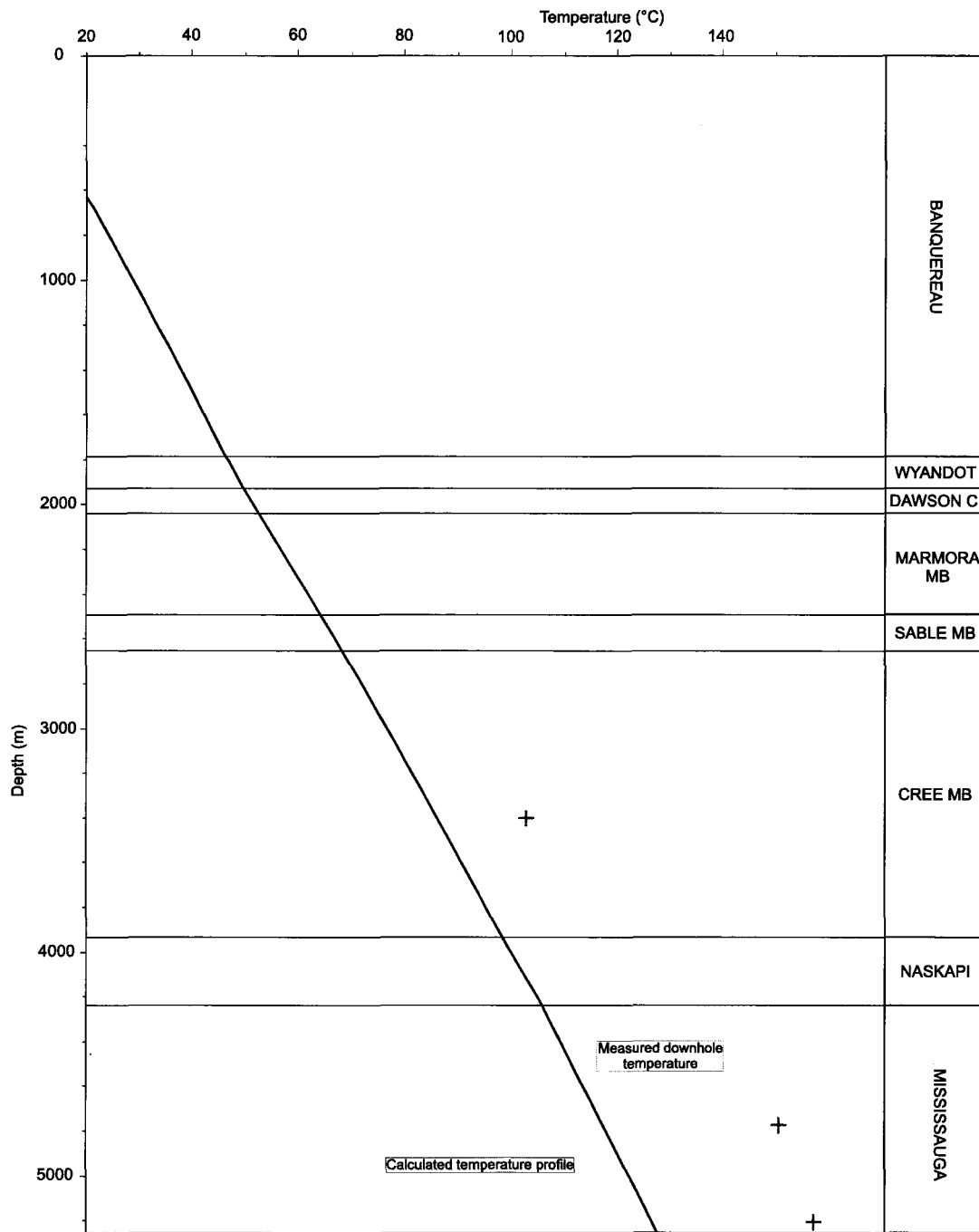
Figure 5.16: Model D modeled temperature vs measured downhole temperature for Chebucto K-90

140
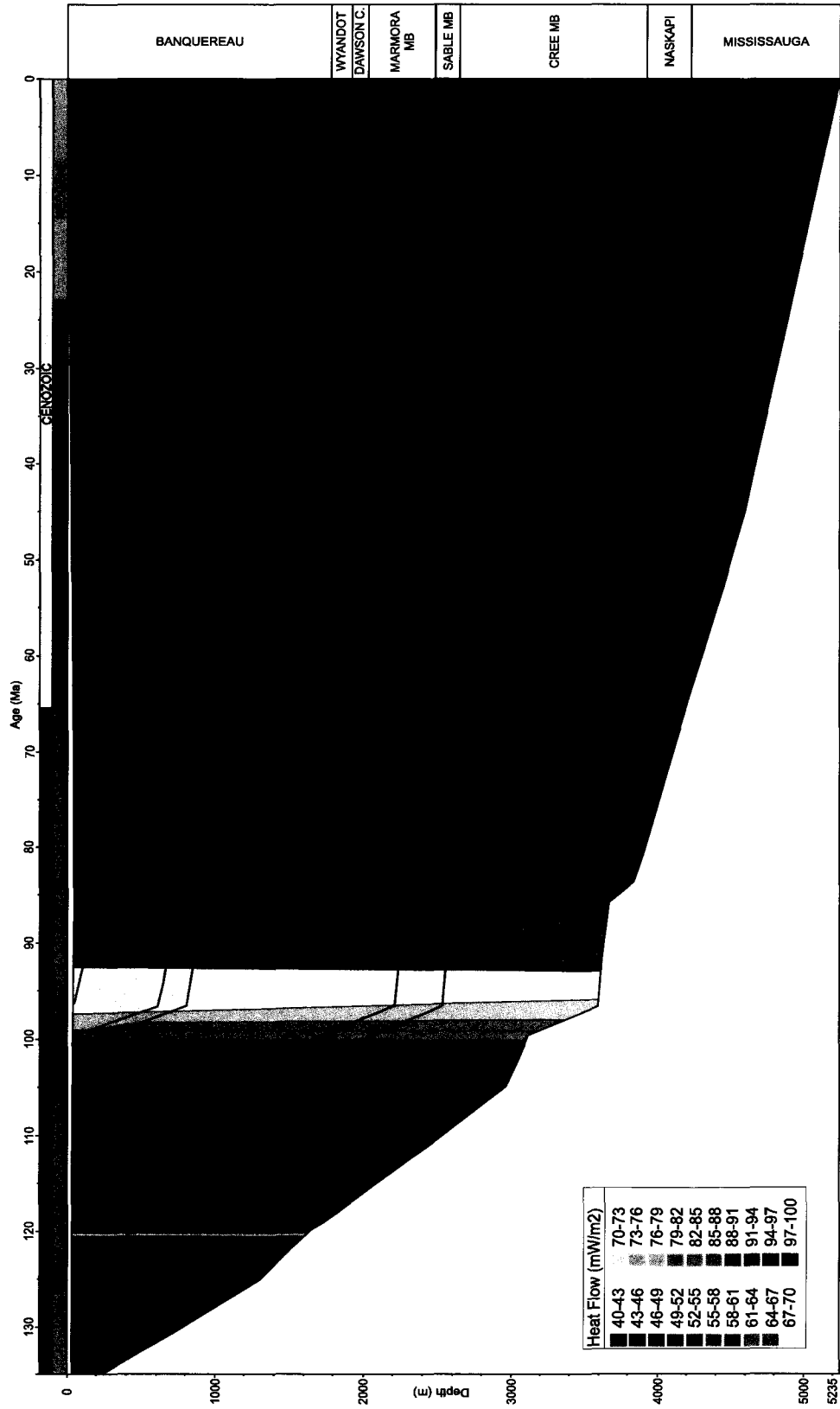
Figure 5.17: Burial history plot with heat flow overlay for model D in the Chebucto K-90 well

141
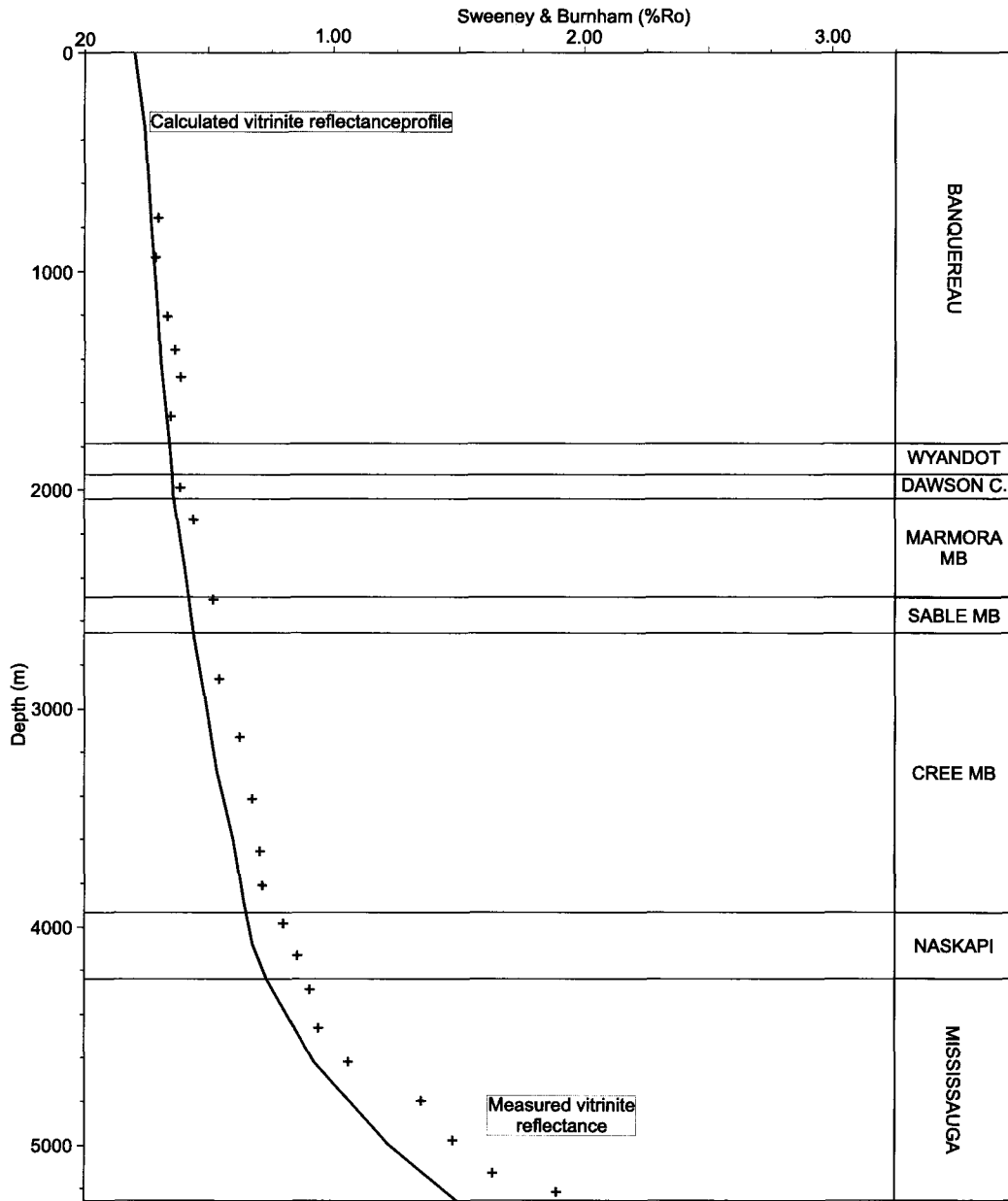
Figure 5.18: Model D modeled vitrinite reflectance profile vs measured vitrinite reflectance for Chebucto K-90

results of model D correlate the best with measured vitrinite reflectance data. The main observation from the results of model D is that calculated temperatures within the Logan Canyon and Mississauga formations were as hot as, or hotter, than present day temperatures. This is similar to the findings of the authors mentioned above, therefore it can be said that a regional post-rift heat flow lasting the duration of volcanism in the Orpheus Graben and Scotian Shelf is possible. The implications of a regional heat flow will be discussed in the next chapter.

5.6 Application to the SW Grand Banks

On the SW Grand Banks, availability and quality of measured data such as reliable biostratigraphy and vitrinite reflectance was limited and thus two wells were chosen which had enough data to model. The two wells are the Mallard M-45 well which contains a thick succession of volcanic and pyroclastic rocks and the Emerillon C-56 well which contains a Cretaceous sill or dyke. Although the measured age of the sill or dyke in Emerillon C-56 is younger than the lower Cretaceous extrusional volcanism on the SW Grand Banks, this well allows the opportunity to model the effect of an intrusion on the heat flow and maturation of surrounding sediments. As with the Jason C-20 and Chebucto K-90 well in the Orpheus Graben and Scotian Shelf, four models were generated (A-D). On the SW Grand Banks, the timing of volcanism is within the lower Cretaceous Berriasian to Barremian stages, and thus model C and D were generated with heat flow introduced at 145 Ma. Unlike the Orpheus Graben and Scotian Shelf, the volcanism does not occur after rifting but rather is synchronous with it.

5.6.1 Mallard M-45

In the Mallard M-45 well, there are three Horner corrected measured downhole temperature values to compare with the modeled downhole temperature profile. In model A, maximum temperatures in all formations were reached at the maximum burial depth. The modeled temperature profile does not match the measured temperature. In terms of the vitrinite reflectance profile, unfortunately the Mallard M-45 well has only 2 measured vitrinite reflectance points within the Mic Mac Formation to compare with the modeled profile. The modeled profile is a close fit with the limited measured values. Model B and C generated results similar to model A. Figures corresponding to the results of models A-C can be found in Appendix 2.

Model D generated a burial history plot with a temperature overlay which shows temperature spikes within the Mic Mac Formation during the time of rifting and volcanism, however the maximum temperatures reached are identical to models A, B and C (Figure 5.19). The modeled temperature profile is identical with model A, B and C, and does not match the measured temperatures (Figure 5.20). The model also generated a burial history plot with a heat flow overlay which shows the increase and decay of heat flow over time within the system (Figure 5.21). The vitrinite reflectance profile is also identical to model A, B and C (Figure 5.22).

5.6.2 Emerillon C-56

As Emerillon C-56 includes a sub-volcanic intrusion, model A was run once without the intrusion to estimate normal burial conditions without igneous activity, and then run again with the intrusion included. The first run without the intrusion generated a

144
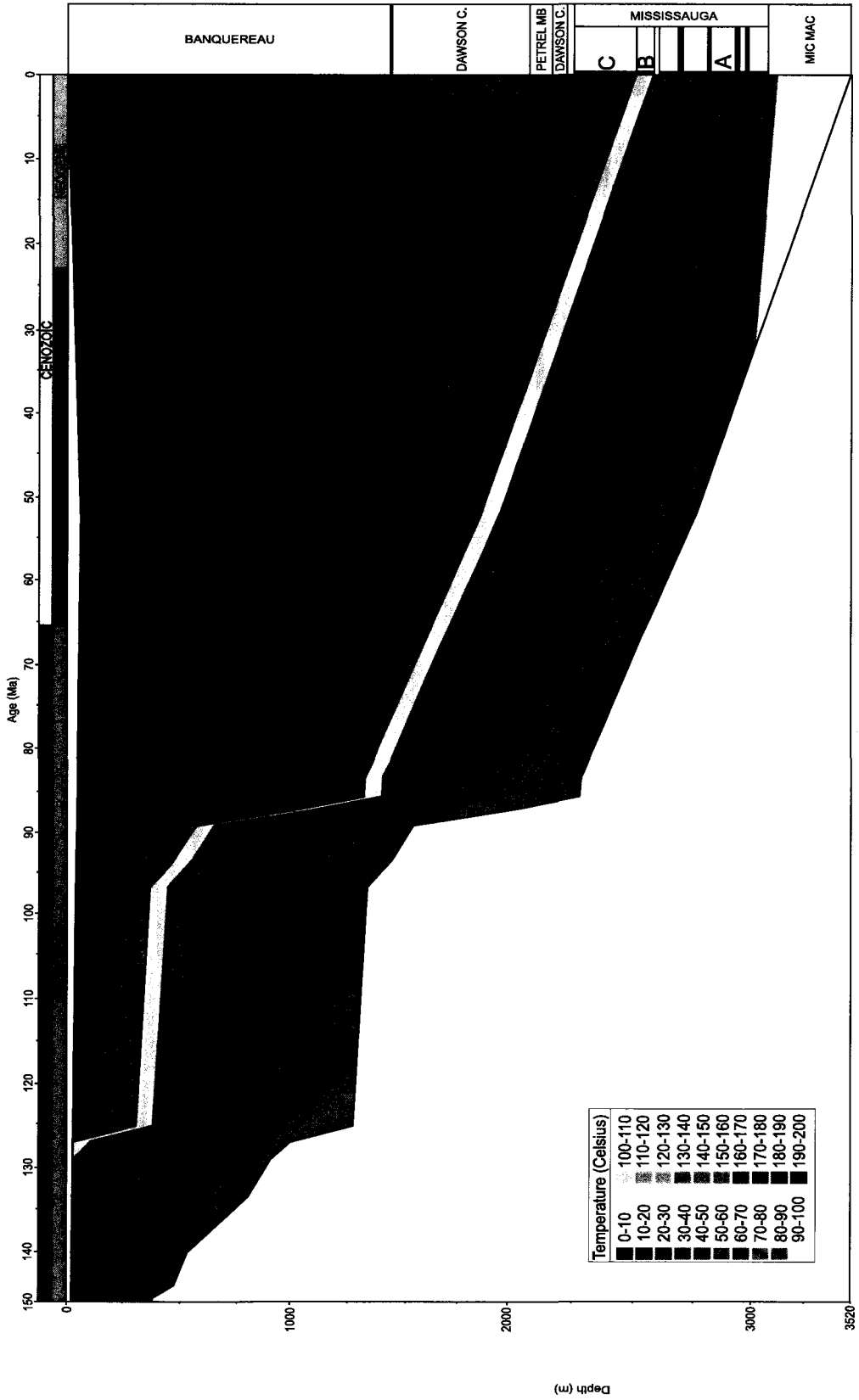
Figure 5.19: Burial history plot with temperature overlay for model D in the Mallard M-45 well

145
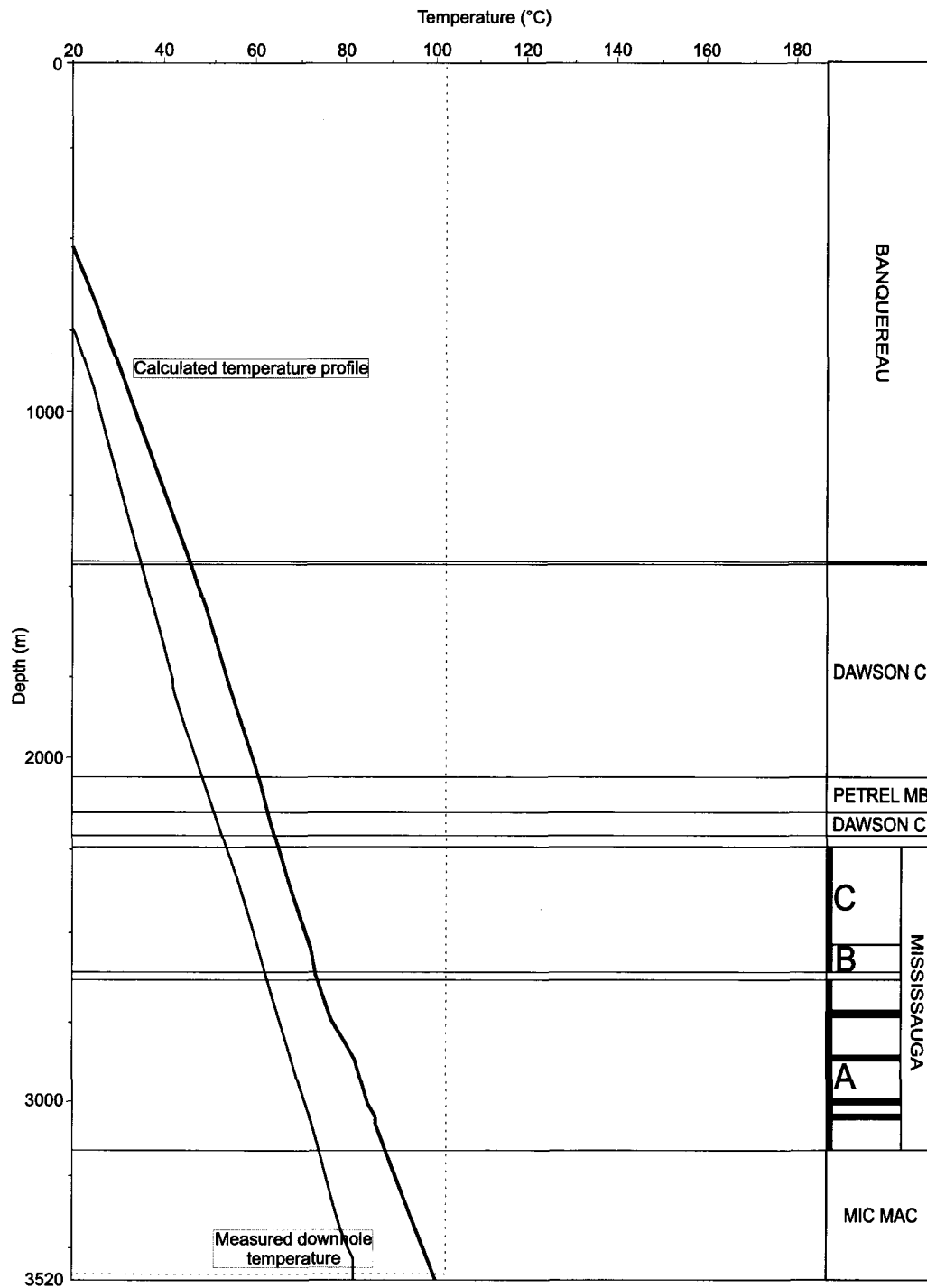
Figure 5.20: Modeled downhole temperature versus measured downhole temperature for model D in the Mallard M-45 well
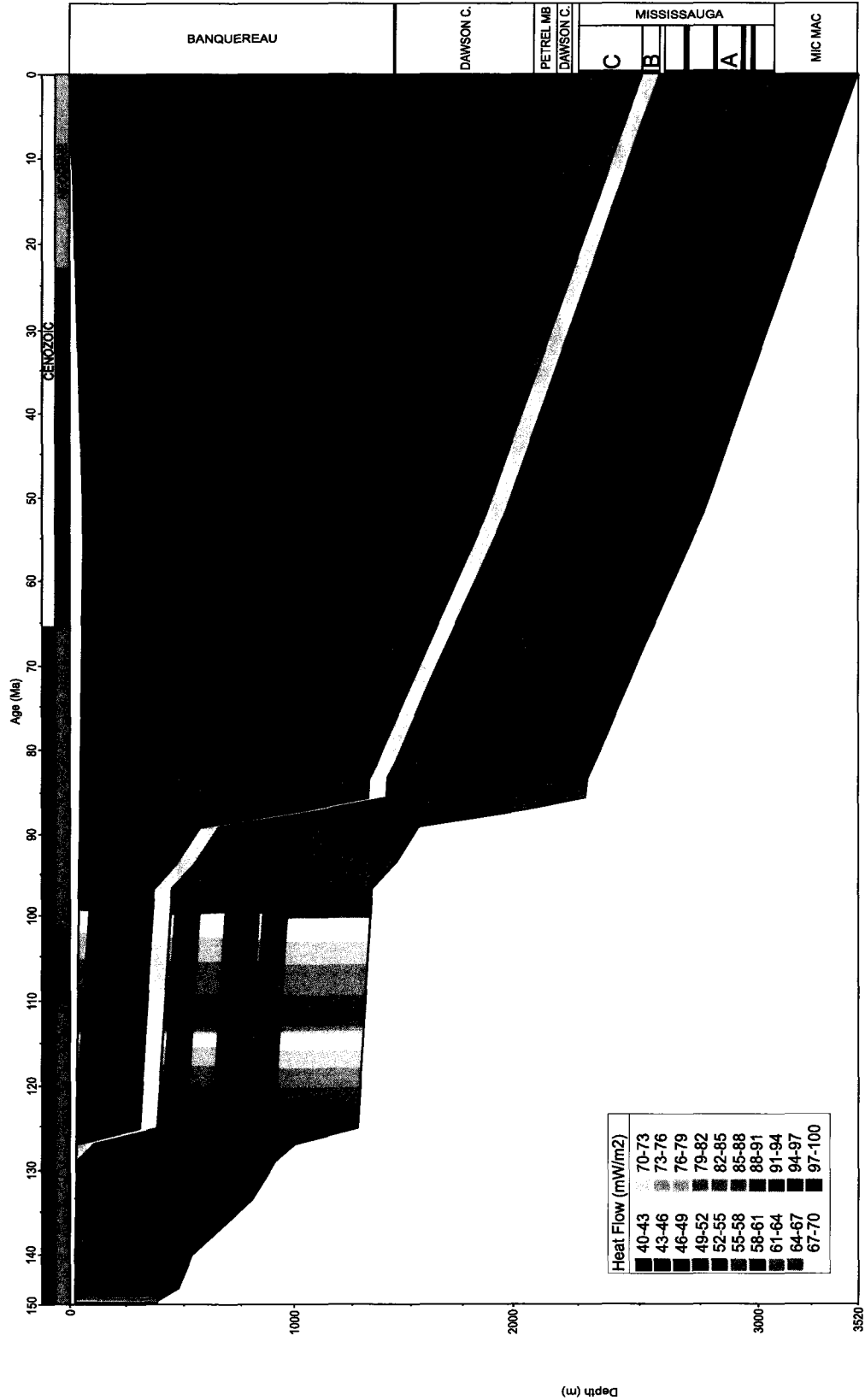
Figure 5.21: Burial history plot with heat flow overlay for model D in the Mallard M-45 well

147
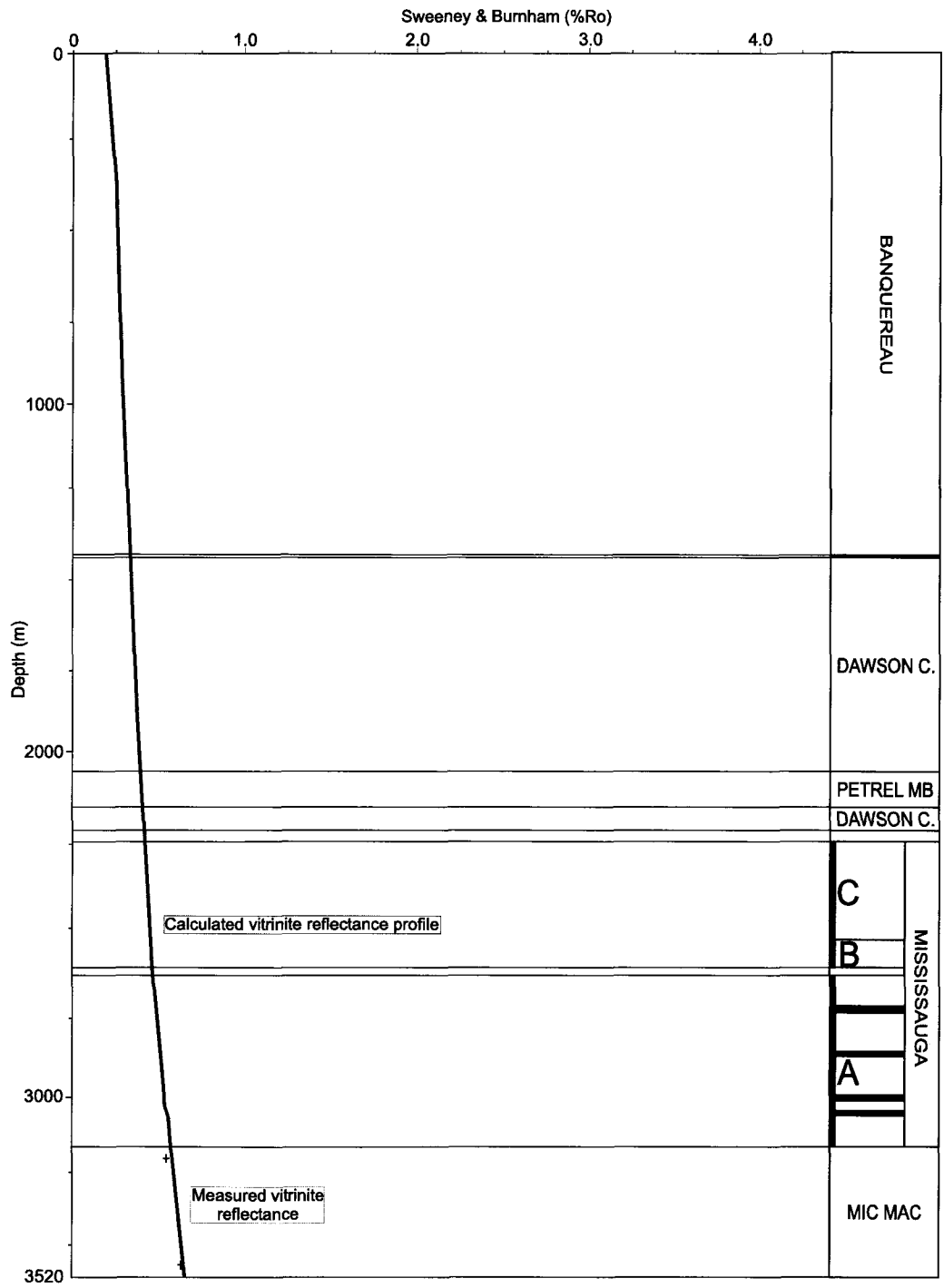
Figure 5.22: Modeled vitrinite reflectance profile versus measured vitrinite reflectance for model D in the Mallard M-45 well

148

burial history plot with temperature overlay similar to all other wells with the maximum temperature of all formations reached at maximum burial depth. In the Emerillon C-56 well, there are only two Horner corrected measured downhole temperature values to compare with the modeled downhole temperature profile. The modeled temperature profile does not match the measured temperature values. The modeled vitrinite reflectance profile does not match the measured vitrinite reflectance points as the modeled profile is less mature than the measured values. The second run of model A, which included the intrusion, is markedly different from the first run without the intrusion. The burial history plot with temperature overlay shows a high temperature spike at the time of intrusion up to 200°C with maximum temperatures of formations below the Eider Unit (Logan Canyon Formation) reached at this time. Maximum burial temperatures are the same as the first run of model A. The modeled temperature profile is identical to the profile of the first run, but the modeled vitrinite reflectance profile increase dramatically directly above and below the intrusion presumably due to the intense heat at the contact with the intrusion. Models B-D were run with the intrusion included and are similar to the results of the second run of model A. Figures corresponding to the results of models A-D can be found in Appendix 2.

5.7 Synthesis of SW Grand Banks results

The overall result of models on the SW Grand Banks indicates that a regional heat flow, of which the volcanism within the SW Grand Banks was a manifestation, may or may not have had a significant effect on the heat flow, temperature and maturation of the sediments. No apatite fission track or fluid inclusion such studies are available for

sedimentary rocks of the SW Grand Banks and measured data values such as vitrinite reflectance data are scarce. Thus it is unclear if any of the tested hypotheses of regional heat flow are close to reality. Sediment thicknesses at the time of volcanism on the SW Grand Banks are much less than sediments thicknesses at the time of volcanism in the Orpheus Graben and Scotian Shelf, which may have an effect on the heat flow in the area. In the case of the Emerillon C-56 well, it appears that the local heat effect of the Cretaceous intrusion masks any regional heat flow effect associated with volcanism within the SW Grand Banks.

CHAPTER 6
DISCUSSION AND CONCLUSIONS

6.1 Style and source of volcanism

The volcanic rocks in the Orpheus Graben consist of ~20 m thick subaerial

basaltic lava flows within the Cree Member of the Logan Canyon Formation (Figure 3.7).

The basalt flows have the geochemical signature of within-plate alkalic basalts (Jansa and

Pe-Piper, 1985). In the Jason C-20 and Hercules G-15 wells these basalt flows are

overlain by tens of metres of Cree Member sediments and ~75 m of subsequent

pyroclastic rocks (Figure 3.7). The basalt flows and thick pyroclastic rocks appear to be

confined to the Orpheus Graben, with the exception of a ~20 m thick basalt flow

intersected by the Hesper I-52 well at the same stratigraphic level as the flows found

within the Orpheus Graben (Figure 3.7 and 6.1). The known extent of the basalt flows

and associated pyroclastic rocks is small, which indicates a Strombolian eruptive style.

Strombolian eruptions may begin as a Hawaiian style effusive eruption of basaltic

lava, which then transitions to a more explosive Strombolian-type eruption of

pyroclastics (Martin and Nemeth, 2006). According to Wilson et al. (1995), this

transition may be based solely on the magma rise speed, with Strombolian activity

occurring at low rise speeds and Hawaiian activity at higher rise speeds. Hawaiian-style

basalt flows have been known to travel up to 50-100 km from their source with

thicknesses of 3-20 m (Kilburn, 2000, Spitzer et al., 2008). Strombolian activity is

characterized by short explosive bursts of pyroclastic ejecta tens to hundreds of metres in

the air (Francis and Oppenheimer, 2004); however, over half of pyroclastic material

ejected falls less than 1 km away from the source forming scoria cones (Vergniolle and
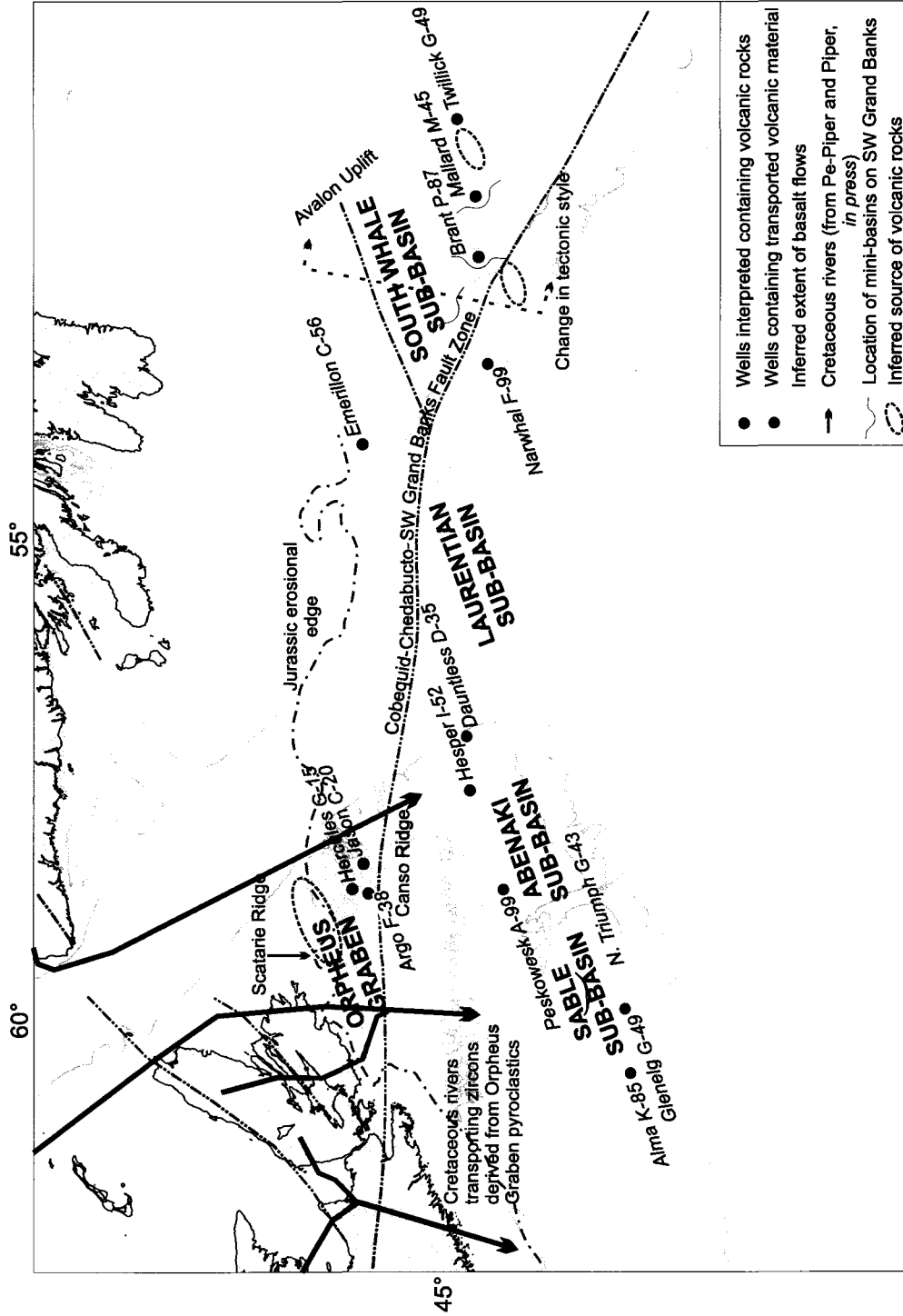
Figure 6.1: Paleogeography map of the Orpheus Graben, SE Scotian Shelf and SW Grand Banks showing the position and extent of volcanism, its inferred source location and the location of ancestral rivers which may have transported pyroclastics to Scotian Basin (Wade and MacLean, 1990; Pe-Piper and Piper, *in press*)

Mangan, 2000). The rest of the pyroclastic material forms a thin sheet over the existing topography, diminishing to less than 10% of its original near-source thickness at a distance of approximately 10 km from the source (Vergniolle and Mangan, 2000). However, the strength and direction of prevailing winds during an eruption may carry pyroclastic material farther from the source than expected.

Strombolian eruptions are characterized by short-lived, mildly explosive eruptions that often generate scoria cones (also known as cinder cones), which are among the most common forms of subaerial volcanic features on Earth (Vespermann and Schmincke, 2000). Scoria cones deposits are most typically composed of bombs, lapilli and minor ash (Vespermann and Schmincke, 2000). These scoria cones are the most common expression of volcanism in uplifted intraplate plateaus in continental extensional settings, often occurring within grabens or on uplifted graben shoulders (Fisher and Schmincke, 1984; Vespermann and Schmincke, 2000).

The type of volcanic activity found within the Orpheus Graben is most likely Strombolian in nature, beginning as a Hawaiian style eruption generating the ~20 m thick basalt flows found within the graben which then flowed south to the SE Scotian Shelf (Figure 6.1). After a period of quiescence, highly vesicular, frothy pyroclastic rocks were deposited, characteristic of a Strombolian style eruption. Pyroclastic material is generally found within 10 km of the source and pyroclastic material is present in the Orpheus Graben wells and not on the SE Scotian Shelf. This suggests that the source of the volcanic activity in this area is near the Orpheus Graben. To date, no remnant volcanoes, nor feeder systems, have been detected in seismic profiles within, or south of, the Orpheus Graben.

However, volcanic rocks were discovered on the Scatarie Ridge (Figure 6.1) that were radiometrically dated by K-Ar dating, yielding an imprecise age of 127 ± 15 Ma (Delabio et al., 1979). The Scatarie Ridge was drilled and two cores were recovered and investigated by Jansa at al. (1993). They discovered the volcanic rocks were part of a diabase dyke or series of dykes outcropping on the seafloor. The sampled dyke was petrographically and geochemically identical to the basalt flows within the Orpheus Graben (Jansa et al., 1993).

Magnetic anomaly data may aid in determining the source of volcanic activity. Mafic materials within volcanic rocks often generate magnetic anomalies as the rocks contain magnetite. Magnetic data within the study area has been collected and processed along 1 km spacings offshore of eastern Canada by the Geological Survey of Canada and made available to the public (Figure 6.2). Shallow short wavelength magnetic anomalies are present along the northern edge of the Orpheus Graben and across the Scatarie Ridge. These anomalies form part of the Collector Magnetic Anomaly, which is thought to be the geophysical expression of the general outline of a suture separating the Avalon and Meguma terranes (Haworth and Lefort, 1979). This suture zone along the northern edge of the Orpheus Graben is considered to be the Cobequid-Chedabucto-SW Grand Banks fault system. According to Jansa et al. (1993), magnetic anomalies on the Scatarie Ridge closely correspond to the locations of the Cretaceous dykes sampled in this area and may indicate the presence of further dykes along the ridge. The dykes on the Scatarie Ridge are the most likely source of the Strombolian system that fed the volcanic activity within the Orpheus Graben 20- 50 km away and the SE Scotian Shelf ~140 km away (Figure 6.1).

Figure 6.2: Magnetic anomaly map indicating possible sources of volcanism in the Orpheus Graben, SE Scotian Shelf and SW Grand Banks Map is a total field magnetic anomaly map, corrected to the pole (Magnetic Anomaly data from Canadian Aeromagnetic Database, 2010)

The style of eruption recorded by rocks in the Brant P-87 and Mallard M-45 wells on the SW Grand Banks appears to be of a more explosive character than that in the Orpheus Graben and Scotian Shelf, based on the presence of a much thicker pyroclastic succession interbedded with basalt flows (Figure 3.6). However, although eruptions were more violent on the SW Grand Banks, they may also have been Strombolian in nature. Recent studies have shown that more violent Strombolian eruptions characterized by high eruption columns, and simultaneous ash and basalt effusion may be more common than once thought (Martin and Nemeth, 2006). The scoria cones built by these more violent Strombolian style eruptions consist of lava flows, bombs, lapilli, lapilli tuff and vesicular ash (Martin and Nemeth, 2006) This is similar to the succession of volcanic material found within the Brant P-87 and Mallard M-45 wells discussed in Chapter 3 and shown in Figure 3.1 and 3.2.

These two wells show very different volcanic stratigraphies among themselves (Figure 3.6).This may be due to a difference in distance from a single source, or may indicate two different sources. If the volcanic deposits in the two wells are derived from the same volcanic centre but are located at different distances from the source, the well closest to the source would have a thicker succession of coarser volcanic rocks while the well farther away from the source would contain a thinner succession of finer volcanic material. The Mallard M-45 well contains a thicker succession of volcanic rocks than the Brant P-87 well; however, the Brant P-87 well contains coarser volcanic breccia compared to the lapilli tuff found in the Mallard M-45 well (Figure 3.1 and 3.2). Thus, the source cannot be identified from stratigraphy alone.

Different volcanic centres may have flows of different chemical composition. The concentration of the trace element Nb is higher in the basalts of the Mallard M-45 well compared to that of the Brant P-87 well (Pe-Piper et al., 2007). This may indicate that the two are sourced from two different volcanic centres.

Interpretation of the seismic profiles at, and around, these wells has shown high amplitude reflections corresponding to basalt flows on one side of a mini basin and abrupt stoppage of the flows halfway into the mini basins. This implies that the basalt flows were sourced from one side of the mini basins. Thus, basalt flows in the Brant P-87 well appear to have been sourced from the south to southwest (Figure 4.12a), while basalt flows in the Mallard M-45 well appear to have been sourced from the east (Appendix Figure 1.15).

As in the Orpheus Graben and SE Scotian Shelf, magnetic anomaly data may aid in determining a source for the volcanic and pyroclastic rocks in the Brant P-87 and Mallard M-45 wells. The Narwhal F-99 well contains proven Mesozoic age volcanic rocks and is located directly above a prominent magnetic anomaly (Figure 6.2). By analogy, magnetic anomalies may represent sources of volcanic rocks. In seismic profiles at the Brant P-87 (Figure 4.12a) and Mallard M-45 wells (Appendix Figure 1.15), horsts are located in the direction of the inferred source of basalt flows. Therefore, magnetic anomalies at horsts may be volcanic sources analogous to the Scatarie Ridge. Magnetic anomaly data shows anomalies southwest of Brant P-87 and east of Mallard M-45 (Figure 6.2). The magnetic anomaly south of the Brant P-87 well is located along the Cobequid-Chedabucto-SW Grand Banks fault zone, while the magnetic anomaly east of the Mallard M-45 well is north of the fault zone. The inferred source of the volcanic

rocks in the Mallard M-45 well may also have been the source of the volcanic rocks at the Twillick G-49 well.

There is also not enough information available to conclude anything about the diorite unit in the Emerillon C-56 well besides the fact that it is a sill or dyke intruding Jurassic sediments which has been dated by K-Ar dating as ~97 Ma. No conclusions different from Pe-Piper et al. (2007) were obtained from study of the volcanic rocks found at the base of the Narwhal F-99.

6.2 Age of volcanism

Volcanic activity on the SW Grand Banks is concentrated in the lower Cretaceous, possibly from Berriasian, but definitely from Hauterivian to Barremian (136-125 Ma). Volcanic activity within the Orpheus Graben and SE Scotian Shelf is concentrated in the lower Cretaceous from Aptian to Albian (125-100 Ma) as determined by an examination of biostratigraphic and radiometric data in wells intersecting volcanic rocks (Figure 6.3).

Detrital zircons provide additional evidence for the age of volcanism. Piper et al. (*in prep*) have identified detrital zircons within the Upper Member of the Mississauga Formation and the Cree Member of the Logan Canyon Formation in the Alma K-85, Peskowesk A-99, Dauntless D-35, Glenelg G-49 and North Triumph G-43 wells on the Scotian Shelf (Figure 6.1). Zircons are the products of volcanic activity and thus the age of the zircons may indicate a volcanic source. The error range for reported zircon dates may be between 2-10 Ma (D.J.W. Piper, pers comm., 2010). Within the lowermost sandstone of the Cree Member in the Alma K-85 and Peskowesk A-99 wells, Piper et al.
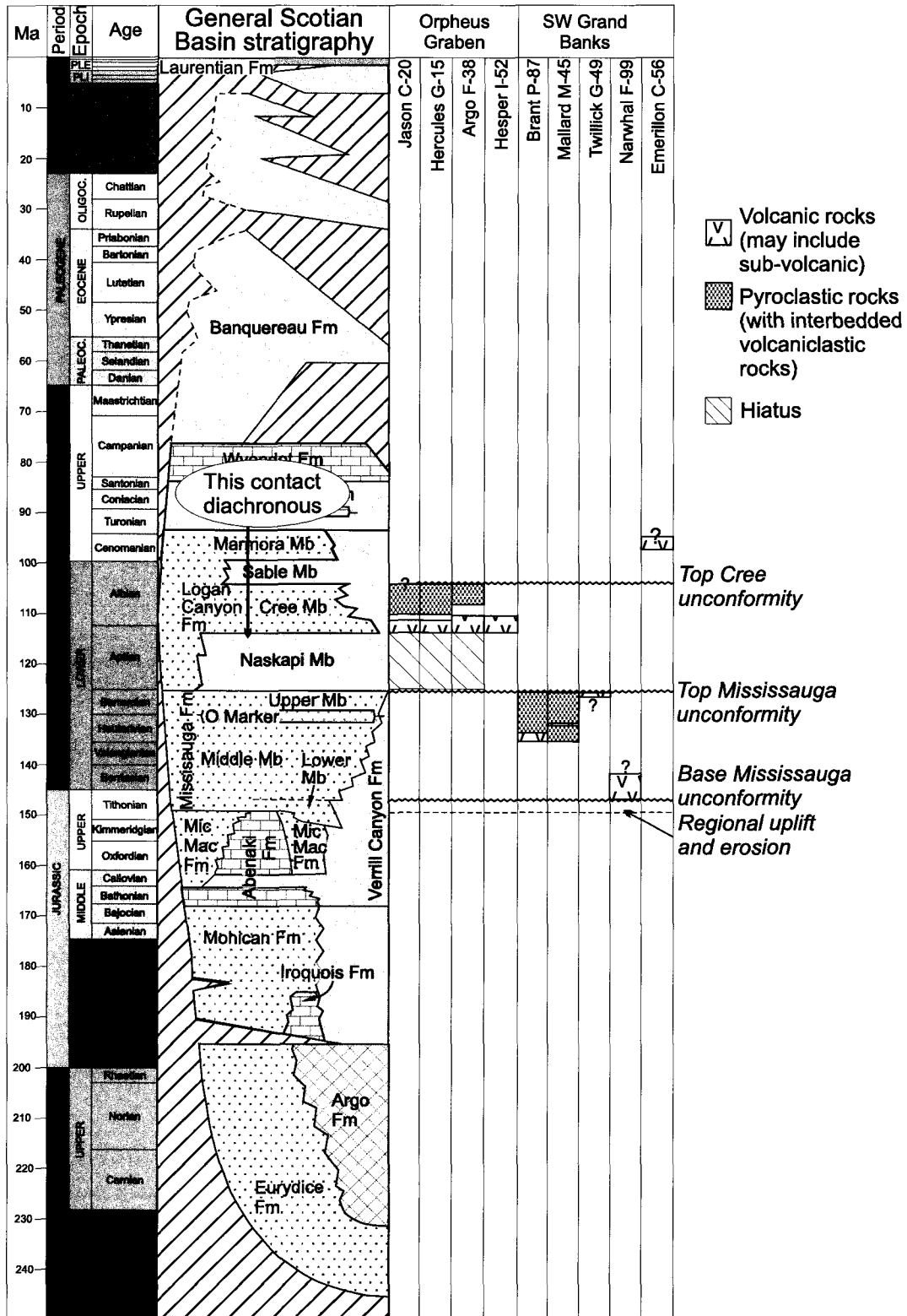
Figure 6.3: Generalized stratigraphy of the Scotian Shelf and SW Grand Banks. General position of volcanic rocks are indicated. (modified from Piper et al., *in prep*)

(*in prep*) identified zircons which have been dated as ~105-106 Ma, the same age as basaltic lapilli pyroclastic rocks dated at 103.9±2.6 Ma in the Cree Member in the Hercules G-15 well in the Orpheus Graben. The pyroclastic rocks in the Hercules G-15 well, and the possible pyroclastic rocks in the Argo F-38 well are capped by the Top Cree unconformity (Figure 3.11). It is unclear how much material was eroded by the Top Cree unconformity, but it is likely that some of the pyroclastic material from these wells was removed and transported elsewhere. The similarity in age of the zircons found within the Alma K-85 and Peskowesk A-99 wells and the pyroclastic rocks dated within the Hercules G-15 well at a similar stratigraphic level indicates the strong possibility that the zircons are sourced from the Hercules G-15 pyroclastic rocks. The mean grain size of zircons found by Piper et al. (*in prep*) is 105 μm. The maximum distance of direct airfall pyroclastic material of that grain size is approximately 100 km from the source, with an average of 50 km from the source (Fisher and Schmincke, 1984). The Peskowesk A-99 and Alma K-85 wells are located approximately 150 and 325 km from the Hercules G-15 well. Thus, direct airfall ash deposits of the dated zircons are unlikely. However, at the time of volcanism in the Orpheus Graben, river systems were cutting through the landscape near the Orpheus Graben which may have picked up the proximal pyroclastic material and deposited it more distally in the Scotian Basin (Figure 6.1).

Other zircon dates determined by Pe-Piper et al. (*in press*) are older, at 118 Ma and 127 Ma, and are found within the Upper Member of the Mississauga Formation in the Dauntless D-35, North Triumph G-43, Glenelg G-49 and Alma K-85 wells. Pe-Piper and Piper (*in press*) have determined that the sediments in the Dauntless D-35 well were sourced from a different drainage basin than the North Triumph G-43, Glenelg G-49 and

160

Alma K-85 wells. The source of these older zircons might have been the volcanoes on the SW Grand Banks or the Scatarie Ridge. Based on the error range in zircon dates, the older zircons may also be sourced from the Orpheus Graben. However, a source on the SW Grand Banks is unlikely due to the large distance from the inferred volcanic source to the wells that contain these detrital zircons on the Scotian Shelf and the fact that there are no detrital zircons older than Barremian (Piper et al., *in prep*) despite volcanic activity on the SW Grand Banks from at least the Hauterivian to the Barremian. Based on the inferred location of Cretaceous rivers (Pe-Piper and Piper, *in press*) (Figure 6.1), a source within the Laurentian sub-basin is also unlikely as there would be no path to transport detrital zircons into the Sable sub-basin. The dredged dyke on the Scatarie Ridge gave an age that falls in the Barremian (Delabio et al., 1979), but with an error range from top Aptian to top Berriasian. Thus it is possible that there was older volcanism on the Scatarie Ridge as well as Aptian to mid-Albian volcanism.

6.3 Style of regional tectonics and its relationship to volcanism

There are several rift-related tectonic events over the time of the extrusion of the Cretaceous volcanic rocks within the Scotian Basin (Figure 6.3). The Orpheus Graben, SE Scotian Shelf and SW Grand Banks have experienced a long and complex tectonic history. In the mid-Devonian there was convergence of the Avalon and Meguma terranes. This was followed by mid-Carboniferous to Permian dextral shear along the Cobequid-Chedabucto fault system, as a result of the convergence of Gondwana. Subsequent breakup during the late Triassic-early Jurassic proceeded in a south to north direction reactivating the Gondwana-Meguma suture as North America separated from

Africa. This resulted in crustal extension as well as strike-slip motion along the fault system which generated interconnected sub-basins, including the Orpheus Graben, separated by intervening basement ridges (Welsink et al., 1989a). The rifting of the Scotian margin also affected the Grand Banks by generating broad rift basins such as the Jeanne D'Arc, Whale and Horseshoe basins, which are present-day inboard basins (Tucholke et al., 2007). Syn and postrift sediments of the Eurydice, Argo, Iroquois, Abenaki, Mic Mac and Verrill Canyon formations were deposited during the late Triassic-Jurassic (Wade and MacLean, 1990).

A second phase of rifting between the Grand Banks and Iberia formed the relatively shallow rift basins of the SW Grand Banks, such as the South Whale sub-basin (Tucholke et al., 2007). In the eastern portion of the study area, near the Brant P-87 and Mallard M-45 wells, there are small rift basins such as that shown in the seismic profile at the Mallard M-45 well (Figure 4.13). Although the Mallard M-45 well does not penetrate sediments older than late Jurassic, the seismic profile in Figure 4.13 shows sedimentation within what appears to be a small basin well below the depth of the Mallard M-45 well. These basins may have begun developing long before rifting between Grand Banks and Iberia.

The pre-rift phase began during the latest Jurassic and generated the uplift, deformation, and erosion of Jurassic and older strata. The uplift has been termed the Avalon Uplift (Grant and McAlpine, 1990). The uplift is expressed in seismic profiles at the Emerillon C-56 well on the SW Grand Banks (Figure 4.10) with the peneplanation of the Jurassic strata by what has been termed the Base Cretaceous unconformity, which is equivalent to the Base Mississauga unconformity traced throughout the study area within

the seismic data. The Base Mississauga unconformity is also present on the SE Scotian

Shelf (Figure 4.5a and b) and Orpheus Graben (Figure 4.7), but it is not clear whether the

tilting of Jurassic strata in this area is exclusively due to uplifting on the Grand Banks or

a combination of uplift and post-rift subsidence of the Scotian margin sub-basins south of

the Jurassic hinge zone. Within the eastern portion of the SW Grand Banks, east of the

Puffin B-90 well, correlation of the Base Mississauga unconformity may be inconsistent,

as the area was peneplained by the Top Mississauga unconformity and thus can only be

traced based on lithostratigraphic picks by MacLean and Wade (1993).

Rifting of the Grand Banks from Iberia began following the uplift and erosion in

the Tithonian-Berriasian. Tucholke et al. (2007) claimed rifting occurred in three stages

culminating at the end Berriasian, end Hauterivian and end Aptian. However, the first

two stages seem to only be apparent on the Iberian side of the rift margin and are not

expressed on the Newfoundland side of the margin. Synchronous with the rifting on the

SW Grand Banks was the formation of the Fogo Seamounts. The seamounts are

generally parallel to the Cobequid-Chedabucto-SW Grand Banks fault zone. The J-

Anomaly Ridge is generally orthogonal to the fault system but parallel to the spreading

margin. Both are located to the south of the SW Grand Banks. The J-Anomaly Ridge

consists of mid-ocean ridge basalts overlain by upper Barremian or lower Aptian to lower

Albian carbonates (Tucholke et al., 1979) and is assumed to be a result of anomalous

melt production at this time south of the rifting margin (Tucholke and Ludwig, 1982).

The Fogo seamounts include the basalts of the Narwhal F-99 well that have been shown

to be older than Berriasian (from biostratigraphy) (Pe-Piper et al., 2007).

In the eastern portion of the study area, possibly Berriasian, but definitely Hauterivian (based on biostratigraphy) to Barremian sediments are preserved only in the small extensional basins as further tectonic movement induced the base Aptian Top Mississauga unconformity which peneplained pre-Aptian strata. Also preserved in these small basins and constrained by the Base Mississauga and Top Mississauga unconformities were the Hauterivian to Barremian volcanic and pyroclastic rocks found in the Mallard M-45 and Brant P-87 wells. The seismic profile near the Twillick G-49 well shows the peneplanation of strata underlying the Top Mississauga unconformity. Approximately 13 m of basalt survived the peneplanation and may indicate that it is a remnant of a basalt flow or flows similar to those found within the Brant P-87 and Mallard M-45 wells.

The Top Mississauga unconformity is also present on the SE Scotian Shelf and in the Orpheus Graben (Figure 4.5a and b) and records a change from the deposition of the underlying Mississauga Formation and the overlying sands and shales of the Logan Canyon Formation. This unconformity may be a result of continued post-rift subsidence or a more widespread tectonic event, as a similar unconformity is found to the north within the Jeanne D'Arc basin (Driscoll et al., 1995). Multiple occurrences of syn-rift volcanism clustering along the general alignment of the Cobequid-Chedabucto-SW Grand Banks fault zone, point to tectonic movement along this fault zone which may have opened pathways for magma migration through the crust and to the surface.

Following the Top Mississauga unconformity, volcanic and pyroclastic rocks were erupted in the Orpheus Graben and SE Scotian Shelf. This activity is partly synchronous with the latter part of rifting of the Grand Banks from Iberia which is

interpreted to have culminated near the Aptian-Albian boundary (Tucholke et al., 2007). The only interruption to sedimentation noted during this time is after the deposition of the Cree Member, as there is a local Top Cree unconformity within the Orpheus Graben, SE Scotian Shelf and at the edge of the margin of the southeast portion of the SW Grand Banks. This unconformity is a transgressive unconformity as determined by Weir-Murphy (2004). The only other volcanic occurrence on the SW Grand Banks is the sill or dyke of possible Cenomanian age in the Emerillon C-56 well but no conclusion can be drawn from it.

Onshore Nova Scotia, the lower Cretaceous Chaswood Formation, which is the onshore equivalent of the Mississauga and Logan Canyon Formations (Stea and Pullen, 2001), accumulated within fault-bounded basins. These onshore basins (including the Elmsvale Basin and West Indian Road Pit) formed within the early Cretaceous (Falcon-Lang et al., 2007) and unconformably overlie Carboniferous strata (Pe-Piper and Piper, 2004). The basal unconformity may correspond to the Base Mississauga unconformity discussed in this study. Also found within this formation is a mid-Cretaceous unconformity (Piper et al., 2005) which most likely corresponds to the Top Mississauga unconformity in this study. This suggests that there was regional and correlative activity on faults throughout the early Cretaceous, including along the Cobequid-Chedabucto-SW Grand Banks fault zone and along NE-SW trending faults that bound most Chaswood Formation basins.

Related tectonic movement may also be expressed by NE-SW trending faults on the SE Scotian Shelf, imaged in seismic profile 82-603 (Figure 4.18). Similar trending faults have been identified within the Chaswood Formation onshore of Nova Scotia

165

(Gobeil et al., 2006). The faults on the SE Scotian Shelf appear to be normal faults dipping basinwards and trending NE-SW. They seem to have been active from the late Jurassic through to sometime within the Tertiary.

6.4 Implications for lower Cretaceous sediments

The tectonic movement and corresponding regional and local unconformities have implications for the deposition, erosion and transport of lower Cretaceous sediments of the Mississuaga and Logan Canyon Formations across the study area.

The SE Scotian Shelf consists of relatively thick (~1800 m) and generally conformable Mississauga and Logan Canyon Formation strata. This includes the "O" marker, a limestone unit marking local transgression within the Mississauga Formation. The "O" marker has been shown in seismic profiles to be present in the SE Scotian Shelf and across part of the Laurentian Channel until it onlaps the Base Mississauga unconformity (Figures 4.5a and Appendix 1 Figure 1.9a). This marks the extent of deposition of fully marine sediments related to the transgression during the early Cretaceous.

The Naskapi Member of the Logan Canyon Formation is a marine shale which marks a major regional marine transgression. The interpretation of the stratigraphic position of the Aptian volcanic rocks in the Orpheus Graben and SE Scotian Shelf has shown the Naskapi Member to be absent in the wells on the Orpheus Graben (with the possible exception of the Argo F-38 well). It has also shown that the subaerial basalt flow, intersected by the Hesper I-52 and Hesper P-52 wells, encountered the paleoshoreline in this location and stopped as imaged in Figure 4.4. Therefore, the extent

166

of the shoreline during the early Aptian can be inferred to have not transgressed much

farther inboard than the Hesper I-52 and Hesper P-52 wells. Hindrances to this

transgression are most likely the tilting of lower Cretaceous strata inboard of the Hesper

wells upon which overlying Logan Canyon strata are seen to onlap (as imaged in Figure

4.5a and b) and the positive relief of the Canso Ridge.

Within the Orpheus Graben there is a question as to the existence of the Naskapi

Member within the Argo F-38 well. As the Naskapi Member is absent in the Hercules G-

15 and Jason C-20 wells, it might be expected to be absent in the nearby Argo F-38 well.

However, MacLean and Wade (1993) have interpreted the presence of the Naskapi

Member and an overlying 50 m of Cree Member sediments underlying the basalt flows in

this well, which clearly correlate with those in the Hercules G-15 and Jason C-20 wells.

Thus, either the Argo F-38 well experienced a slightly different depositional history with

greater accommodation, or the interpretation of MacLean and Wade (1993) is wrong.

The log character of the gamma and sonic velocity logs at the base of the Cree Member

in the Hercules G-15 and Jason C-20 wells (gamma= 20 API, sonic velocity= 350 μs/m^2)

is similar to the log character of the Argo F-38 well approximately 15 m below the basal

basalt flow (Figure 3.7). Biostratigraphy by Bujak (1979) indicates sediments at this

level are of Aptian age. This horizon at 1057 m depth in the Argo F-38 well is the most

probable position of the base Logan Canyon unconformity.

The SW Grand Banks also presents implications for lower Cretaceous

sedimentation. As tectonic movement due to pre-rift uplift is more predominant in this

area, the effects of reworking and erosion of older sediments are much more obvious.

This is exemplified by the thin Mississauga and Logan Canyon Formation sediments near

the Emerillon C-56 well in comparison with the thick succession on the SE Scotian Shelf and Orpheus Graben (Figure 4.10). However, there is also a thick succession of Mississauga and Logan Canyon Formation sediments at the southern edge of the SW Grand Banks as exemplified at the Puffin B-90 well (Figure 4.11). The proximal shoreline south of the Emerillon C-56 well is imaged in seismic profiles (Appendix Figure 1.16) and shows a thickening of both Mississauga and Logan Canyon sediments beyond the shoreline. Thus it would seem that sediments shed from the uplifted region near the Emerillon C-56 well, which is generally an uplifted zone from the Canso Ridge to the Ermerillon C-56 well, were deposited to the southwest into the Laurentian sub-basin.

East of the Puffin B-90 well, the tectonic style changes and there was significant sediment erosion at both the Base Mississauga and Top Mississauga unconformities. Based on lithostratigraphic picks by the CNLOPB (2007) and biostratigraphic picks by multiple authors over multiple years, the Aptian-Cenomanian Logan Canyon Formation overlies Jurassic and older strata in many wells east of the Puffin B-90 well. However, in small extensional basins such as that at the Brant P-87 and Mallard M-45 wells, and near the Twillick G-49 well, Mississauga Formation sediments are preserved. Well biostratigraphy and seismic profiles near the Brant P-87 and Mallard M-45 wells (Figures 4.12a, b and 4.13), show the Logan Canyon Formation is present but is very thin. Seismic profiles near the Narwhal F-99 well cross the proximal shoreline and show what appears to be eroded material deposited into deep water (Appendix Figure 1.17)

6.5 Thermal implications

Thermal modeling of wells in the Orpheus Graben, Scotian Shelf and SW Grand Banks has shown that the extruded volcanic and pyroclastic rocks did not have a significant local effect on the heat flow. However the regional effects of high heat flow, associated with volcanism, might have played an important role. The wells studied in this thesis are only a part of the widespread volcanism in eastern North America (Figure 6.4).

There have been several studies conducted within sub-basins on the Scotian Shelf which point to a regional heating event within the Cretaceous in the Scotian Basin (Grist et al., 1992; Li et al., 1995; Wierzbicki et al., 2006; Karim et al., 2009, 2010). Locations of samples in these studies are shown in Figure 6.5. Apatite fission track data has been investigated by Grist et al. (1992) and Li et al. (1995) in samples taken from the Mississauga and Logan Canyon Formations within wells across the Scotian Shelf. Their results indicate that the current basin temperature is insufficient to account for the observed fission track annealing and thus the basin must have been hotter in the past. Their method could constrain the peak temperatures up to 55°C hotter than at present, but could not constrain the timing of this heating event. They determined a broad range for timing of the event, from 100-40 Ma. These authors suggested that the heat influx was due to a rapid expulsion of overpressured hot fluids, which may have been related to regional volcanism.

Wierzbicki et al. (2006) discovered high temperature values of 85-147°C in fluid inclusions from calcites and dolomites of the Abenaki platform carbonates in the Deep Panuke area. These temperatures are higher than expected based on the present day

169
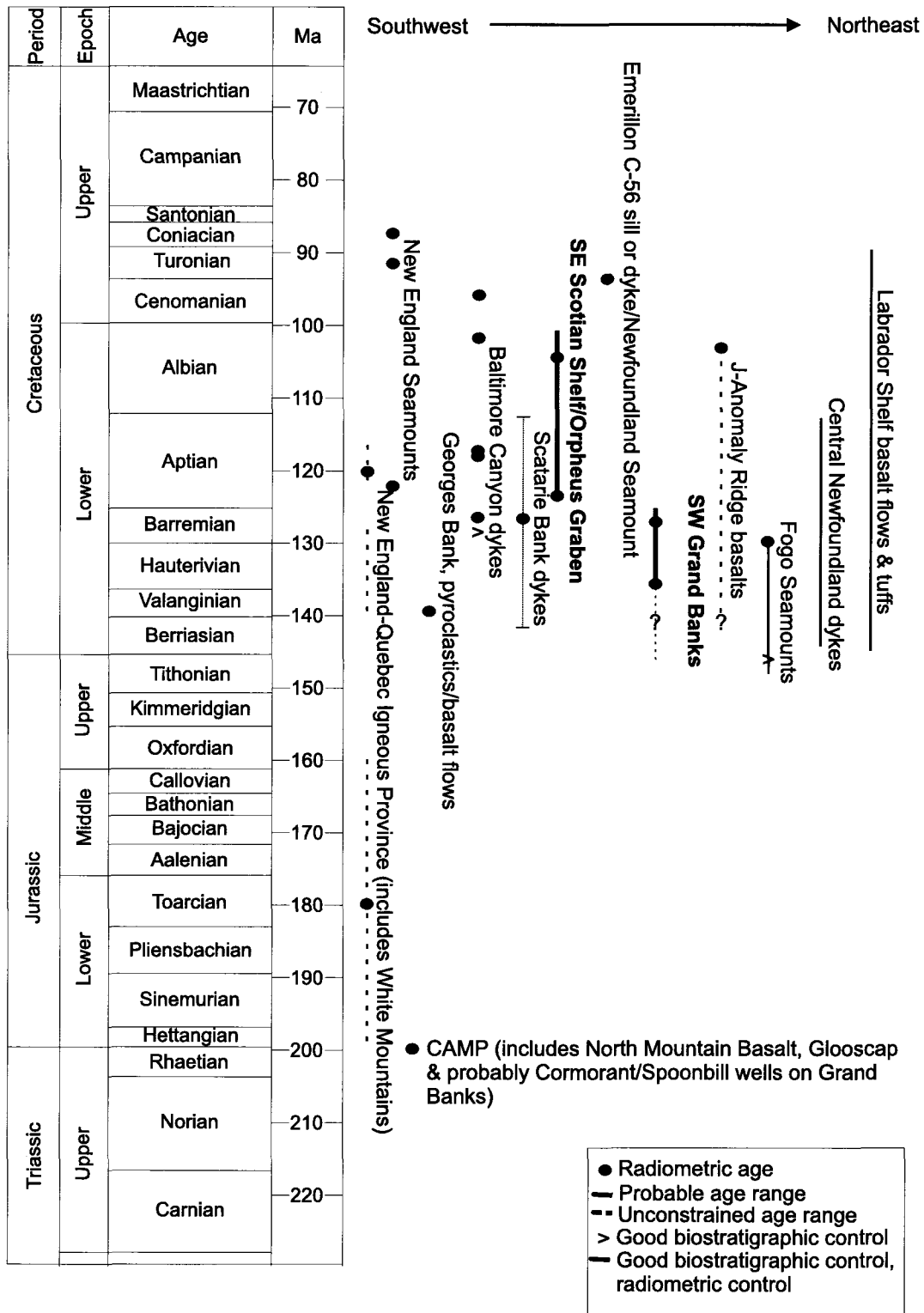
Figure 6.4: Timescale showing timing of volcanic occurrences in eastern Canada (Strong and Harris, 1974; Schlee et al., 1976; Keen at al., 1977; Hall et al., 1977; McHone, 1978; Delabio et al., 1979; Houghton et al., 1979; Tucholke and Ludwig, 1982; Eby, 1985; Jansa and Pe-Piper, 1985; Jansa and Pe-Piper, 1986)

170

Figure 6.5: Map showing location of Cretaceous volcanism in eastern Canada as well as the locations of samples investigated for apatite fission track and fluid inclusions investigations by other authors (Grist et al., 1992; Li et al., 1995; Wierzbicki et al., 2006; Karim et al., 2009, 2010)

geothermal gradient. They attributed the higher than expected temperatures to the passage of hydrothermal fluids through faults, which they proposed may be associated with the final breakup stage of the Grand Banks and Iberia in the Aptian.

Fluid inclusions were also studied in wells on the Scotian Shelf by Karim et al. (2009) and Karim et al. (2010). Karim et al. (2009) found primary fluid inclusions within lower Cretaceous sandstones of the Mississauga Formation in the Glenelg G-43, Thebaud I-93 and Chebucto K-90 wells. The primary fluid inclusions indicate temperatures up to 130°C, much hotter than present day (Karim et al., 2009). Further studies of primary fluid inclusions in the lower member of the Mississauga Formation in wells within the Venture field on the Scotian Shelf (Venture 1, Venture 2, and Venture B-52) determined higher than expected temperatures of 82-135°C. Karim at al. (2010) attributes the high temperatures to a thermal event at ~105 Ma synchronous with known active faulting in the Orpheus Graben and consistent with the approximate age of faulting described by Wierzbicki et al. (2006).

Further regional evidence of a high heat flow is the presence of Cretaceous volcanic and sub-volcanic rocks found at the New England seamounts, Baltimore Canyon and in the New England-Quebec igneous province (Strong and Harris, 1974; Schlee et al., 1976; Keen et al., 1977; Hall et al., 1977; McHone, 1980; Houghton et al., 1979; Jansa and Pe-Piper, 1985) (Figure 1.3). An investigation by Beck and Housen (2003) determined that the paleomagnetic poles in the Appalachians contained an unexpected mid-Cretaceous overprint. The authors proposed the overprint may be due to partial thermal remagnetization associated with mid-Cretaceous (~122 Ma) igneous activity.

These independent discoveries of unexpected high heat flow in wells across the Scotian Basin points to a regional thermal event within the Cretaceous. Previous authors have speculated that the heating event occurred within the late Cretaceous (Grist et al., 1992; Li et al., 1995). However it is not unreasonable to think that any thermal event occurred in the mid-Cretaceous at the same time as the regional evidence of igneous activity and tectonism. Although a heat pulse generated from the volcanism within the Orpheus Graben and SE Scotian Shelf did not produce a high conductive heat flow, convective heat flow is possible. The regional thermal input manifested by volcanism could have generated hot hydrothermal fluids, which then migrated laterally through the basin. Strike-slip faults in the Scotian Basin, along with active NE-SW trending faults, reactivated by the final separation of the Grand Banks from Iberia in Aptian time, may have opened pathways not only for the Orpheus Graben volcanism but also associated hydrothermal fluids. Thus, although the volcanism within the Orpheus Graben and SE Scotian Shelf would not have generated enough heat flow to significantly alter sediments locally, the heating of nearby hydrothermal fluids which propagated throughout the basin may have regionally increased burial temperatures. These increased burial temperatures would not have been enough to alter the maturation of sediments, as shown by the thermal modeling, but may have impacted the speed of diagenetic precipitation.

The thermal implications of volcanism on the SW Grand Banks are not as well constrained as the SE Scotian Shelf and Orpheus Graben. However, if there is a regional high heat flow, as manifested by volcanism, the thermal implications of the SW Grand Banks are likely quite similar to those of the SE Scotian Shelf and Orpheus Graben.

6.6 Conclusions

Meeting the objectives of this study has resulted in a better understanding of the eruptive style and correlation of Cretaceous volcanic and pyroclastic rocks within the Orpheus Graben, SE Scotian Shelf and SW Grand Banks along with their relation to regional tectonic events and regional heat flow.

1) The volcanic and pyroclastic rocks in the Argo F-38, Jason C-20 and Hercules G-15 wells correlate. The volcanic rock in the Hesper I-52 well is a basalt flow which is correlatable to the Orpheus Graben. The source of these volcanic and pyroclastic rocks is most likely the Scatarie Ridge to the north of the Orpheus Graben. As a result of the correlation of these volcanic rocks, the position of the base Logan Canyon has been refined in wells in the Orpheus Graben. The Naskapi transgression did not reach parts of the SE Scotian Shelf and Orpheus Graben (nor much of the Laurentian or South Whale subbasins).

2) Volcanic and pyroclastic rocks on the SW Grand Banks were extruded during Hauterivian to Barremian time in local mini basins. Basalt flows can be traced to the basin margin and are likely sourced from at least two volcanic centres on horsts at major magnetic highs.

3) Volcanic rocks on the SW Grand Banks, Orpheus Graben and SE Scotian Shelf are the product of varying intensities of Strombolian eruptions. Pyroclastic rocks and

trachytes follow periods of major basaltic eruption and mark the waning of volcanic activity.

4) Evidence of a regional heat flow is found in widespread Cretaceous volcanic activity in eastern North America, apatite fission track data, fluid inclusion data and paleomagnetic resetting, all reported in previous literature. The eruption of volcanic and pyroclastic rocks in the Orpheus graben, SE Scotian Shelf and SW Grand Banks is a manifestation of this high heat flow and was most likely facilitated by strike-slip faulting in the early to mid-Cretaceous.

5) The eruption of volcanic materials during the Cretaceous did not produce a significant local thermal effects on maturation. However, it was a manifestation of high regional heat flow that may have heated basinal hydrothermal fluids which propagated along reactivated faults, transmitting high heat flow into the western part of the Scotian Basin and perhaps elsewhere.

REFERENCES

Ascoli, P. 2008. Biostratigraphic picks: Mallard M-45. Online
http://basin.gdr.nrcan.gc.ca/wells/single_biostrat_e.php?well=D089

Blackwell, D. 1983. Heat flow in the Northern Basin and Range Province. *In* The role of
heat in the development of energy and mineral resources in the Northern Basin
and Range Province, Special Report 13. *Edited by* Geothermal Research Council,
p. 81-93

Bujak, J.P. 1979. Biostratigraphic picks: Argo F-38. Online
http://basin.gdr.nrcan.gc.ca/wells/single_biostrat_e.php?well=D017

Canadian Aeromagnetic Database. 2010. Magnetic Anomaly Map. Airborne Geophysics
Section, GSC-Central division, Geological Survey of Canada, Earth Sciences
Sector, Natural Resources Canada

Clague, D. 1987. Hawaiian xenolith populations, magma supply rates, and development
of magma chambers. Bulletin of Volcanology, v. 49, p. 577-587

CNLOPB. 2007. Schedule of wells. Online http://www.cnlopb.nl.ca/well_intro.shtml
Accessed March 2010

Cornen, G.; Beslier, M.-O.; Girardeau, J., 1996. Petrology of the mafic rocks cored in
the Iberia Abyssal Plain. *In* Proceedings of the ODP, Scientific Results, 149.
Edited by Whitmarsh, R.B., Sawyer, D.S., Klaus, A., and Masson, D.G. College
Station, TX (Ocean Drilling Program), p. 449–469

Dehler, S.; Keen, C. 1993. Effects of rifting and subsidence on thermal evolution of
sediments in Canada's east coast basins. Canadian Journal of Earth Sciences, v.
30, p. 1782-1798

Delabio, R.; Lachance, G.; Steens, R.; Wanless, R. 1979. Age determinations and
geological studies, K-Ar isotopic ages, Report 14. Geological Survey of Canada
Paper 79-02, 67p.

Driscoll, N.W.; Hogg, J.R.; Christie-Blick, N; Karner, G.D. 1995. Extensional tectonics
in the Jeanne D'Arc basin, offshore Newfoundland: Implication for timing and
breakup between Grand Banks and Iberia. *In* The Tectonics, Sedimentation and
Paleooceanography of the North Atlantic Region. *Edited by* Scrutton, R.A.;
Stoker, M.S.; Shimmield, G.B.; Tudhope, A.W. Geological society of London,
Special Publications 90, p. 1-28

Eby, G.N. 1985. Age relations, chemistry and petrogenesis of mafic alkaline dykes from the Monteregian Hills and younger White Mountains Igneous Province. Canadian Journal of Earth Science, v. 22, p. 1103-1111

Eldholm, O.; Sundvor, E.; Vogt, P.; Hjelstuen, B.; Crane, K.; Nilsen, A.; Gladczenko, T. 1999. SW Barents Sea continental margin heat flow and Håkon Mosby mud volcano. Geo-Marine Letters, v. 19, p. 29-37

Enachescu, M. 1988. Extended basement beneath the intracratonic rifted basins of the Grand Banks of Newfoundland. Canadian Journal of Exploration Geophysics, v. 24, no. 1, p. 48-65

Falcon-Lang, H.J.; Fensome, R.A.; Gibling, M.R.; Malcolm, J.; Fletcher, K.R.; Holleman, M. 2007. Karst-related outliers of the Cretaceous Chaswood Formation of Maritime Canada. Canadian Journal of Earth Sciences, v. 44, no. 5, p. 619-642

Fisher R.V.; Schmincke, H-U. 1984. Pyroclastic rocks. Springer, New York, 472p.

Francis, P.; Oppenheimer, C. 2004. Volcanoes (Second Edition). Oxford University Press, New York, 521p.

Given, M.M. 1977. Mesozoic and early Cenozoic geology of offshore Nova Scotia. Bulletin of Canadian Petroleum Geology, v. 25, p. 63-91

Gradstein, F.M.; Ogg, J.; van Kranendonk, M. 2008. On the geologic timescale 2008. Newsletters on Stratigraphy, v. 43, no. 1, p. 5-13

Gradstein, F.M. 1977. Biostratigraphic picks: Brant P-87. Online http://basin.gdr.nrcan.gc.ca/wells/single_biostrat_e.php?well=D114

Grant, A.C.; McAlpine, K.D. 1990. The continental margin around Newfoundland. *In* Geology of the Continental Margin of Eastern Canada. *Edited by* M.J. Keen and G.L. Williams. Geological Survey of Canada, Geology of Canada, no.2 (also Geology of North America, Vol. I-1), p. 241-292

Grist, A.M.; Reynolds, P.H.; Zentilli, M.; Beaumont, C. 1991. The Scotian Basin offshore Nova Scotia: thermal history and provenance of sandstones from apatite fission track and $^{40}Ar/^{39}Ar$ data. Canadian Journal of Earth Sciences, v. 29, p. 909-924

Hall, J.M.; Barrett, D.L.; Keen, C.E. 1977. The volcanic layer of the ocean crust adjacent to Canada- a review. *In* Volcanic Regimes of Canada. *Edited by* Baragar, W.R.; Coleman, L.C.; Hall, J.M. Geological Association of Canada, Special paper 16, p. 425-444

Haworth, R.T.; Lefort, J.P. 1979. Geophysical evidence for the extent of the Avalon zone in Atlantic Canada. Canadian Journal of Earth Sciences, v. 16, p. 552-567

Hellinger, S.; Sclater, J. 1983. Some comments on two-layer extensional models for the evolution of sedimentary basins. Journal of Geophysical Research, v. 88, p. 8251-8269

Hinz, K.; Winterer, E. et al. 1984. Initial reports of the Deep Sea Drilling Project, Volume 79, Washington, D.C., US Government Printing Office, 934p.

Houghton, R.L.; Thomas, J.E.; Diecchio, R.J.; Tagliacozzo, A. 1979. Radiometric ages of basalts from DSDP Leg 43: sites 382 and 385 (New England seamounts), 384 (J Anomaly), 386 and 387 (central and western Bermuda Rise). *In* Initial reports of the Deep Sea Drilling Project, volume 43, *Edited by* Tucholke, B.C.; Vogt, P.R. et al., p. 721-738

Issler, D.; McQueen, H.; Beaumont, C. 1988. Thermal and isostatic consequences of simple shear extension of the continental lithosphere. Earth and Planetary Science Letters, v. 91, p. 341-358

Issler, D.; Beaumont, C. 1986. Estimates of terrestrial heat flow in offshore eastern Canada: Discussion. Canadian Journal of Earth Sciences, v.23, p. 2083-2085

Jansa, L.F.; Pe-Piper, G.; Loncarevic, B.D. 1993. Appalachian basement and its intrusion by Cretaceous dykes, offshore southeast Nova Scotia, Canada. Canadian Journal of Earth Sciences, v. 30, p. 2495-2509

Jansa, L.F. 1991. Regional geology and geophysics: pre-Mesozoic basement and Mesozoic igneous rock occurrences. Map. *In* East Coast Basin Atlas Series: Scotian Shelf, Geological Survey of Canada, 25p.

Jansa, L.F.; Pe-Piper. 1988. Middle Jurassic to Early Cretaceous igneous rocks along eastern North American continental margin. The American Association of Petroleum Geologists Bulletin, v. 72, p. 347-366

Jansa, L.F.; Pe-Piper, G. 1986. Geology and geochemistry of middle Jurassic and early Cretaceous igneous rocks on the eastern North American continental shelf. Geological Survey of Canada Open File 1351, 95p.

Jansa, L.F.; Pe-Piper, G. 1985. Early Cretaceous volcanism on the northeastern American margin and implications for plate tectonics. Geological Society of America Bulletin, v. 96, p. 83-91

Jansa, L.F.; Wade, J.A. 1975. Geology of the continental margin off Nova Scotia and Newfoundland. *In* Offshore Geology of Eastern Canada, Volume 2: Regional

Geology. *Edited by:* W. Van der Linden and J.A. Wade. Geological Survey of Canada paper 74-30, p. 51-106

Jarvis, G.; McKenzie, D. 1980. Sedimentary basin formation with finite extension rates. Earth and Planetary Science Letters, v. 48, p. 42-52

Jones, S.; Wielens, H.; Williamson, M-C.; Zentilli, M. 2007. Impact of magmatism on petroleum systems in the Sverdrup basin, Canadian Arctic Islands, Nunavut: A numerical modeling study. Journal of Petroleum Geology, v. 30, no. 3, p. 237-256

Karim, A.; Pe-Piper, G.; Piper, D.; Hanley, J. 2010. Thermal history and the relationship between diagenesis and the reservoir connectivity: Venture field, offshore Nova Scotia, eastern Canada. Geological Survey of Canada Open File 6557, 69p.

Karim, A.; Hanley, J.J.; Pe-Piper, G.; Piper, D.J.W. 2009. Fluid inclusions in Mississauga Formation sandstones and their implications. Core 09, Petroleum society Technical Sessions, October 06-08, Halifax, NS

Keen, C.; Dehler, S. 1993. Stretching and subsidence: rifting of conjugate margins in the North Atlantic region. Tectonics, v. 12, no. 5, p. 1209-1229

Keen, C.; Courtney, R.; Dehler, S.; Williamson, M-C. 1993. Decompression melting at rifted margins: Comparison of model predictions with the distribution of igneous rocks on the eastern Canadian margin. Earth and Planetary Science Letters, v. 121, p. 403-416

Keen, M.J.; Piper, D.J.W. 1990. Geological and historical perspectives. *In* Geology of the Continental Margin of Eastern Canada. *Edited by* M.J. Keen and G.L. Williams. Geological Survey of Canada, Geology of Canada, no.2 (also Geology of North America, Vol. I-1), p. 7-30

Keen, C.; Beaumont, C. 1990. Geodynamics of rifted continental margins. *In* Geology of the continental margin of eastern Canada. *Edited by* Keen, M. and Williams, G. Geological Survey of Canada, no.2, p. 391-472

Keen, C.E.; Loncarevic, B.D.; Reid, I.; Woodside, J.; Haworth, R.T.; Williams, H. 1990. Tectonic and geophysical overview. *In* Geology of the Continental Margin of Eastern Canada. *Edited by* M.J. Keen and G.L. Williams. Geological Survey of Canada, Geology of Canada, no.2 (also Geology of North America, Vol. I-1), p. 33-85

Keen, C.; Hall, B.; Sullivan, K. 1977. Mesozoic evolution of the Newfoundland basin. Earth and Planetary Science Letters, v. 37, p. 307-320

Kilburn, C. 2000. Lava flows and flow fields. *In* Encyclopedia of Volcanoes. *Edited by* Sigurdsson, H.; Houghton, B.; McNutt, S.; Rymer, H.; Stix, J. Academic Press, Toronto, 1417p.

Klitgord, K.; Schouten, H. 1986. Early Mesozoic reconstruction from sea-floor spreading data: Eos (Transactions, American Geophysical Union), v. 63, 307p.

Li, G.; Ravenhurst, C.; Zentilli, M. 1995. Implications of apatite fission track analysis for the thermal history of the Scotian Basin, offshore Nova Scotia, Canada. Bulletin of Canadian Petroleum Geology, v. 43, no. 2, p. 127-144

Littler, K.; Robinson, S.; Bown, P.; Nederbragt, A.; Pancost, R. 2009. High sea-surface temperatures in the Early Cretaceous (Berriasian – Barremian): a problem for ice? Geological Research Abstract, v. 11, EGU2009-2464-1, 19 – 24 April, Vienna, Austria.

Louden, K. 2002. Tectonic evolution of the east coast of Canada. CSEG Recorder, p. 37-48

Louden, K.; Lau, H. 2001. Insights from scientific drilling on rifted continental margins. Geoscience Canada, v. 28, no. 4, p. 87-95

Lyngberg, E. 1984. The Orpheus Graben, offshore Nova Scotia: palynology, organic geochemistry, maturation and time-temperature history. M.Sc. thesis, University of British Columbia, 172p.

MacKenzie, A.; Beaumont, C.; Boutilier, R.; Rullkotter, J. 1985. The aromatization and isomerization of hydrocarbons and the thermal subsidence history of the Nova Scotia margin. Philosophical Transactions of the Royal Society of London, v. 315, p. 203-232

McKenzie, D. 1978. Some remarks on the development of sedimentary basins. Earth and Planetary Science Letters, v.40, p. 25-32

MacLean, B., Wade, J. 1993. Seismic markers and stratigraphic picks in the Scotian Basin wells: East coast basin atlas series. Geological Survey of Canada, 276p.

MacLean, B.; Wade, J. 1992. Petroleum geology of the continental margin south of the islands of St. Pierre and Miquelon, gulf of St. Lawrence. Canadian Society of Petroleum Geologists Bulletin, v. 40, p. 222-253

Martin, U.; Nemeth, K. 2006. How Strombolian is a "Strombolian" scoria cones? Some irregularities in scoria cone architecture from the Transmexican Volcanic Belt, near Volcan Ceboruco (Mexico), and AlHaruj (Libya). Journal of Volcanology and Geothermal Research, v. 155, p. 104-118

McHone, J. 1978. Distributions, orientations and ages of mafic dikes in central New England. Geological Society of America Bulletin, v. 89, p. 1645-1655

McIver, N. 1971. Cenozoic and Mesozoic stratigraphy of the Nova Scotia shelf. Canadian Journal of Earth Sciences, v. 9, p. 54-70

New Mexico Tech: New Mexico Bureau of Geology and Mineral Resources. 2008. K/Ar and ^{40}Ar/^{39}Ar Methods. Online: http://geoinfo.nmt.edu/labs/argon/methods/home.html Accessed June, 2010

Pe-Piper, G.; Piper D.J.W. submitted. Volcanic ash in the lower Cretaceous Chaswood Formation of Nova Scotia, source and implications. 42p.

Pe-Piper, G.; Piper, D.J.W., in press. Cretaceous re-activation of the passive-margin Scotian Basin. In: *Recent advances in tectonics of sedimentary basins*, ed. C. Busby and A. Azor.

Pe-Piper, G.; Piper, D.J.W.; Jansa, L.; de Jonge, A. 2007. Early Cretaceous opening of the North Atlantic ocean: implications of the petrology and tectonic setting of the Fogo Seamounts off the SW Grand Banks, Newfoundland. Geological society of America Bulletin, v. 119, no. 5/6, p. 712-724

Pe-Piper, G.; Piper, D.J.W. 2004. The effects of strike-slip motion along the Cobequid-Chedabucto-southwest Grand Banks fault system on the Cretaceous-Tertiary evolution of Atlantic Canada. Canadian Journal of Earth Sciences, v. 41, p. 799-808

Pe-Piper, G.; Jansa, L.F.; Palacz, Z. 1994. Geochemistry and regional significance of the Early Cretaceous bimodal basalt-felsic associations on Grand Banks, eastern Canada. Geological Society of America Bulletin, v. 106, p. 1319-1331

Pe-Piper, G.; Jansa, L.F.; Lambert, R. 1992. Early Mesozoic magmatism on the eastern Canadian margin: Petrogenetic and tectonic significance. *In* Eastern North American Mesozoic Magmatism. *Edited by:* J. Puffer and P. Ragland. Geological Society of America Special Paper 268, p. 13-36

Pe-Piper, G.; Piper, D.J.W.; Keen, M.J.; McMillan, N.J. 1990. Igneous rocks of the continental margin. *In* Geology of the Continental Margin of Eastern Canada. *Edited by* M.J. Keen and G.L. Williams. Geological Survey of Canada, Geology of Canada, no.2 (also Geology of North America, Vol. I-1), p. 75-82

Pe-Piper, G.; Jansa, L.F. 1987. Geochemistry of late Middle Jurassic-Early Cretaceous igneous rocks on the eastern North American margin. Geological Society of American Bulletin, v. 99, p. 803-813

Pe-Piper, G; Jansa, L. 1986. Geology and geochemistry of Middle Jurassic and Early Cretaceous igneous rocks on the eastern North American continental shelf. Geological Survey of Canada Open File 1351

Piper, D.J.W.; Pe-Piper, G.; Tubrett, M. Triantaphyllidis, S.; Strathdee, G., in prep. Detrital zircon geochronology and polycyclic sediment sources, Cretaceous Scotian Basin, southeastern Canada.

Piper, D.J.W.; Pe-Piper, G.; Douglas, E.V. 2005. Tectonic deformation and its sedimentary consequences during deposition of the Lower Cretaceous Chaswood Formation, Elmsvale basin, Nova Scotia. Bulletin of Canadian Petroleum Geology, v. 53, no. 2, p. 189-199

Renne, P.; Swisher C.; Deino, A.; Karner, D.; Owens, T.; DePaolo, D. 1998. Intercalibration of standards, absolute ages and uncertainties in $^{40}Ar/^{39}Ar$ dating. Chemical Geology, v. 145, p. 117-152

Royden, L.; Keen, C. 1980. Rifting process and thermal evolution of the continental margin of eastern Canada determined from subsidence curves. Earth and Planetary Science Letters, v. 51, p. 343-361

Sarna-Wojcicki, A.; Champion, D.; Davis, J. 1984. Holocene volcanism in the conterminous United States and the role of silicic volcanic ash layers in correlation of the latest Pleistocene and Holocene deposits. *In* Late-Quaternary environments of the United States: The Holocene. *Edited by* Wright, H. University of Minnesota Press, p. 52-77

Schlee, J.S.; Behrendt, J.C.; Grow, J.A.; Robb, J.M.; Mattick, R.E.; Taylor P.T.; Lawson, B.J. 1976. Regional geologic framework off northeastern United States. American Association of Petroleum Geologists Bulletin, v. 60, p. 926-951

Schlumberger. 2007. PetroMod 10 computer software.

Schmincke, H-U. 2004. Volcanism. Springer, New York, 324p.

Schoene, B.; Bowring, S.A.; 2006. U-Pb systematics of the McClure Mountain syenite: thermochronological constraints on the age of the 40Ar/39Ar standard MMhb. Contributions to Mineralogy and Petrology, v. 151, p. 615-630

Sheridan, R. 1983. Phenomena of pulsation tectonics related to the breakup of the eastern North American continental margin. Tectonophysics, v. 94, p. 169-185

Silvestri, S. 1961. Proposal for a genetic classification of hyaloclastites. Bulletin of volcanology, v. 25, no. 1, p. 315-321

SMT (Seismo-Micro Technology). 2009. The KINGDOM Suite computer software.

Spitzer, R.; White, R.; Christie, P. 2008. Seismic characterization of basalt flows from the Faroes margin and the Faroe-Shetland basin. Geophysical Prospecting, v. 56, p. 21-31

Stea, R.; Pullan, S. 2001. Hidden Cretaceous basins in Nova Scotia. Canadian Journal of Earth Sciences, v. 38, p. 1335-1354

Steiger, R.H.; Jager, E. 1977. Subcommission on geochronology: convention on the use of decay constants in geochronology and cosmochronology. Earth and Planetary Science Letters, v. 36, p. 359-362

Strong, D.R.; Harris, A. 1974. The petrology of Mesozoic alkaline intrusives of central Newfoundland. Canadian Journal of Earth Sciences, v. 11, p. 1208-1219

Tankard, A. J.; H. J. Welsink, 1989, Mesozoic extension and styles of basin formation in Atlantic Canada, *In* Extensional tectonics and stratigraphy of the north Atlantic margins. *Edited by* Tankard, A. and Balkwill, H. American Association of Petroleum Geology Memoir 46, p. 175–195

Tucholke, B.; Sawyer, D.; Sibuet, J.-C. 2007. Breakup of the Newfoundland-Iberia rift. *In* Imaging, Mapping and Modelling Continental Lithosphere extension and Breakup. *Edited by* Karner, G.; Manatschal, G.; Pinheiro, L. Geological Society of London, Special Publications 282, p. 9-46

Tucholke, B.; Ludwig, W. 1982. Structure and origin of the J Anomaly Ridge, western North Atlantic Ocean. Journal of Geophysical Research, v. 87, no. B11, p. 9389-9407

Tucholke, B., et al. 1979. Site 384: The Cretaceous/Tertiary boundary, Aptain reefs, and the J Anomaly Ridge. Initial Report of the Deep Sea Drilling Project, v. 143, p. 107-165

Vazquez, J.; Shamberger, P.; Hammer, J. 2007. Plutonic xenoliths reveal the timing of magma evolution at Hualalai and Mauna Kea, Hawaii. Geology, v. 35, no. 8, p. 695-698

Vergniolle, S.; Mangan, M. 2000. Hawaiian and Strombolian eruptions. *In* Encyclopedia of Volcanoes. *Edited by* Sigurdsson, H.; Houghton, B.; McNutt, S.; Rymer, H. Stix, J. Academic Press, New York, 1417p.

Vespermann, D.; Schmincke, H-U. 2000. Scoria cones and tuff rings. *In* Encyclopedia of Volcanoes. *Edited by* Sigurdsson, H.; Houghton, B.; McNutt, S.; Rymer, H. Stix, J. Academic Press, New York, 1417p.

Wade, J.A.; MacLean, B.C. 1990. The geology of the southeastern margin of Canada. *In* Geology of the Continental Margin of Eastern Canada. *Edited by* M.J. Keen and G.L. Williams. Geological Survey of Canada, Geology of Canada, no.2 (also Geology of North America, Vol. I-1), p. 167-238

Weir-Murphy, S. 2004. The Cretaceous rocks of the Orpheus graben, offshore Nova Scotia. M.Sc. thesis, Saint Mary's University, 168p.

Welsink, H.; Dwyer, J.; Knight, R. 1989a. Tectono-stratigraphy of the passive margin off Nova Scotia. *In* Extensional tectonics and stratigraphy of the north Atlantic margins. *Edited by* Tankard, A. and Balkwill, H. American Association of Petroleum Geology Memoir 46, p. 215-231

Welsink, H.; Srivastava, S.; Tankard, A. 1989b. Basin architecture of the Newfoundland continental margin and its relationship to ocean crust fabric during extension. *In* Extensional tectonics and stratigraphy of the north Atlantic margins. *Edited by* Tankard, A. and Balkwill, H. American Association of Petroleum Geology Memoir 46, p. 197-213

Wierzbicki, R.; Dravis, J.; Al-Aasm, I.; Harland, N. 2006. Burial dolomitization and dissolution of upper Jurassic Abenaki platform carbonates, Deep Panuke reservoir, Nova Scotia, Canada. American Association of Petroleum Geology, v. 90, no. 11, p. 1843-1861

Williams, G. 1975. Dinoflagellate and spore stratigraphy of the Mesozoic-Cenozoic, offshore eastern Canada. *In* Offshore Geology of Eastern Canada, Volume 2: Regional Geology. *Edited by:* W. Van der Linden and J.A. Wade. Geological Survey of Canada paper 74-30, p. 107-161

Williamson, M-C.; Courtney, R.; Keen, C.; Dehler, S. 1995. The volume and rare earth concentrations of magmas generated during finite stretching of the lithosphere. Journal of Petrology, v. 36, no. 5, p. 1433-1453

Wilson, L.; Parfitt, E.; Head, J. 1995. Explosive volcanic eruptions-VIII. The role of magma recycling in controlling the behaviour of Hawaiian-style lava fountains. Geophysical Journal International, v. 121, p. 215-225

Yilmaz, O. 1987. Seismic Data Processing. Society of Exploration Geophysics. Tulsa, Oklahoma, 526p.

Zetaware. 2003. BHT Horner Correction utility. Online http://zetaware.com/utilities/bht/horner.html. Accessed March 2010.

APPENDIX 1
SEISMIC PROFILES

(refer to Chapter 4 Figure 4.1 for map of seismic
profile locations)
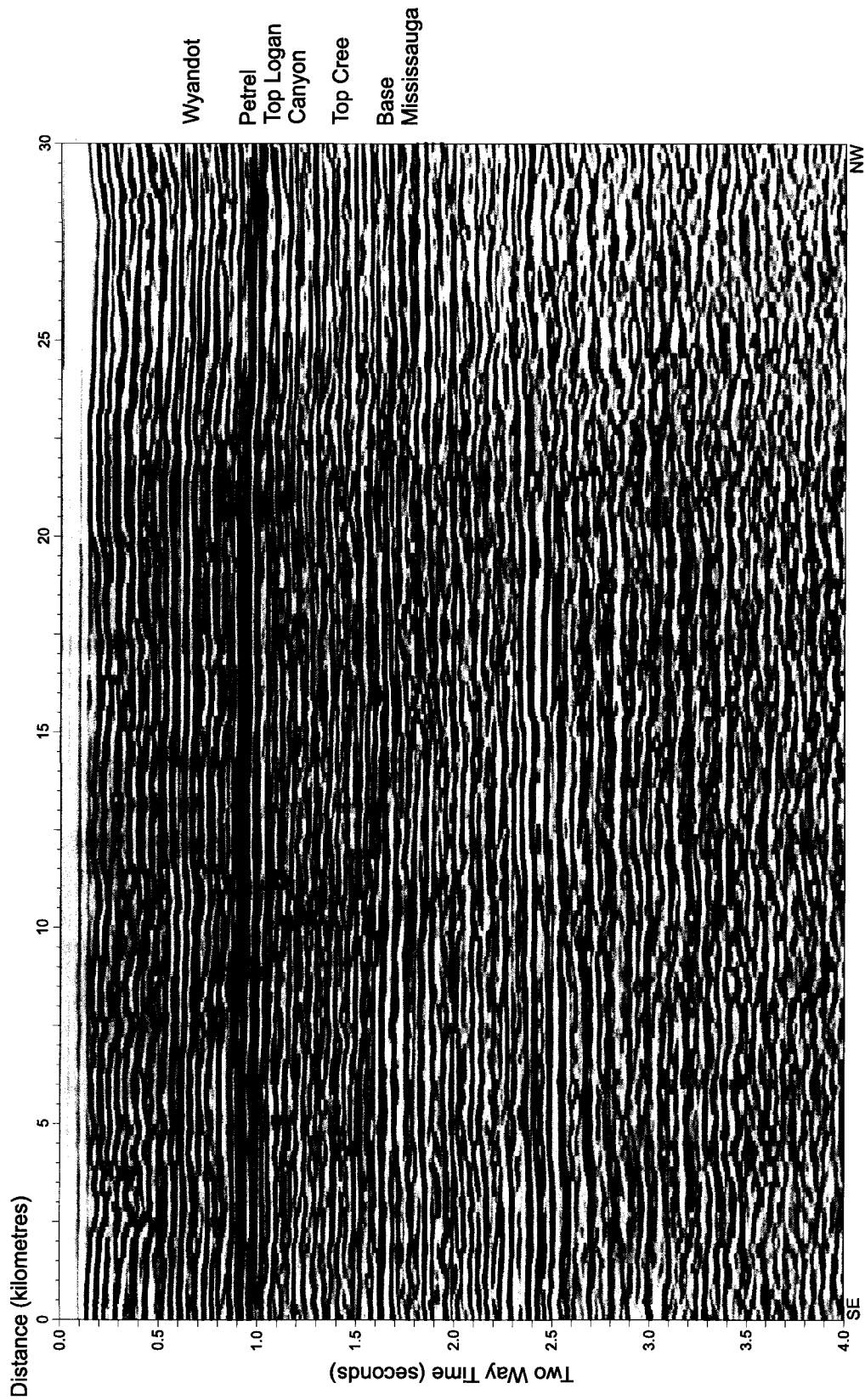
Figure 1.1: NW-SE profile E2-1040 linking the Scotian Shelf towards the Orpheus Graben
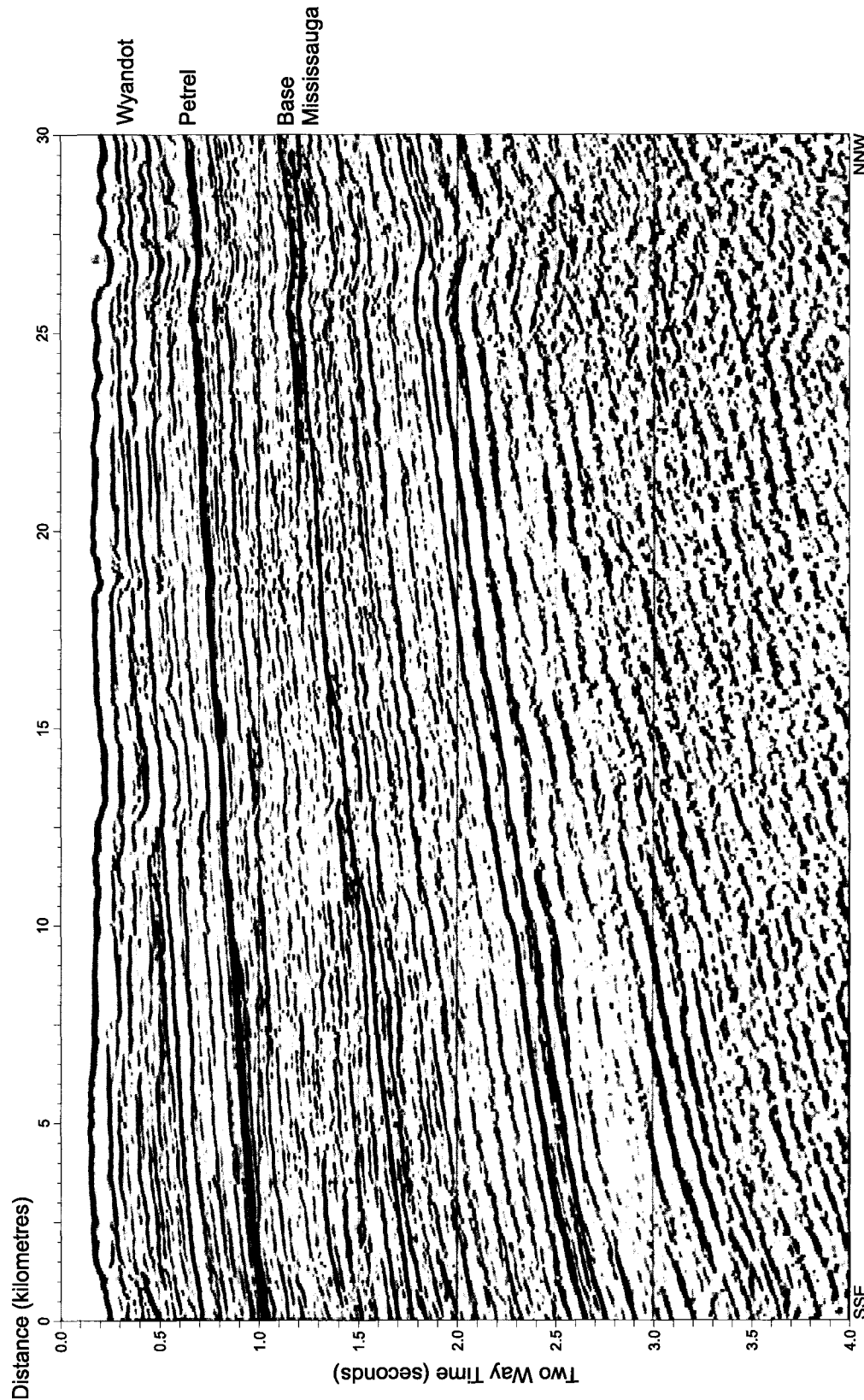
Figure 1.2a: NNW-SSE profile 3606A (part 1) correlating from the Scotian Shelf into the Orpheus Graben near the Jason C-20 well. It is at this point that correlation of all horizons fails.

187
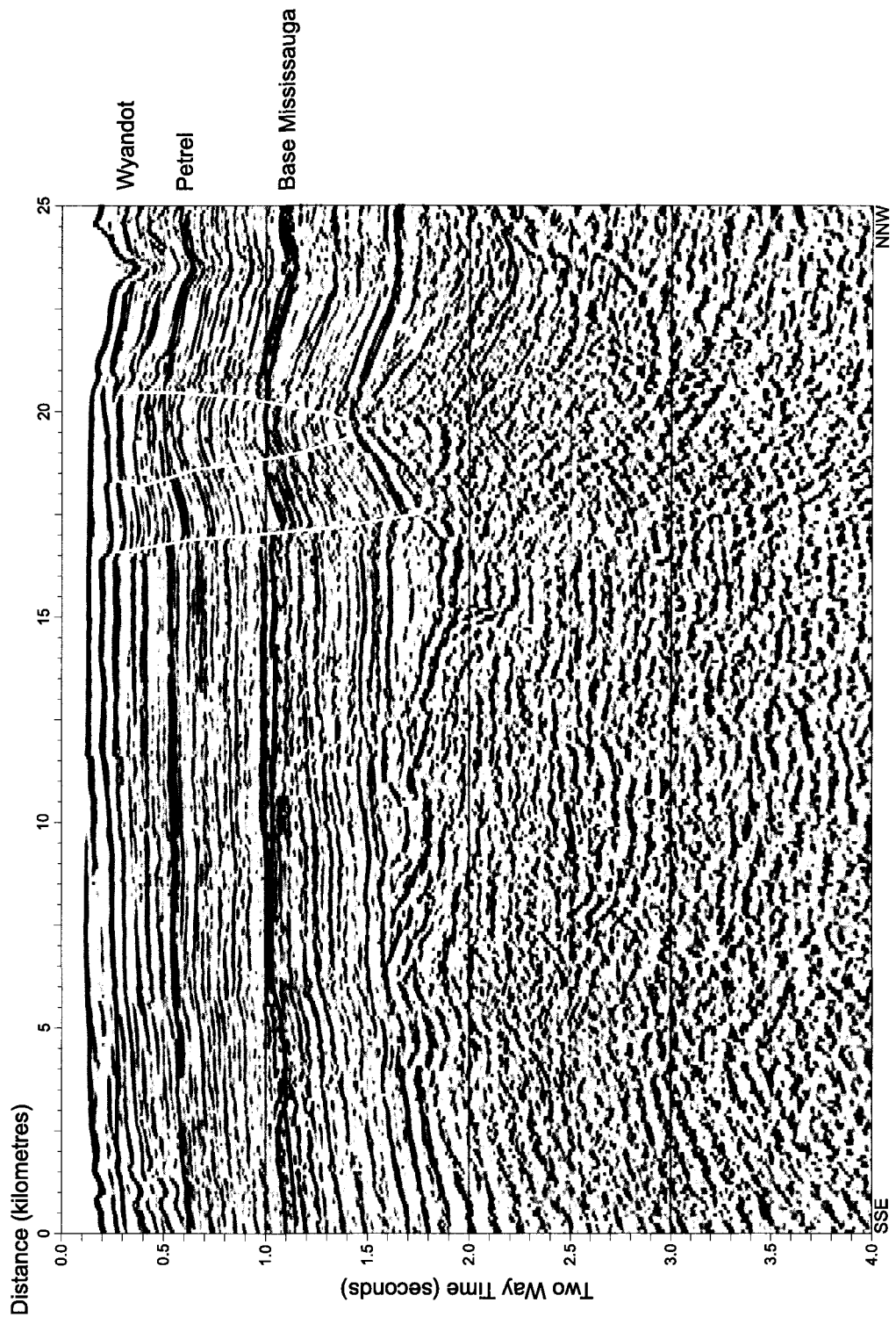
Figure 1.2b: NNW-SSE profile 3606A (part 2) correlating from the Scotian Shelf into the Orpheus Graben near the Jason C-20 well. It is along this profile that correlation of all horizons (with the exception of the Petrel and Base Mississauga horizons) fails
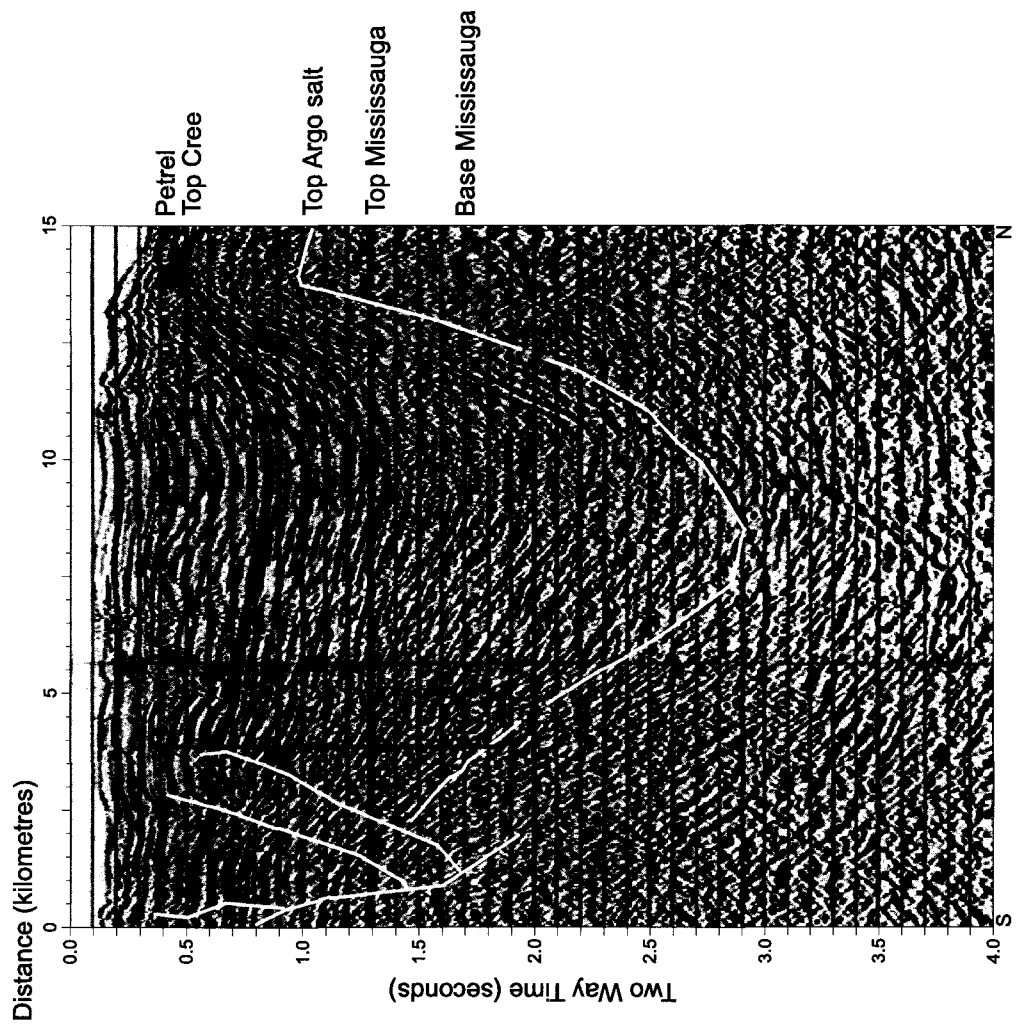
Figure 1.3: Correlation from the Jason C-20 well towards the Argo F-38 and Hercules G-15 wells on profile 81–403A

189
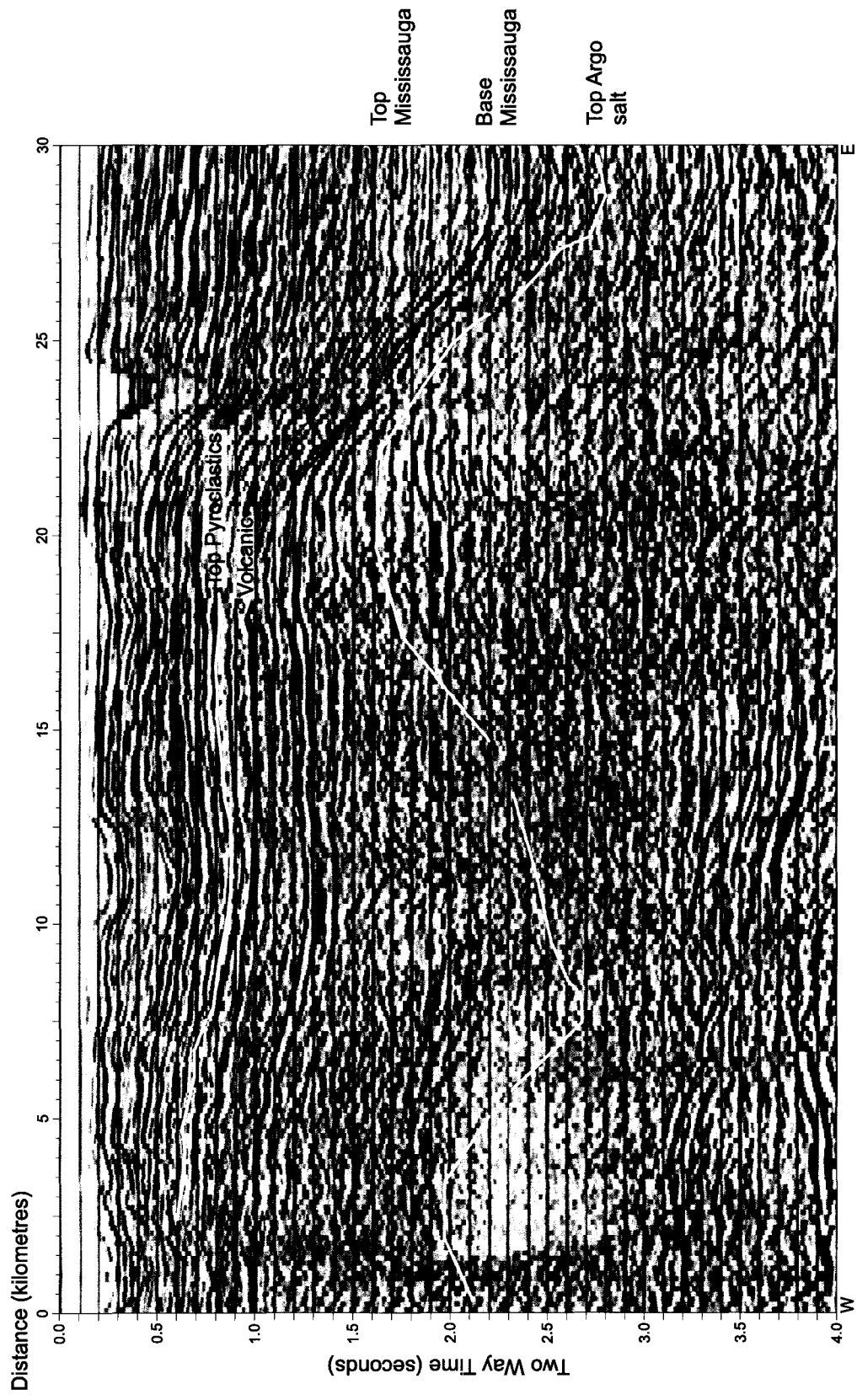
Figure 1.4: W-E profile 81–402A correlating from the Jason C-20 well to the Argo F-38 and Hercules G-15 wells
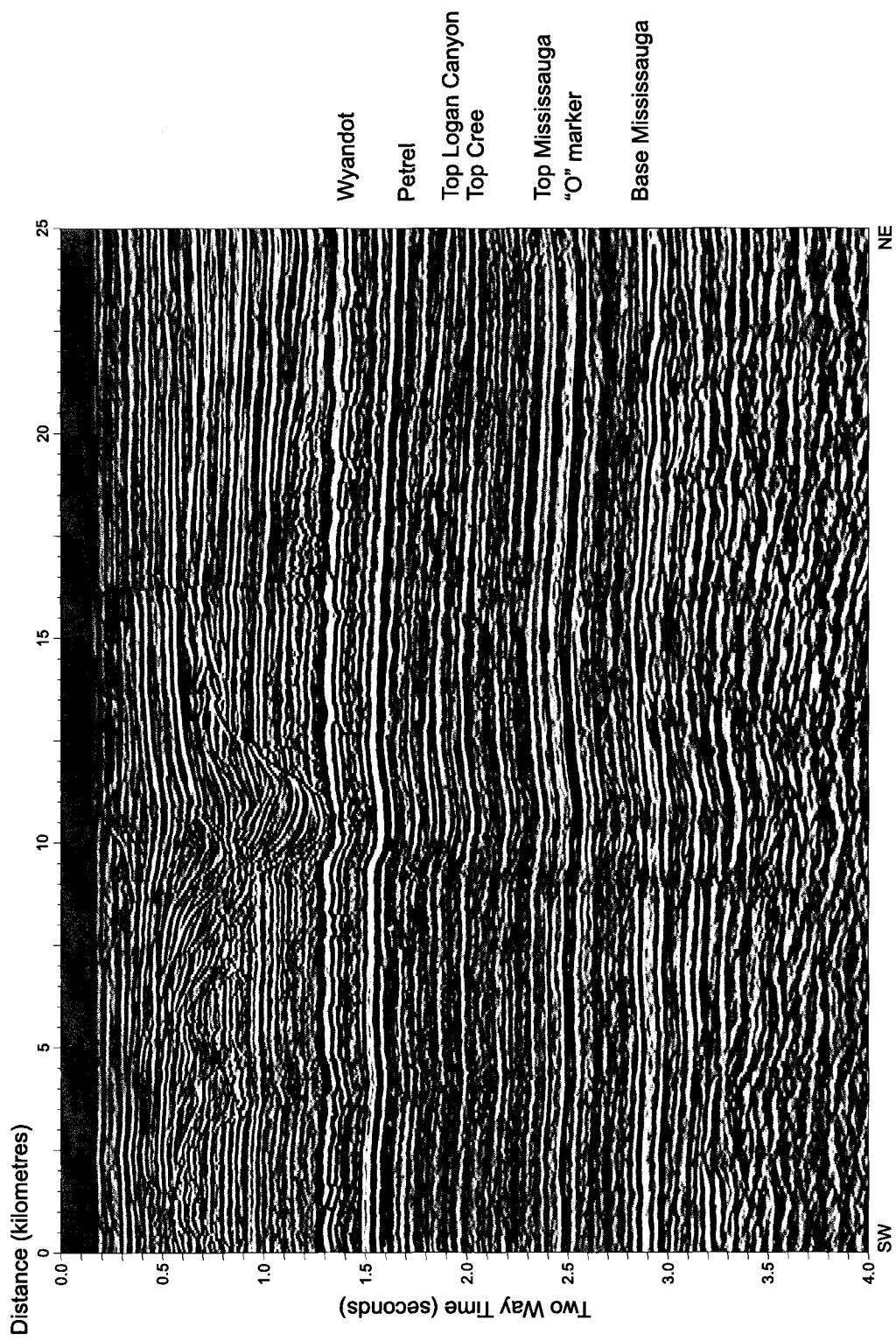
Figure 1.5: NE-SWprofile 83-4449BB correlating the Sachem D-76 well to the Dauntless D-35 well

191
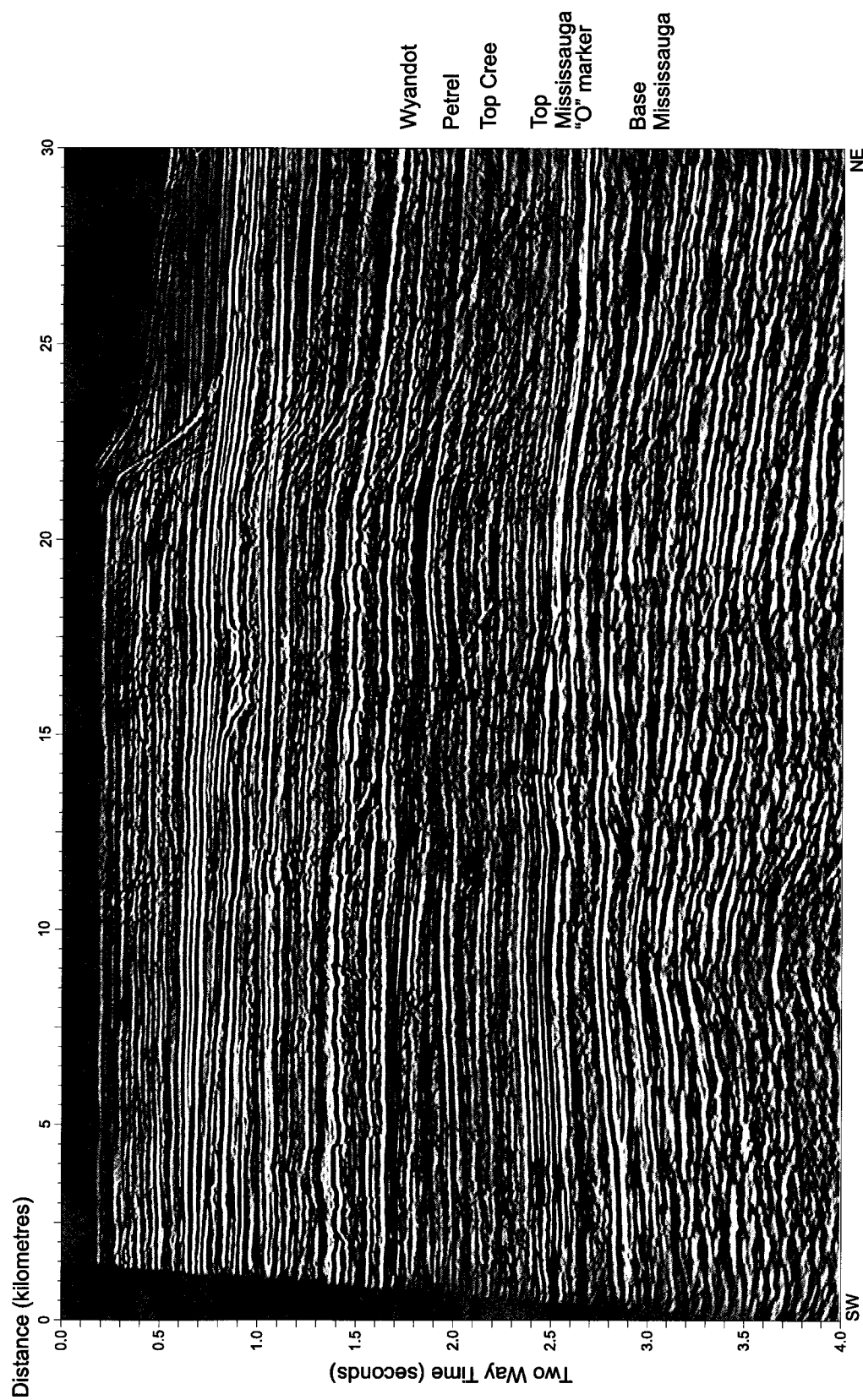
Figure 1.6: NE-SW profile 83-4449BA correlating the Sachem D-76 well to the Dauntless D-35 well
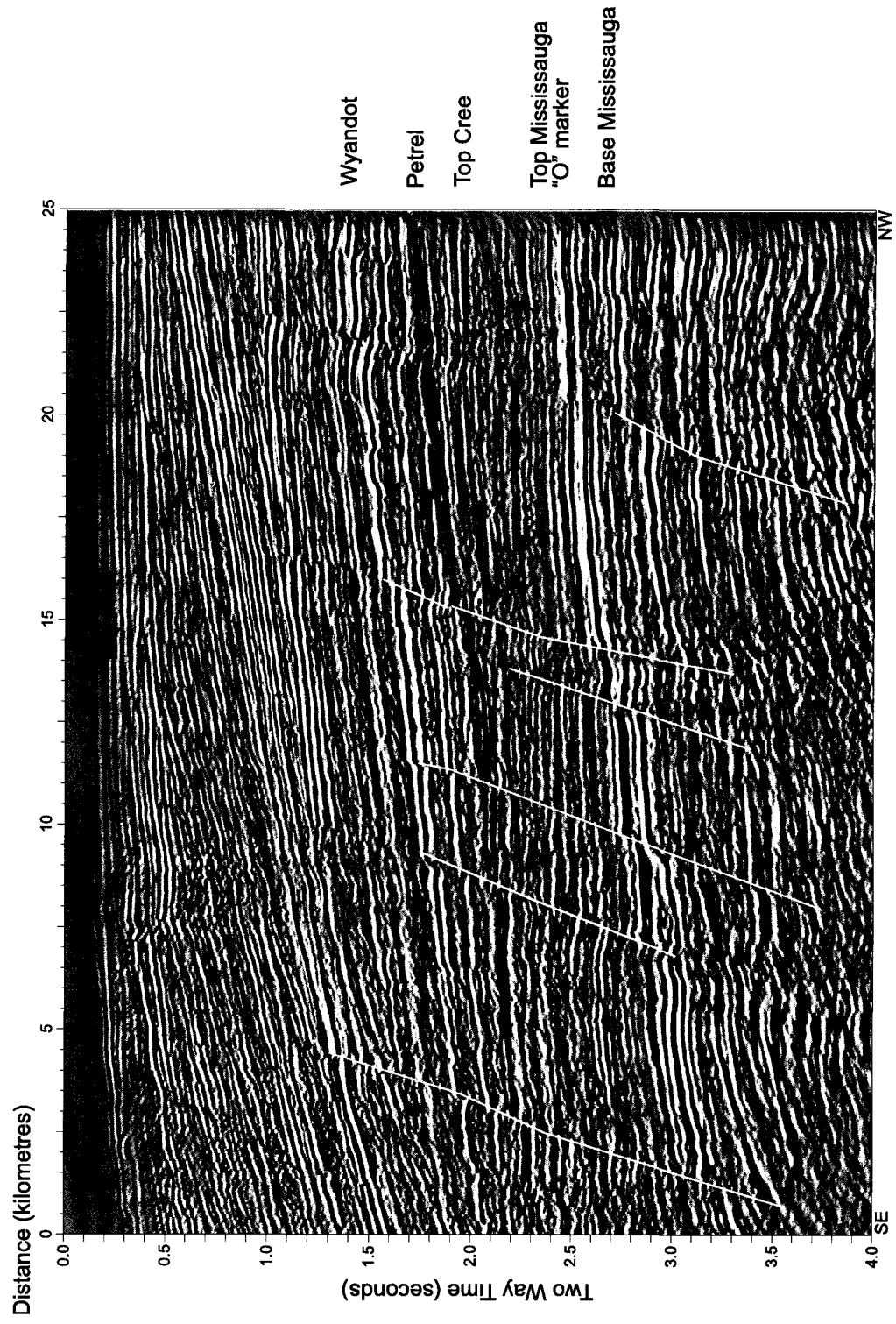
Figure 1.7: NW-SE profile 83-1403B correlating the Sachem D-76 well to the Dauntless D-35 well

193
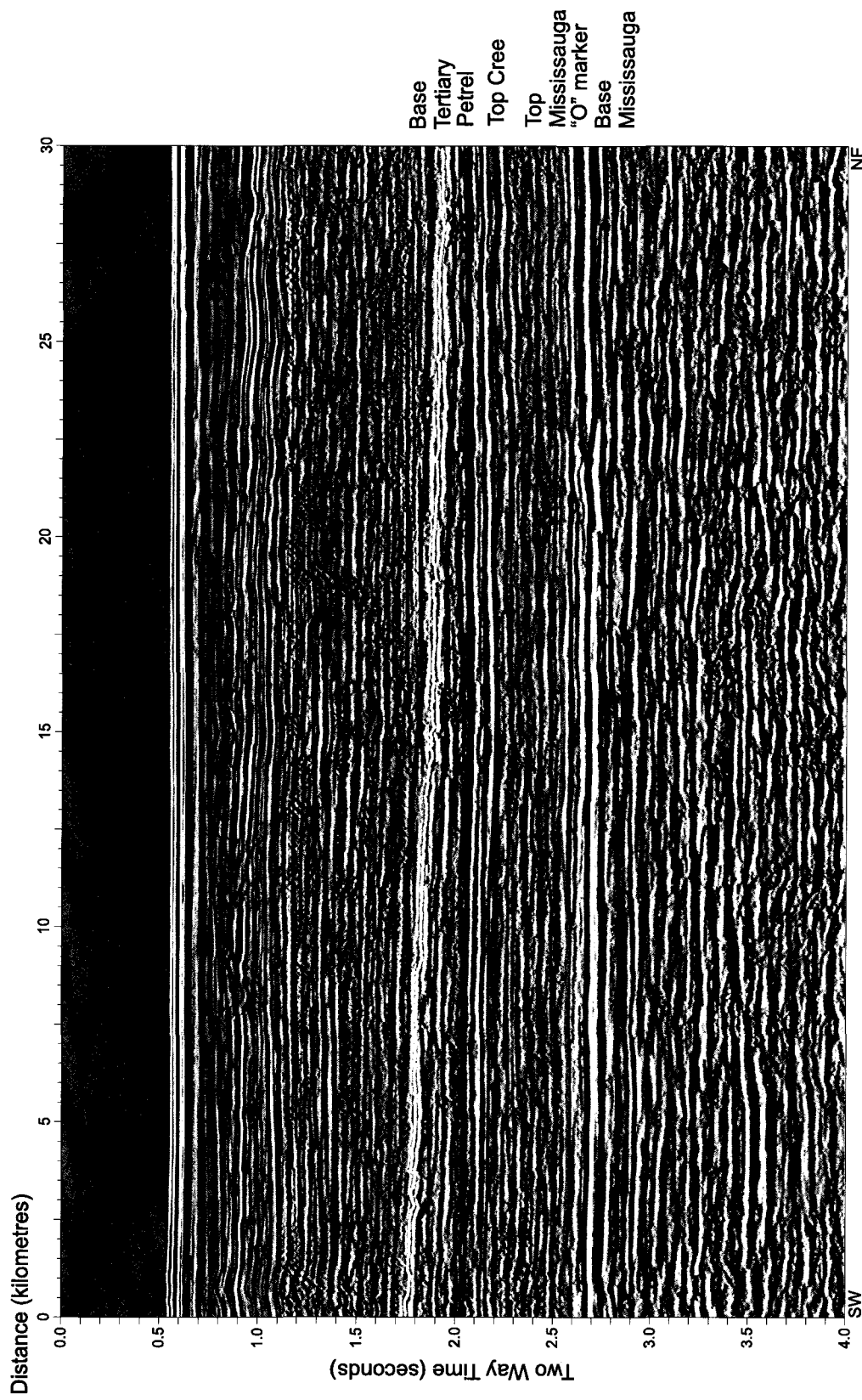
Figure 1.8a: NE-SW peofile STP2 (part 2) correlating the Scotian Shelf with the SW Grand Banks
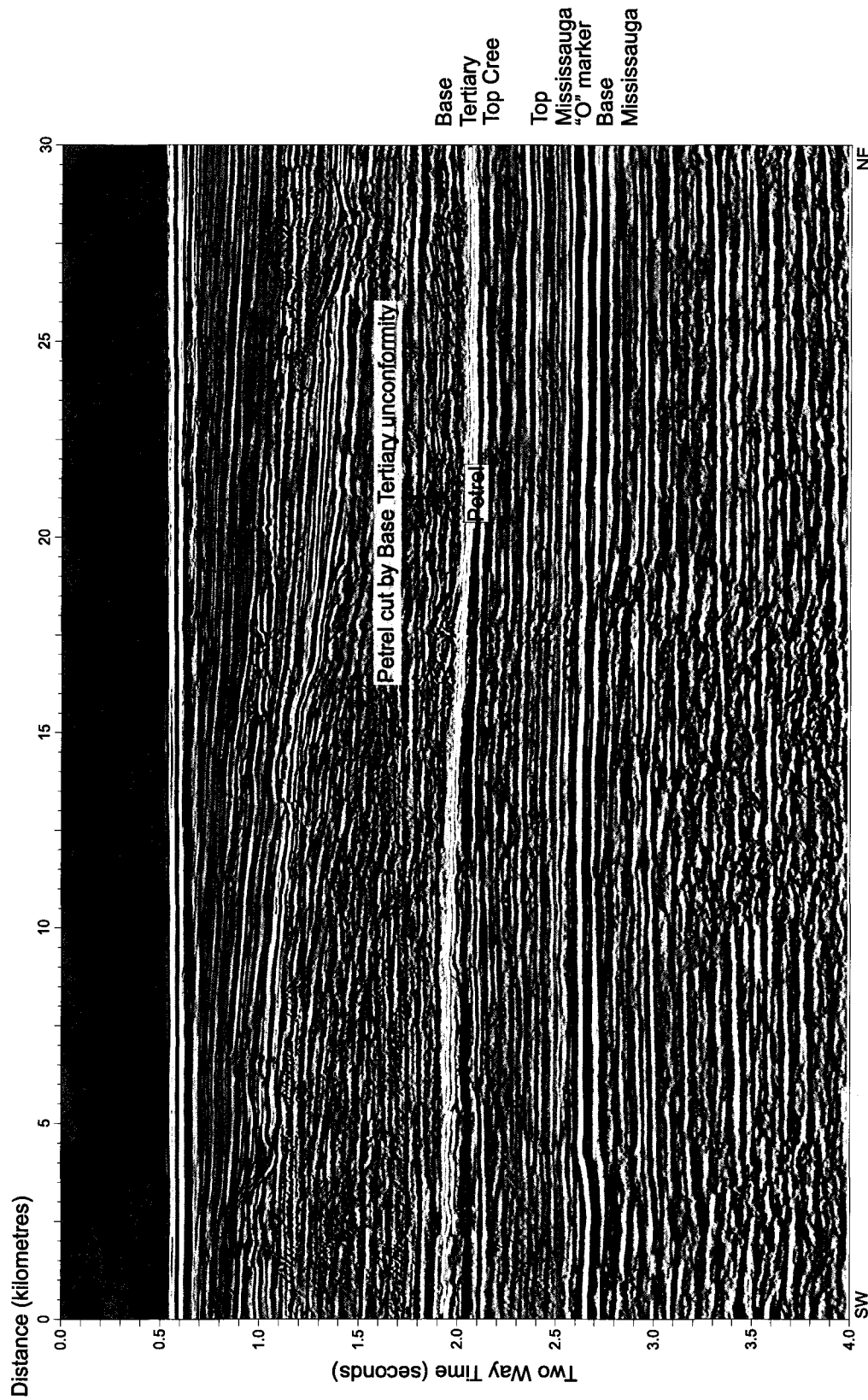
Figure 1.8b: NE-SW profile STP2 (part 3) correlating the Scotian Shelf with the SW Grand Banks
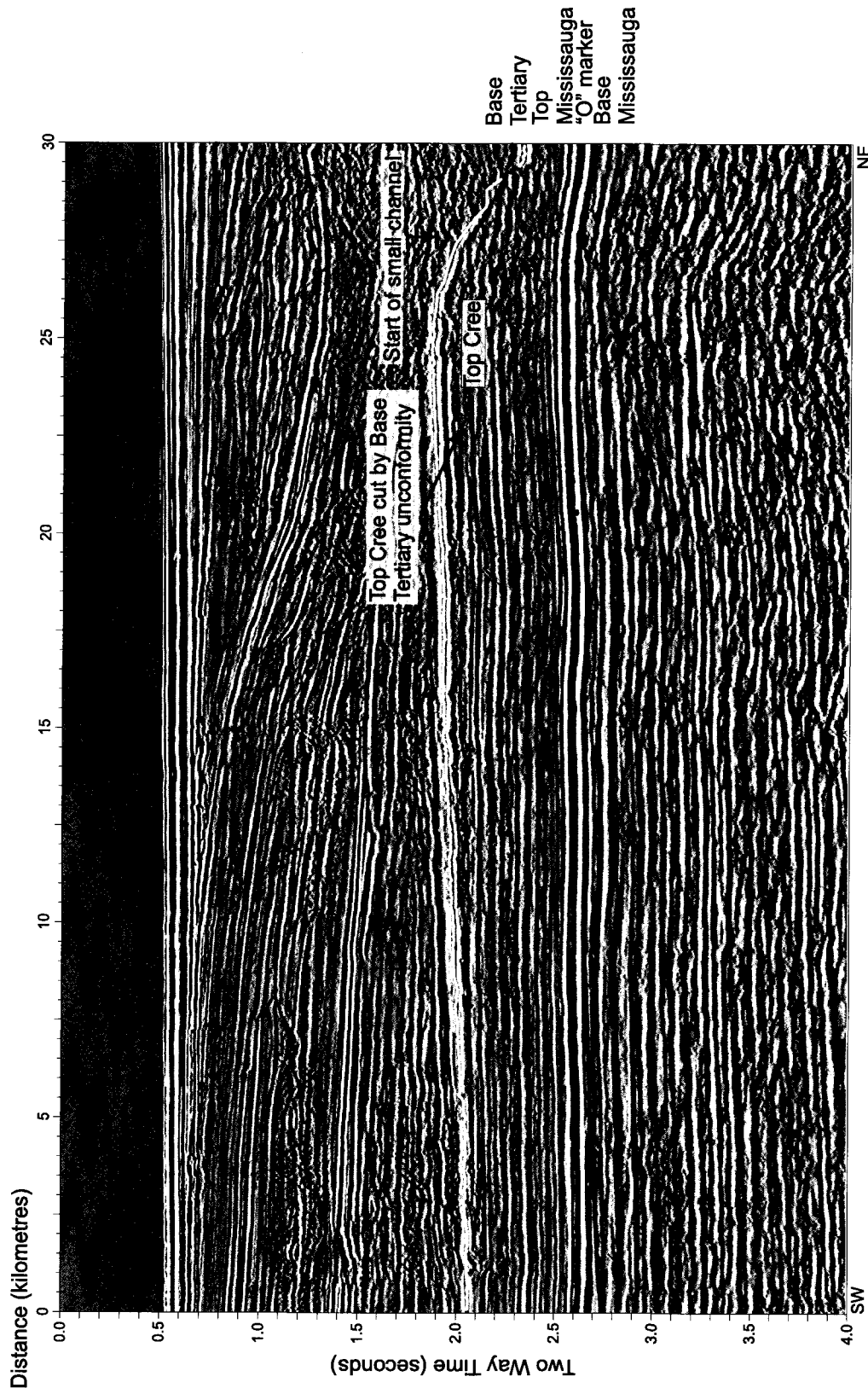
Figure 1.8c: NE-SW profile STP2 (part 4) correlating the Scotian Shelf with the SW Grand Banks

196
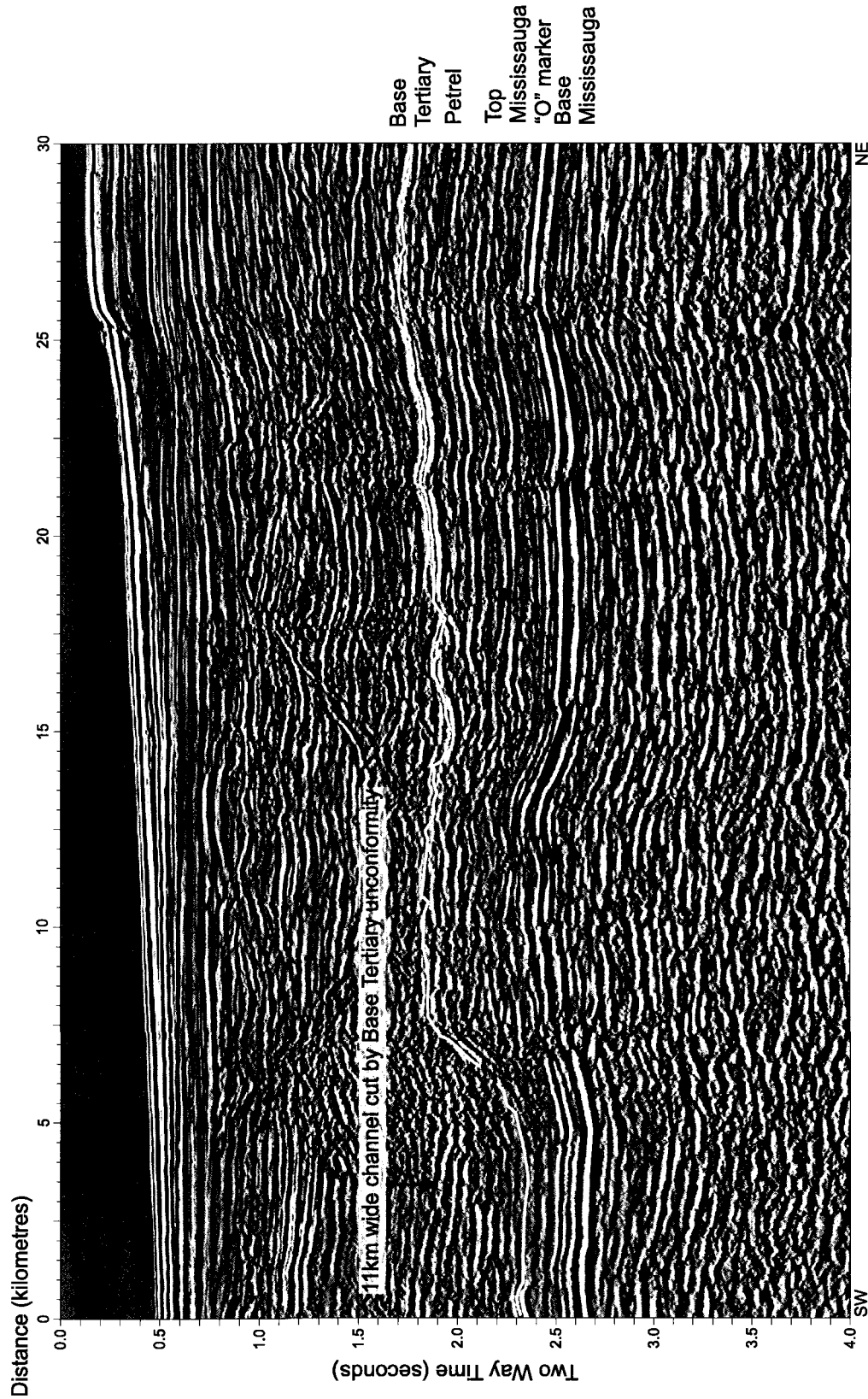
Figure 1.8d: NE-SW profile STP2 (part 5) correlating the Scotian Shelf to the SW Grand Banks
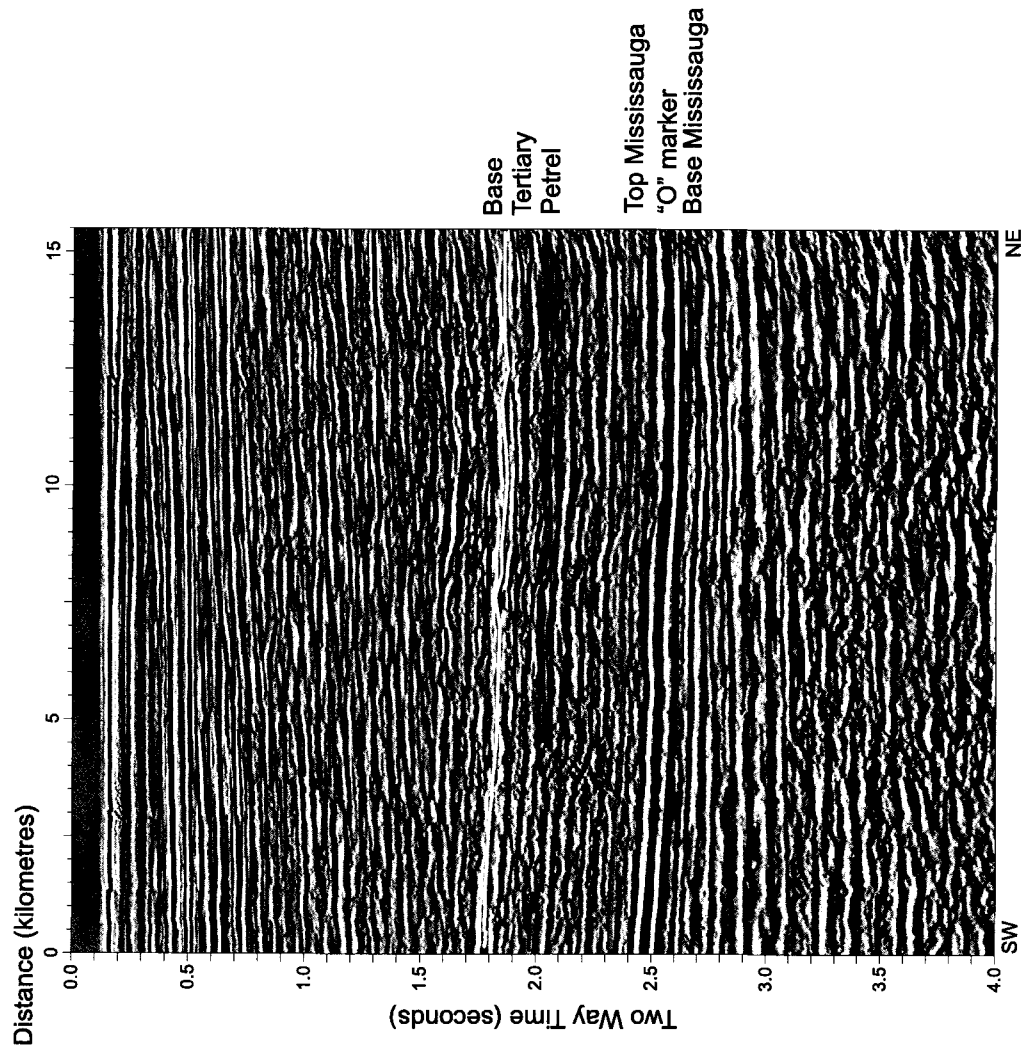
Figure 1.8e: NE-SW profile STP2 (part 6) correlating the Scotian Shelf to the SW Grand Banks

198
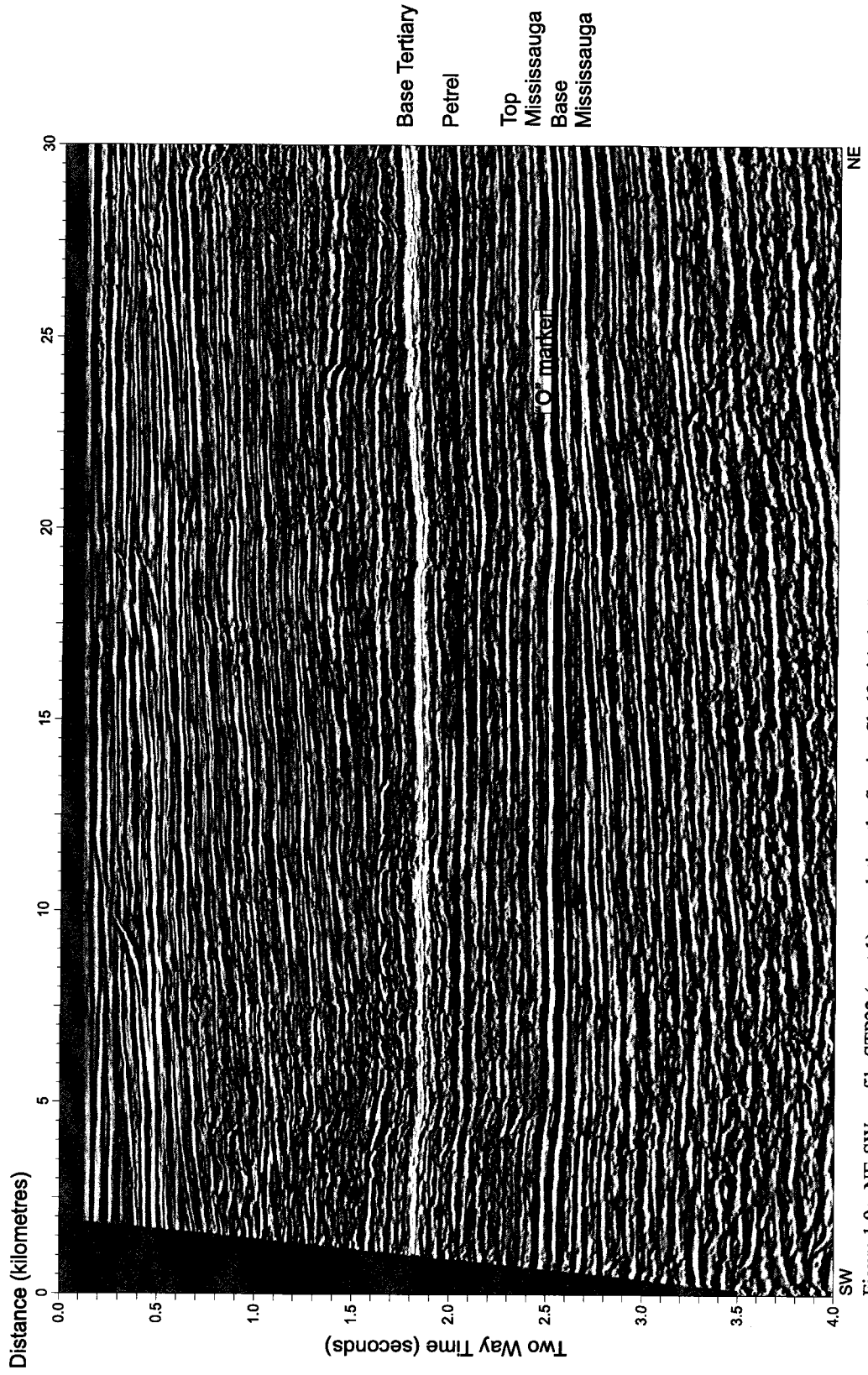
Figure 1.9a: NE-SW profile STP22 (part 1) correlating the Scotian Shelf with the SW Grand Banks
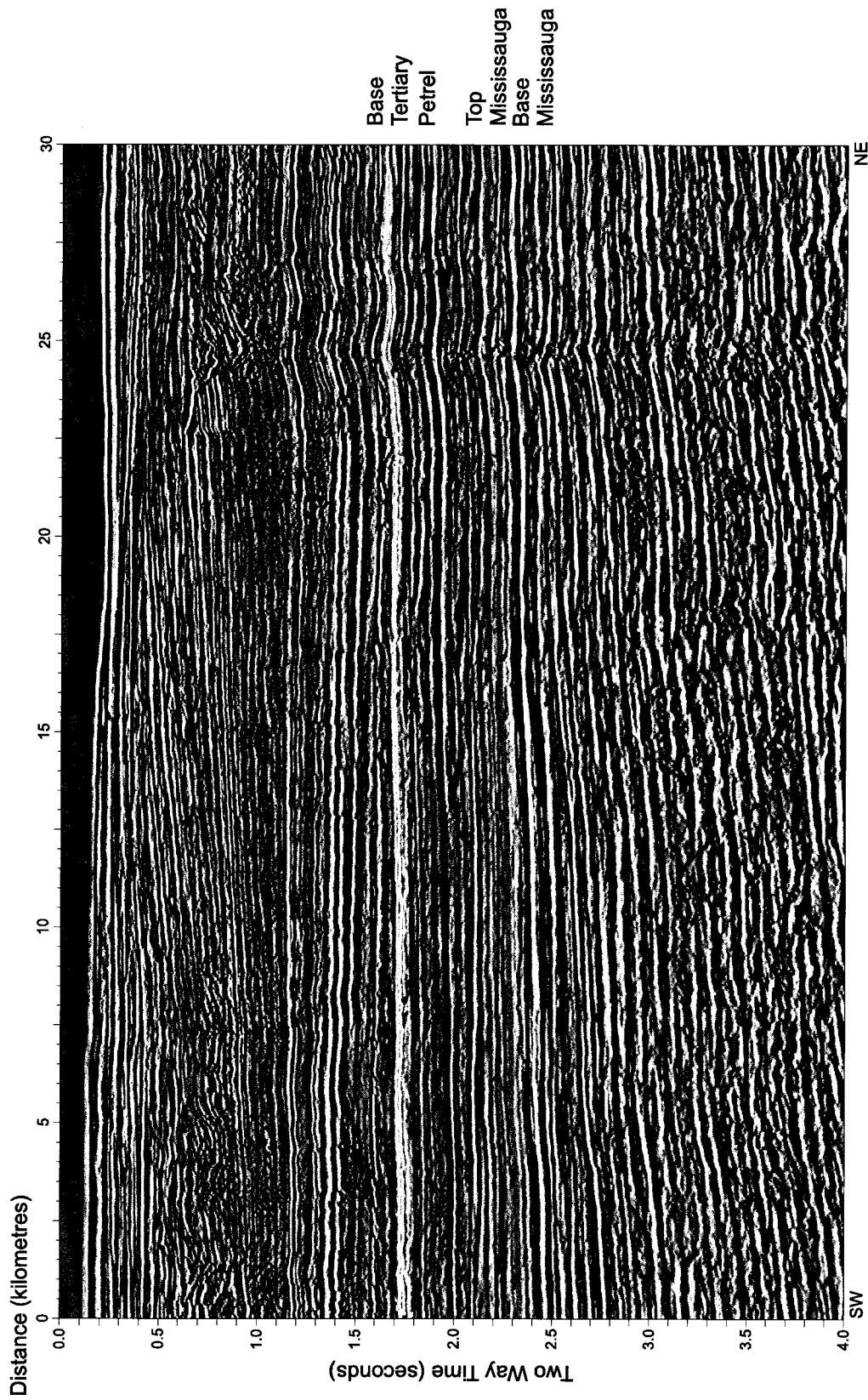
Figure 1.9b: NE-SW profile STP22 (part 2) correlating the Scotian Shelf with the SW Grand Banks
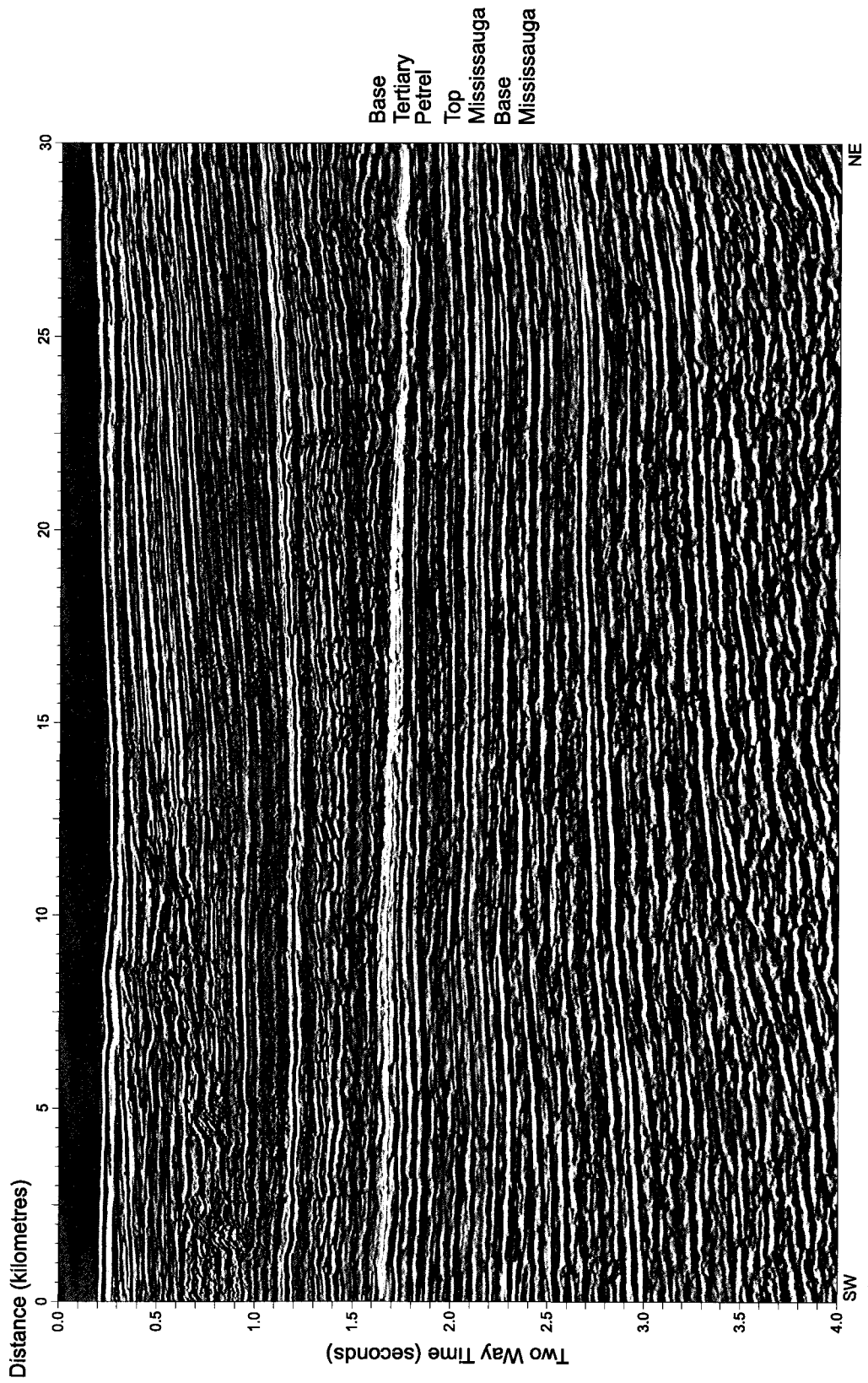
Figure 1.9c: NE-SW profile STP22 (part 3) correlating the Scotian Shelf with the SW Grand Banks
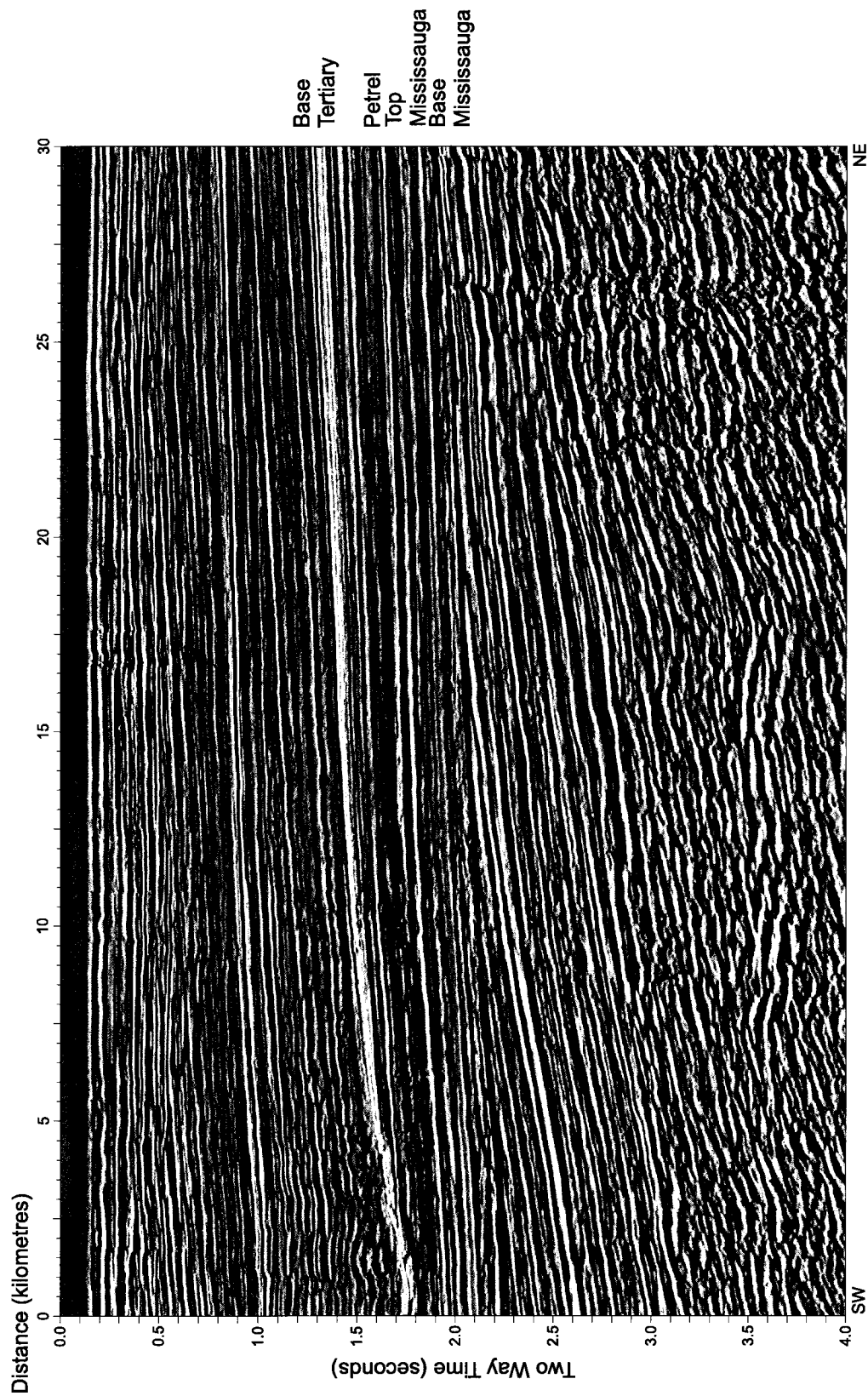
Figure 1.9d: NE-SW lprofile STP22 (part 4) correlating the Scotian Shelf with the SW Grand Banks
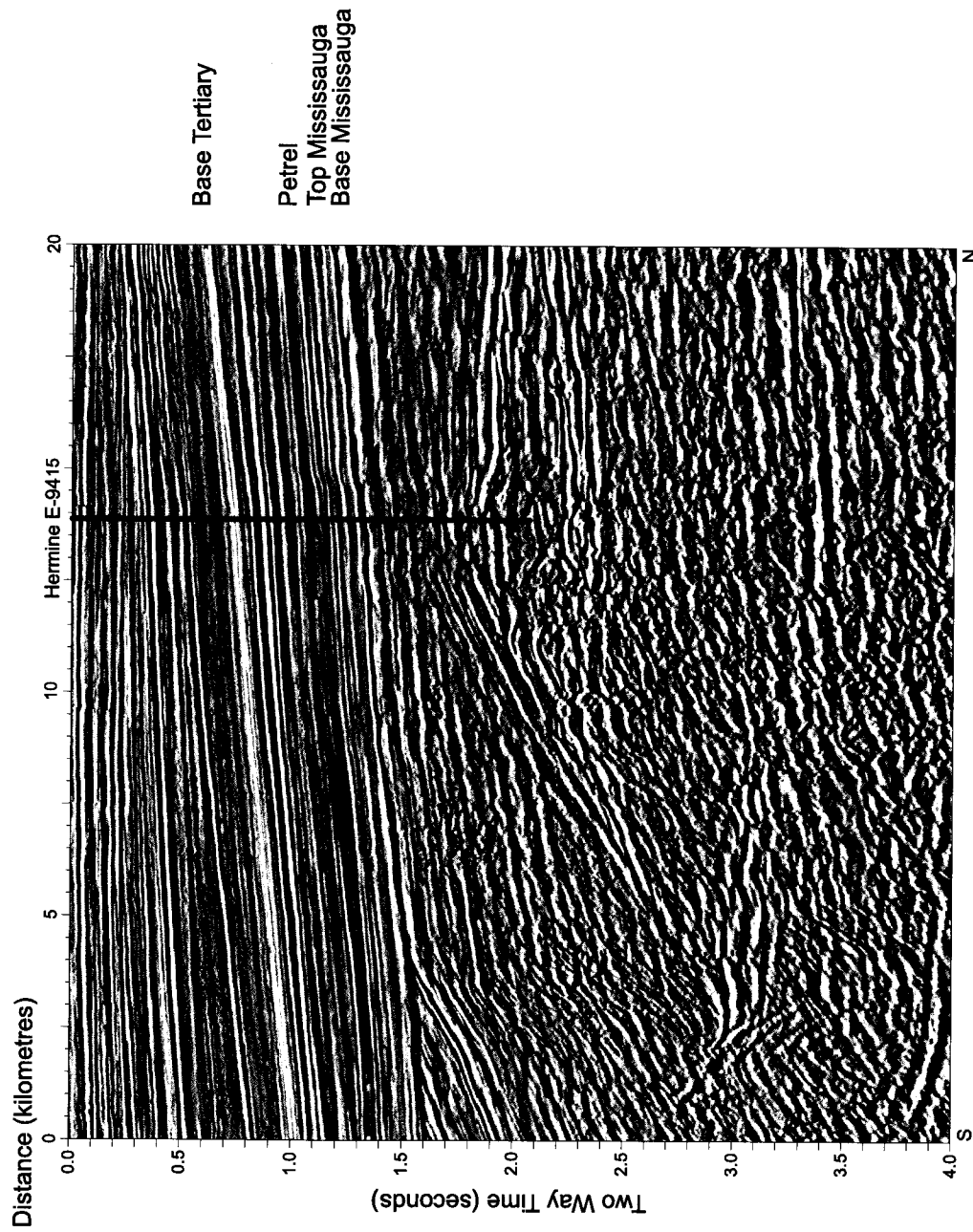
Figure 1.10a: N-S profile STP17 (part 1) correlating the Hermine E-94 well with the rest of the SW Grand Banks

203
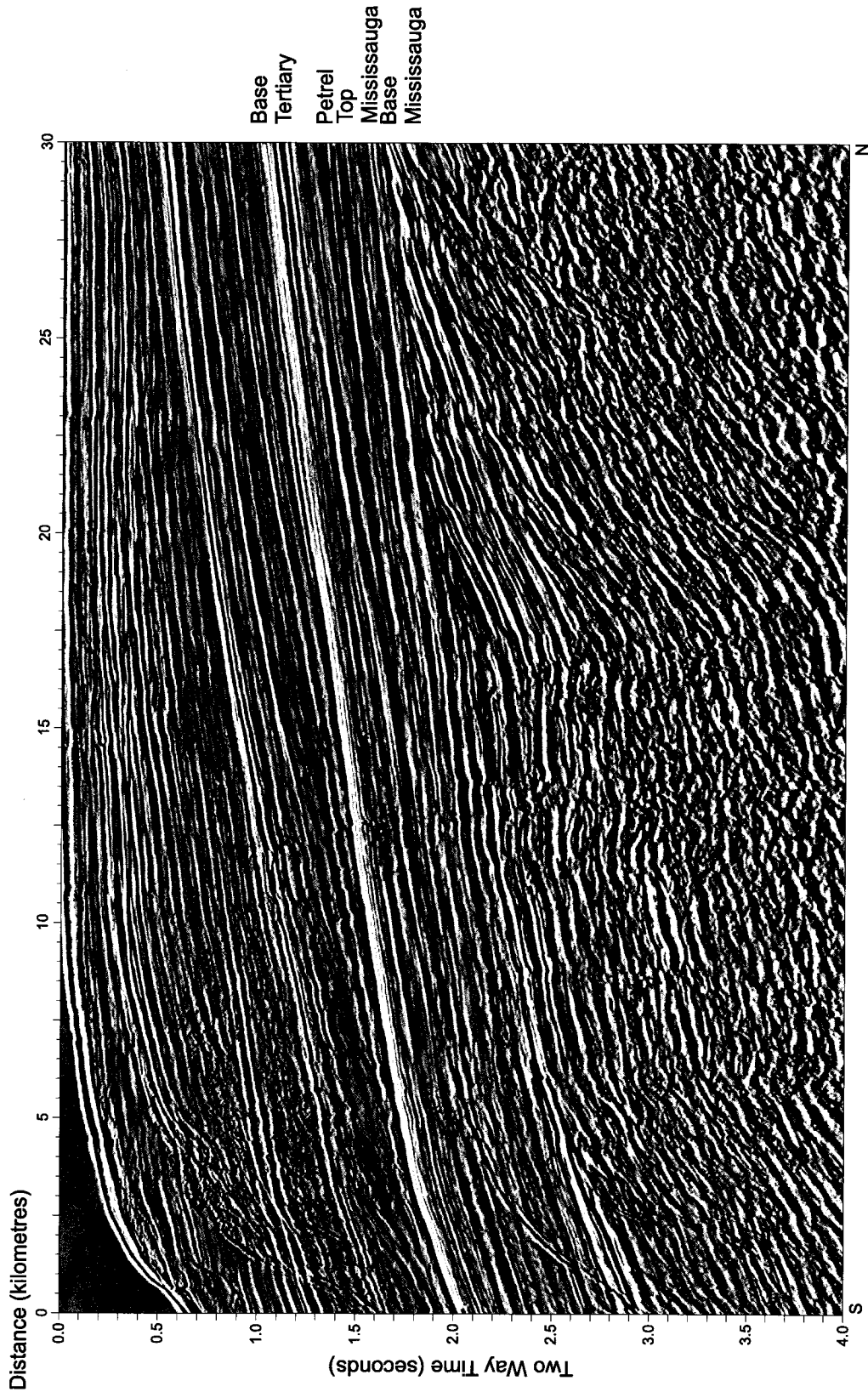
Figure 1.10b: N-S profile STP17 (part 1) correlating from near the Hermine E-94 well to the rest of SW Grand Banks

204
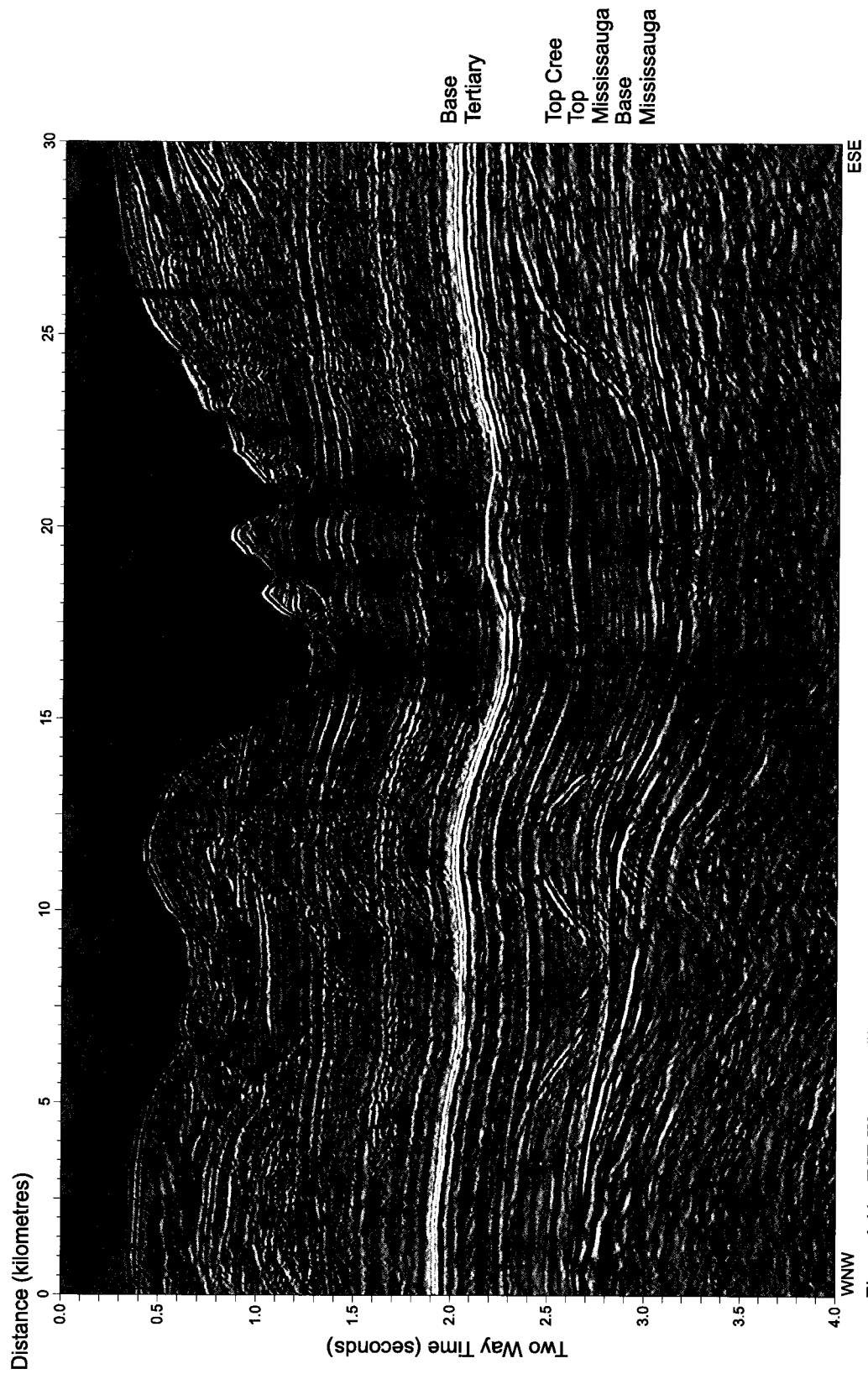
Figure 1.11a: ESE-WNW profile 83-4512 (part 1) correlating the SW Grand Banks

205
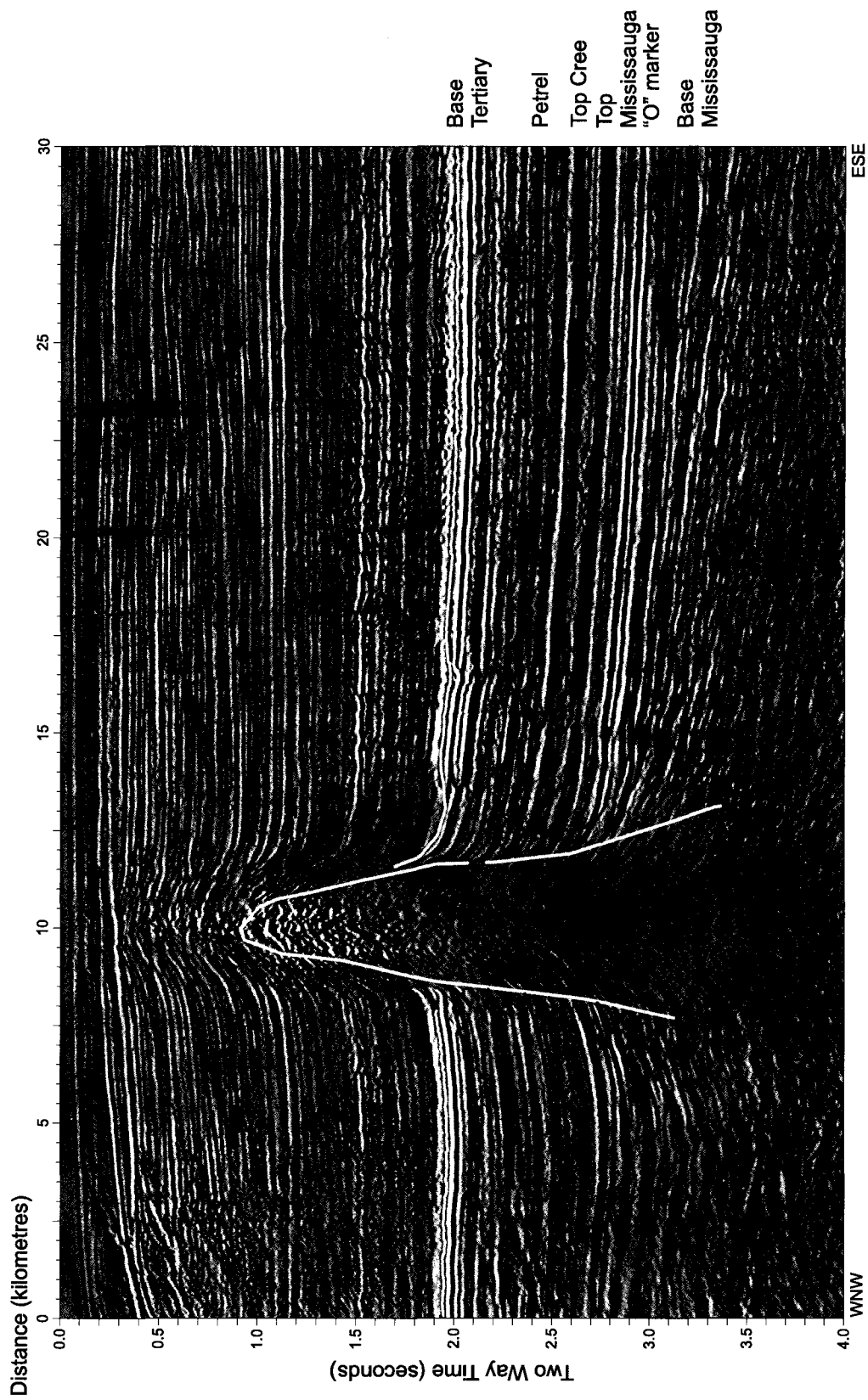
Figure 1.11b: ESE-WNW profile 83-4512 (part 2) correlating the SW Grand Banks
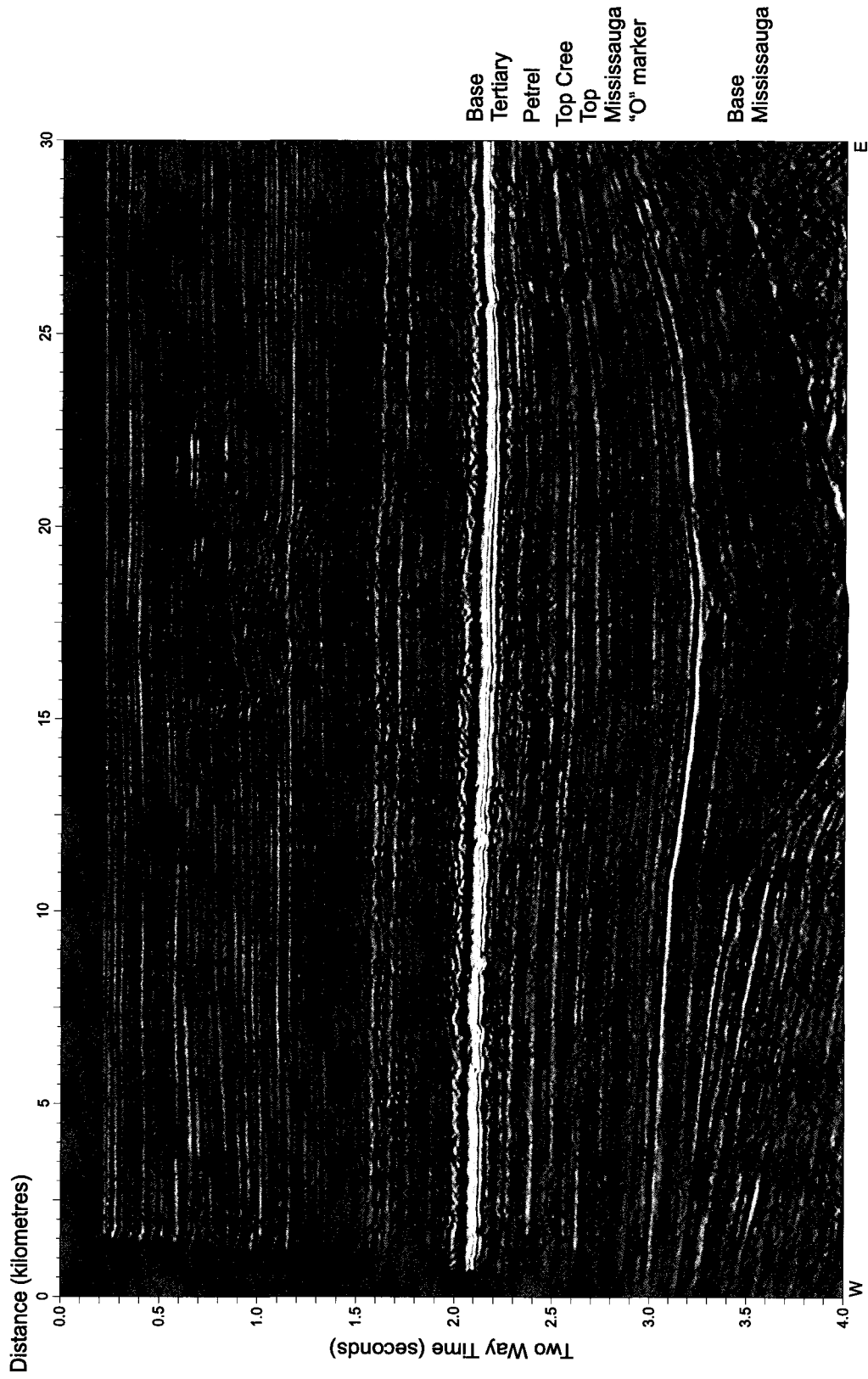
Figure 1.12a: E-W profile 80-1206d (part 1) correlating the SW Grand Banks near the Puffin B-90 well

207
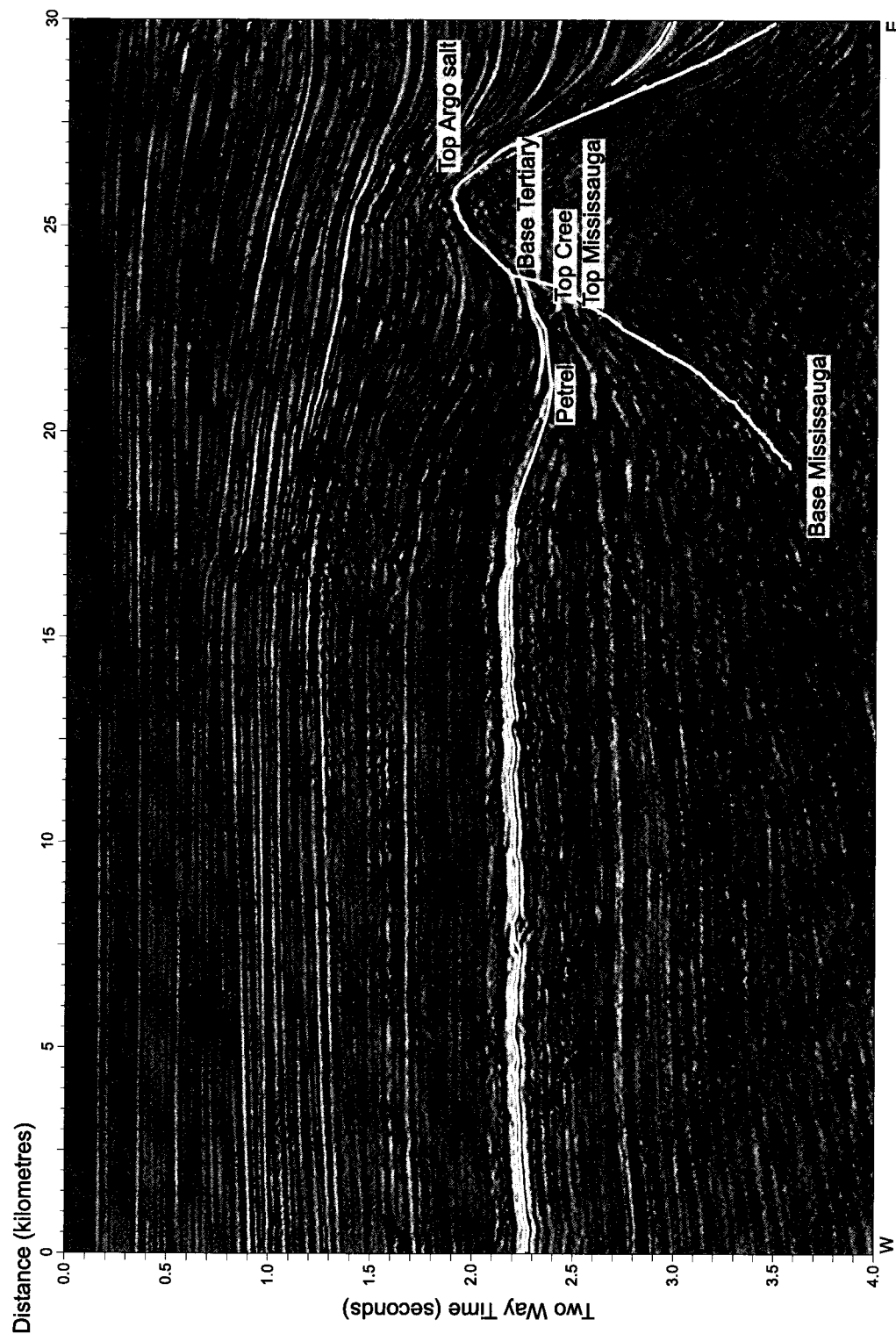
Figure 1.12b: E-W profile 80-1206d (part 3) correlating the SW Grand Banks near the Puffin B-90 well

208
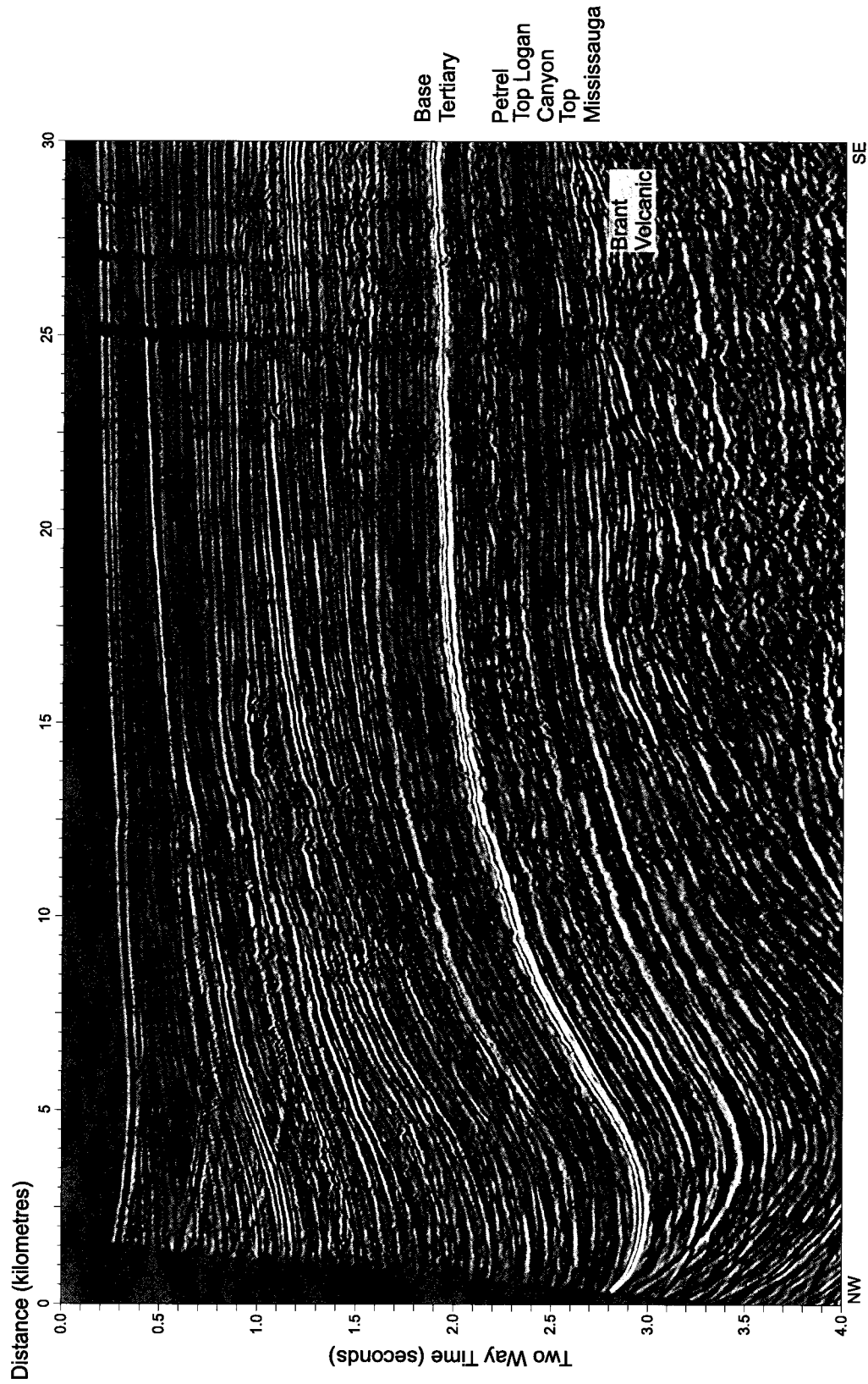
Figure 1.13a: NW-SE profile 80-1206e (part 1) correlating the SW Grand Banks towards the Brant P-87 well

209
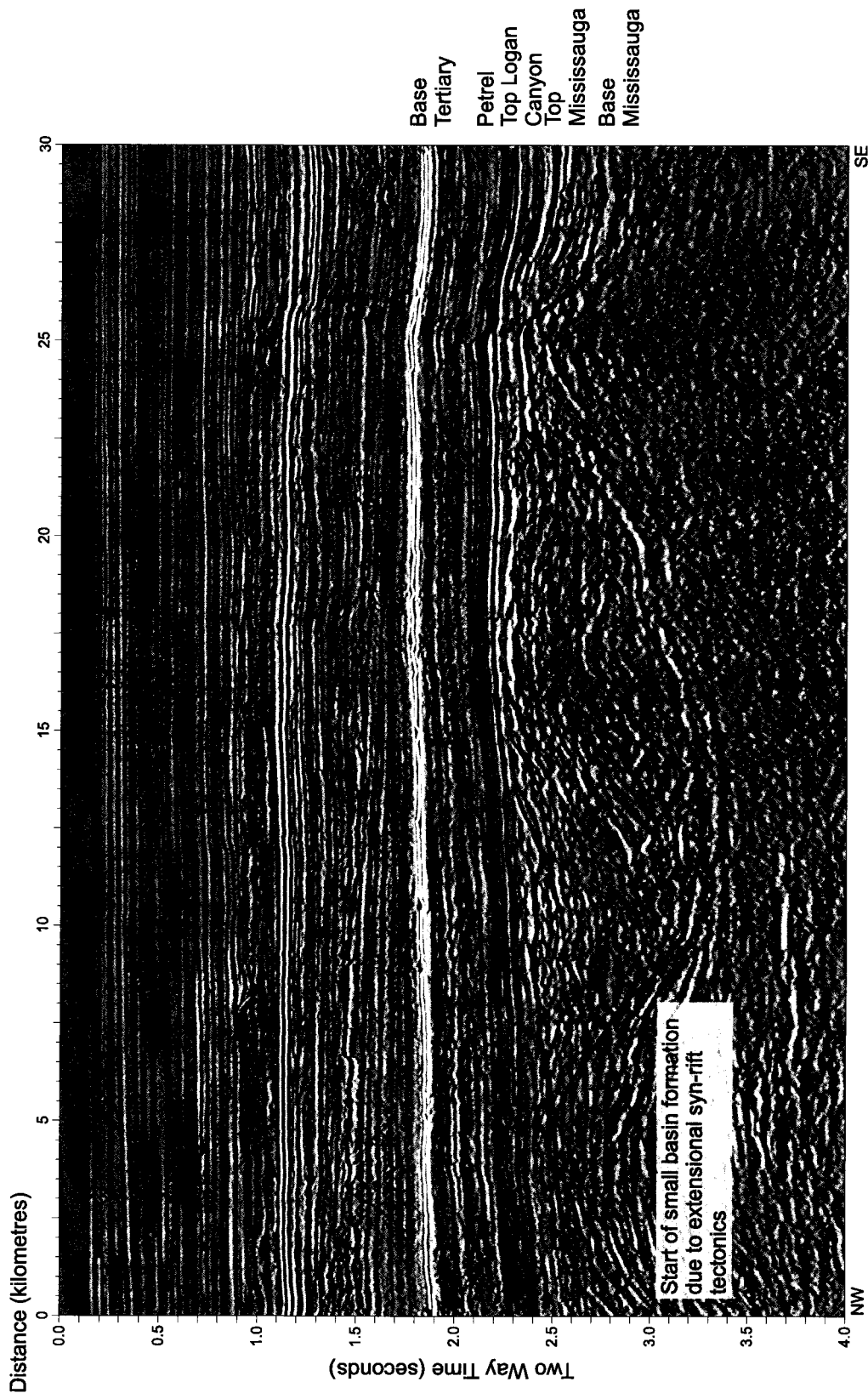
Figure 1.13b: NW-SE profile 80-1206e (part 2) correlating the SW Grand Banks toward the Brant P-87 well

210
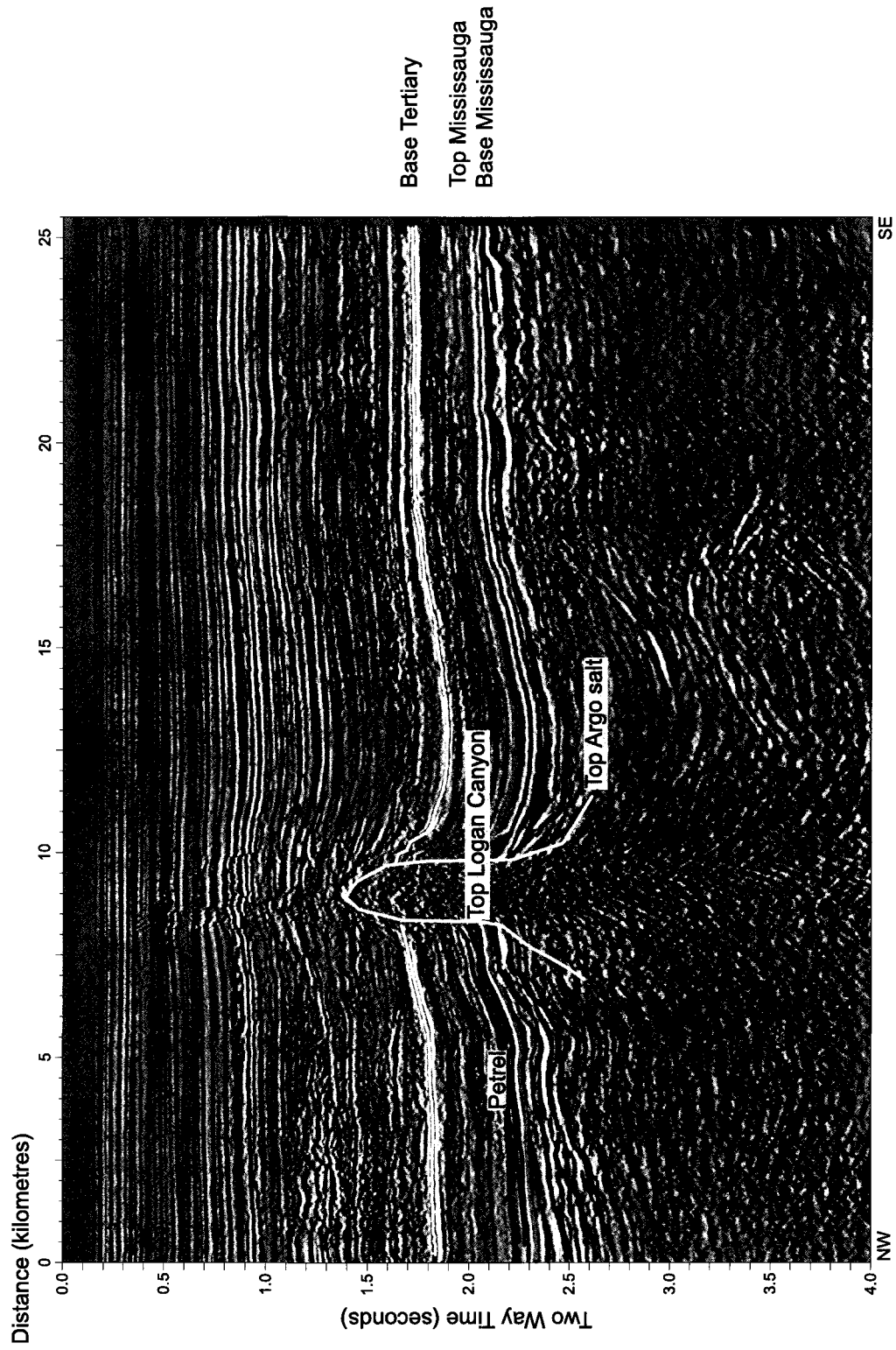
Figure 1.13c: NW-SE profile 80-1206e (part 3) correlating SW Grand Banks toward the Brant P-87 well

211
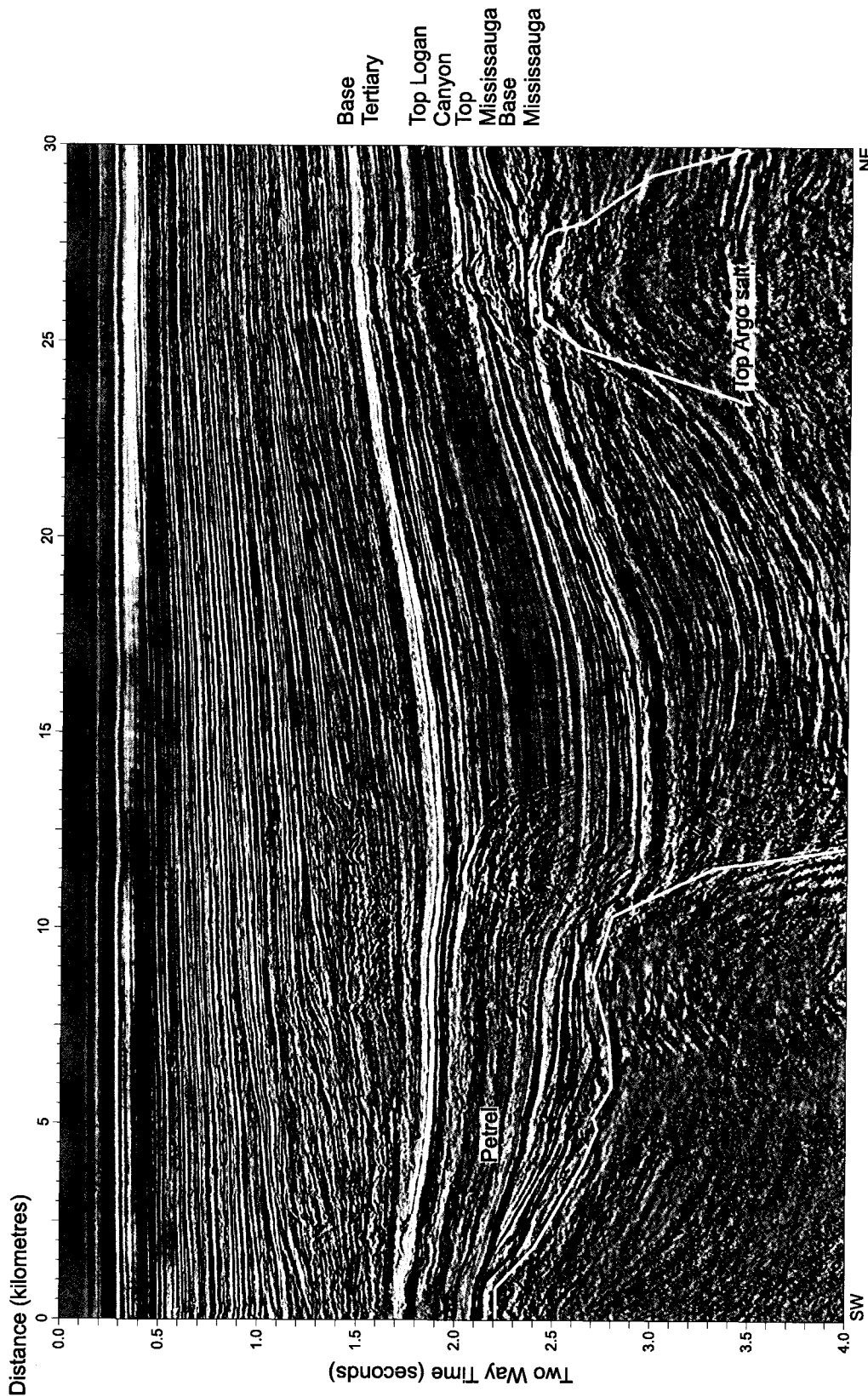
Figure 1.14: NE-SW profile hm82-81 correlating the SW Grand Banks near the Mallard M-45 well
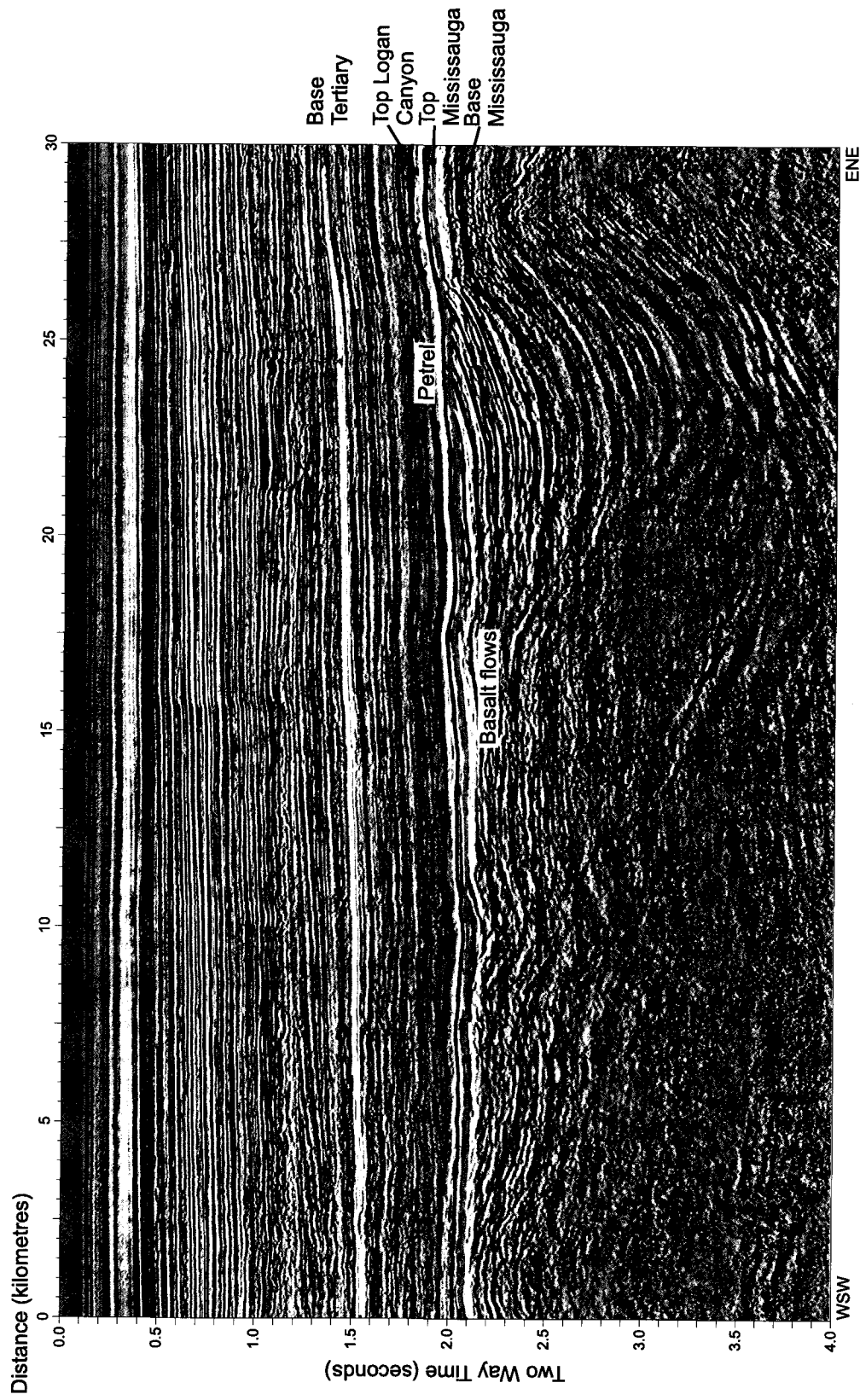
Figure 1.15: ENE-WSW profile HM82-138 highlighting the abrupt ending of basalt flows within a mini basin near the Mallard M-45 well on the SW Grand Banks

213
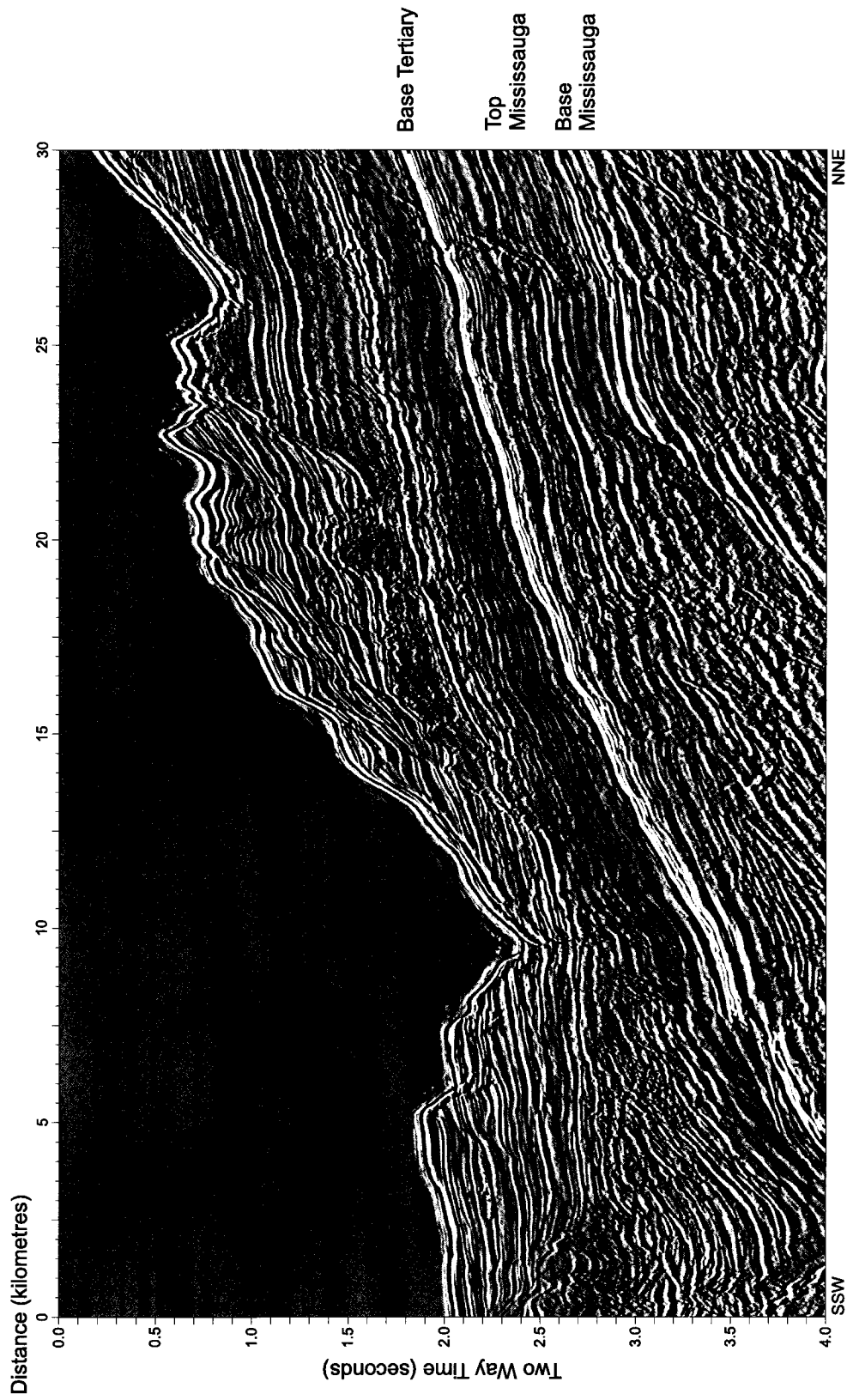
Figure 1.16: NNE-SSW profile STP17 highlighting the proximal shoreline, and increased sediment deposition, near the Emerillon C-56 well on the SW Grand Banks

214
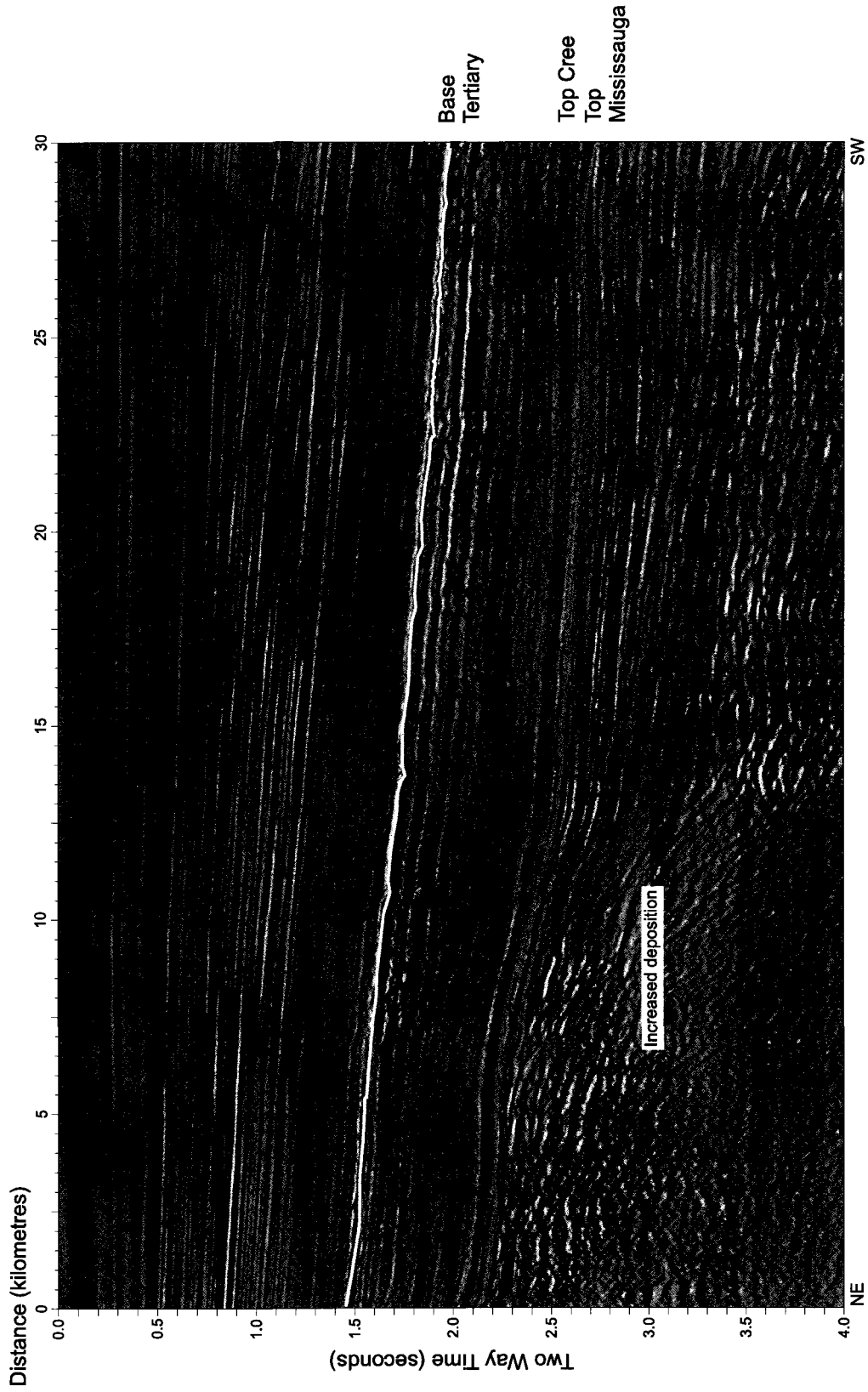
Figure 1.17: E-W profile 6309 highlighting the proximal shoreline near the Narwhal F-99 well, and increased deposition on the SW Grand Banks

215

APPENDIX 2
MODELING RESULTS

-Chebucto K-90 (models A-C)
-Mallard M-45 (models A-C)
-Emerillon C-56 (models A-D)
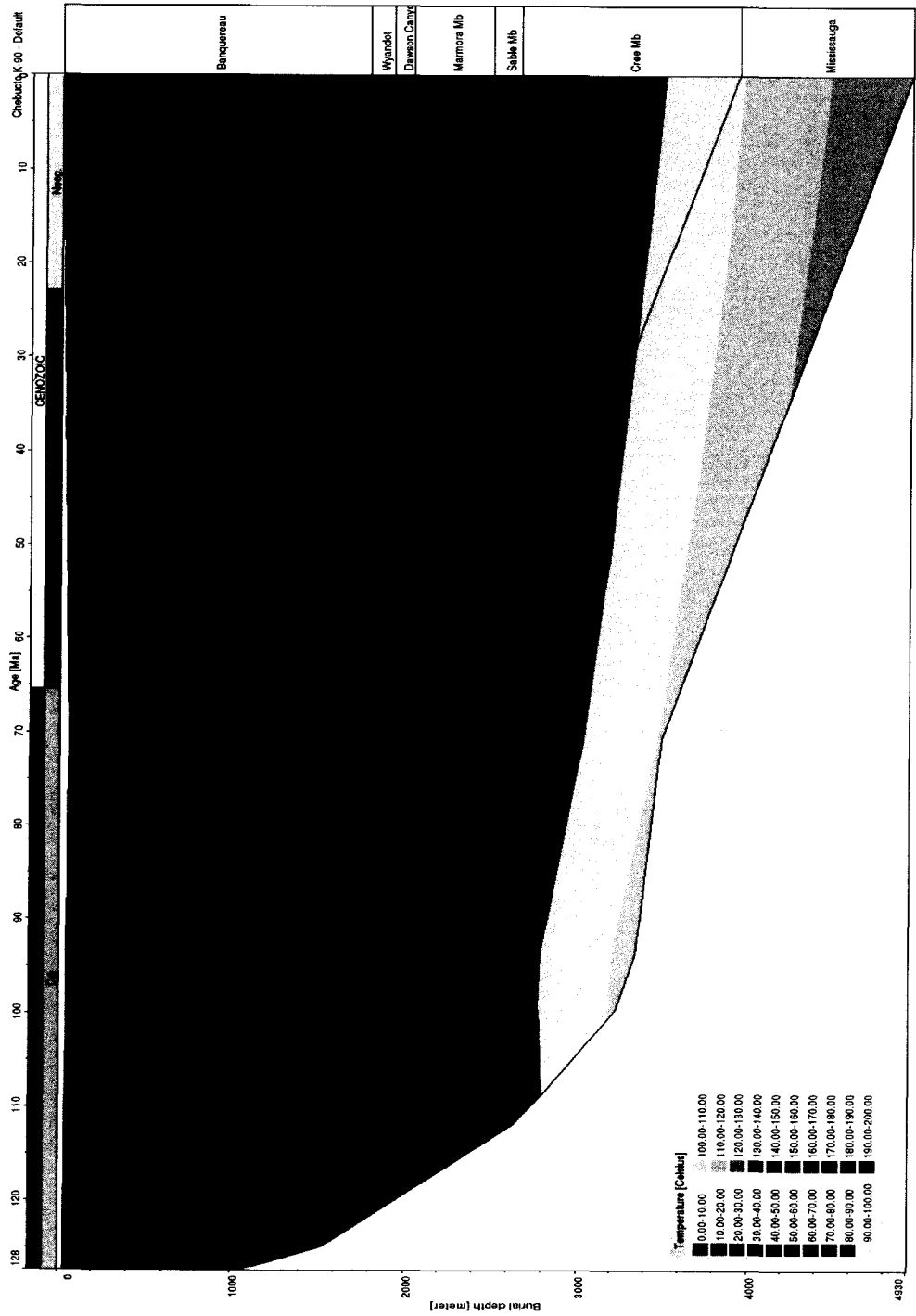
Figure 2.1: Results of Model A burial history plot with temperature overlay for Chebucto K-90
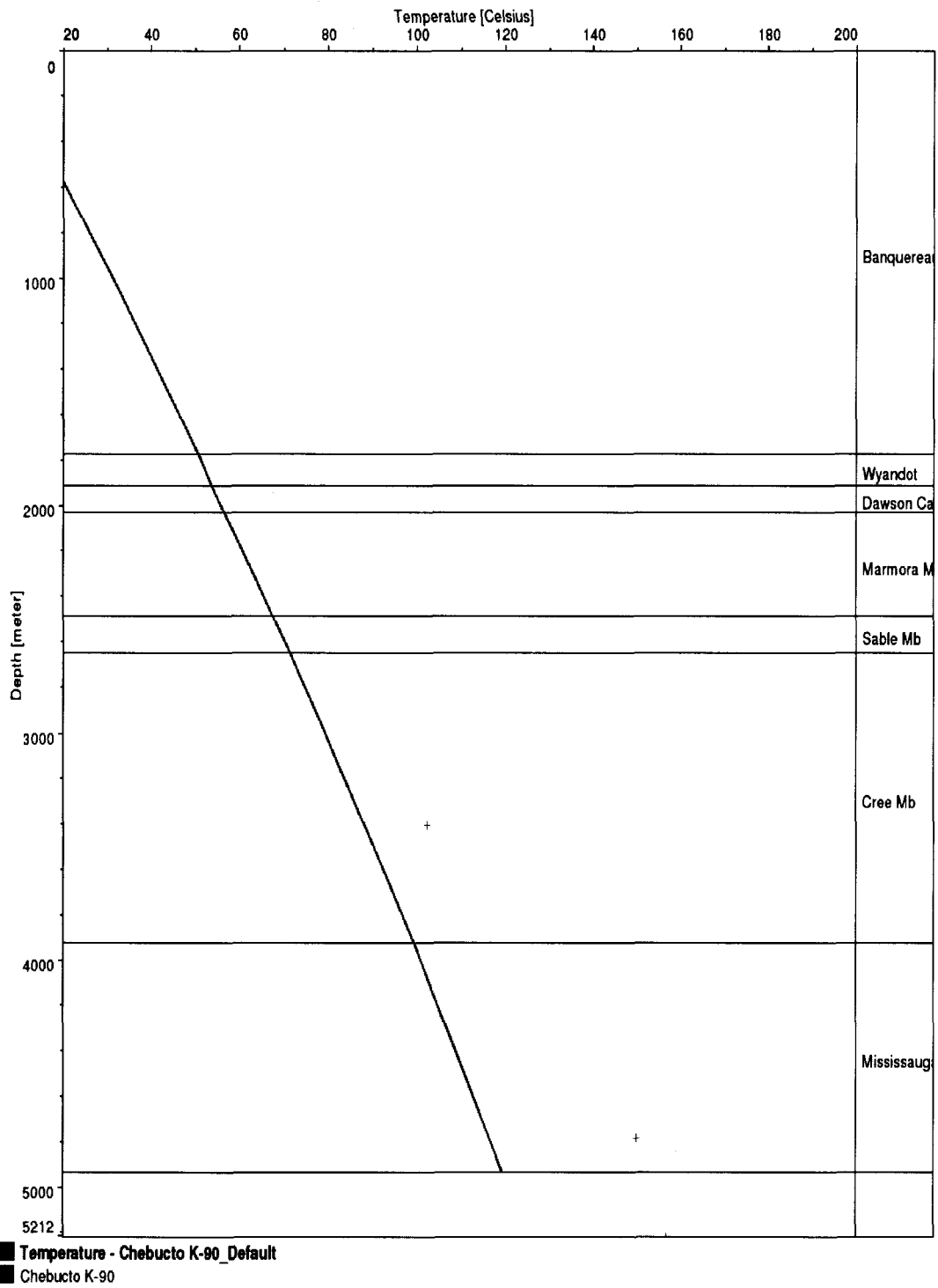
Figure 2.2: Model A modeled temperature profile vs measured downhole temperature for Chebucto K-90
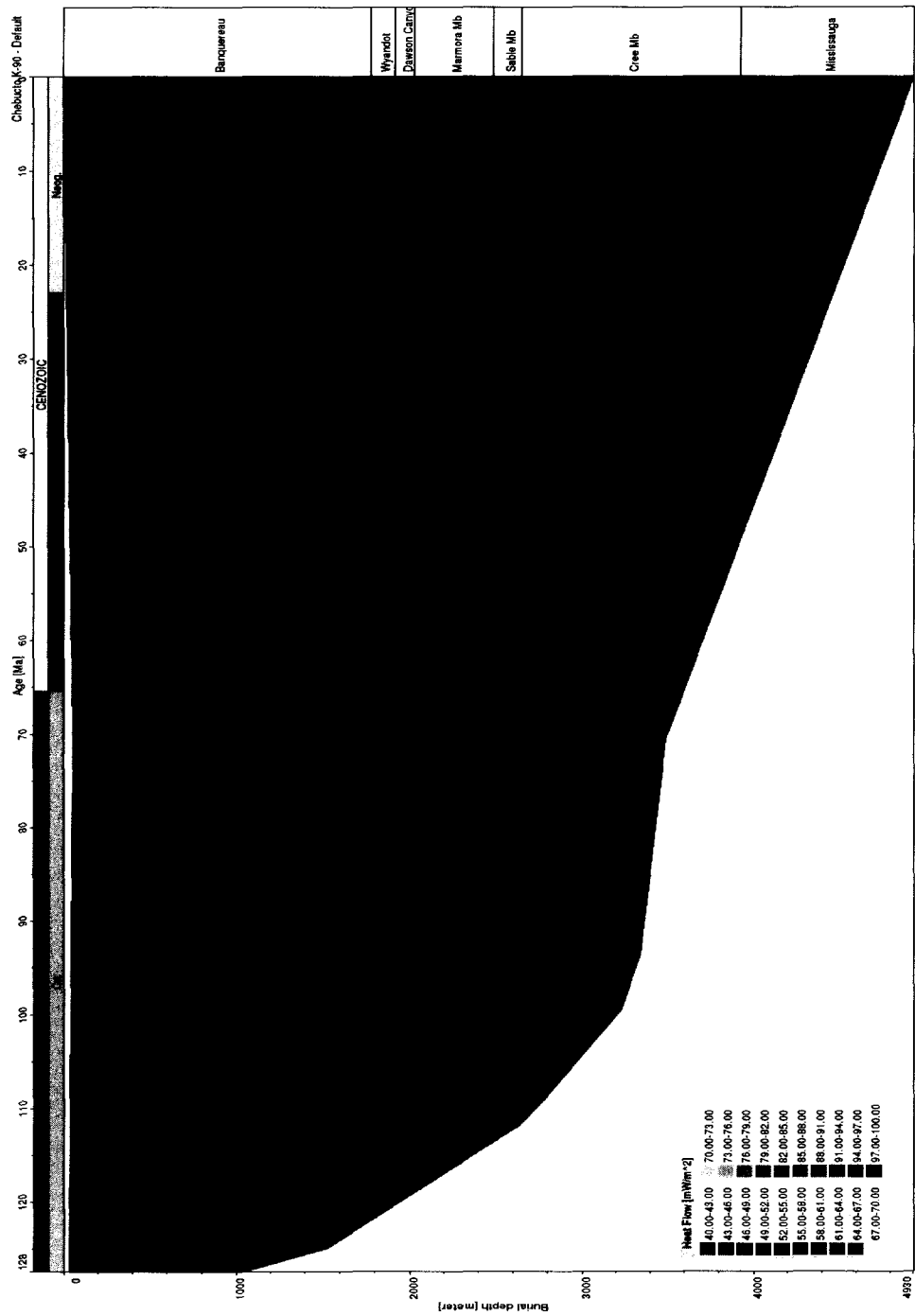
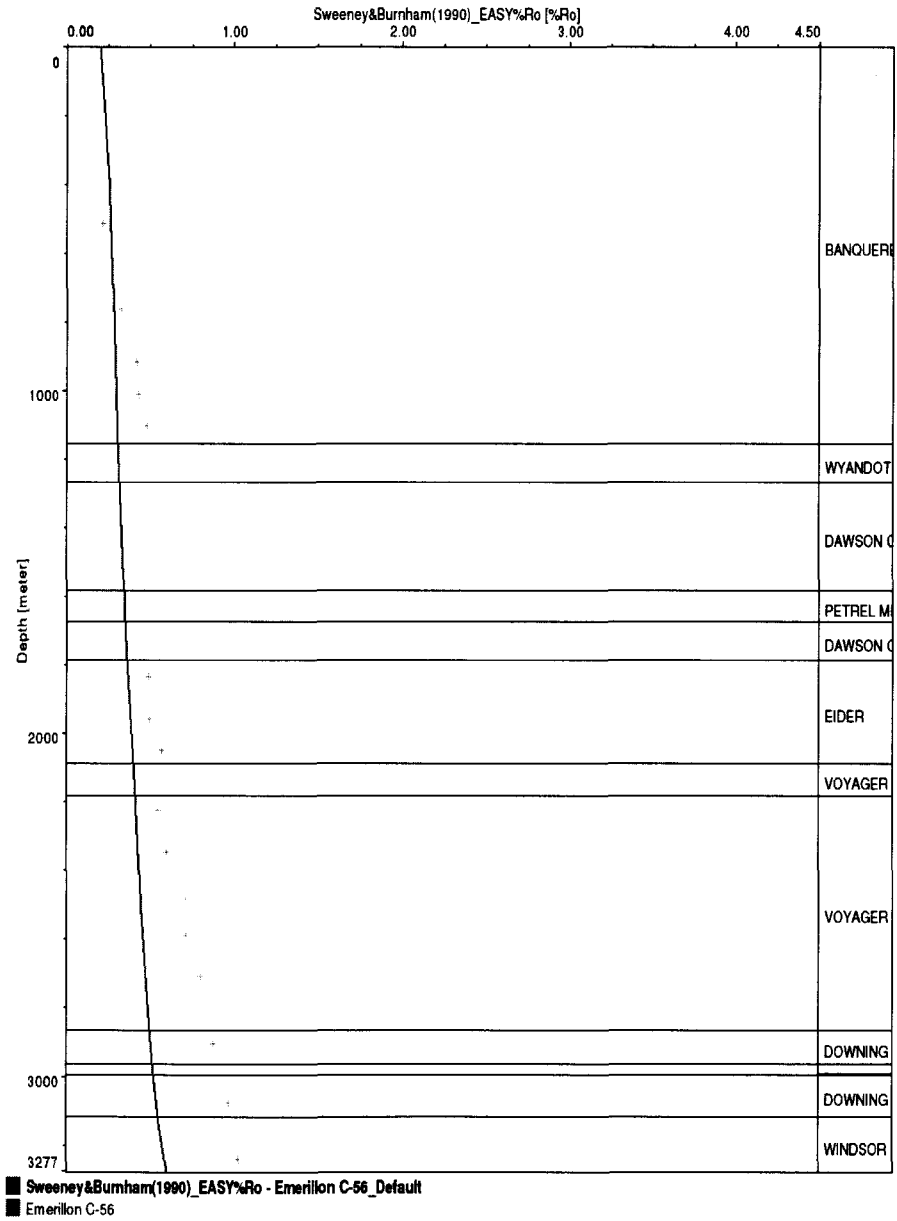Figure 2.3: Result of Model A burial history plot with heat flow overlay for Chebucto K-90

219
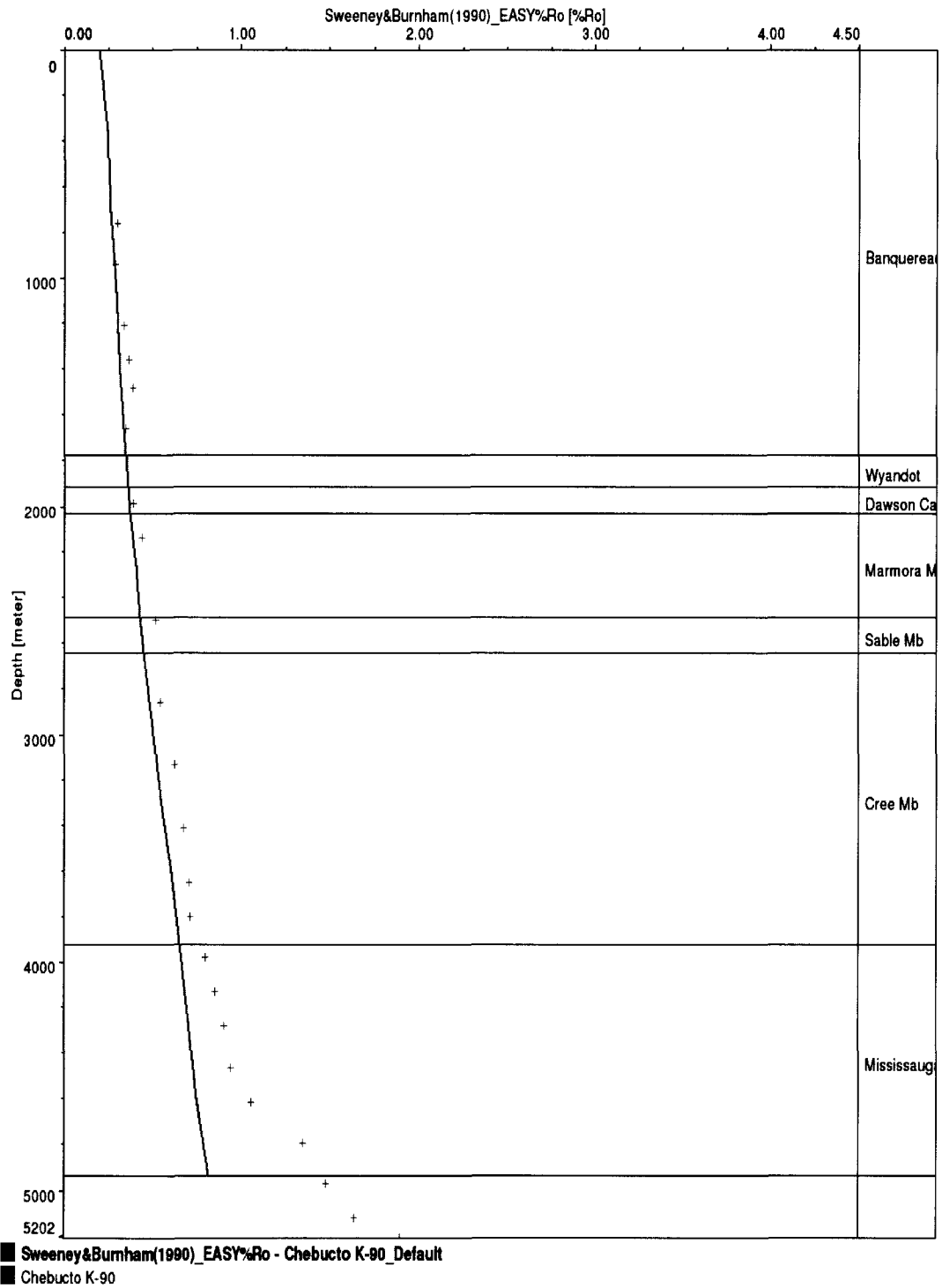
Figure 2.4: Model A modeled vitrinite reflectance profile vs measured vitrinite reflectance for Chebucto K-90
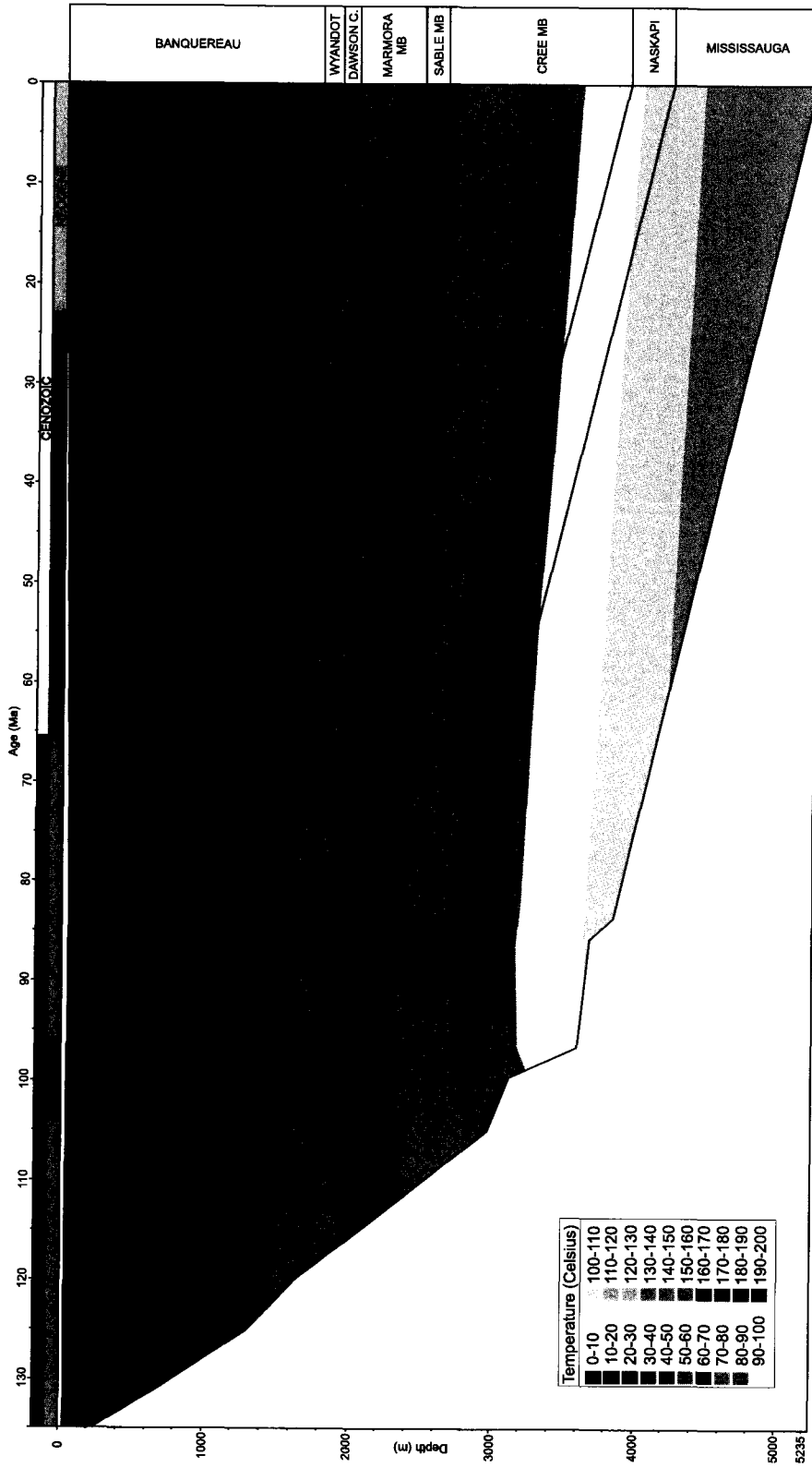
Figure 2.5: Results of Model B burial history plot with temperature overlay for Chebucto K-90
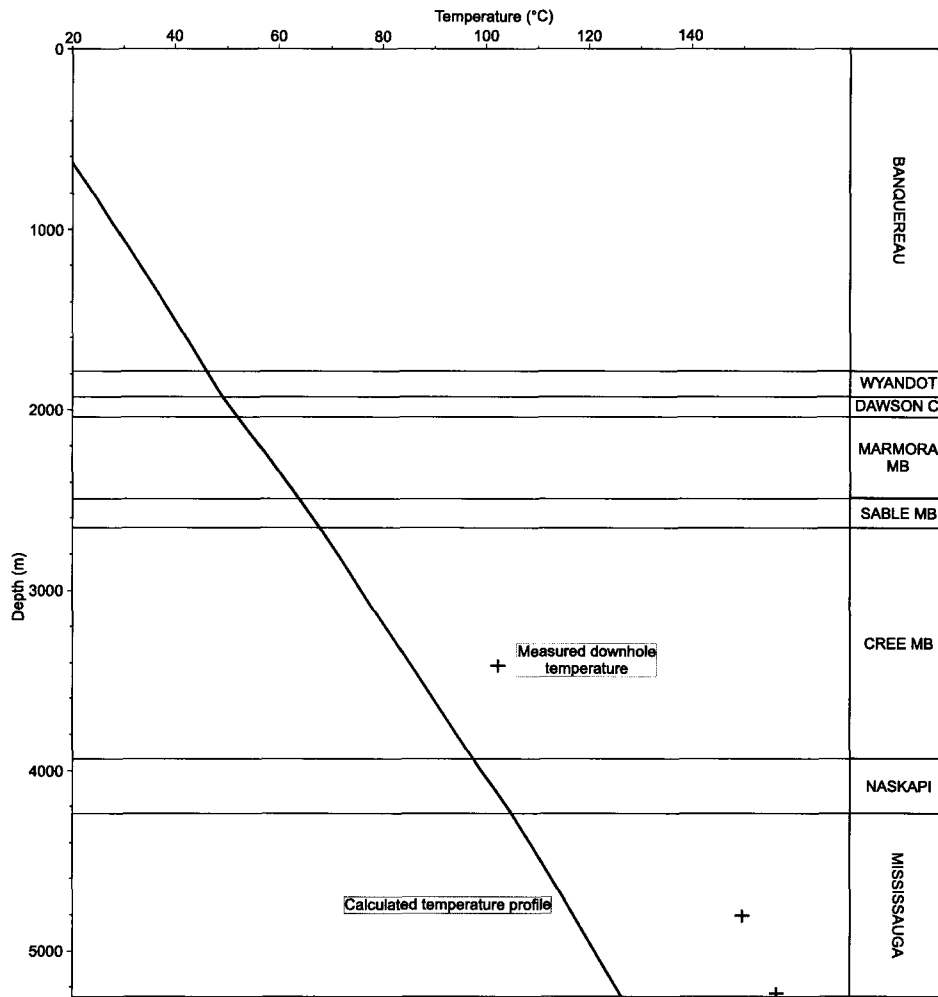
Figure 2.6: Model B modeled temperature vs measured downhole temperature for Chebucto K-90
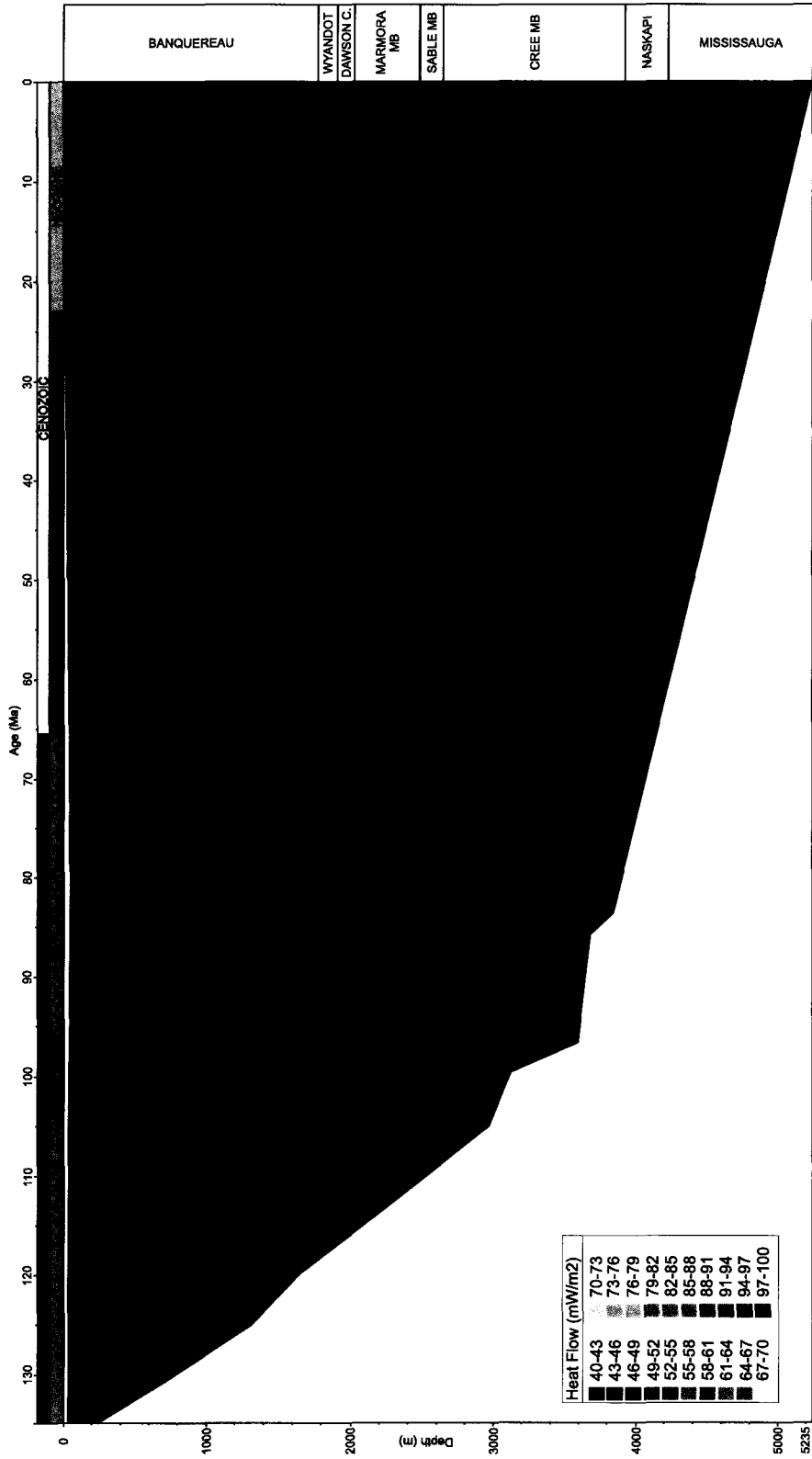
Figure 2.7: Results of Model B burial history plot with heat flow overlay for Chebucto K-90

223
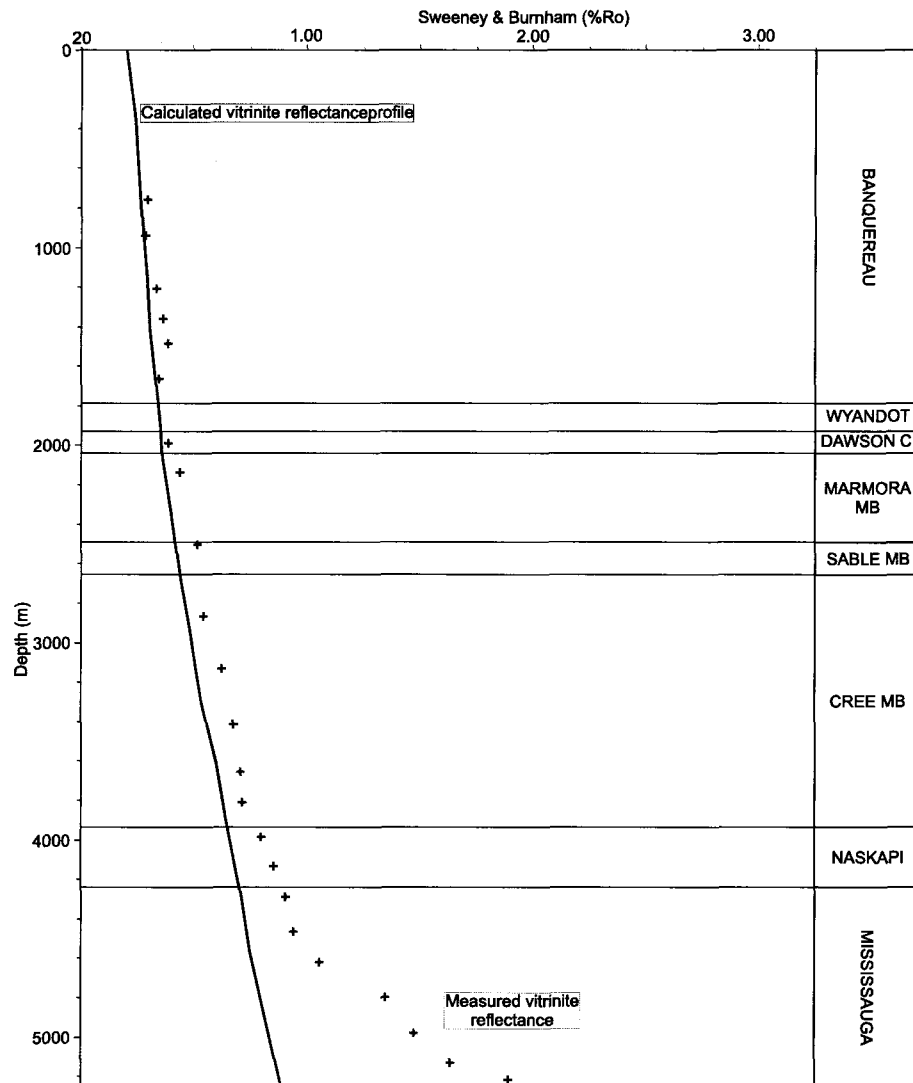
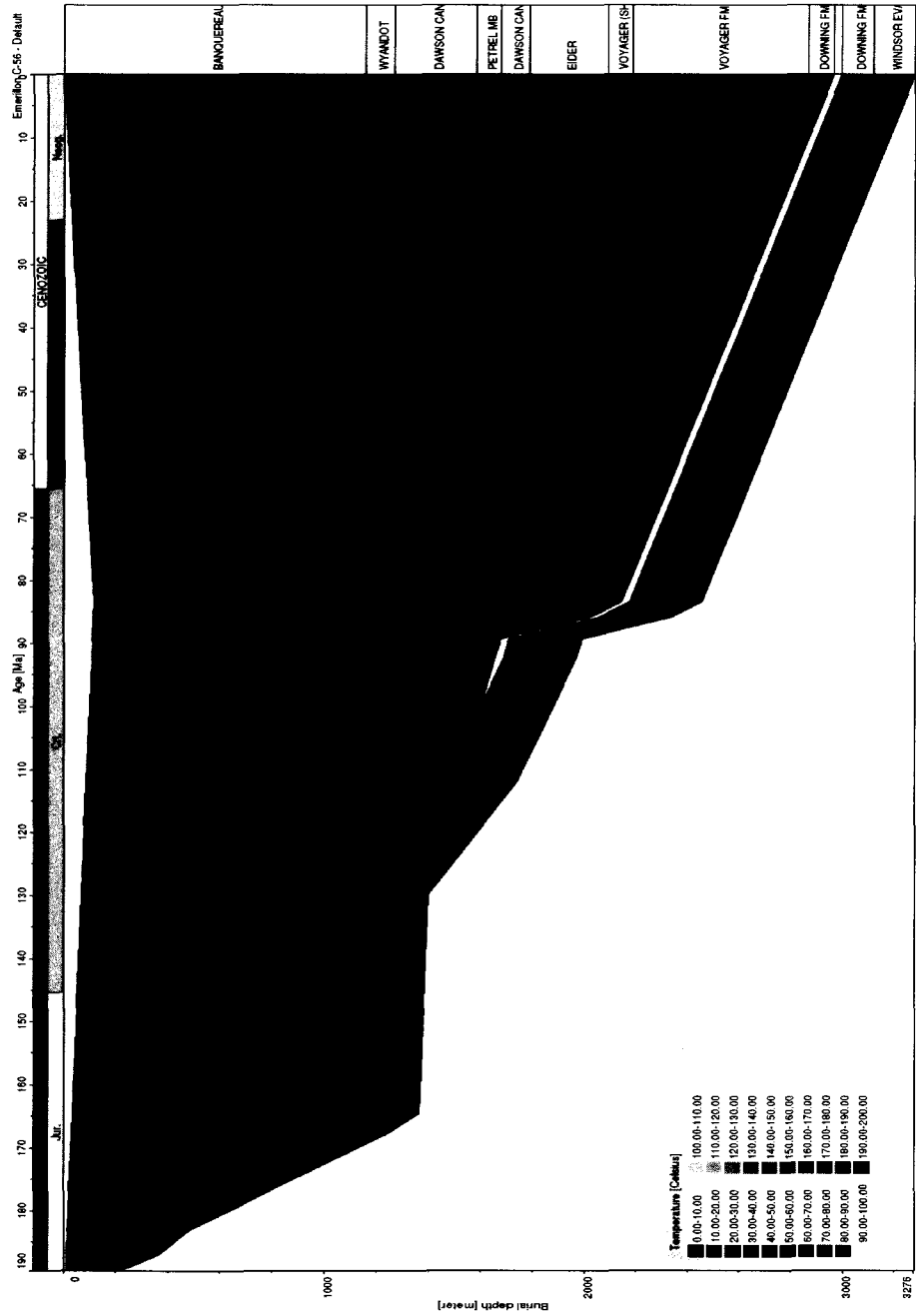Figure 2.8: Model B modeled vitrinite reflectance profile vs measured vitrinite reflectance for Chebucto K-90
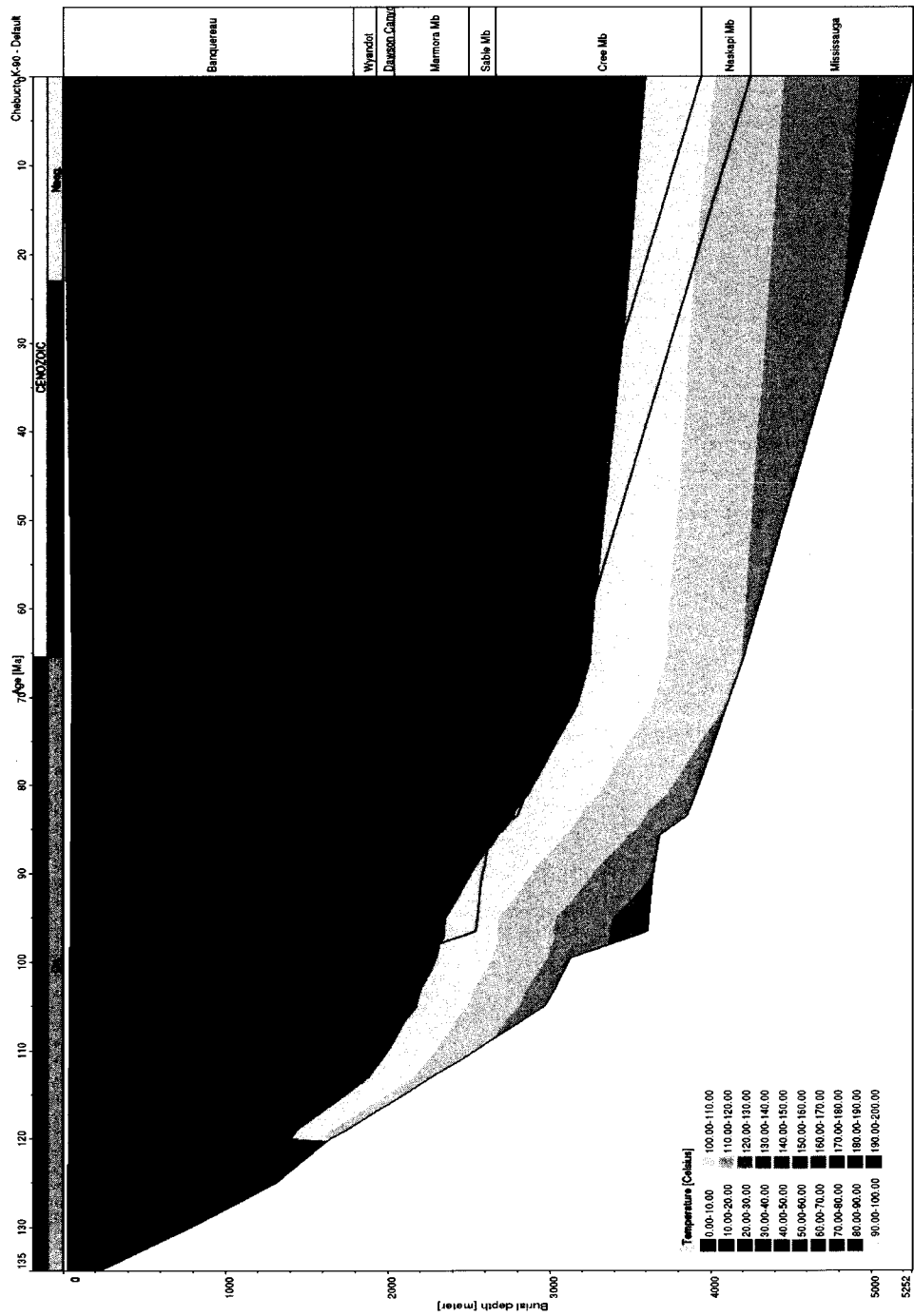
Figure 2.9: Results of Model C burial history plot with temperature overlay for Chebucto K-90
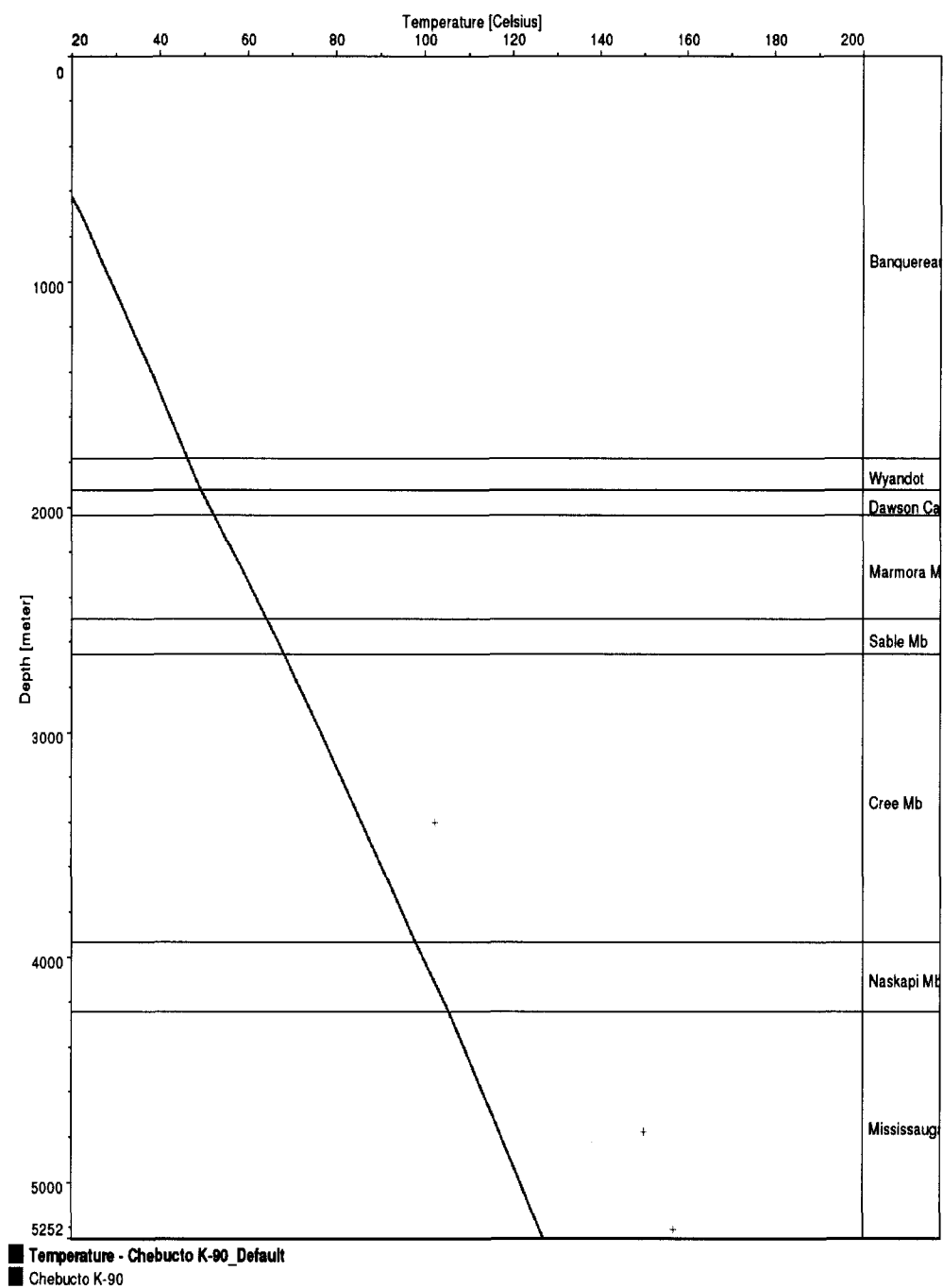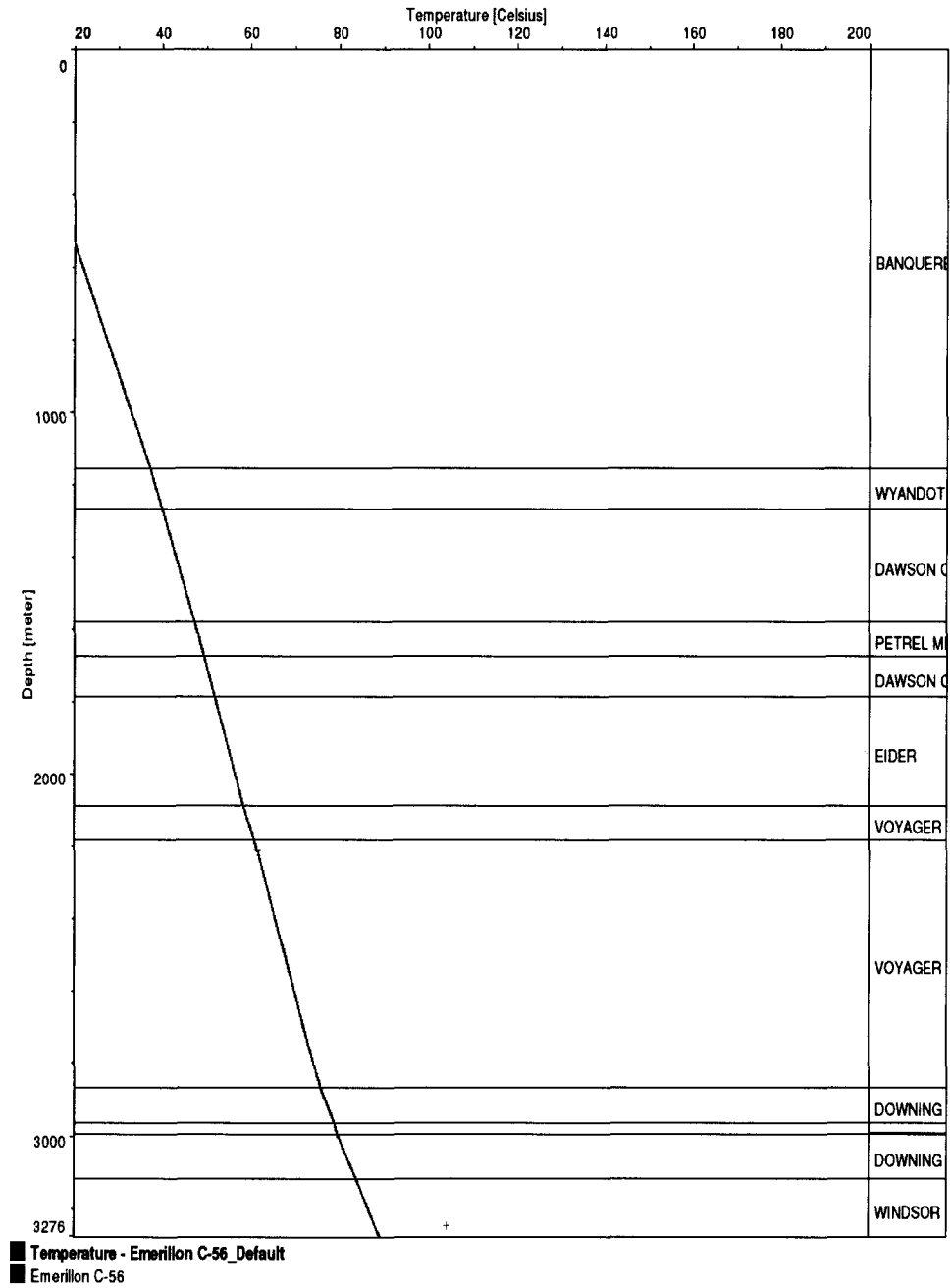
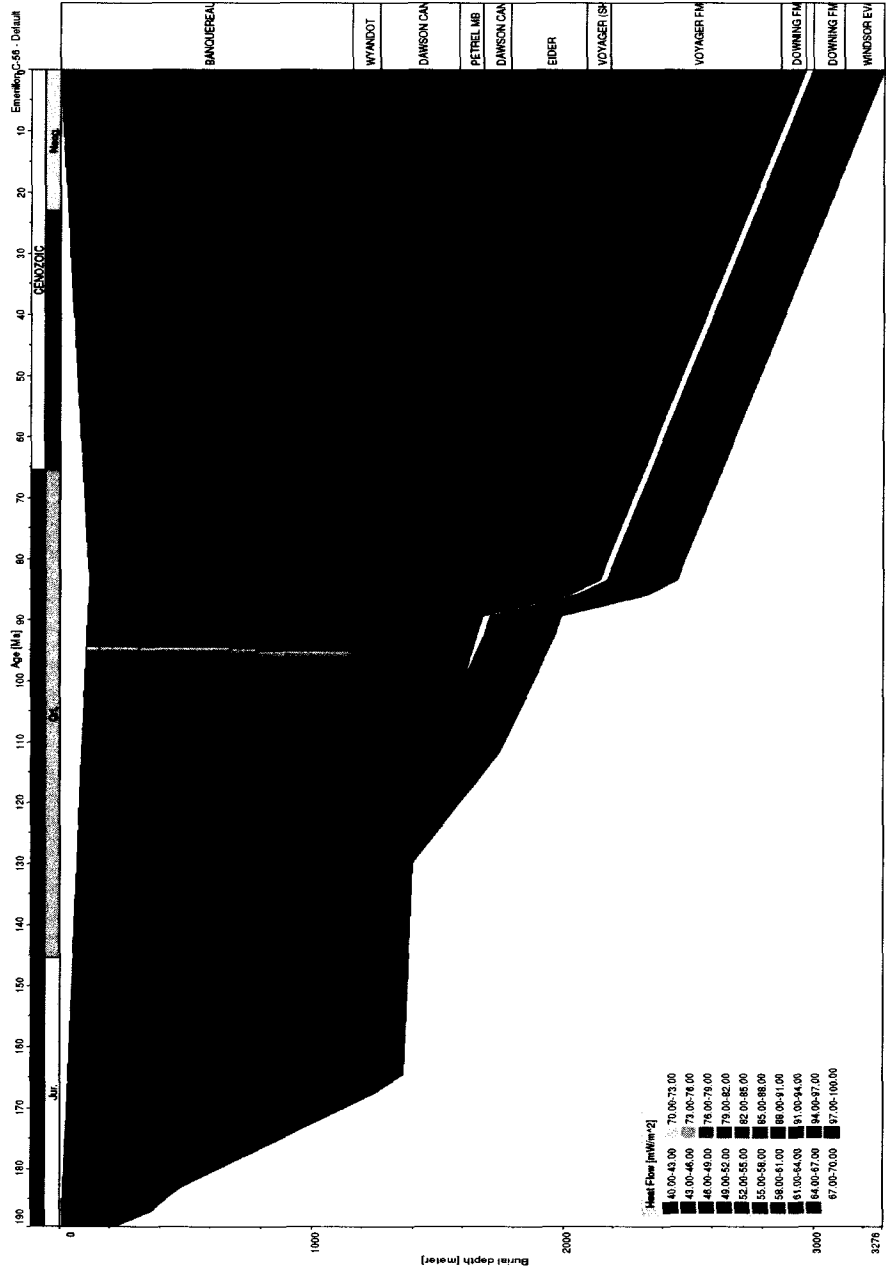Figure 2.10: Model C modeled temperature vs measured downhole temperature for Chebucto K-90

227
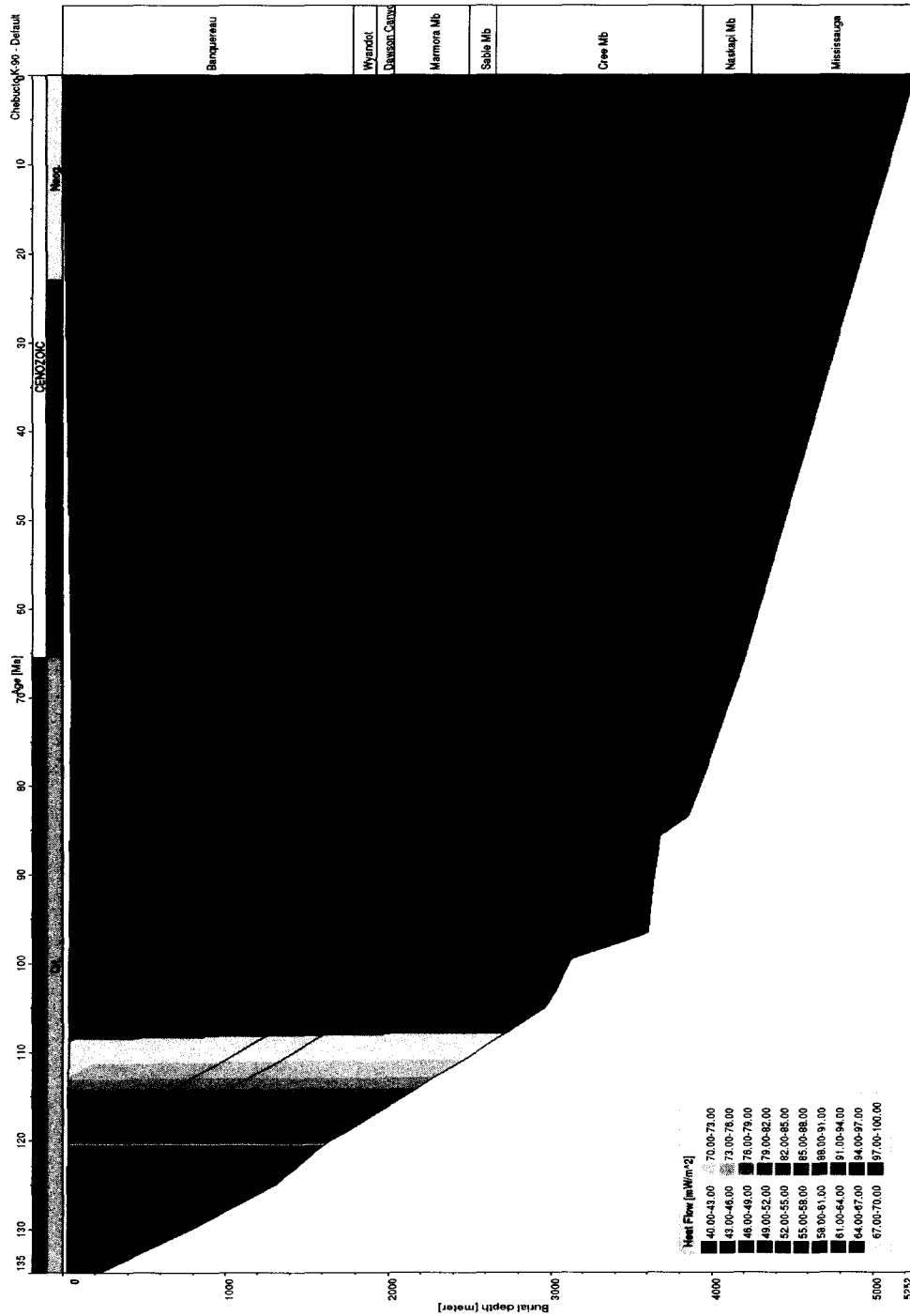
Figure 2.11: Results of Model C burial history plot with heat flow overlay for Chebucto K-90
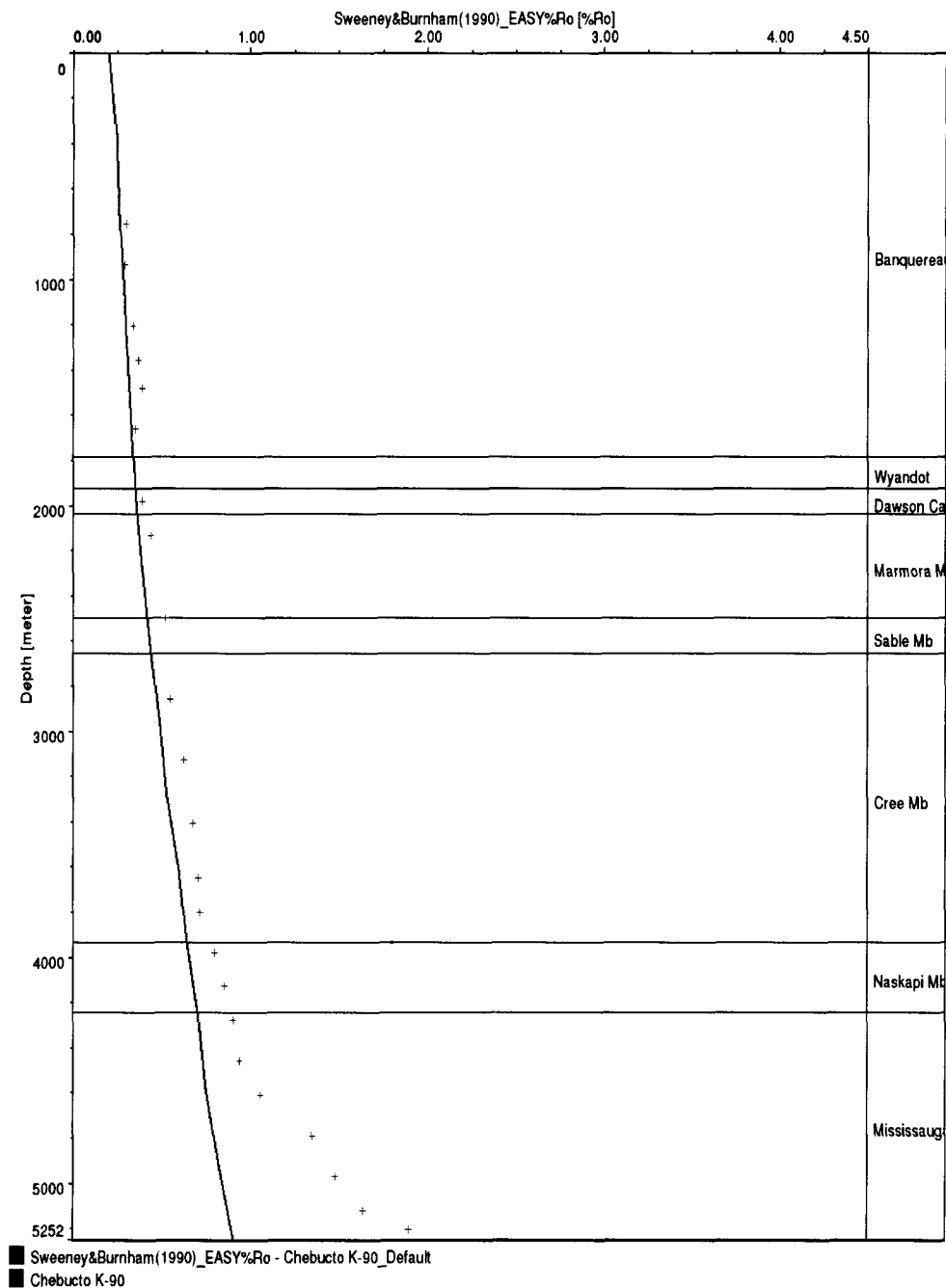
Figure 2.12: Model C modeled vitrinite reflectance profile vs measured vitrinite reflectance for Chebucto K-90
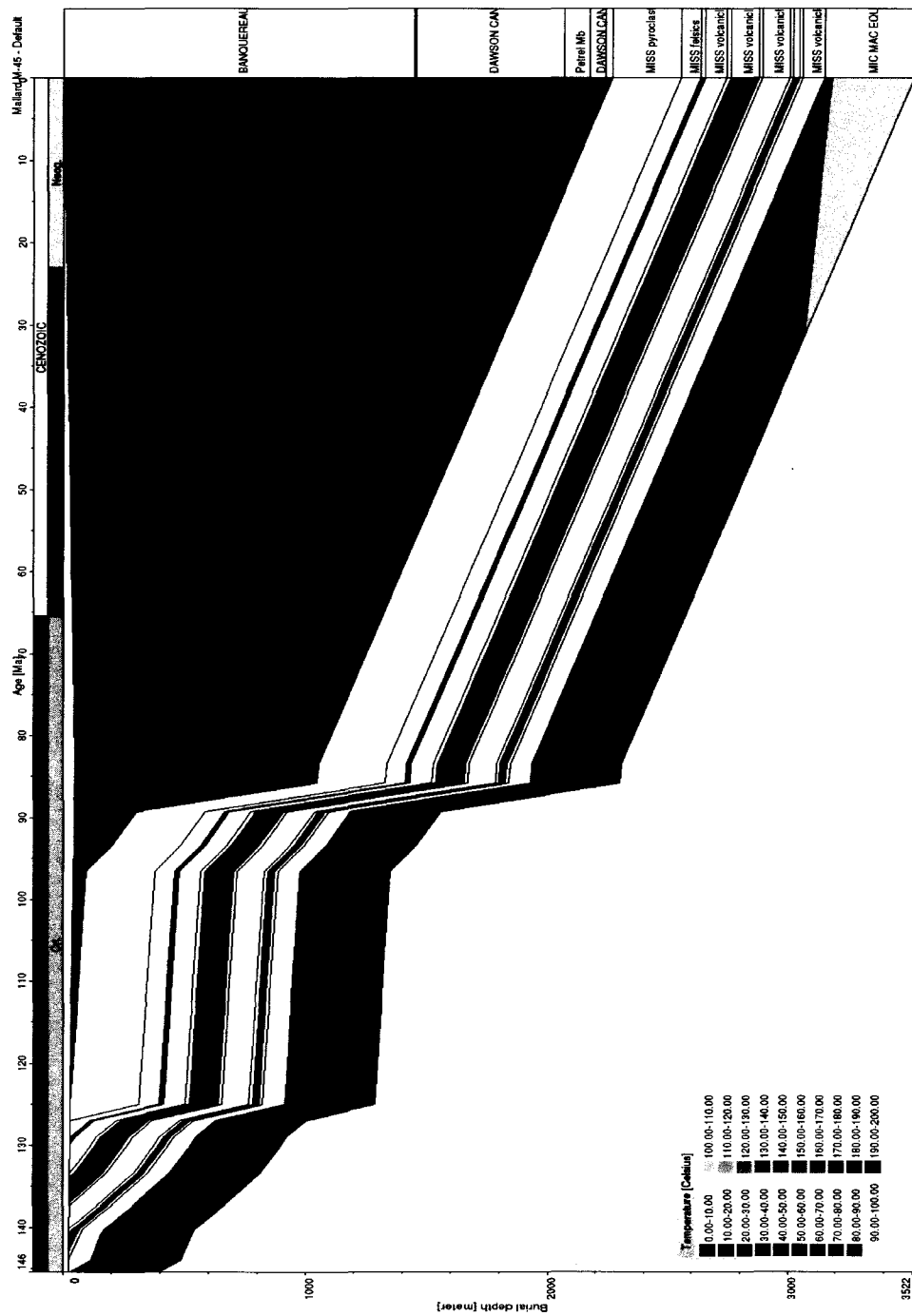
Figure 2.13: Results of Model A burial history plot with temperature overlay for Mallard M-45
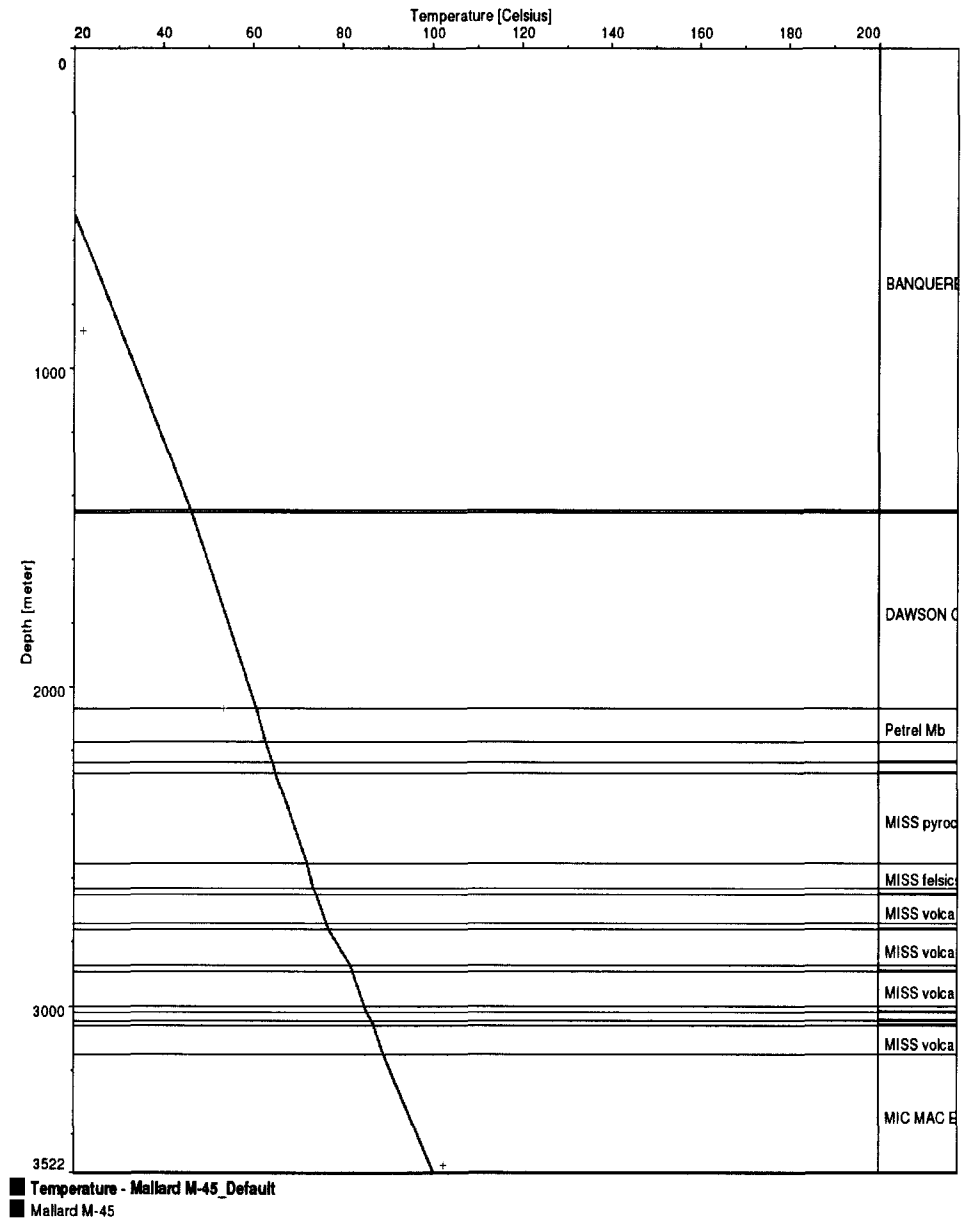
Figure 2.14: Model A modeled temperature vs measured downhole temperature for Mallard M-45
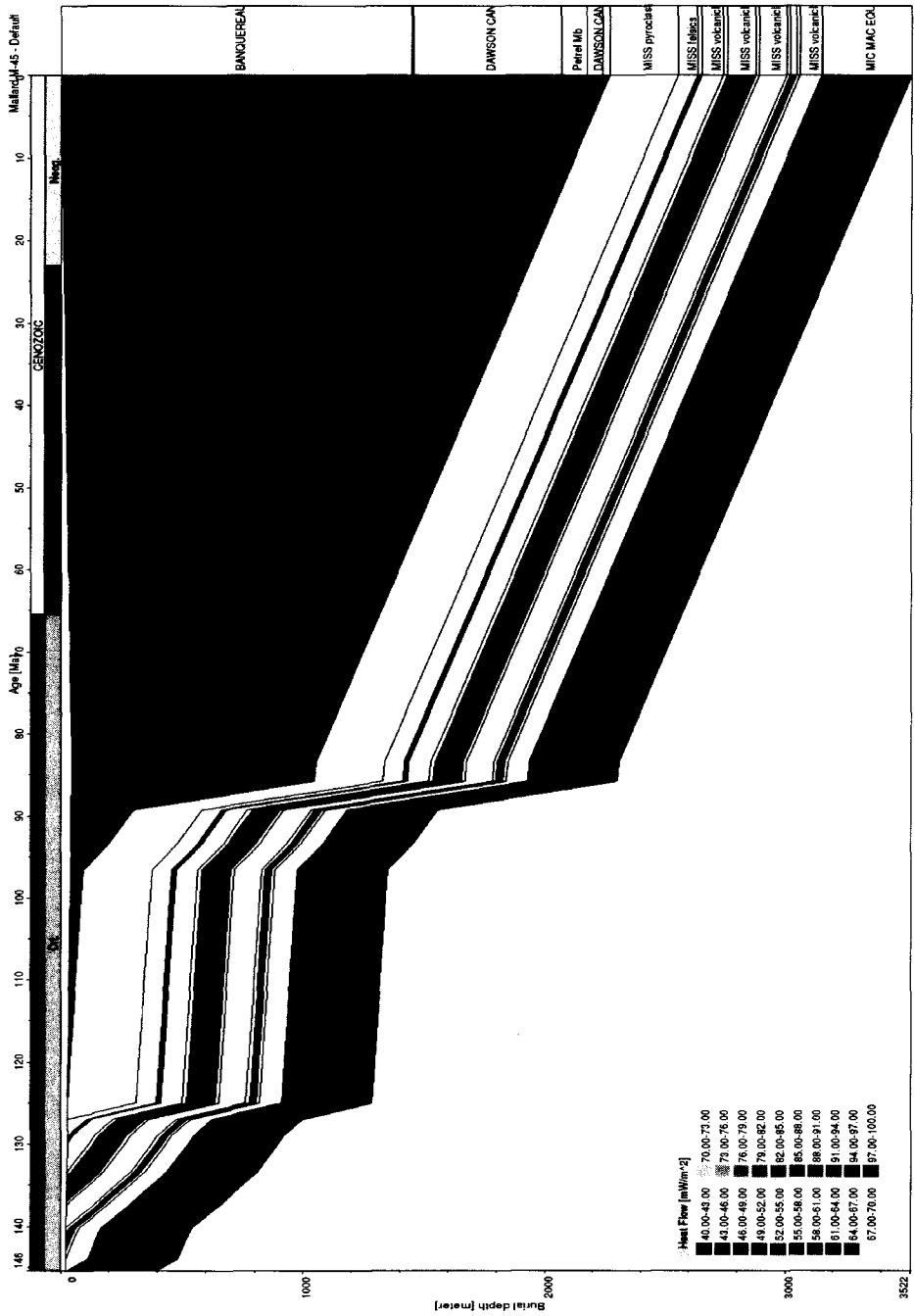
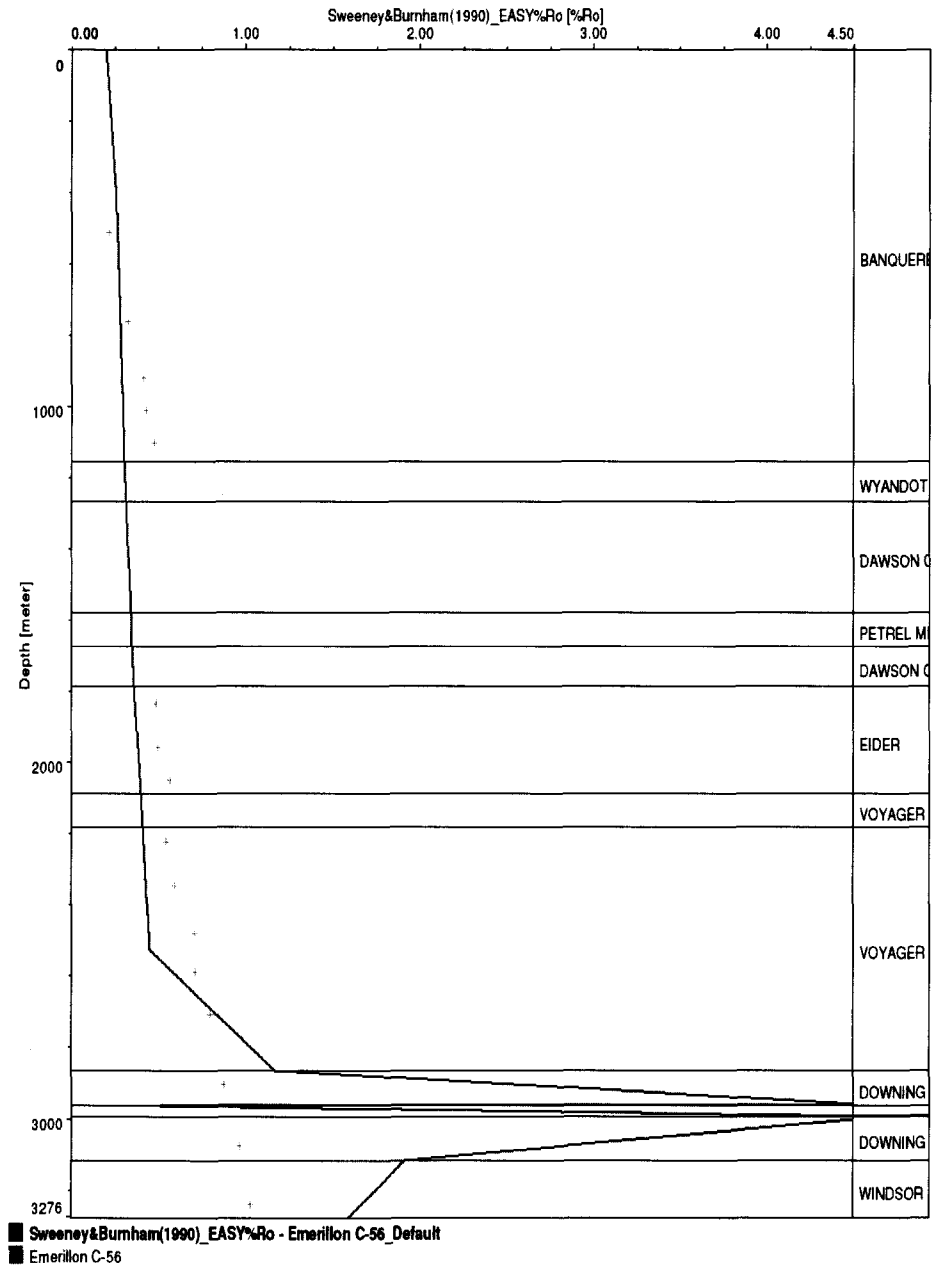Figure 2.15: Results of Model A burial history plot with heat flow overlay for Mallard M-45
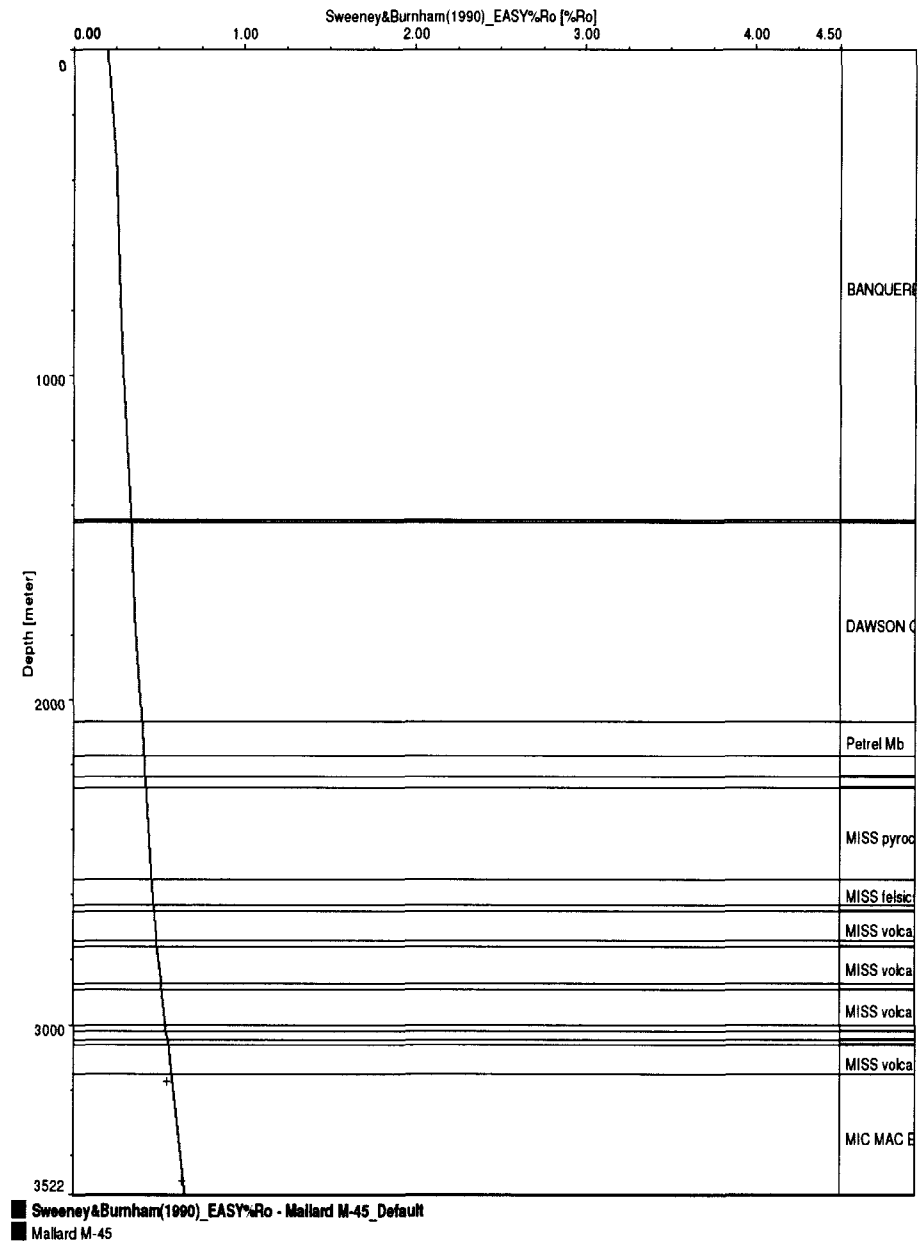
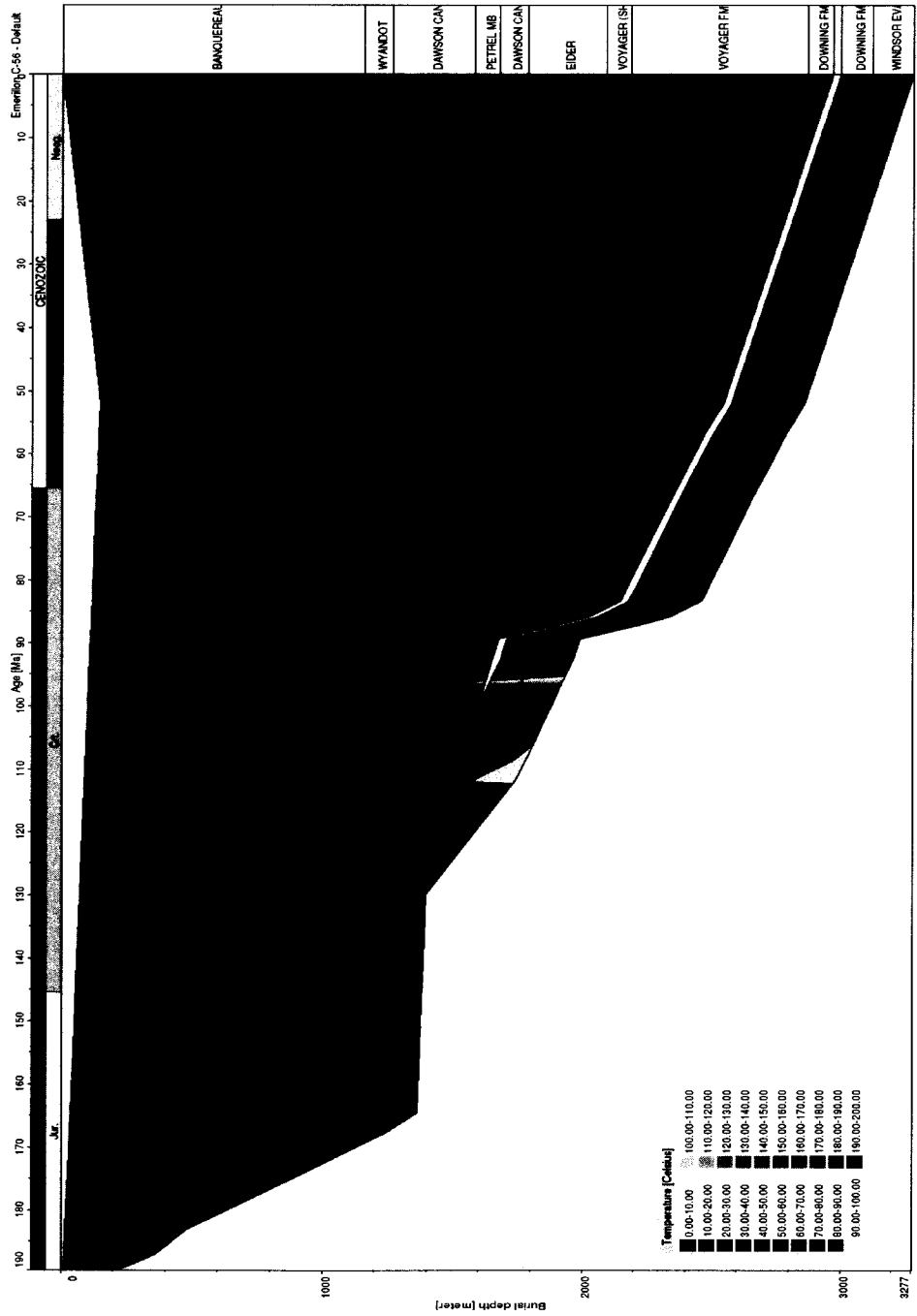Figure 2.16: Model A modeled vitrinite reflectance profile vs measured vitrinite reflectance for Mallard M-45
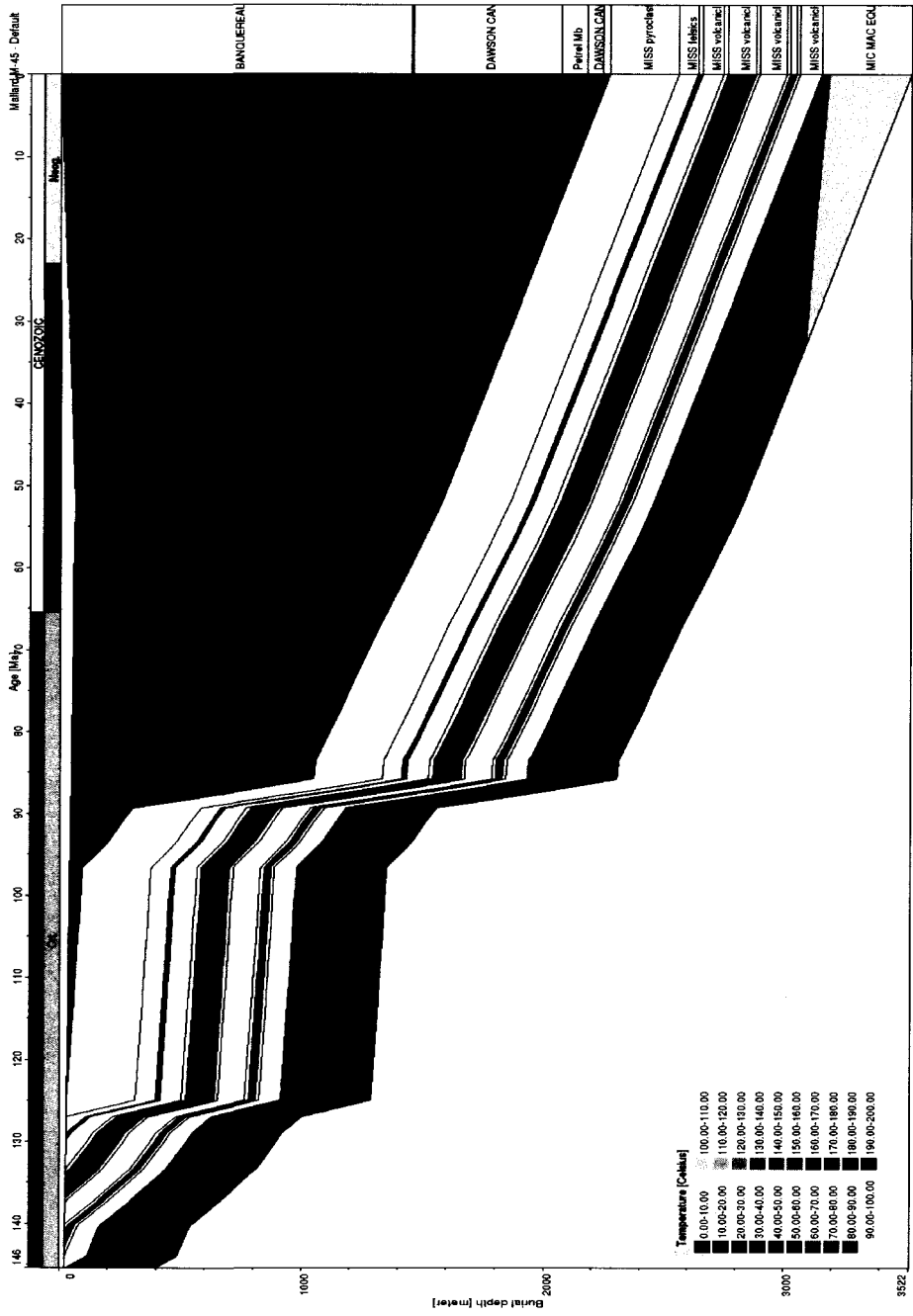
Figure 2.17: Results of Model B burial history plot with temperature overlay for Mallard
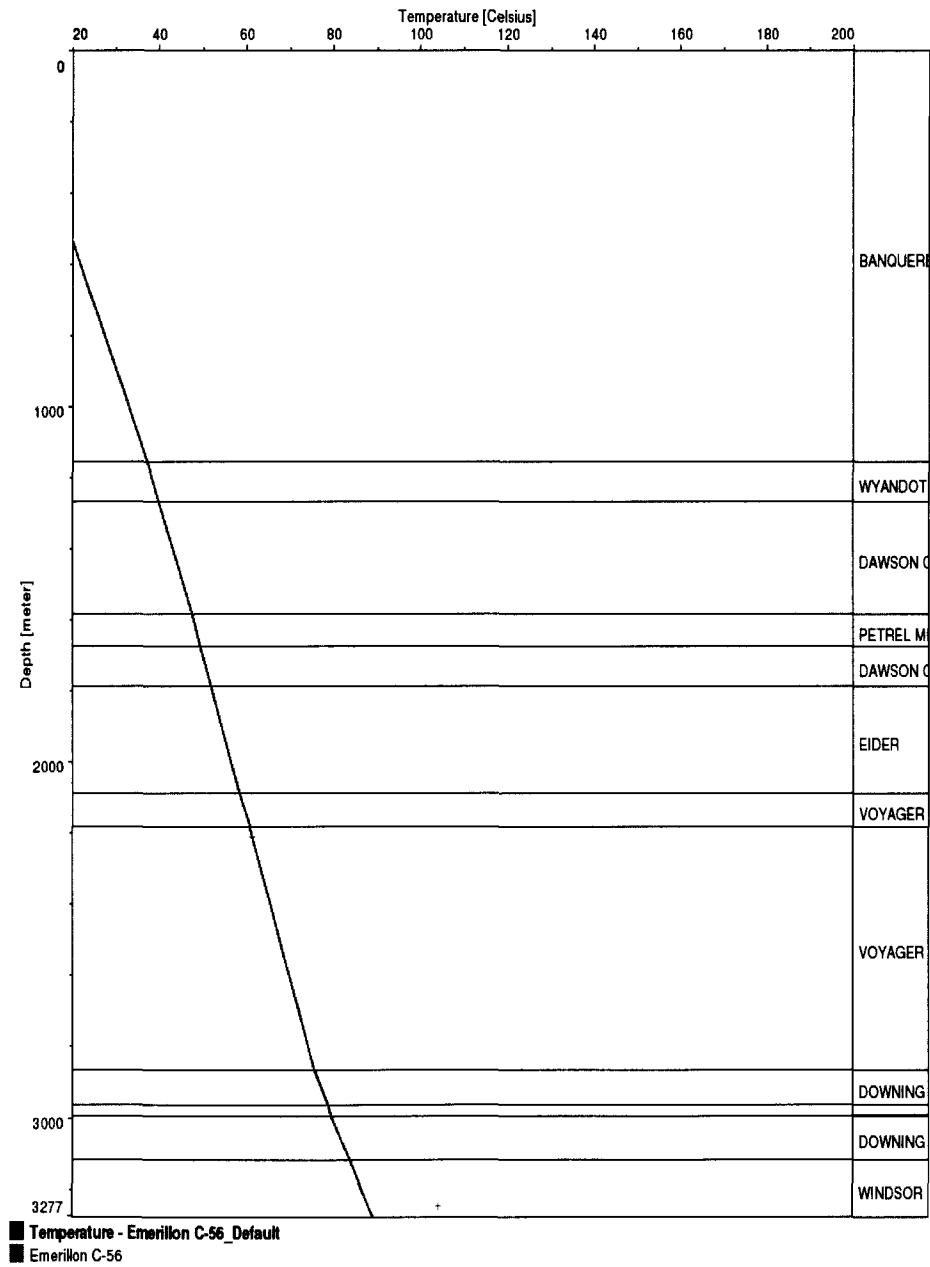M-45
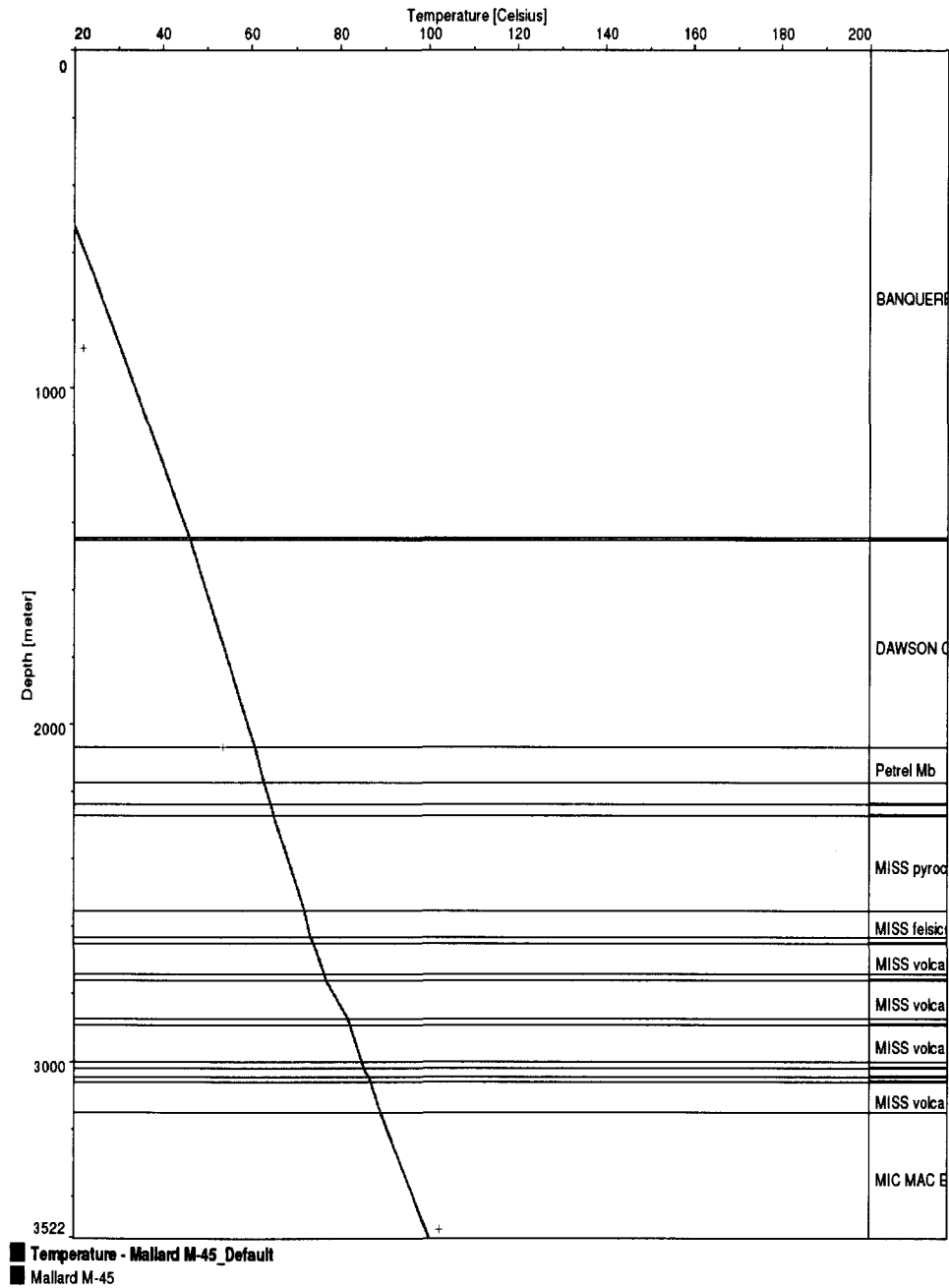
Figure 2.18: Model B modeled temperature vs measured downhole temperature for
Mallard M-45

235
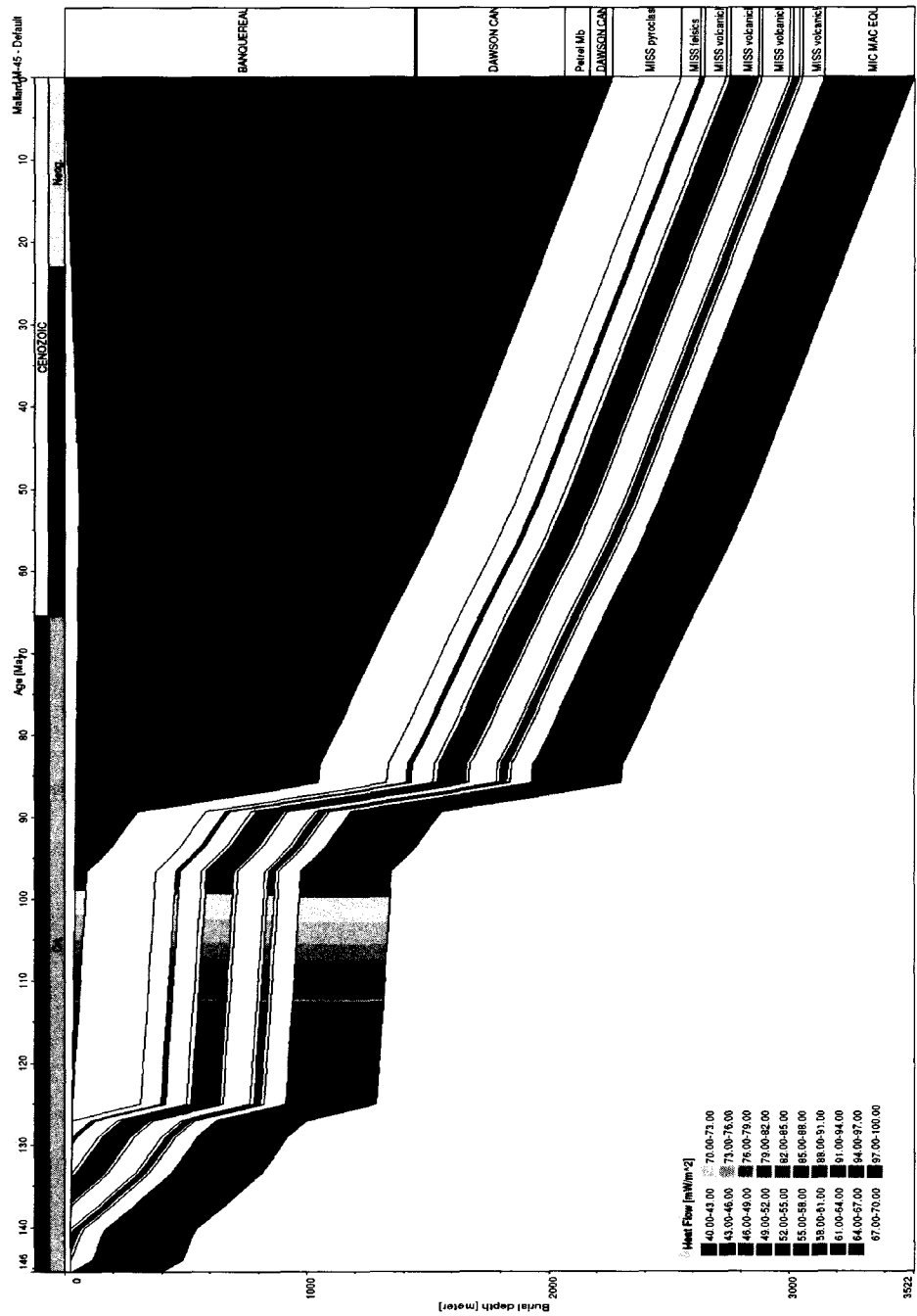
Figure 2.19: Results of Model B burial history plot with heat flow overlay for Mallard M-45
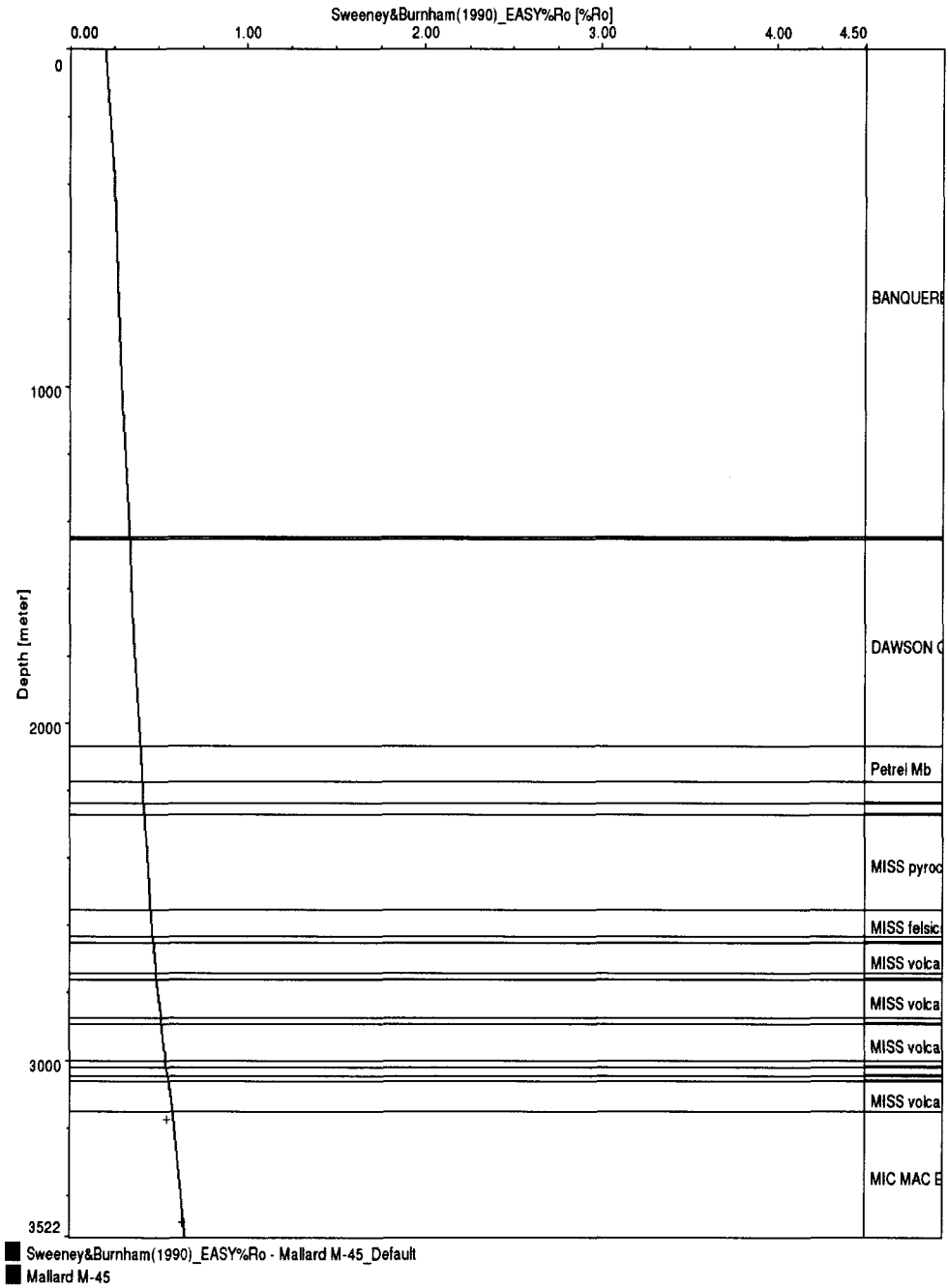
Figure 2.20: Model B modeled vitrinite reflectance profile vs measured vitrinite reflectance for Mallard M-45

Figure 2.21: Results of Model C burial history plot with temperature overlay for Mallard M-45
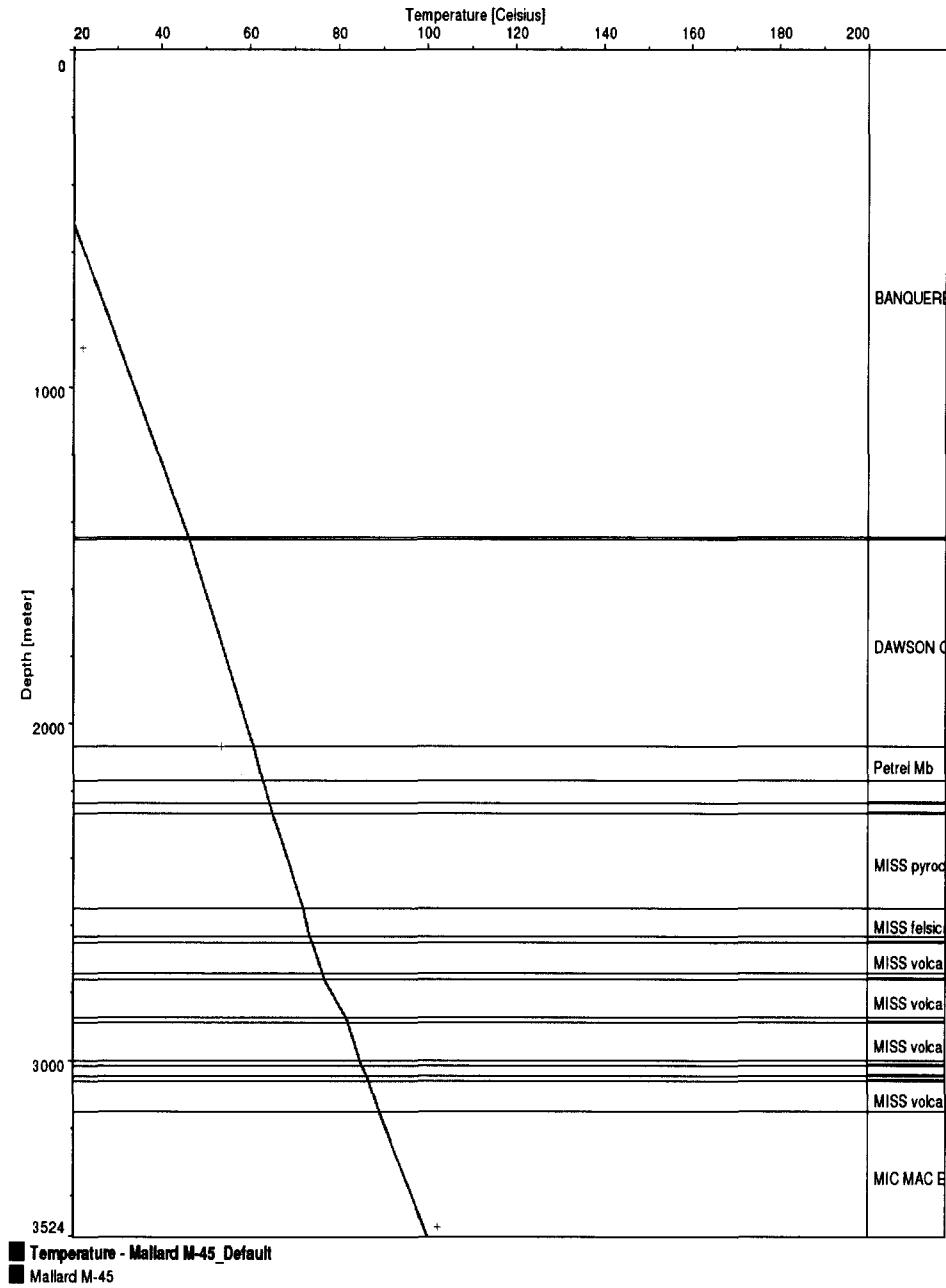
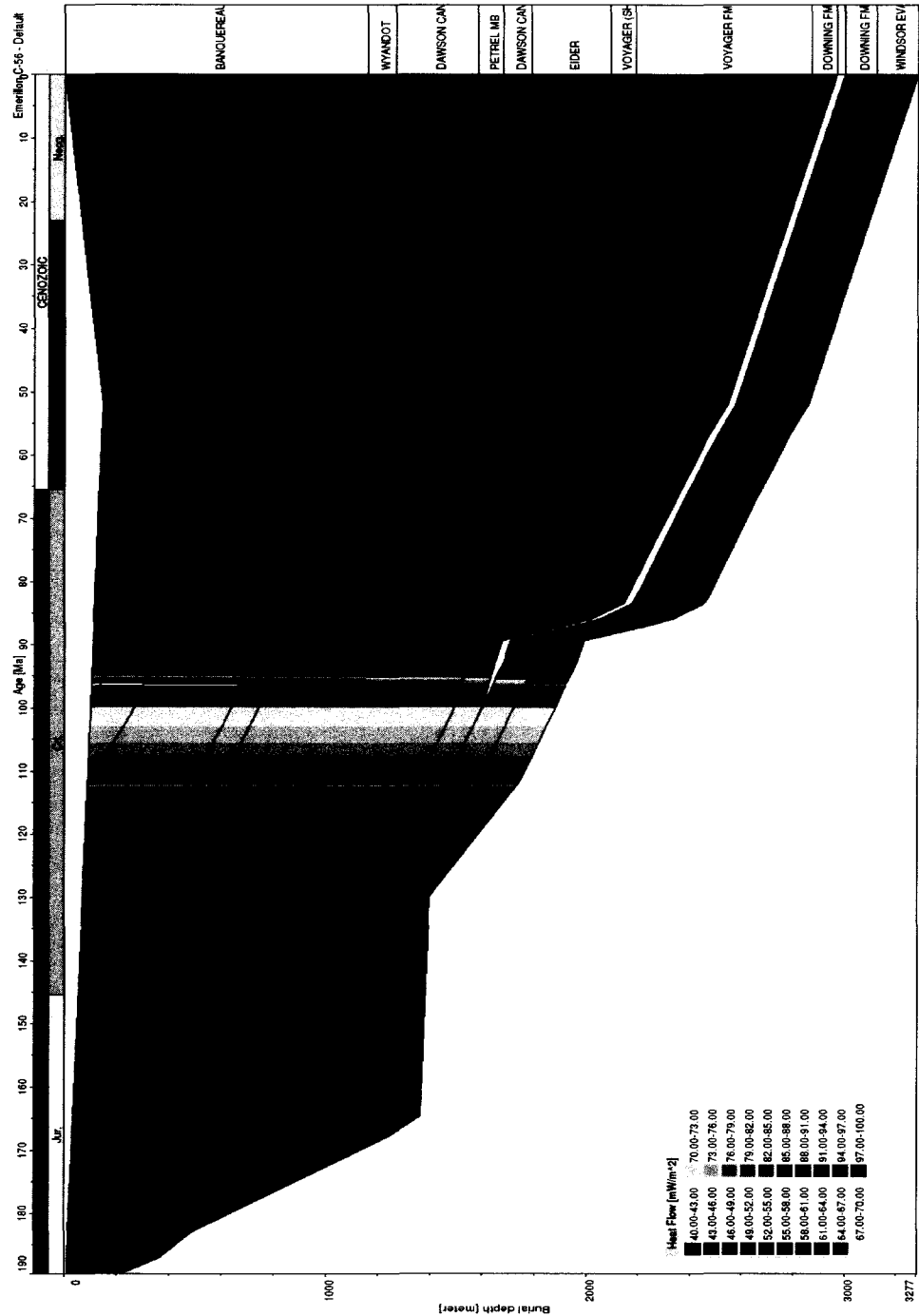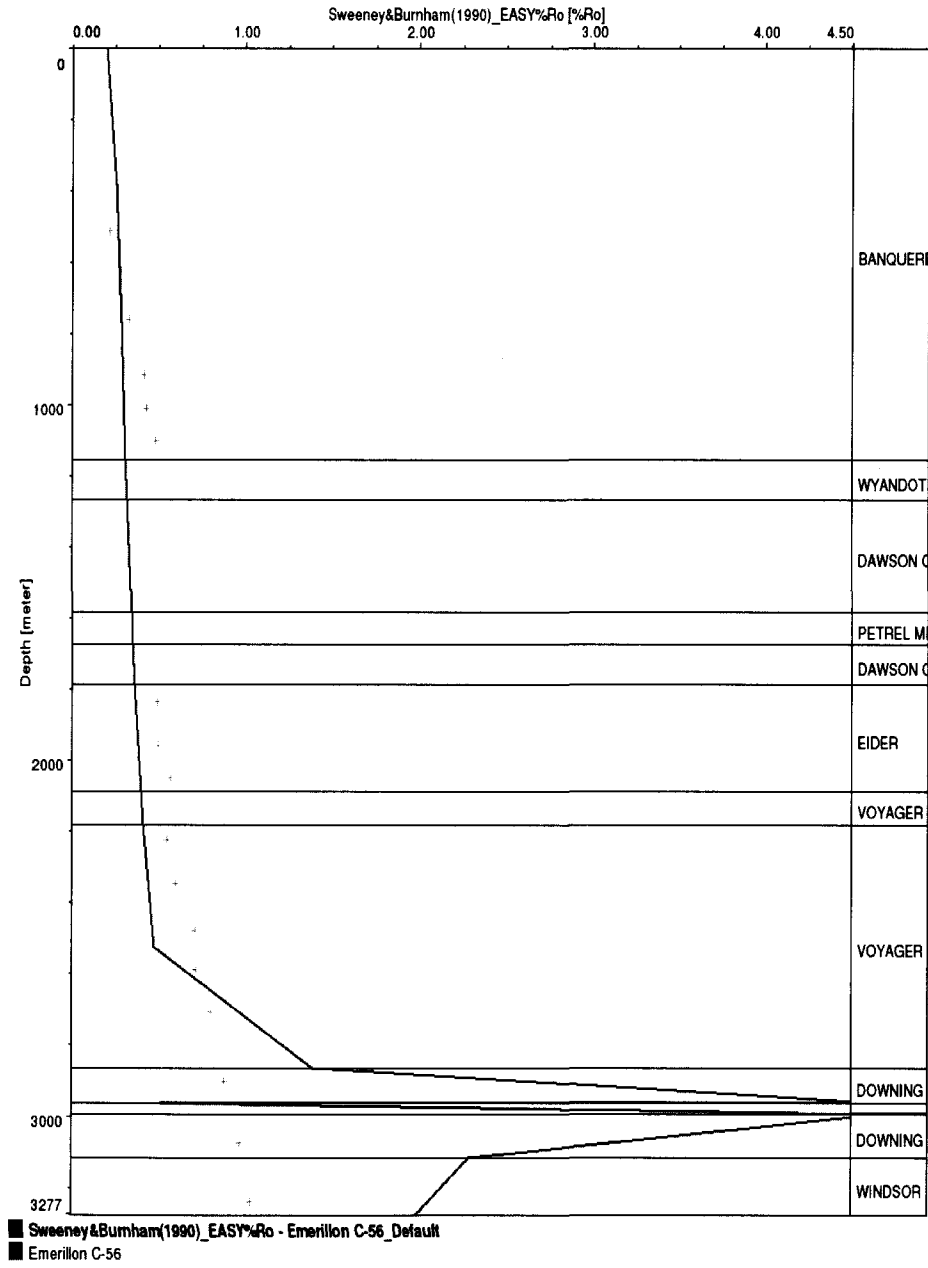Figure 2.22: Model C modeled temperature vs measured downhole temperature for Mallard M-45
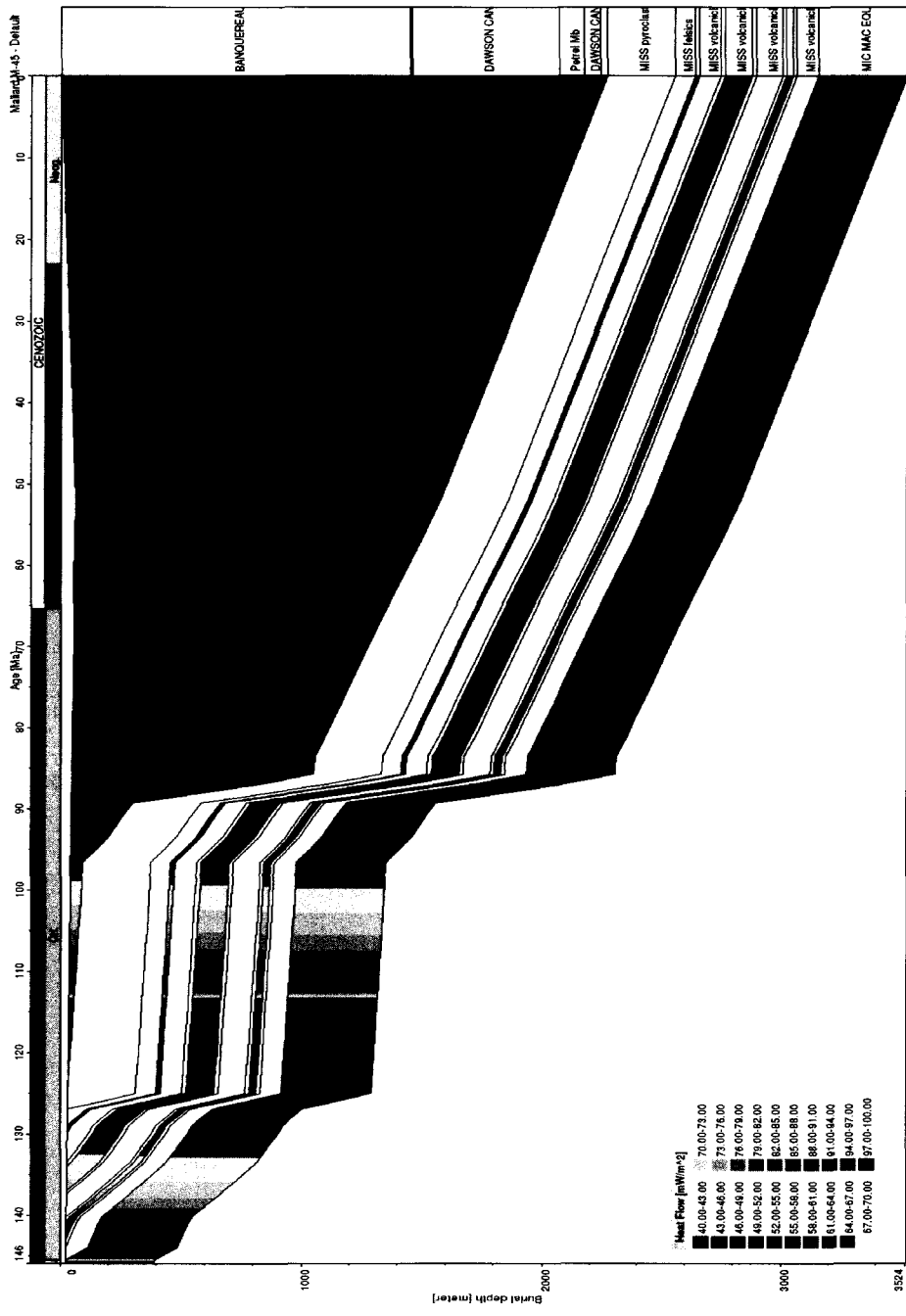
Figure 2.23: Results of Model C burial history plot with heat flow overlay for Mallard M-45
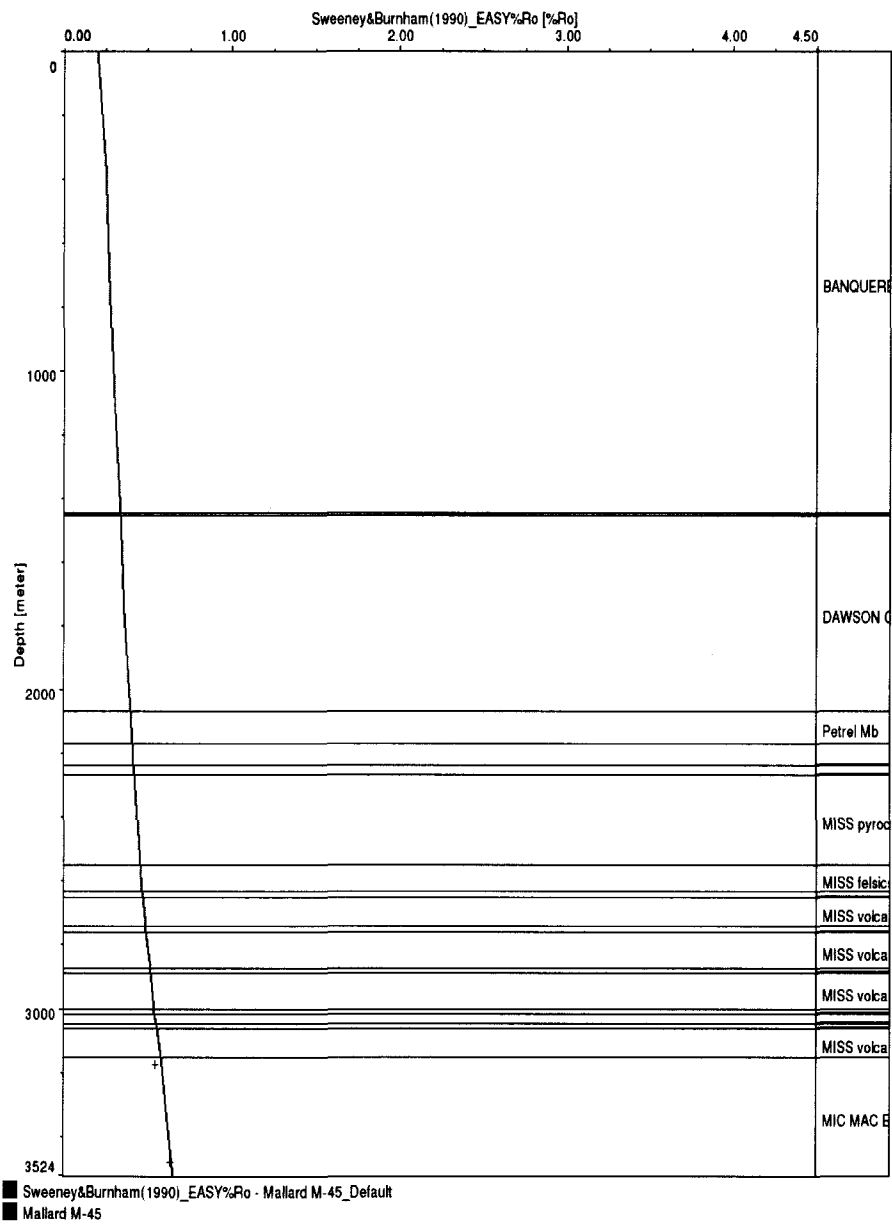
Figure 2.24: Model C modeled vitrinite reflectance profile vs measured vitrinite reflectance for Mallard M-45

Figure 2.25: Results of Model A (no intrusion) burial history plot with temperature overlay for Emerillon C-56
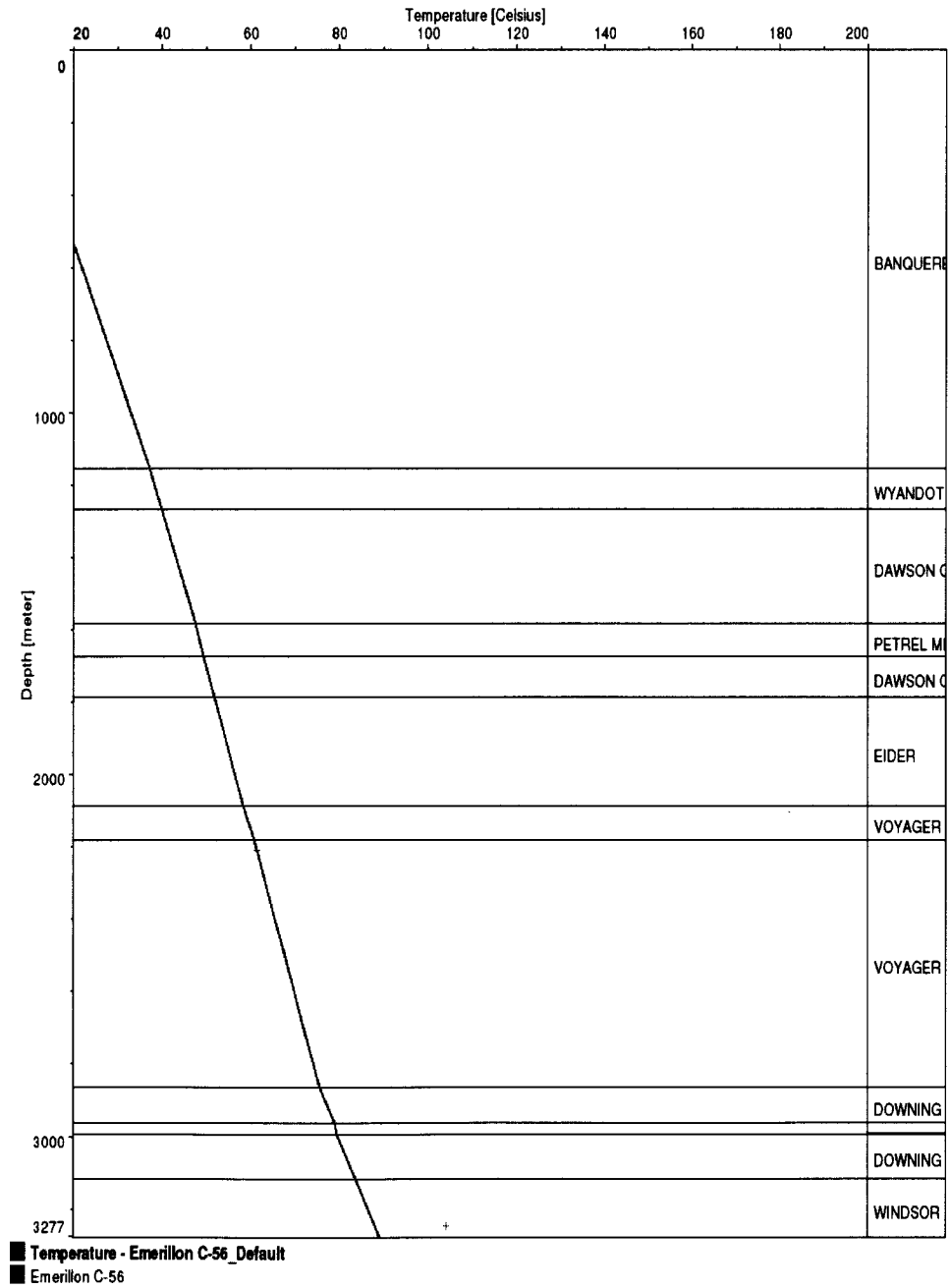
Figure 2.26: Model A (no intrusion) modeled temperature vs measured downhole temperature for Emerillon C-56
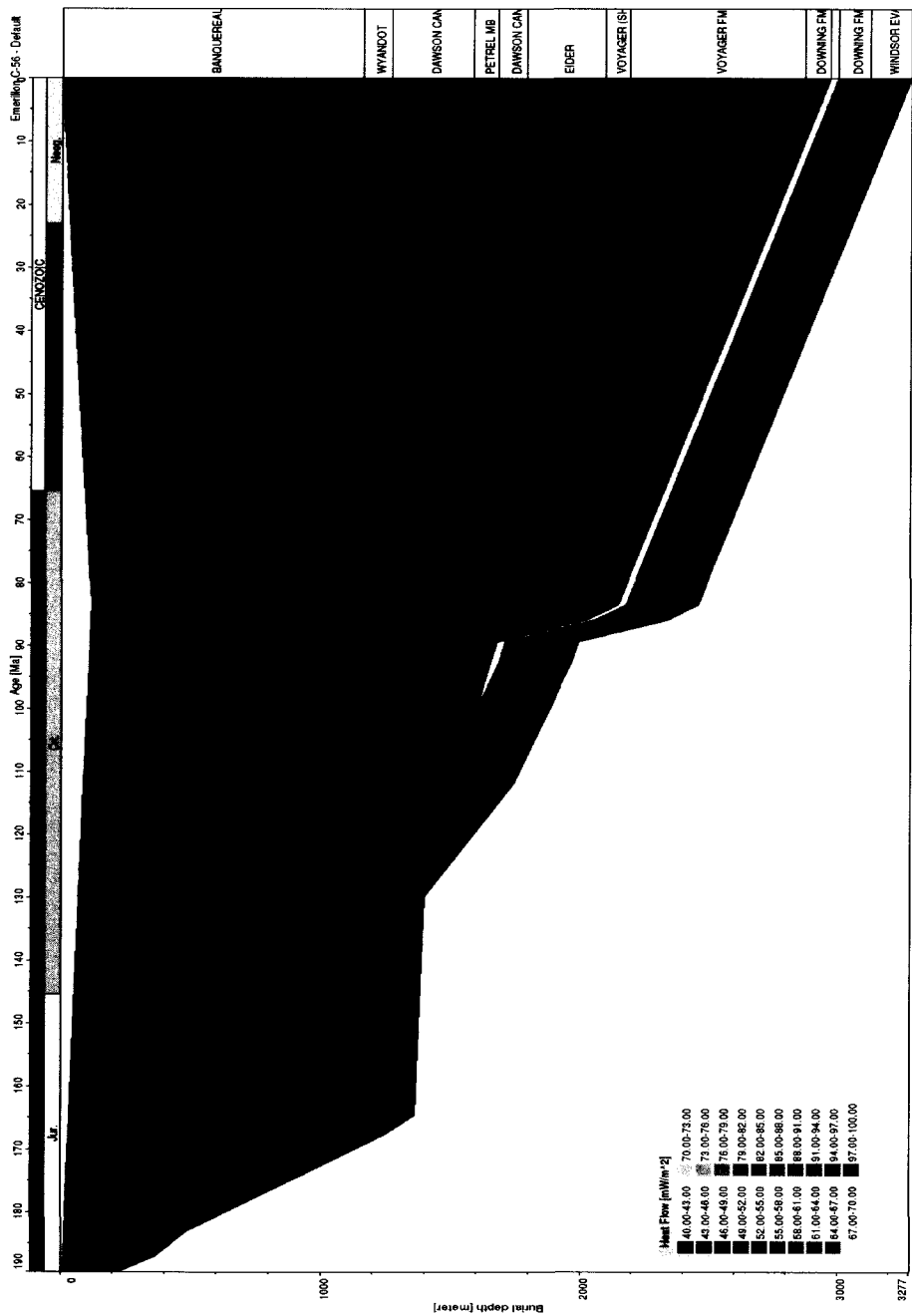
Figure 2.27: Results of Model A (no intrusion) burial history plot with heat flow overlay for Emerillon C-56

Figure 2.28: Model A (no intrusion) modeled vitrinite reflectance profile vs measured vitrinite reflectance for Emerillon C-56
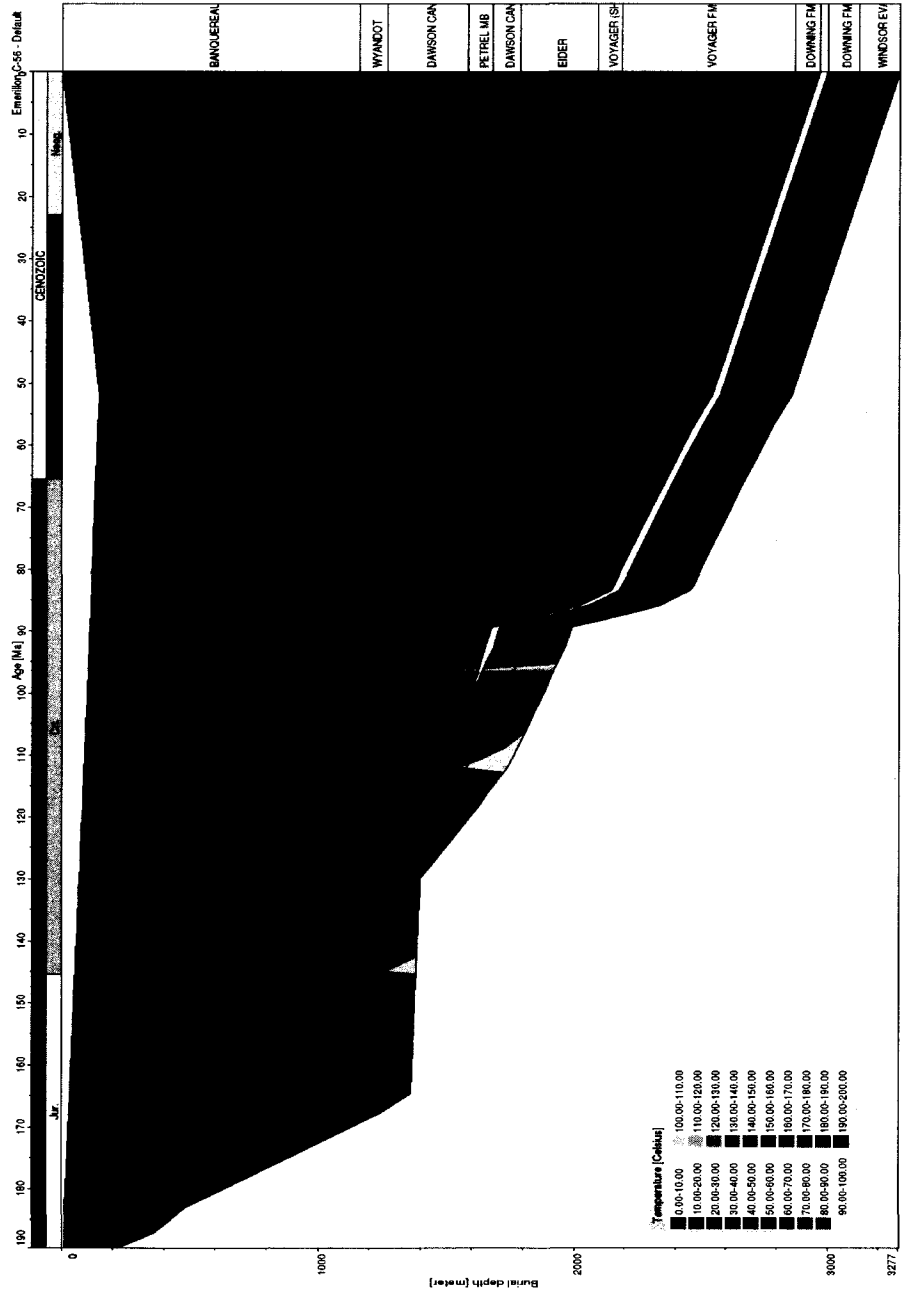
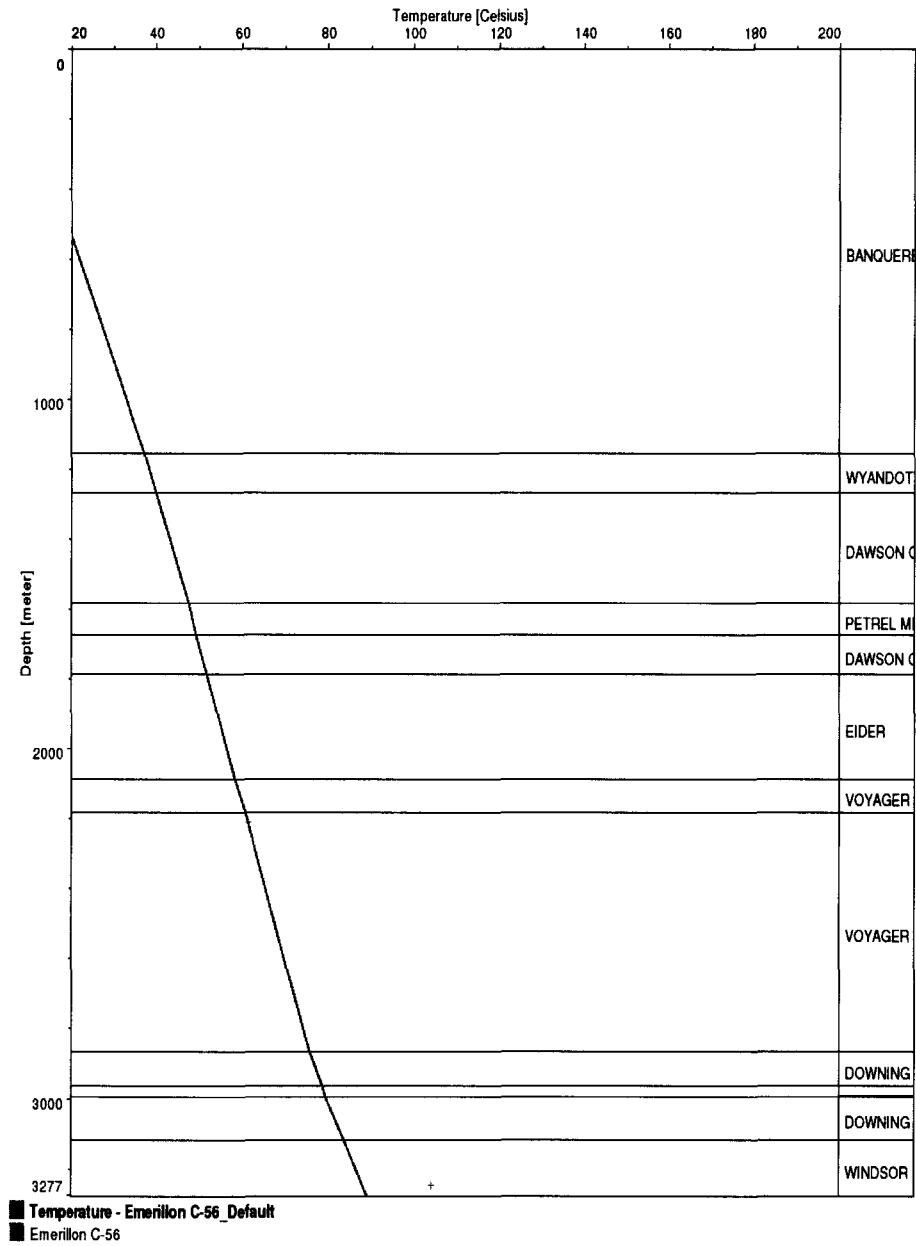Figure 2.29: Results of Model A burial history plot with temperature overlay for Emerillon C-56

Figure 2.30: Model A modeled temperature vs measured downhole temperature for
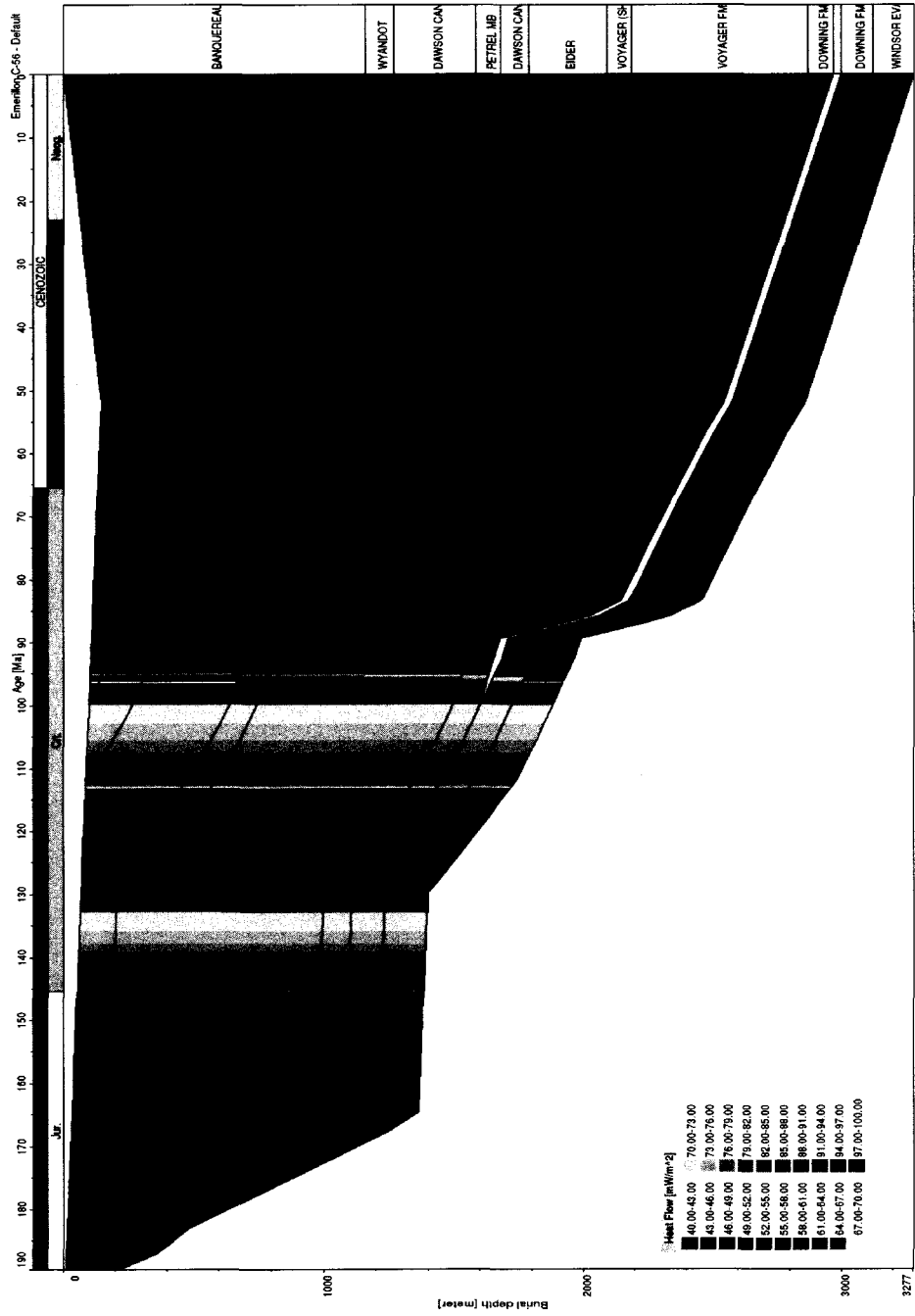Emerillon C-56

Figure 2.31: Results of Model A burial history plot with heat flow overlay for Emerillon C-56

Figure 2.32: Model A modeled vitrinite reflectance profile vs measured vitrinite reflectance for Emerillon C-56

Figure 2.33: Results of Model B burial history plot with temperature overlay for Emerillon C-56

Figure 2.34: Model B modeled temperature vs measured downhole temperature for Emerillon C-56

Figure 2.35: Results of Model B burial history plot with heat flow overlay for Emerillon
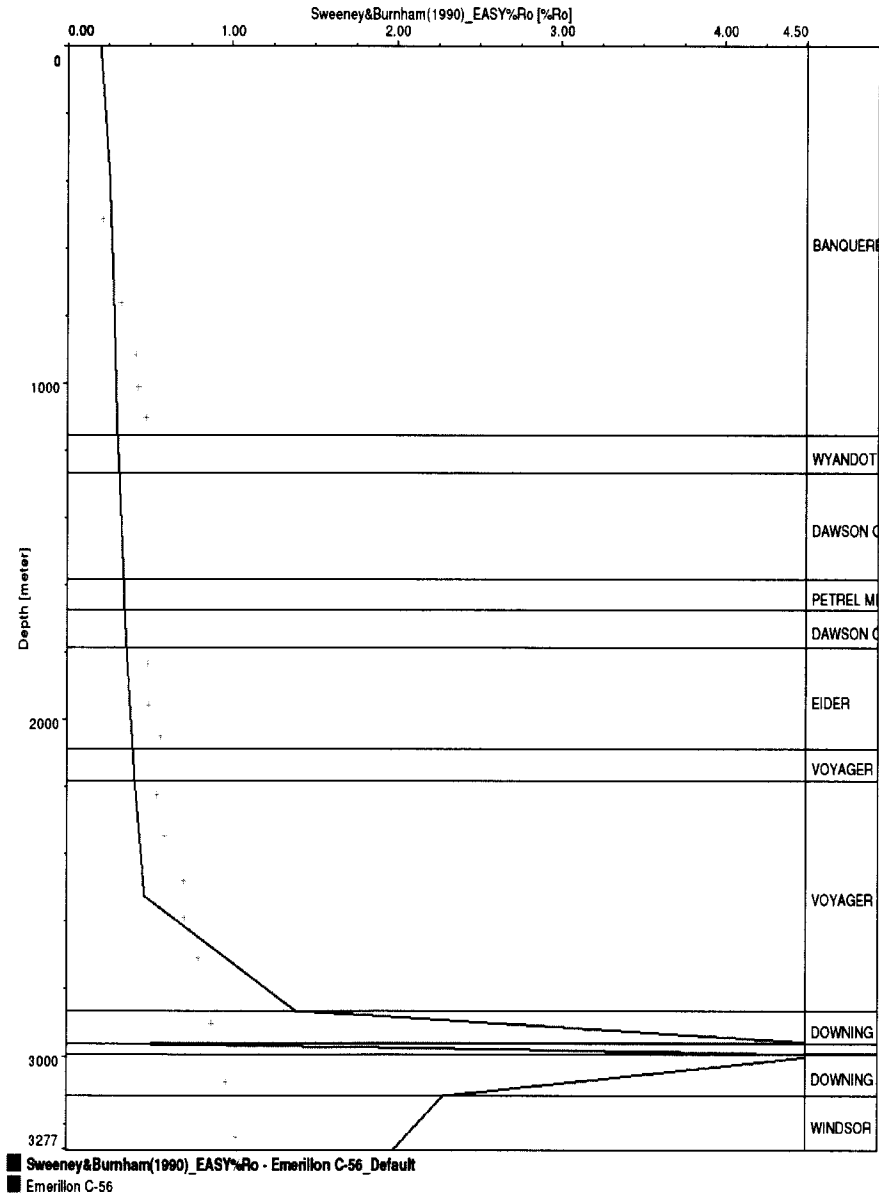C-56

252

Figure 2.36: Model B modeled vitrinite reflectance profile vs measured vitrinite reflectance for Emerillon C-56
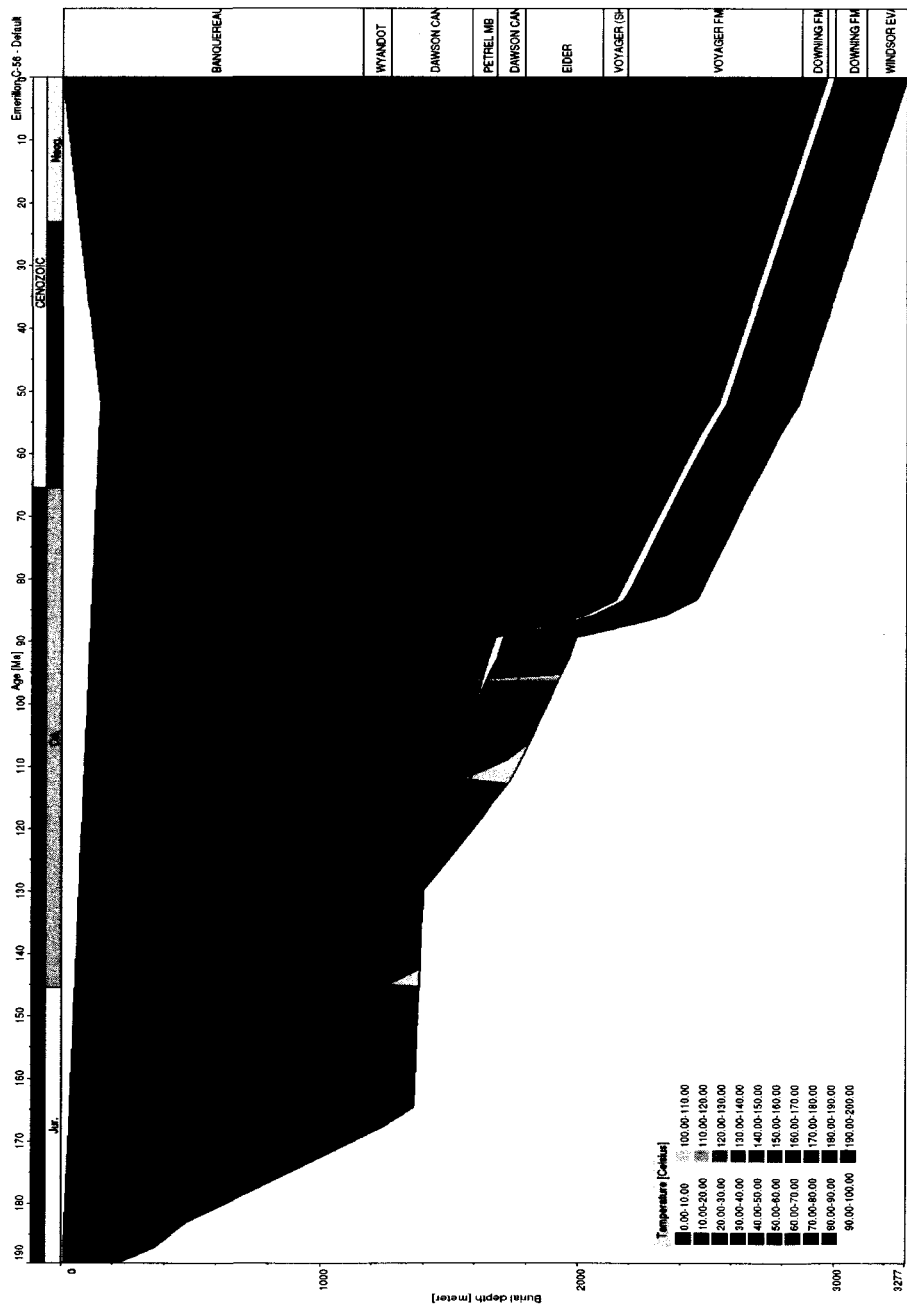
Figure 2.37: Results of Model C burial history plot with temperature overlay for Emerillon C-56
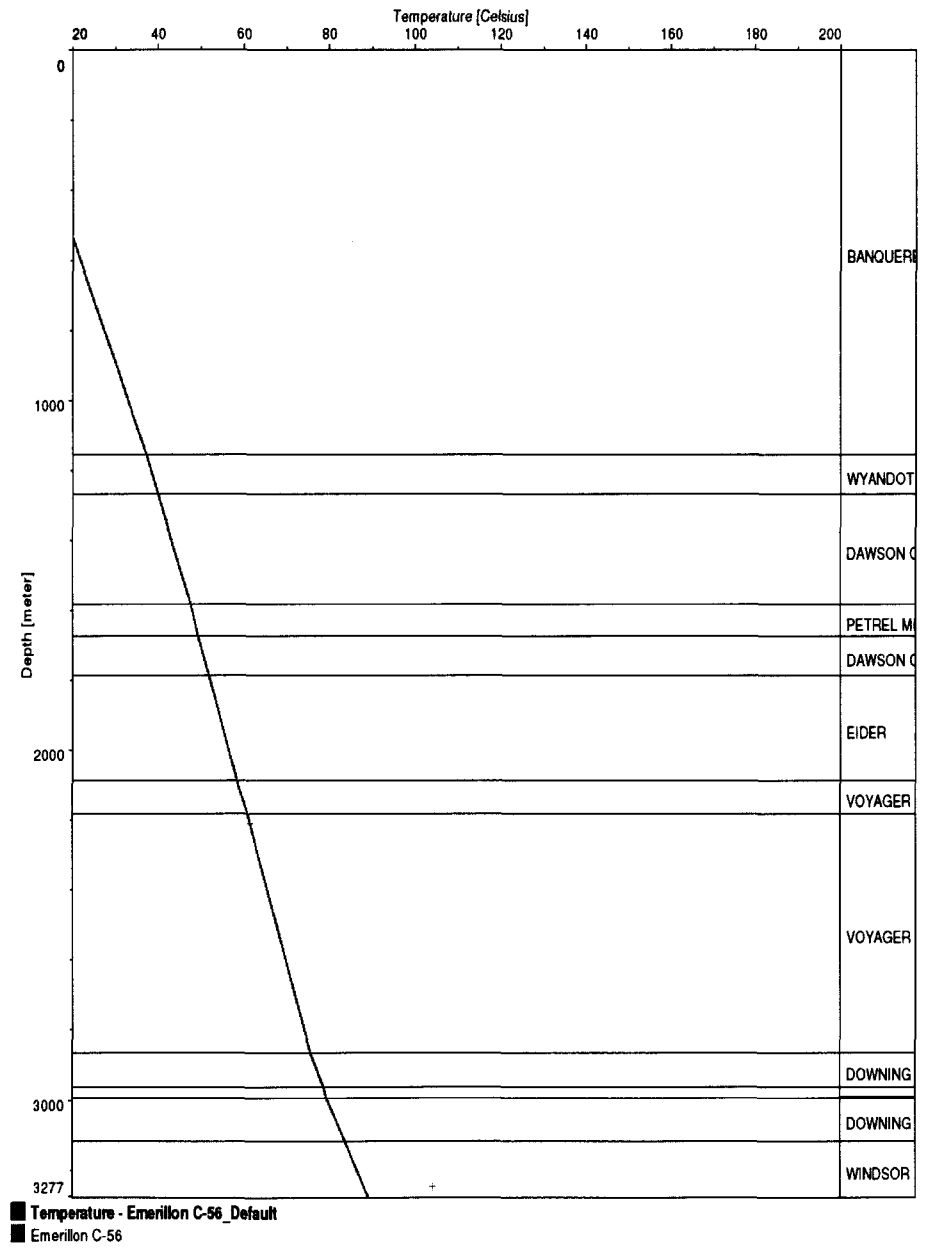
Figure 2.38: Model C modeled temperature vs measured downhole temperature for Emerillon C-56

Figure 2.39: Results of Model C burial history plot with heat flow overlay for Emerillon C-56

Figure 2.40: Model C modeled vitrinite reflectance profile vs measured vitrinite reflectance for Emerillon C-56

Figure 2.41: Results of Model D burial history plot with temperature overlay for Emerillon C-56

Figure 2.42: Model D modeled temperature vs measured downhole temperature for Emerillon C-56
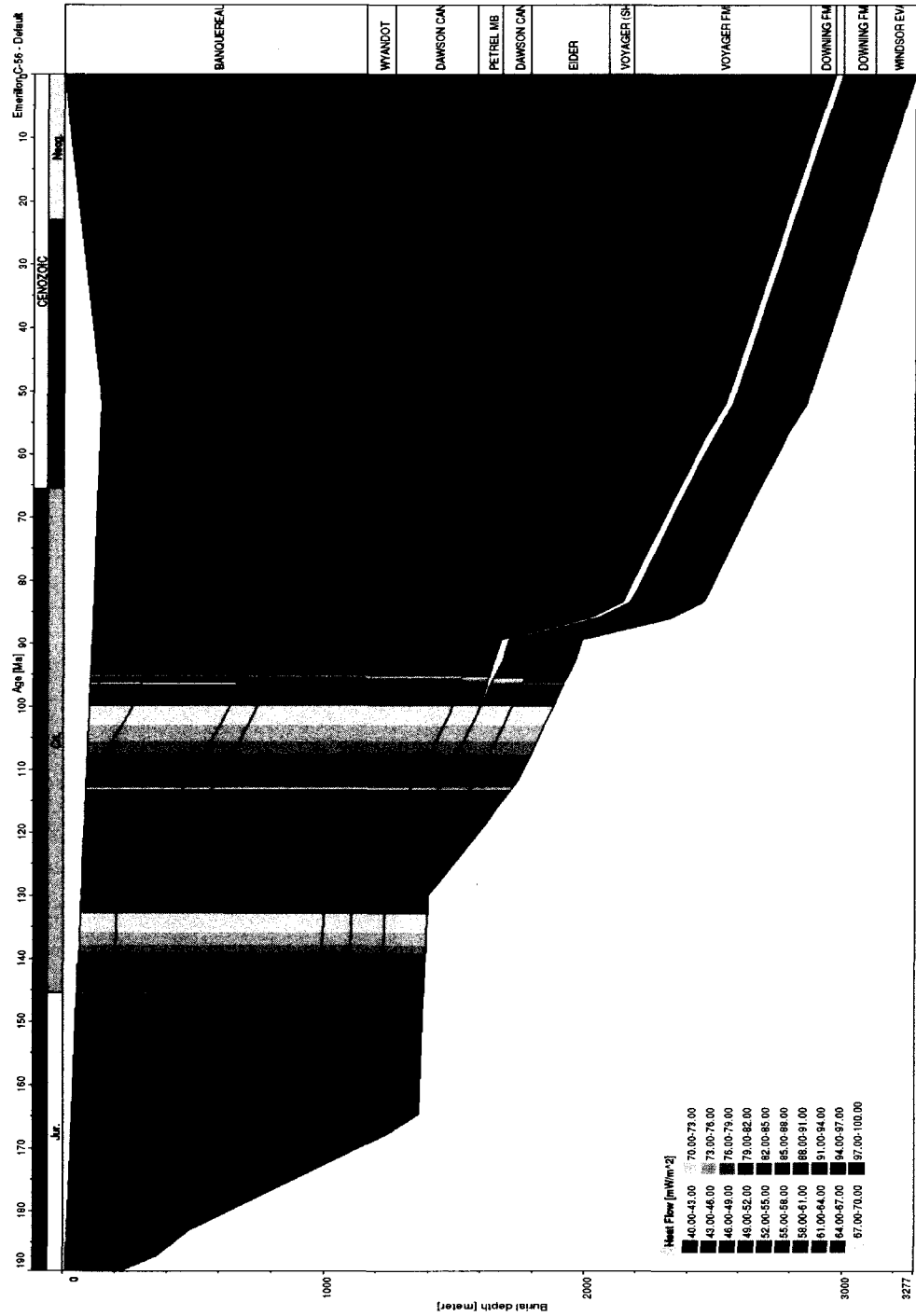
Figure 2.43: Results of Model D burial history plot with heat flow overlay for Emerillon C-56
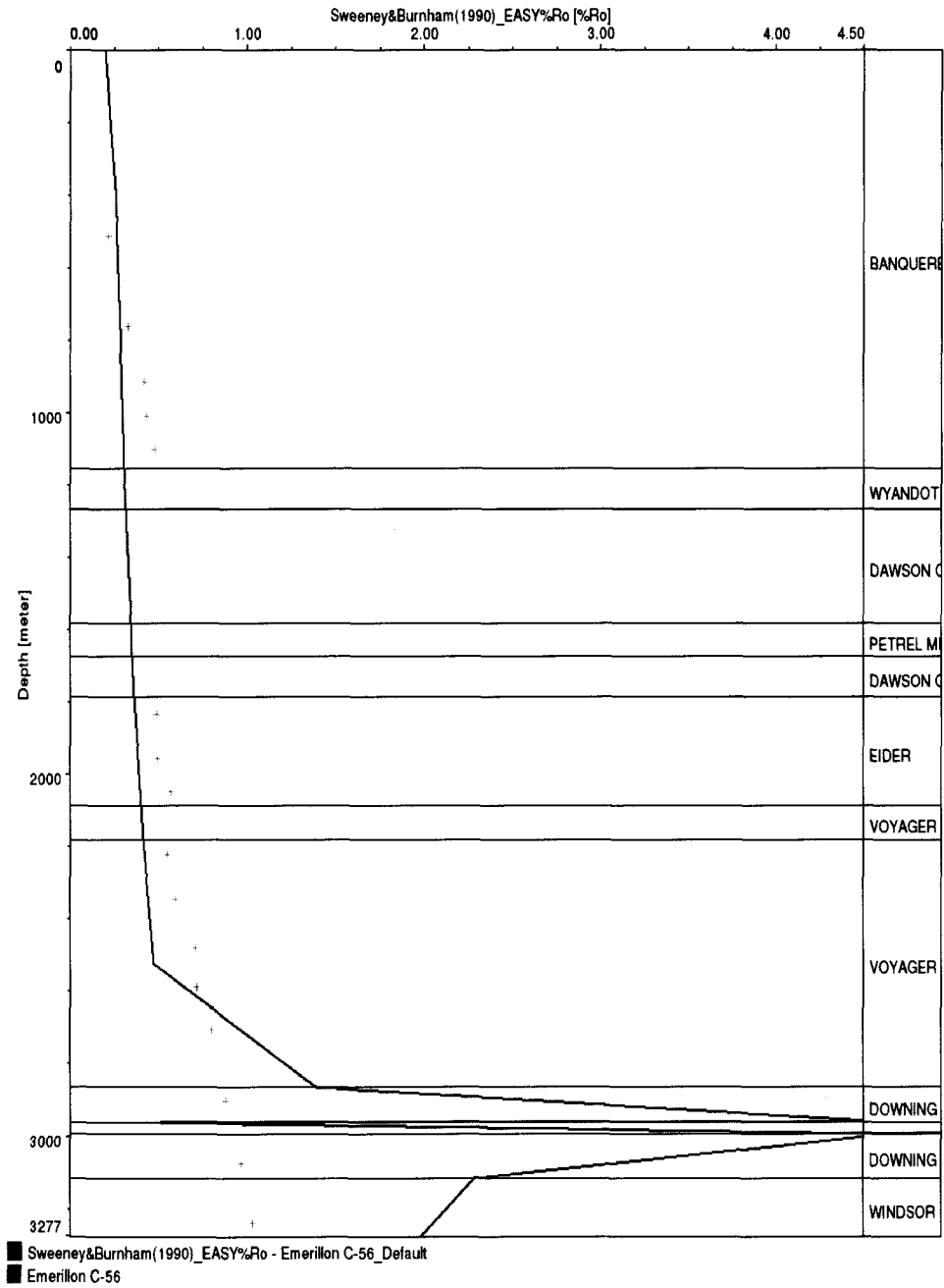
Figure 2.44: Model D modeled vitrinite reflectance profile vs measured vitrinite reflectance for Emerillon C-56